

ENGINEERING AEQUORIN AS AN INDICATOR OF CALCIUM SIGNALS NEAR THE BK CHANNEL

Pablo Reviriego Santos

**A thesis submitted to Cardiff University in accordance with
the requirements for the degree of Philosophiae Doctor**

September 2009

**Cardiff University
Welsh School of Pharmacy
Redwood Building
King Edward VII Avenue
Cardiff CF10 3NB**

UMI Number: U584365

All rights reserved

INFORMATION TO ALL USERS

The quality of this reproduction is dependent upon the quality of the copy submitted.

In the unlikely event that the author did not send a complete manuscript and there are missing pages, these will be noted. Also, if material had to be removed, a note will indicate the deletion.



UMI U584365

Published by ProQuest LLC 2013. Copyright in the Dissertation held by the Author.
Microform Edition © ProQuest LLC.

All rights reserved. This work is protected against
unauthorized copying under Title 17, United States Code.



ProQuest LLC
789 East Eisenhower Parkway
P.O. Box 1346
Ann Arbor, MI 48106-1346

**“Any living cell carries with it the experience of a billion
years of experimentation by its ancestors.”**

Max Delbrück

SUMMARY

The BK channel is a large conductance calcium-activated voltage-dependent potassium channel. This channel plays a key role as a negative feedback mechanism of membrane excitability and cellular Ca^{2+} . There is substantial evidence suggesting that the Ca^{2+} activation of the BK channel is regulated by localised Ca^{2+} release from intracellular stores. The aim of the work presented in this thesis was to develop a novel method of measuring the local Ca^{2+} concentration controlling the BK channel activation. The $\beta 2$ subunit, an auxiliary protein of the BK channel, was extracted from MG63 cells and cloned. Subsequently, the aequorin sequence was attached to its C-terminus using splicing by overlapping extension.

The recombinant protein retained the features of the native proteins emitting light in response to Ca^{2+} and showed correct targeting to the cell membrane. The resultant light emission of the new protein was diminished in comparison to the native aequorin. The $\beta 2$ -Aequorin and a cytosolic Luciferase-aequorin were successfully transfected in a HEK293 cell line which stably express the BK channel α subunit. The expression of the aequorin constructs in HEK293 cells in suspension revealed the presence of intracellular mechanosensitive Ca^{2+} channels.

The main finding of this thesis was that the Ca^{2+} affecting the BK channel is regulated independently of cytosolic Ca^{2+} in HEK293 cells. Stimulation with agonists such as carbachol, ATP and cyclopiazonic acid demonstrated clear differences in the magnitude of BK channel microdomain and cytosolic Ca^{2+} signals. Short term exposure to caffeine induced a significant decrease in the Ca^{2+} signals near the channel. The addition of extracellular Ca^{2+} led to large Ca^{2+} transients close to the BK channel suggesting a store-operated Ca^{2+} mechanism. The Ca^{2+} effects produced by carbachol, ATP, caffeine and cyclopiazonic acid indicate a coupling between IP_3 -induced Ca^{2+} release from the ER and Ca^{2+} - activation of the BK channel.

TABLE OF CONTENTS

Summary	i
Declaration	ii
Table of contents	iii
Acknowledgments	xi
List of figures & tables	xii
Abbreviations	xvi
<u>CHAPTER 1. Introduction</u>	1
1.1. CELLULAR CALCIUM	4
1.1.1. <i>Historical perspective</i>	4
1.1.2. <i>Physiological relevance of calcium</i>	5
1.1.3. <i>Mechanisms of control of cellular calcium</i>	6
1.2. ION CHANNELS	10
1.1.4. <i>Overview</i>	10
1.1.5. <i>Localisation</i>	11
1.1.6. <i>Structure, gating and selectivity</i>	11
1.3. BK CHANNELS	12
1.3.1. <i>BK channels diversity</i>	12
1.3.1.1. <i>Splice variants</i>	14
1.3.1.2. <i>β Subunit Modulation</i>	14
1.3.2. <i>BK channel structure</i>	14
1.3.3. <i>BK channel characteristics</i>	17
1.3.4. <i>Other BK channels</i>	19
1.4. <i>β SUBUNITS: THEIR IMPORTANCE</i>	21

Table of contents

1.4.1. <i>Specific features of each β subunit</i>	21
1.4.2. <i>Stoichiometry</i>	26
1.4.3. <i>Channelopathies</i>	27
1.5. BIOLUMINESCENCE	31
1.5.1. <i>Aequorin</i>	31
1.5.1.1. <i>Mechanism of light emission in aequorin</i>	31
1.5.1.2. <i>Structure of aequorin</i>	33
1.5.1.3. <i>Converting aequorin light emission into calcium</i>	35
1.5.1.4. <i>Aequorin as a Ca^{2+} reporter.</i>	36
1.6. MEASURING INTRACELLULAR CALCIUM	37
1.6.1. <i>Optical Techniques</i>	38
1.6.1.1. <i>Fluorescence indicators</i>	38
1.6.1.2. <i>GFP-based Ca^{2+} indicators</i>	40
1.6.1.3. <i>Aequorin</i>	41
1.6.2. <i>Non-optical techniques</i>	43
1.6.2.1. <i>Ca^{2+}-selective electrodes</i>	43
1.6.2.2. <i>Electrophysiology</i>	43
1.6.3. <i>Use of luminescence techniques in ion channels</i>	44
1.7. AIMS OF THE THESIS	45
CHAPTER 2. Material and Methods.	48
2.1. MATERIALS REAGENTS	49
2.1.1. General reagents	49
2.1.1.2. <i>Chemicals.</i>	49
2.1.1.2. <i>Enzymes and molecular biology reagents.</i>	49
2.1.2. General solutions	50

Table of contents

2.1.2.1. <i>Physiological solutions</i>	52
2.2 MOLECULAR BIOLOGY TECHNIQUES	53
2.2.1. <i>Polymerase chain reaction</i>	53
2.2.1.1. <i>High-fidelity PCR</i>	53
2.2.1.2. <i>Primer design</i>	54
2.2.1.3. <i>DNA quantification</i>	54
2.2.1.4. <i>DNA sequencing</i>	55
2.2.2. <i>Agarose Gel electrophoresis</i>	59
2.2.3. <i>RNA isolation</i>	57
2.2.3.1. <i>DNase treatment</i>	57
2.2.3.2. <i>RNA quantification</i>	58
2.2.4. <i>Reverse transcription PCR</i>	58
2.2.5. <i>TA Cloning into pTarget vector</i>	59
2.2.5.1. <i>Ligation of DNA insert into pTarget</i>	59
2.2.5.2. <i>Preparation of competent bacteria</i>	59
2.2.5.3. <i>Transformation of competent cells</i>	60
2.2.5.4. <i>Screening transformant colonies for DNA insert</i>	60
2.2.6. <i>Isolation of plasmid</i>	61
2.2.6.1. <i>Isolation of large quantities of plasmid DNA.</i>	62
2.2.7. <i>Protein expression</i>	63
2.2.7.1 <i>In vitro Protein transcription/translation</i>	63
2.2.7.2. <i>Expression of recombinant proteins in living cells.</i>	64
2.2.7.2.1. <i>Lipid mediated transfection</i>	64
2.2.7.2.1.1. <i>Cell seeding</i>	64

Table of contents

2.2.7.2.1.2. <i>Lipofectamine 2000 transfection</i>	65
2.2.7.2.1.3. <i>Lipofectamine LTX and PLUS transfection</i>	65
2.2.7.2.1.4. <i>FUGENE HD transfection</i>	65
2.2.8. Aequorin expression and extraction from bacteria	66
2.2.9. Protein extraction from eukaryotic cells	67
2.2.9.1. <i>Subcellular fractionation</i>	67
2.3. CELL BIOLOGY TECHNIQUES	68
2.3.1. <i>Cell culture</i>	68
2.3.1.1. <i>Cell husbandry of MG63 and HBO.</i>	68
2.3.1.2. <i>Cell husbandry of HEK293.</i>	68
2.3.2. <i>Cell storage</i>	69
2.4. CALCIUM IMAGING TECHNIQUES	69
2.4.1. Apoequorin reconstitution	69
2.4.1.1. <i>Coelenterazine</i>	69
2.4.1.2. <i>Reconstitution of apoequorin in translation products</i>	70
2.4.1.3. <i>Reconstitution of apoequorin in bacteria cell extracts</i>	70
2.4.1.4. <i>Reconstitution of apoequorin in living cells</i>	71
2.4.2 Luminometers	71
2.4.2.1. <i>Home-built luminometer</i>	71
2.4.2.1.1 <i>Calibration of the home-built luminometer</i>	73
2.4.2.2. ICCD camera	75
2.4.2.2.1. <i>Sample handling</i>	77
2.4.2.2.1. <i>Perfusion system</i>	78
2.4.2.2.3. <i>Data Analysis</i>	80
2.4.3. <i>Converting aequorin light emission into calcium</i>	81

2.5. ELECTROPHYSIOLOGICAL TECHNIQUES	82
<i>2.5.1. The patch-clamp technique</i>	84
<i>2.5.2. Seeding on to glass coverslips</i>	84
<i>2.5.3. Microelectrodes production</i>	84
<i>2.5.4. Electrophysiological Recording</i>	84
<i>2.5.5. Data analysis.</i>	85
2.6 . STATISTICAL ANALYSIS	86
 <u>CHAPTER 3.</u> Engineering and characterisation of a β2-Aequorin chimera targeting the BK channel.	87
 3.1. INTRODUCTION	88
3.2. METHODS	91
<i>3.2.1. Primer design.</i>	91
<i>3.2.2. Polymerase Chain Reaction.</i>	92
<i>3.2.3. Cloning of the β2 subunit.</i>	92
<i>3.2.4. Engineering and cloning of β2-Aequorin.</i>	92
<i>3.2.5. Cell-free protein expression.</i>	94
<i>3.2.6. MTS Cell proliferation assay.</i>	94
<i>3.2.7. Assessment of aequorin reconstitution.</i>	95
3.3. RESULTS	96
<i>3.3.1. MG63 and HEK293 α cell assessment.</i>	96
<i>3.3.2. β2 subunit cloning.</i>	97
<i>3.3.3. Engineering and cloning of β2-Aequorin.</i>	104
<i>3.3.4. Expression of β2-Aequorin in a cell-free system.</i>	111
<i>3.3.5. Evaluation of reconstitution conditions for β2-Aeq.</i>	113

3.3.6. Subcellular distribution of recombinant aequorin.	118
3.3.7. Effects of $\beta 2$ -Aeq in cell growth.	120
3.4. DISCUSSION	122
3.4.1. Cell Assessment	122
3.4.2. Engineering of $\beta 2$ -Aeq and functional evaluation.	124
3.4.3. Assessment of best conditions for aequorin reconstitution	127
3.4.4.. Differences between $\beta 2$ -Aeq and Luc-Aeq	128
3.4.4.. Conclusions	131
<u>CHAPTER 4. Evidence for local regulation of the calcium</u>	132
signals in the proximity of the BK channel in living cells.	
4.1 INTRODUCTION	133
4.2 METHODS	135
4.2.1 Transfection efficiency.	135
4.2.2 Fluorescence-activated cell sorting.	136
4.2.3 Calcium-dependent signal from living cells.	137
4.2.3.1. Effects of the addition of an isosmotic solution on intracellular free Ca^{2+} detected using a home-built luminometer.	137
4.2.3.2 Effects of addition of extracellular Ca^{2+} on intracellular free Ca^{2+} recorded using an ICCD camera.	138
4.2.3.3 Analysis of individual Ca^{2+} signals.	139
4.3 RESULTS	139
4.3.1. Transfection efficiency.	139
4.3.2 Effects of the addition of an isosmotic solution on intracellular free Ca^{2+} in transfected HEK293 cells in suspension.	147

4.3.3. <i>Effects of the addition of extracellular calcium on intracellular free Ca^{2+}.</i>	148
4.3.4. <i>Individual Ca^{2+} responses in HEK293 cells.</i>	156
4.4 DISCUSSION	163
4.4.1. <i>Assessment of the best conditions for Ca^{2+} imaging in HEK293 and MG63 cells: evidence of mechanosensitive channels in HEK293.</i>	163
4.4.2. <i>Effects of extracellular calcium.</i>	166
4.4.3. <i>Individuality of Ca^{2+} responses in HEK293 cells.</i>	172
4.4.4. <i>Conclusions</i>	176
CHAPTER 5. Regulation of local calcium signals near the BK channel by agonists and intracellular calcium release.	178
5.1. INTRODUCTION	179
5.2. METHODS	182
5.2.1. <i>Ca^{2+} monitoring in living cells in response to diverse agonists.</i>	182
5.2.2. <i>Ca^{2+} monitoring in living cells in response to diverse drugs.</i>	182
5.2.3. <i>Data analysis</i>	184
5.2 RESULTS	185
5.3.1 <i>Effects of agonist-induced Ca^{2+} responses in HEK293 cells.</i>	186
5.3.2 <i>Effects of K^+ channel blockers on intracellular free Ca^{2+} in HEK293 cells.</i>	189
5.3.2 <i>Effects of caffeine.</i>	190
5.3.3. <i>Effects of cyclopiazonic acid.</i>	196
5.4 DISCUSSION	198
5.4.1 <i>Effects of receptor-operated agonists.</i>	199
5.4.2. <i>Effects of K^+ channel blockers.</i>	205

5.4.3. <i>ER and BK channel coupling: investigation using caffeine and cyclopiazonic acid.</i>	206
5.4.3.1 <i>The effects of caffeine on intracellular free Ca^{2+}.</i>	207
5.4.3.2 <i>The effects of CPA on intracellular free Ca^{2+}.</i>	212
5.4.4. <i>The potential role of mitochondria in buffering calcium in the BK channel microdomain.</i>	216
5.4.5. <i>Conclusions</i>	220
<u>CHAPTER 6. Conclusions and general discussion.</u>	222
6.1. SUMMARY OF MAIN FINDINGS	223
6.2. FUTURE PROSPECTS	225
6.2.1. <i>Further assessment of the functional properties of the $\beta 2$-Aeq chimera.</i>	225
6.2.2. <i>Investigation of the role of mitochondria on Ca^{2+} signalling near the BK channel.</i>	227
6.2.3. <i>Does the local Ca^{2+} regulation of the BK channel vary with cell function?</i>	228
6.2.4. <i>Does the BK channel form complexes with Ca^{2+} channels?</i>	229
<u>REFERENCES</u>	231
Appendix 1	258
Appendix 2	260
Appendix 3	261
Appendix 4	265

Acknowledgements

I would never have been able to succeed on my research and complete my dissertation were it not for the tremendous support of my supervisors, Dr Ken Wann and Prof. Anthony Campbell. Dr Wann's rigorous attitude and approach in science research, as well as solid academic background and sharp grasp of cell biology, have taught me the true essence of being a good scientist. Prof. Campbell's passion, dedication and aspiration for science have provided me the constant guidance and encouragement to continue my persistently assiduous study in the doctoral degree. Thanks to both for placing me on a solid path to finish my doctoral degree and getting me ready for a bright future career on science research.

I am thankful to Neil Henney and Bo Li, as well as the others who have provided me with succour one way or the other in these several years.

I wish to thank Bronwen Evans and Carole Elford for valuable conversations and guidance on the genetic studies. I would also like to acknowledge all members in the Pharmacy School for their assistance in all these years.

I also need to extend my thank-you note to AKRainbow Ltd. for providing me with financial support, expertise and facilities to bring this project to a successful conclusion. Furthermore the excellent R&D environment of AKRainbow Ltd. gave me the full display to show my talent on the research work.

None of my accomplishments would have been possible without the love and support of my dear family and my wonderful partner, Beatriz Casado. I am deeply indebted to my family in Spain and very grateful to my parents for bringing me up and nurturing me in a love-caring environment devoting their love to me unreservedly.

In particular I dedicate the dissertation to the best person I ever known, my partner Beatriz. Her selfless love, devotion and support always accompany my academic journey, giving me the strength and confidence when most needed.

LIST OF FIGURES

Fig 1.1.	Number of scientific publications on calcium.	3
Fig 1.2.	The complex mechanism controlling Ca^{2+} signalling inside the cell	10
Fig 1.3	Molecular diversity of the potassium channels	13
Fig 1.4	Structure of the α and β subunit of the BK channel	15
Fig 1.5	Stoichiometry of α and β subunits in the BK channel complex	27
Fig 1.6	The basic chemical reaction of bioluminescence	32
Fig 1.7	Crystal structure of aequorin	34
Fig 2.1	Picture of the home-built luminometer	73
Fig 2.2	Calibration of the home-built luminometer.	75
Fig 2.3	Schematic representation of the ICCD325 camera	77
Fig 2.4	Picture and schematic representation of the components of the ICCD camera system.	79
Fig 2.5	Light emission of cell clusters following the addition of a high Ca^{2+} lysis solution.	81
Fig 2.6	Schematic representation of a single ion channel being recorded within the patch pipette.	83
Fig 3.1	Location of primers in the $\beta 2$ sequence	92
Fig 3.2	Subunit composition of the BK channel in human osteoblast.	100

Fig 3.3	Single channel recording of BK channels in HEK293 α cells in a cell-attached patch.	101
Fig 3.4	PCR amplification of the BK α subunit in HEK293 α .	102
Fig 3.5	Cloning of the β 2 subunit.	102
Fig 3.6	Engineering and cloning of β 2-Aequorin.	106
Fig 3.7	Hydropathy analysis of the β 2 subunit.	110
Fig 3.8.	Cell-free expression of β 2Aeq and LucAeq.	112
Fig 3.9	Reconstitution efficiency of aequorin constructs in HEK293 in different media.	115
Fig 3.10	Relative reconstitution efficiency of aequorin constructs in HEK293 in different media.	116
Fig 3.11	Effects of coelenterazine concentration in the reconstitution efficiency of aequorin constructs in HEK293.	117
Fig 3.12	Subcellular fractionation of HEK 293 transfected with either β 2Aeq or LucAeq.	120
Fig 3.13	Effects of β 2-Aeq transfection on cell number.	122
Fig 4.1	Comparative analysis of different transfection reagents.	143
Fig 4.2	FACS analysis of transfection efficiency in HEK293.	144
Fig 4.3	FACS analysis of transfection efficiency in MG63.	145
Fig 4.4	Light emission of MG63 cells transfected with Luc-Aeq.	146
Fig 4.5	Effect of mechanical stimuli on free Ca^{2+} HEK293 cells in suspension.	150
Fig 4.6	Visual evaluation of effects of extracellular calcium in Luc-Aeq and β 2-Aeq.	153

Fig 4.7	Effects of extracellular calcium on intracellular free Ca^{2+} from HEK293 cells.	154
Fig 4.8	Individual Ca^{2+} transients induced by addition of extracellular Ca^{2+} .	159
Fig 4.9	Individual Ca^{2+} transients induced by a second addition of extracellular Ca^{2+} .	160
Fig 4.10	Comparison of Ca^{2+} signals to the total expression of aequorin in individual cell clusters.	161
Fig 5.1	Effects of carbachol in individual clusters of HEK293 cells.	187
Fig 5.2	Effects of intracellular Ca^{2+} modulators on Ca^{2+} responses in HEK293 cells.	188
Fig 5.3	Effects of TEA on intracellular free Ca^{2+} in individual clusters of HEK293 cells.	191
Fig 5.4	Effects of K^+ channel blockers on intracellular free Ca^{2+} in HEK293 cells.	192
Fig 5.5	Effects of caffeine on intracellular free Ca^{2+} in individual HEK293 cell clusters	194
Fig 5.6	Effects of caffeine on intracellular free Ca^{2+} in HEK293.	195
Fig 5.7	Effects of cyclopiazonic acid on intracellular free Ca^{2+} in HEK293 cells.	197
Fig. 5.8	Schematic representation of the effects of ER Ca^{2+} release on the Ca^{2+} activation the BK channel.	202

LIST OF TABLES

Table 1.1.	Characteristics of the BK channels	18
Table 1.2	Characteristics of other BK channels	20
Table 1.3	Expression of BK α and β subunits in different tissues.	22
Table 3.1.	List of α and β 1-4 primers.	91
Table 3.2	β 2 nucleotide and protein sequence comparisons.	103
Table 3.3	Amino acid modifications in the β 2-Aeq protein sequence.	107
Table 3.4	β 2-Aequorin nucleotide and protein sequence comparisons.	108
Table 4.1	Transfection efficiency in HEK293 and MG63 cells.	144
Table 4.2	Comparison of basal intracellular free Ca^{2+} concentrations in HEK293 cells.	155
Table 4.3	Variability of the individual Ca^{2+} responses.	162

ABBREVIATIONS

AA	Amino acid
Aeq	Aequorin
ATP	Adenosine triphosphate
bp	base pair
Bcl-2	B cell lymphoma gene-2
BRET	Bioluminescence resonance energy transfer
BSA	Bovine serum albumin
C-terminus	Carboxyl-terminus
CCD	Charged coupled device
cDNA	complementary DNA
CCD	Charge couple device
CCh	Carbachol
CDS	Coding sequence
CMV	Cytomegalovirus
CPA	Cyclopiazonic acid
CICR	Calcium induced calcium release
CRAC	Calcium release-activated current
CTX	Charybdotoxin
CV	Coefficient of variation
DHS-1	Dehydrosoyasaponin-1
DMEM	Dulbecco's modified Eagle medium
DMSO	Dimethyl sulphoxide
DNA	Deoxyribonucleic acid
dNTP	Deoxynucleotide triphosphate
EDTA	Ethylenediaminetetra acetic acid
EGFP	Enhanced green fluorescent protein
EGTA	Ethyleneglycolbis-(β -aminoethyether)-N,N,N',N' tetra acetic acid
ER	Endoplasmic reticulum
ERK	extracellular signal-regulated kinase

Abbreviations

FRET	Fluorescence resonance energy transfer
GFP	Green fluorescent protein
GPCR	G-protein-coupled receptors
h	hours
HEPES	N-2-hydroxyethylpiperazine-N'-2-ethanesulphonic acid
IbTX	Iberiotoxin
ICCD	Intensified charged coupled device
IPTG	Isopropyl β-D-thiogalactoside
IP₃	Inositol triphosphate
KRH	Krebs-Ringer-HEPES
LB	Luria Bertani
Luc	Luciferase
MAPK	Mitogen-activated protein kinase
MEM	Minimum Essential Medium
MOPS	3-[N-morpholino] propanesulfonic acid
mRNA	messenger RNA
MTS	3-(4,5-dimethylthiazol-2-yl)-5-(3-carboxy methoxyphenyl)-2-(4-sulfophenyl)-2H-tetrazolium
MW	Molecular weight
N-terminus	amino-terminus
OAS	Odd area set
PCR	Polymerase chain reaction
PMS	Phenazine methosulfate
PMT	Photomultiplier
RCK	Regulator of conductance for potassium
RT	Reverse transcription
SD	Standard deviation
SEM	Standard error of the mean
SOC	Store operated calcium
SOP	Splicing by overlap extension
STIM	Stromal interaction molecule

Abbreviations

TAE	Tris-acetic acid-EDTA
TEA	Tetraethylammonium
TRP	Transient receptor potential
TE	Tris-EDTA buffer
Tris	Tris(hydroxymethyl)aminomethane
UV	Ultra violet
v/v	volume / volume

INTRODUCTION

The survival of all living organisms depends on the maintenance of suitable concentrations of inorganic ions such as sodium, potassium, chloride and calcium. Calcium in particular is now widely recognized as a vital regulator of many cellular processes including metabolic processes, enzymatic activities, gene regulation and electrochemical responses. There has been a vast increase in research on calcium signalling in recent years which has widened our understanding. The majority of this research has focused mainly on the cytosol. It is now well-known that small variations in intracellular free calcium may have significant repercussions on some of these essential processes. Some of these events are triggered by calcium within milliseconds whereas others require the presence of Ca^{2+} over minutes to hours. Not only the temporal aspects but also the spatial pattern of Ca^{2+} concentrations affects these processes. Some of them respond to localised Ca^{2+} concentrations whereas others to more diffuse Ca^{2+} signals. The activity of Ca^{2+} -dependent protein complexes such as enzymes or ion channels is modulated by the Ca^{2+} concentration in their vicinity. It is becoming evident that in order to understand how Ca^{2+} controls the activity of these ion channels, the measuring of the exact local Ca^{2+} concentrations near to these elements is required.

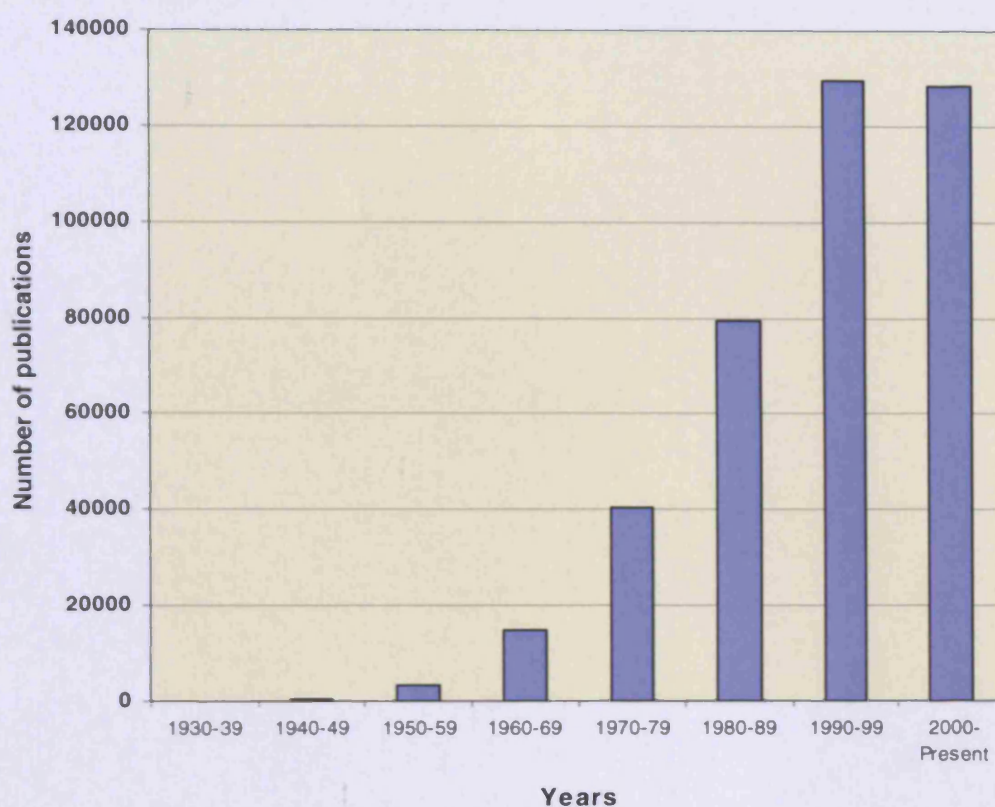
Fig. 1.1 Number of scientific publications on calcium.

Fig. 1.1 Number of biomedical scientific publications on calcium over the last decades. The graph represents the number of publications which are related to calcium in biomedical journals. An exponential growth can be observed until the year 2000. Interestingly, the number of publications of the last two decades is maintained. A web search was carried out using the term calcium and the publication dates indicated in the graph on the web-based search engine Pub Med (<http://www.ncbi.nlm.nih.gov/pubmed/>) during March 2009.

1.1. CELLULAR CALCIUM

1.1.1 Historical Perspective: The first 100 years.

The work carried out by Sidney Ringer (Ringer, 1883) nearly 125 years ago is considered the first evidence of the crucial role of calcium in physiological processes. This brilliant physiologist realised that small amounts of Ca^{2+} in the perfusion solution were required for the maintenance of the normal heartbeat of isolated rat hearts. He concluded that Ca^{2+} was not only an structural component of the body but also responsible for initiating physiological processes such as heart contraction. Subsequently a number of investigators (see Campbell, 1983 for details) followed his work providing more evidence of the important role of Ca^{2+} in cell stimuli. Among many others, one could quote the work of two pioneers: Heilbrunn and Bailey. Heilbrunn (Heilbrunn, 1940) proved that Ca^{2+} applied to the cut ends of frog muscle fibers diffused to their contractile elements eliciting contraction. Bailey (Bailey, 1942) showed that the ATPase activity of myosin was increased in the presence of Ca^{2+} (but not Mg^{2+}) and concluded that the release of Ca^{2+} in the proximity of the myosin triggered muscle contraction. The synthesis and characterisation of EDTA led to the compelling evidence that the removal of Ca^{2+} by EDTA relaxed muscle fibers (Bozler, 1954). In the following fifty years, the interest in Ca^{2+} has experienced a continuous growth, slowly at first and then more rapidly. Calcium is now recognised as an essential messenger involved in a

myriad of key cell processes (for a general overview of the historical aspects, see Carafoli, 2002; for comprehensive review, see Campbell, 1983).

1.1.2 Physiological relevance of calcium.

Calcium is thought to play a key role in the regulation of a multitude of cellular processes such as ion channel modulation, neurotransmitter and hormone release, muscle contraction, proliferation, exocytosis, apoptosis, gene regulation, control of kinase and phosphatase activity and general enzymatic activation (Carafoli & Klee, 1998; McDonough, 2003). Perturbed Ca^{2+} homeostasis is also thought to be involved in the pathogenesis of disorders of the immune, cardiovascular and nervous system (Orrenius *et al.*, 2003) i.e. heart failure (Go *et al.*, 1995) and Alzheimer's disease (Mattson *et al.*, 2000).

The function of calcium in apoptosis is particularly fascinating, especially when we consider that cell death is behind many of the mentioned disorders. There is considerable evidence supporting the major role of calcium in apoptosis involving well-known apoptosis regulators such as the oncogene Bcl-2 family members, cytochrome c and caspases (Rizzuto *et al.*, 2003). 'Ca²⁺ communication' between ER and mitochondria is a clear example. An increase in ER Ca²⁺ release induces the augmentation of Ca²⁺ loading of mitochondria causing the release of cytochrome c, fragmentation and swelling of the mitochondria (Pinton *et al.*, 2001; Boehning *et al.*, 2003). Furthermore, proteins of

the Bcl-2 family have been found in these two organelles (Scorrano *et al.*, 2003). Other elements involved in the apoptotic process such as the proteases calpains, some caspases and reactive oxygen species have been shown to be Ca^{2+} dependent (Rizzuto *et al.*, 2003). All these facts emphasize that programmed cell-death seems to be tightly related to alterations in intracellular Ca^{2+} homeostasis.

1.1.3 Mechanisms of control of cellular calcium.

It is clear that calcium ions affect many vital cellular processes. However, it must be noted that only the free Ca^{2+} ions serve as a second messenger tightly controlling all these processes. The resting levels of free Ca^{2+} found in the cytosol are maintained near 100 nM while extracellular calcium is around four orders of magnitude higher (1-1.5 mM) (Baker, 1972). The total cell calcium (free, bound to calcium-binding proteins and within intracellular compartments) is estimated to be much higher (10^5 times the amount of cytosolic free Ca^{2+}) (Hurwitz *et al.*, 1991).

As a general rule, Ca^{2+} -binding proteins such as aequorin and fluorescent Ca^{2+} indicators such as the Fura-2 dye only detect free Ca^{2+} in their proximity. Unless otherwise stated, in this thesis we will refer to free intracellular calcium simply as intracellular calcium.

Since intracellular enzymes and receptors display different affinities for calcium, minor variations of intracellular calcium can lead to diverse

intracellular results. Therefore, the correct calcium balance must be preserved to maintain cell functions. The plasma membrane calcium ATPase (PMCA) and the $\text{Na}^+/\text{Ca}^{2+}$ -exchanger are responsible for Ca^{2+} extrusion. On the other hand, the two predominant mechanisms of intracellular Ca^{2+} increase are Ca^{2+} entry from the extracellular milieu and Ca^{2+} release from intracellular stores. For the purpose of this work, we will focus on the sources of Ca^{2+} entry.

The lipid membrane is very impermeable to Ca^{2+} ions and Ca^{2+} only enters through Ca^{2+} channels. There are mainly three types of Ca^{2+} channels: voltage-gated Ca^{2+} channels, receptor-operated Ca^{2+} channels and store-operated Ca^{2+} (SOC) channels.

Voltage-gated Ca^{2+} channels mediate the entry of Ca^{2+} ions in response to electrical depolarisation of the plasma membrane. According to their biophysical and pharmacological properties, voltage-gated Ca^{2+} channels can be classified as L, N, T and P/Q type (Tsien *et al.*, 1988; Miller *et al.*, 1992; Zamponi *et al.*, 2005). It is thought that different Ca^{2+} channel subtypes govern distinct physiological functions (McDonough, 2003).

The receptor-operated Ca^{2+} channels respond to agonists such as glutamate, ATP or histamine in the plasma membrane allowing Ca^{2+} entry through the membrane. The binding of agonists to some receptors in the plasma membrane such as muscarinic or purinergic receptors results in the production of IP_3 which in turn causes the release of Ca^{2+}

from intracellular organelles (McMillian *et al.*, 1988). IP₃ receptors have been also found in the plasma membrane (Khan *et al.*, 1992). Ryanodine, caffeine and inositol 1,4,5-triphosphate (IP₃) are typical effectors which cause Ca²⁺ release by binding to these receptors contained in the ER. In particular, IP₃ is generally considered a second messenger (Streb *et al.*, 1983; Berridge, 1984).

SOC channels are involved in the replenishment of intracellular Ca²⁺ stores after depletion by the mechanism known as store-operated Ca²⁺ entry, also termed capacitative Ca²⁺ entry (Putney, 2007). The most studied SOC channels are calcium-release activated calcium (CRAC) channels (Putney, 1986). The main characteristics of CRAC channels are: an extremely small conductance (<1 pS); high selectivity for Ca²⁺ and sensitivity to channel blockers such as La³⁺, Gd³⁺ and Ni²⁺ (Putney, 2001). Although The precise mechanism of CRAC channels activation has remained elusive for the past 20 years, the recent discovery of the Orai and Stim proteins brings new light to this problem. Stim1 is mainly localised in the ER where detects Ca²⁺ fluctuations, while Orai1 is embedded in the plasma membrane. Orai1 and Stim1 interact functionally and together can emulate most of the features of CRAC entry (Putney, 2007). Second messenger particles such as the Calcium influx factor (CIF) and TRP channels have been also suggested to play an important role in this mechanism (Birnbaumer *et al.*, 1996). In light of these new findings, these hypotheses need a close re-examination.

Some TRP channels have been reported to be CRAC channels. However, the role of TRP channels in SOC entry is controversial. because their electrophysiological signature (Ca^{2+} selectivity, conductance and pharmacology) does not coincide with that displayed by CRAC channels (Birnbaumer *et al.*, 1996; Clapham, 2003). Like all the other Ca^{2+} -permeant channels they probably affect this mechanism of Ca^{2+} entry but more research is needed to decide whether TRP channels are CRAC channels.

Cells possess many ways of controlling intracellular Ca^{2+} (Fig. 1.2) and in most cases more than one of these mechanisms affect stimuli-induced Ca^{2+} responses. In this work, we will address the effects of these mechanisms when studying the resultant Ca^{2+} responses.

Comprehensive reviews about the important role of intracellular Ca^{2+} in the physiological context and the cellular mechanisms of controlling Ca^{2+} can be found first in Campbell (1983) and also in Carafoli & Klee (1998), Clapham (2003) and Putney (2007).

Cells use Ca^{2+} signalling to modulate the signals received from the environment and from other cells. They can also alter their electrical potential across the plasma membrane to regulate these signals. Consequently, cells need a means of controlling both mechanisms simultaneously. The tight regulation of membrane potential and Ca^{2+} concentrations is achieved by means of Ca^{2+} -activated voltage-dependent ion channels such as the large conductance Ca^{2+} -activated

potassium channel (BK channel). The BK channel plays a key role acting as a negative feedback regulator for these processes.

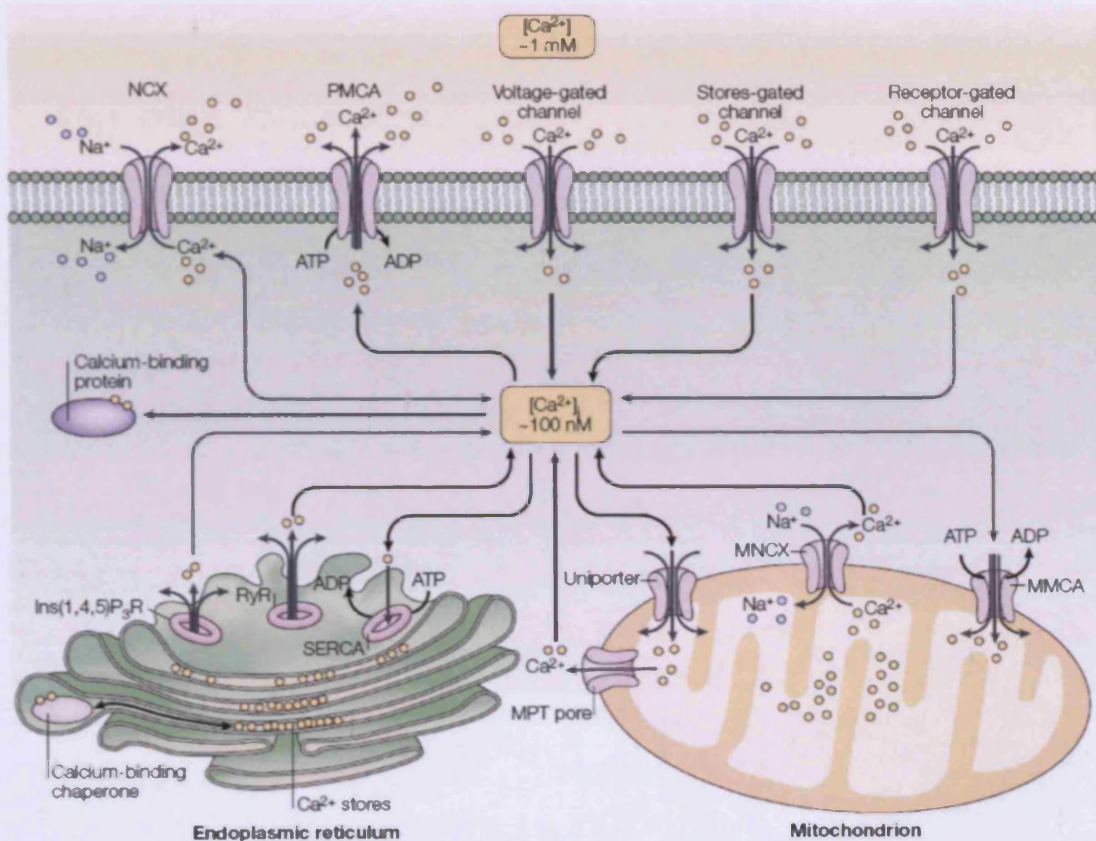


Fig 1.2. Schematic illustration of the complex mechanism controlling Ca^{2+} inside the cell (from Syntichaki & Tavernarakis, 2003).

1.2. ION CHANNELS

1.2.1 Overview.

Every single cell possesses a membrane which enables it to keep its interior characteristics (pH, charge, concentrations) suitable to perform optimally all the biological processes inside the cell. This membrane is a

lipid bilayer impermeable to polar molecules (sugars, amino acids, ions). The ion channels, together with ion pumps and exchangers, are the mechanisms embedded in the membrane that control the pathway of the ions. These ionic movements account for the membrane potential fluctuations. Changes in this potential trigger intracellular processes including the release of chemical signals that enable the cells to communicate with other cells. Therefore, at a physiological level, it may be said that the ion channels are in charge of the brain synapses, the heart beating and muscle contraction.

1.2.2. Localisation.

The ion channels can be expressed in all membrane domains. They may be found in the plasma membrane as well as in internal membranes such as those of the nucleus, Golgi complex, endoplasmic reticulum, lysosomes, endosomes and mitochondria.

1.2.3. Structure, gating and selectivity.

Ion channels are composed of diverse proteins assembled with an aqueous pore in the centre that can be either open or closed. We refer to this as gating. The opening is produced by means of conformational changes which allow the flow of ions through the channel at rates up to 10^8 ions per second. The gating of the channel can be triggered as a result of the binding of one or more compounds (ligand-gated channels), changes in the membrane potential (voltage-gated

channels), sensory stimuli of various kinds (mechanosensitive channels) or a combination of these factors (Ca^{2+} - voltage-activated channels).

Different channels show different selectivity. Potassium channels are up to 100 times more permeable to K^+ than Na^+ because the K^+ gating is a thermodynamically favoured process. Broadly speaking, the gating and selectivity are independent processes.

For an extended review of ion channel function see (Aidley, 1996; Hille, 2001; Sperelakis, 2001).

1.3 BK CHANNELS

The BK channel is one of the most widely studied K^+ channels. It is activated by both membrane depolarization and increases in cytosolic Ca^{2+} (Marty, 1981; Pallotta, *et al.*, 1981) and is present in almost all organisms (mammals, fruit flies, bacteria, virus...). It is involved in many physiological processes but its main role in the human body is controlling neuronal excitability, secretion and smooth muscle tone.

1.3.1 BK CHANNEL DIVERSITY

The molecular diversity of the K^+ channel family is vastly greater than the rest of ion channel families.

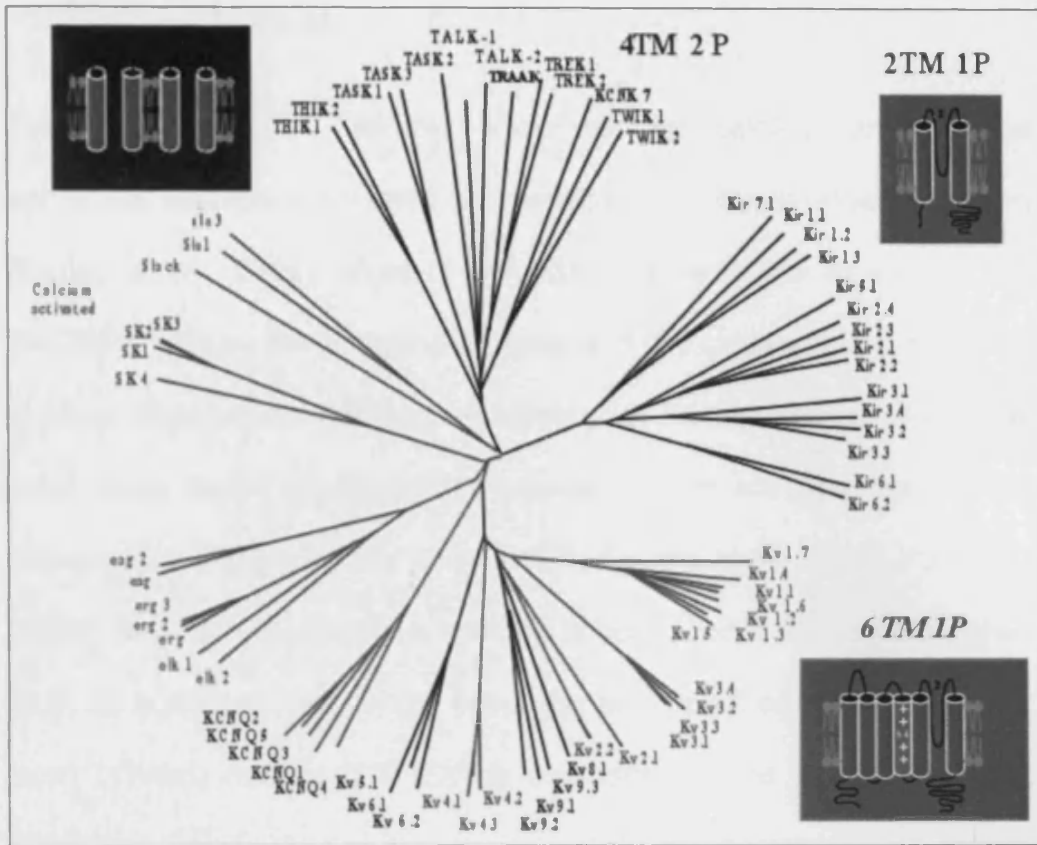


Fig 1.3. This diagram illustrates the great molecular diversity of the potassium channels (Institut de Pharmacologie Moléculaire et Cellulaire).

This enormous molecular diversity (Fig 1.3) is attributable to the combination of heteromultimeric formation, accessory subunits, alternative splicing, RNA editing and posttranslational modification (Coetzee *et al.*, 1999). In particular for BK channels, the majority of the research on their molecular diversity has been predominantly based on the alternative splicing sites and β subunit co-expression (Orio *et al.*, 2002).

1.3.1.1 *Splice Variants.*

The different splice variants show distinct calcium and voltage sensitivity, surface expression and sensitivity to protein phosphorylation (Curley *et al.*, 2004). Most of the splice variants are located in the COOH terminus. These splice variants are tissue dependent and their number depends on the tissue studied. For instance 9 splice variants have been found in the brain, whereas there are only two in the myometrium (Tseng-Crank *et al.*, 1994; Curley *et al.*, 2004; Yu *et al.*, 2006). Part of this alternative splicing is controlled by stress hormones such as corticosterone. In the presence of adrenal corticosterone, the exon (174bp) named “STREX” is expressed in rat (Xie & McCobb, 1998).

1.3.1.2. *β Subunit Modulation.*

The co-expression of BK channel four α subunits with the β -subunit alters their Ca^{2+} sensitivity, gating kinetics and pharmacological properties (Orio *et al.*, 2002). These aspects are explained in more detailed in section 1.4.

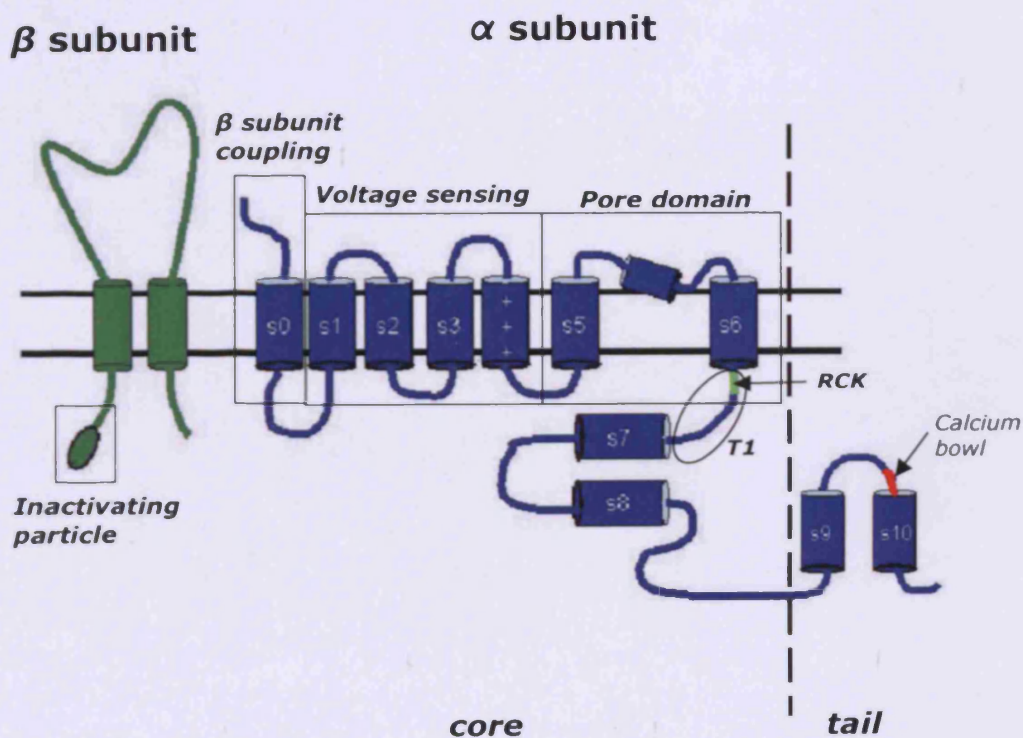
1.3.2 BK CHANNEL STRUCTURE

BK channels essentially belong to the family of 6 transmembrane K_v channels such as *Shaker* K^+ channel, but differ from them because BK channels contain an extra N-terminus transmembrane segment (Fig

1.4) which is exoplasmic and their characteristic tail at the C-terminus is much longer.

The minimum functional BK channel is formed by a tetramer of α subunits which shows Ca^{2+} and voltage dependence. However, the co-assembly of the α subunit with β subunits is needed to obtain a completely functional channel with all the relevant kinetics and pharmacological properties.

The following diagram schematically illustrates the structure of a single BK channel α subunit coupled with its β subunit:



T1: Tetramerization 1 domain
RCK: regulator of conductance for K^+

Figure 1.4: Diagram of the structure of the 7TM α subunit of the BK channel and the 2TM auxiliary β subunit (modified from Latorre & Brauchi, 2006).

The extensive research on the BK channel structure has clarified the role of specific domains:

Core: Initial studies divided the channel in two parts, namely core and tail according to the different Ca^{2+} sensitivity properties. The core includes the S0-S8 region (Wei *et al.*, 1994).

Tail: Domains S9-S10 were initially held responsible for Ca^{2+} affinity. Later studies have shown that a Ca^{2+} -binding site with lower affinity is contained near to the RCK domain (Jiang *et al.*, 2001).

β subunit coupling: The S0 segment is only found in BK channels. This extra transmembrane domain was thought to be required for the assembly of β subunits with the α subunit (Meera *et al.*, 1997) but recent studies have proven otherwise (Morrow *et al.*, 2006). Nevertheless, this exoplasmic N terminus domain is essential for some of the features produced by the $\beta 1$ subunit such as the conductance-voltage (G-V) shift and 17β -Estradiol sensitivity. Apart from this, it can also modulate the activity of the voltage sensor (Koval *et al.*, 2007).

β subunit inactivating particle: The NH_2 terminus of the $\beta 3$ subunit mediates the inactivation of BK channels. Its removal results in a β subunit lacking inactivation properties (Xia *et al.*, 1999).

Pore domain: The S5 and S6 segments form the pore domain which shows, by similarity with *Shaker* K channel, the features of potassium selectivity (Jan & Jan, 1997). There is also a great deal of evidence that

binding sites for channel-specific toxins are located in these transmembrane domains.

Voltage sensing: The S1, S2, S3 and S4 transmembrane segments function as part of the voltage sensor. The S4 segment possesses three positively charged residues (R365, R368, and R371), which contribute significantly to the channel gating (Seoh *et al.*, 1996). The S3 segment has been shown to be sufficient for the physical association between α - β 1 subunits (Jan & Jan, 1997; Diaz, 1998; Morrow *et al.*, 2006).

Calcium bowl: A motif rich in Asp and Glu which enormously decreases the Ca^{2+} sensitivity of the channel when altered by mutations. However, recent findings suggest that BK channels may exhibit the normal calcium sensitivity even after the deletion of the whole COOH-terminal region. Therefore, BK channels must have other Ca^{2+} binding sites (Moczydlowski, 2004).

RCK: A regulator of conductance for K^+ which contains binding sites for Ca^{2+} and Mg^{2+} (Jiang *et al.*, 2001).

T1 Domain: This “Tetramerization 1 domain” promotes the assembly of monomers into functional potassium channels. It includes the RCK domain (Shen *et al.*, 1993).

1.3.3. BK CHANNEL CHARACTERISTICS

In the table below the main features of BK channels may be observed.

CHARACTERISTICS OF THE BK CHANNELS

Description	Large conductance, Ca^{2+} and Voltage-activated potassium channel
Other names	KCNMA1, Slo (hSlo for human), BK channel, Maxi-K channel, KCa1.1
Molecular information	KCNMA1 Human: 1182aa, chr 10q22
Main associated subunits	BK-beta (4 different types: KCNMB1, KCNMB2, KCNMB3, KCNMB4)
Other associated proteins	β 2-adrenergic receptor and Ca^{2+} channels; Protein Kinases, Caveolin-1 and caveolae; Haem and Hemoxygenase-2, Synaptic proteins, Syntaxin 1A, β -Catenin, Cereblon, Microtubule-associated protein 1A and ankyrin-repeat family protein
Conductance (K^+/K^+)	~260 pS (between 200-300 pS)
Ion selectivity	$P_{\text{K}}/P_{\text{Na}} > 50$
Activation	Calcium and voltage
Activators	Intracellular calcium, NS1608, NS1619, BMS204352, DHS-1, CGS7181, estradiol, sulphatides, Mg^{2+}
Modulators	Phosphorylation modifies Ca^{2+} sensitivity. MaxiK activity is increased by inhibition of mitogen-activated protein kinases (MAPKs) such as stress-activated protein kinases (also known as p38s) and extracellular signal-regulated kinases (ERKs).
Blockers (ED_{50})	TEA (0.14mM), charybdotoxin (2.9nM), iberitoxin (1.7nM), paxilline (1.9nM), slotoxin (1.5nM), BmP09 Chinese scorpion toxin (27 nM)
Channel distribution	Ubiquitous, brain, skeletal muscle, smooth muscle, adrenal cortex, cochlear hair cells, odontoblast, pancreatic islet cells, colonic and kidney epithelium
Pharmacological significance	Channel openers may have applications in stroke, epilepsy, bladder over-reactivity, asthma, hypertension, gastric hypermotility and psychoses.

Table 1.1. (Wei, 2005; Chi & Qi, 2006; Li *et al.*, 2006; Lin *et al.*, 2006)

Apart from β subunits, the other BK channel partners mentioned above, mostly identified by co-immunoprecipitation or immunolabelling techniques, are: β_2 -adrenergic receptor and Ca^{2+} channels (L-type, P/Q-type, N-Type and TRPC1) (Berkefeld *et al.*, 2006; Kwan *et al.*, 2009); protein kinases (protein kinase A, focal adhesion kinase, proline-rich tyrosine kinase 2, src tyrosine kinase), caveolin-1 and caveolae; haem and hemoxygenase-2 and synaptic proteins and other partners from brain (syntaxin 1A, β -catenin, cereblon, microtubule-associated protein 1A and ankyrin-repeat family protein). Particularly significant it is the coupling of BK and calcium channels in the central nervous system which may well control transmitter release (Lu *et al.*, 2006). How these complex and diverse partnerships with the BK channel regulate its properties and phenotype is in most cases unclear. Particular attention to the co-assembly of Ca^{2+} channels will be paid for the purpose of this thesis.

1.3.4. OTHER BK CHANNELS

BK channels are characterised by a large single channel conductance and their activation by voltage and other cytoplasmic factors such as Ca^{2+} , pH or phosphorylation. In this context it is worth mentioning that apart from hSlo1 (KCNMA1) there are other BK channels which fit this description. Nonetheless, they differ in conductance, pharmacological properties and protein sequences. Their main aspects are summarised in the table below:

Channel	Characteristics of other BK channels
Slo2.1	<p>Human Gene: KCNT2</p> <p>Alternative names: Slick, K_{Na}, $KCa4.2$</p> <p>Conductance (K^+/K^+): 60-140 pS</p> <p>Voltage-dependence: Low.</p> <p>Blockers: Intracellular ATP, quinidine, Ba^{2+}.</p> <p>Modulators: Na^+ and Cl^-, negatively modulated by G-protein-coupled receptors (GPCRs).</p> <p>Channel distribution: Mainly in the brain.</p> <p>Structure: Lack of S0 TM domain, absence of positive charges in S4, some negative charges in the Ca^{2+} bowl changed to positive.</p>
Slo2.2	<p>Human Gene: KCNT1</p> <p>Alternative names: Slack, K_{Na}, $KCa4.1$</p> <p>Conductance (K^+/K^+): 100-180 pS</p> <p>Voltage-dependence: Low.</p> <p>Modulators: Na^+ and Cl^-, positively modulated by G-protein-coupled receptors (GPCRs).</p> <p>Channel distribution: Mainly in the brain.</p> <p>Structure: Lack of S0 TM domain, absence of positive charges in S4, some negative charges in the Ca^{2+} bowl changed to positive.</p>
Slo3	<p>Human Gene: KCNU1</p> <p>Alternative names: K large-conductance pH sensitive channel, $KCa5.1$</p> <p>Conductance (K^+/K^+): 70-100 pS</p> <p>Voltage-dependence: Marked.</p> <p>Modulators: High dependence of intracellular pH.</p> <p>Channel distribution: Only spermatocytes.</p> <p>Structure: Lack of the Ca^{2+} bowl, high similarity to Slo1</p>
Table 1.2. (Salkoff <i>et al.</i> , 2006)	

To date several heteromultimeric complexes of K_v channels have been found (Patel *et al.*, 1997). Similarly the formation of heteromultimeric complex of different Slo channels has been suggested, although there is no direct evidence. This possibility may well account for part of the molecular and pharmacology differences shown by BK channels in diverse cell types and should be taken into consideration when channel properties are studied.

BK channels interact with several cellular partners (see Table 1.1). The auxiliary β subunits are considered as the main modulators of BK channel activity and pharmacology.

1.4. β SUBUNITS: THEIR IMPORTANCE

The co-expression of BK channel 4 alpha subunits with the β subunits alters their Ca^{2+} sensitivity, gating kinetics and pharmacological properties. At present, four different β subunits have been identified each of which show distinct modulation properties. For instance, the $\beta 1$ increases the stability of the open states whereas $\beta 2$ subunit produces inactivating currents (Orio *et al.*, 2002).

1.4.1. *Specific features of each β subunit.*

Probably the most noteworthy difference amongst β subunits is their high tissue specificity. In the table below (Table 1.3) we can see a rough outline of this fact:

The symbol (-----) indicates that the subunit is expressed at very low level in that specific tissue or is not expressed at all. Different tissues express different subunit genes. The figures were calculated dividing gene expression in a specific tissue by the total gene expression of all tissues evaluated.

Expression of BK α and β subunits in different tissues

Normalized Gene Expression (%)					
Tissue	KCNMA1	KCNMB1	KCNMB2	KCNMB3	KCNMB4
Blood	0.90	8.71	-----	2.45	2.56
bone:	4.96	-----	-----	2.24	2.35
brain:	7.22	0.63	2.97	1.07	10.43
colon:	1.02	4.93	3.86	4.16	10.17
Eye	0.95	1.53	1.20	2.57	6.29
Heart	1.08	-----	4.09	2.93	3.07
kidney:	3.52	1.70	6.65	3.81	5.00
lung	2.03		8.35	2.49	2.62
lymph node	0.74	-----	-----	11.09	9.51
muscle:	8.16	2.19	5.14	1.23	2.58
Ovary	0.59	-----	13.40	-----	-----
Pancreas	3.89	-----	9.36	-----	-----
Prostate:	2.12	6.14	1.60	1.15	7.23
spleen:	8.46	-----	10.65	7.64	-----
Stomach	-----	2.78	-----	1.56	-----
uterus:	8.21	16.75	-----	2.57	-----
vascular:	6.59	21.19	-----	5.95	12.48

Table 1.3. The table shows the main tissues expressing the different BK channel subunits and their level of normalized gene expression for that tissue. Note that figures are calculated dividing gene expression in a specific tissue by total gene expression of all tissues evaluated (Rebhan, *et al.*, 1997; GeneCards encyclopedia, 2008)

Although the normalization was made individually for each subunit, these data suggest that each tissue needs a BK channel with a precise range of properties defined by distinct assembly patterns.

More evidence to support this general fact is reported by Rhodes (Rhodes *et al.*, 1996) revealing that the K_v channel α/β complex has a different distribution and expression depending on the tissue. In this study, it was reported that the expression level of $K_v\beta 2$ in the rat brain is twice that of $K_v\beta 1$. Furthermore, the expression of $K_v\beta 1$ requires the presence of $K_v\beta 2$ while $K_v\beta 2$ may be expressed individually.

The different effects on channel activity mediated by each subunit are as follows:

$\beta 1$ SUBUNIT (KCNMB1): This is by far the most studied β subunit.

These are some of its features:

Channel Modulation: Modulates Ca^{2+} sensitivity and affinity for CTX and IbTX, increases open probability (P_o), especially at high Ca^{2+} ($1\mu M$) and enhances oxidative regulation (Santarelli *et al.*, 2004).

Kinetics: slows down the activation and deactivation kinetics.

Pharmacology: required for binding of the opener dehydrosoyasaponin (DHS-1) and for external binding of the agonist hormone 17β -Oestradiol

Coupling: $\beta 1$ subunit intervenes in the regulation of coupling between Ca^{2+} transients and BK channels by protein kinase C (Hagen *et al.*, 2003).

Disorders: Protects against hypertension and its absence provokes an increase in arterial tone and blood pressure (Fernandez-Fernandez *et al.*, 2004; Ghatta *et al.*, 2005).

Surface expression: regulates BK surface expression levels (Toro *et al.*, 2006).

β2 SUBUNIT (KCNMB2):

Channel Modulation: confers low affinity for CTX and produces inactivation currents thanks to a peptide sequence in NH₂ terminal domain. In absence of this peptide, it exhibits the same properties as β1.

Surface expression: regulates BK surface expression levels (Zarei, 2005).

β3 SUBUNIT (KCNMB3):

Channel Modulation: partially inactivates or slightly decreases the activation time of the channel.

Splice variants: 4 different isoforms have been reported, each one conferring different inactivation properties. Some of them show inactivation kinetics similar to the β2 subunit.

β4 SUBUNIT (KCNMB4): highly expressed in the brain.

Channel Modulation: decreases the apparent Ca²⁺ sensitivity, confers resistance to CTX and IbTX (Meera *et al.*, 2000).

Kinetics: slows down channel activation and accelerates its deactivating effect.

Disorders: implicated in epilepsy (Brenner *et al.*, 2005).

A more detailed description of all these aspects may be found in (Orio *et al.*, 2002).

The role of β subunits as promoters of cell surface expression of the channel has been investigated in more detail in the *shaker* K_v channel which shares a resemblance to BK in many aspects. In this channel β subunits increase α subunit expression and stability (Sutherland *et al.*, 1999). In this case the β subunit behaves as a chaperone-like protein and this is probably one of its fundamental roles. The α/β subunit interaction occurs very rapidly via the cytoplasmic N-terminus of the α subunit (note that this N terminus is not cytosolic in BK channels and may interact differently with the β subunit). Additionally, it has been suggested that electrical activity may be caused by a failure of many of the α subunits to reach the cell surface and that β subunit dysfunction may lead to seizure activity or other neuropathological states in mammals (Nakahira *et al.*, 1996). Unexpectedly, the mechanisms of surface expression of BK channels show a difference among species. During pregnancy, reduced channel expression in rats arises due to diminished transcription, whereas in mice is produced by altering the subunit traffic to the surface (Mansoureh *et al.*, 2003). Furthermore, some highly evolved organisms such as *Drosophila melanogaster* lack β subunits. This may be because the fruit fly possesses a more efficient α subunit than their mammalian counterpart (Nagaya, 1997). All this evidence suggests that β subunits may play a significant role in the adaptation and evolution of animals. Indeed, the $\beta 1$ and $\beta 2$ subunits of

the BK channel are believed to take part in the physiological adaptations to hypoxia since their mechanisms of expression are altered by this condition (Hartness *et al.*, 2003; Del Toro, 2005; Navarro-Antolin, 2005).

Interestingly, in addition to their chaperone activity, β subunits have been reported to behave as kinases as well as being a modulator subunit of the K^+ voltage-gated sensory channel (Cai, 2005).

1.4.2. Stoichiometry.

β subunits form a complex with the α subunits. This complex was initially thought to exist as a 4:4 channel with a 1:1 stoichiometry (Fig. 1.5) (Garcia-Calvo *et al.*, 1994) but further studies have shown evidence of a reduced stoichiometry showing for instance 4 α subunits and only 3 β (Wang *et al.*, 2002).

The modulation of channel properties by β subunits, such as gating and inactivation, is functionally dependent on the average number of β subunits per channel (Manganas & Trimmer, 2000; Wang *et al.*, 2002). Furthermore, according to (Zeng *et al.*, 2003), the mechanism of blockage is related to the number of β subunits.

In chromaffin cells, it has been demonstrated that currents from native BK channels and those from recombinant α/β_2 share many properties but differ in others (the voltage-dependent activation is shifted to the right along the voltage axis) (Uebele *et al.*, 2000). Additionally,

variability in the average number of $\beta 2$ subunits was detected. These features can be explained by the channel having fewer $\beta 2$ subunits or mixtures of different β subunits.

In summary, β subunits contribute greatly to the phenotypic variability of BK channels in native tissues, modulate binding properties, calcium sensitivity, voltage-dependence, current shift, etc; may promote channel expression and stability; are involved in vasoregulation and in hypoxia and must act in concert to show some (if not all) of their properties (e.g. inactivation).

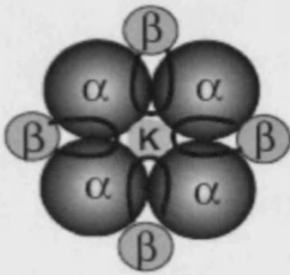


Fig 1.5 Diagram showing the co-assembly of α subunits and β subunits in a stoichiometry of 4:4, from (Toro L., 2005)

1.4.3. Channelopathies.

Channelopathies are by definition diseases connected with ion channel disorders. A large number of channelopathies have been discovered over the past decade highlighting the physiological relevance of ion channels.

Potassium channels are involved somehow with different diseases such as cardiac arrhythmias (long-QT syndrome type 1,2,5, Andersen's syndrome), neurological disorders (depression, genetic ataxia, episodic ataxia with myokymia, some forms of epilepsy), neurodegenerative diseases (Huntington's, Parkinson, Alzheimer's), vision disorders (total colour-blindness), renal disorders (Antenatal variant of Bartter syndrome), endocrine disorders (hypersinsulinemic hypoglycaemia of infancy, type II diabetes) and periodic paralysis (Shieh *et al.*, 2000; Hubner & Jentsch, 2002; Cajal Institute Neuroscience Research Centre, 2005; Heurteaux *et al.*, 2006; Waters *et al.*, 2006).

BK Channels, in particular, are directly involved in several physiological processes and disorders: the mechanism of analgesia, the olfactory system, hearing loss, innate immunity, pregnancy, development, coronary artery disease and senescence, acute ischemic stroke, genetic hypertension, autism, urinary system disorders (Type II Bartter's syndrome, incontinence), erectile dysfunction, schizophrenia, generalized epilepsy and paroxysmal dyskinesia. (Dray & Urban, 1996; Gribkoff, 2001; Marijic, 2001; Clapp & Jabr, 2003; Eghbali *et al.*, 2003; Ahluwalia *et al.*, 2004; Meredith *et al.*, 2004; Ruttiger, 2004; Du, 2005; Werner *et al.*, 2005; Bailey *et al.*, 2006; Laumonnier *et al.*, 2006; Lin *et al.*, 2006; Zhang *et al.*, 2006). BK channels are also thought to be involved in cancer progression since there is data showing an over-expression of BK in cancer cell lines and inhibition of apoptosis with channel blockers (Bronstein-Sitton, 2003; Bauer, 2005). In some cases

it is difficult to say whether the alterations in the ion channels are the cause of the disease or the consequence. Nevertheless, the existence of a close relationship between these factors and BK channels is undeniable.

Recently, two models of BK channel knockout mice have been developed, one with no α -subunit ($\alpha^{-/-}$) and another with no $\beta 1$ subunit ($\beta 1^{-/-}$). The ($\alpha^{-/-}$) shows hearing dysfunction and a cerebellar motor deficit whereas ($\beta 1^{-/-}$) exhibits bowel/colon dysfunction and a decrease of K^{+} secretion. Interestingly, ($\beta 1^{-/-}$) mice have a higher vascular arterial tone and blood pressure than that observed in ($\alpha^{-/-}$) (Ghatta *et al.*, 2005). This fact highlights the key role of β subunit in some of the previously mentioned diseases. For instance, apart from controlling the vascular tone, it is thought that the $\beta 1$ subunit protects against hypertension and is involved in the complications of diabetes, and that $\beta 4$ prevents epilepsy (Fernandez-Fernandez *et al.*, 2004; Brenner *et al.*, 2005; McGahon *et al.*, 2007).

All this evidence stresses the major importance of ion channel research as well as the necessity of finding new techniques to facilitate the study, screening and resolution of ion channel disorders.

1.5 BIOLUMINESCENCE

Bioluminescence is the emission of light produced by a chemical reaction within an organism. This term has currently been extended to

the test-tube biochemical systems derived from such organisms although a more appropriate word would be chemiluminescence because no living organism is involved. In this study we follow this current tendency and will refer to this phenomenon as bioluminescence.

In nature, a wide range of organisms produce bioluminescence such as marine animals (jellyfish, octopus, aristotomias...), insects (fireflies, beetles), worms, bacteria, mushrooms/fungi, etc (Campbell, 1988) for a variety of purposes, such as defence, feeding, breeding, etc. The spectrum of the light depends on the organism and goes from cyan, through blue, green, orange to red.

Bioluminescence represents an extremely sensitive method for determining the concentration of specific ions and molecules and plays a key role in analytical biochemistry and molecular biology (Campbell, 1988). The applications of bioluminescence reach all areas such as medicine (non-invasive imaging), industry (food processing, gas detection, measurement of light emissions...), environment (detection of toxicity levels in water, monitoring of coastal currents, etc), society (cosmetics glowing birthday cards, etc) (Campbell, 1989). In particular, aequorin has been used extensively specially for the detection of calcium concentrations in vivo and as a label in immunoassays.

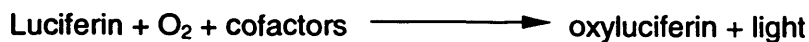
1.5.1. Aequorin.

Aequorin from *Aequorea victoria* jellyfish was the first bioluminescent protein to be isolated by Dr Shimomura in the early 1960s (Shimomura *et al.*, 1963) opening a huge new area of research focused on cell imaging *in vivo*. Since its discovery, aequorin has been widely used to monitor intracellular Ca^{2+} (Ridgway & Ashley, 1967; Cobbold & Lee, 1991). Initially, microinjection was the main method of choice to load the photoprotein into the tissues. The subsequent cloning of the aequorin sequence (Inouye *et al.*, 1985) allowed the use of homogenous aequorin and new methods to introduce the protein into the cells (i.e. cell transfection). Thanks to the constant advances in molecular biology and microscopy techniques, luminescent probes have become an every-day analysis and screening technique.

1.5.1.1 Mechanism of light emission in aequorin.

Aequorin is composed of two distinct units, apoaequorin, with an approximate molecular weight of 22 kDa and the prosthetic group coelenterazine (MW 472 kDa), a molecule belonging to the luciferin family. Luciferin is the chemical substance present in the cells of bioluminescent organisms that emits light when oxidized under the catalytic effects of luciferase and in the presence of molecular oxygen and certain cofactors like ATP or Ca^{2+} (Fig 1.6, A) (Campbell, 1988).

A



B

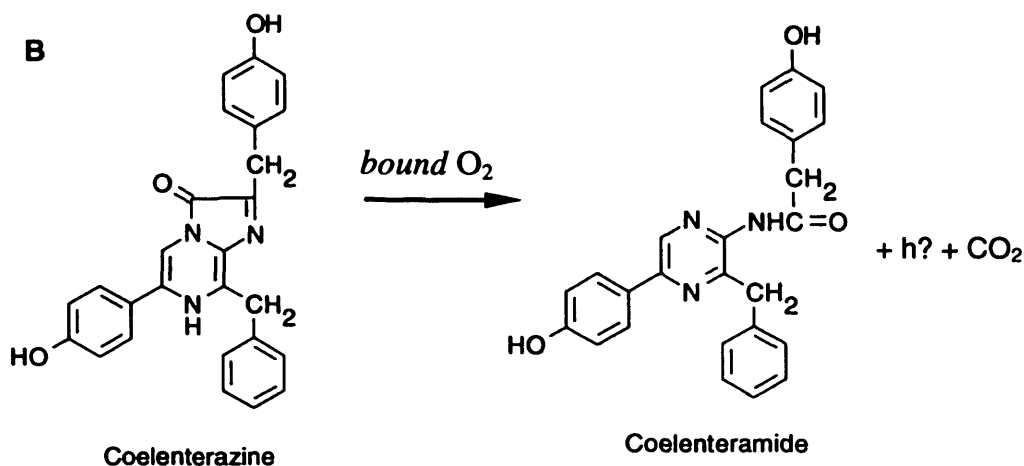


Fig 1.6. (A) The basic chemical reaction that produces bioluminescence (Campbell, 2003). (B) Chemical reaction producing aequorin light emission.

The mechanism of aequorin is as follows: the two components of aequorin form spontaneously the functional protein in the presence of oxygen; then if Ca²⁺ is added, the protein undergoes a conformational change and converts through oxidation its prosthetic group, coelenterazine, into excited coelenteramide and CO₂ (Campbell, 1988). The last step is the relaxation of the excited coelenteramide to the ground state emitting blue light of wavelength of 469 nm (Fig. 1.6 B). Once aequorin is triggered, it can no longer emit light. However, it can be reconstituted into the active photoprotein by the addition of

coelenterazine in the presence of oxygen (Shimomura & Johnson, 1975).

Coelenterazine is a hydrophobic chemical compound, cell permeable and commercially available which allows the reconstitution of apoaequorin both in free solution or inside intact cells (Inouye *et al.*, 1986). A number of coelenterazine analogues have been synthesised and used to reconstitute apoaequorin generating a range of semisynthetic aequorins with different reconstitution rates and Ca^{2+} sensitivities (Shimomura *et al.*, 1993). Aequorin has been also engineered using direct mutagenesis creating new photoproteins with a reduced affinity for Ca^{2+} . This has allowed monitoring of high Ca^{2+} compartments such as ER or mitochondria.

1.5.1.2. Structure of aequorin.

The crystal structure of aequorin (Fig. 1.7) has been elucidated recently showing that it is a dimer (Head *et al.*, 2000). The protein scaffold consists of four helix-loop-helix domains (EF-hands), three of which can bind calcium. Two EF-hands (I & III) exhibited a high affinity for Ca^{2+} whereas the affinity of the third (IV) was 20 times lower (Toma *et al.*, 2005). This is consistent with previous reports showing that between 2 (Shimomura, 1995) and 2.5 (Allen *et al.*, 1977) Ca^{2+} ions are required to trigger the luminescence reaction of aequorin. These domains create a central hydrophobic binding cavity for coelenterazine. Both oxygen and coelenterazine are bound within this cage. In this state, the protein shell

is completely closed not allowing solvent access. The addition of calcium initiates a series of conformational changes in the protein that triggers the internal reaction resulting in light emission and the opening up of the ligand-binding site, releasing the oxyluciferin.

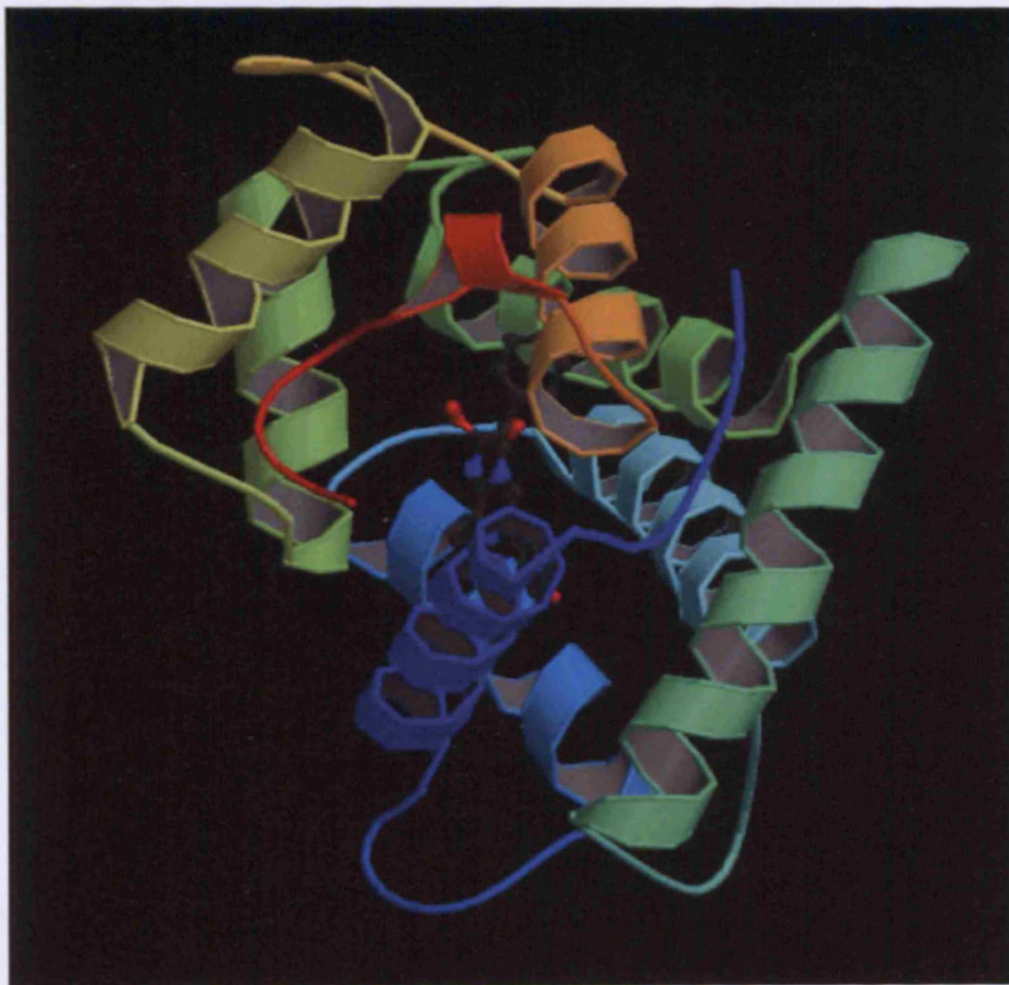


Fig 1.7 Diagram of the crystal structure of aequorin from PDB database (Access number 1EJ3).

1.5.1.3. Converting aequorin light emission into calcium.

The binding of Ca^{2+} ions to the aequorin protein follows a power law relationship of around 2.5 (Shimomura, 1995; Allen *et al.*, 1977). This 2.5 power relationship between light emission and free calcium level entails that a doubling of the Ca^{2+} concentration can lead to a five fold increase in light output. Additionally, aequorin is consumed during this process causing a decrease in light emission while the Ca^{2+} concentration is still rising. The method used to calibrate aequorin takes into consideration both events using by means of two approaches. First the light signal is calibrated over a range of solutions containing different Ca^{2+} concentrations (Allen *et al.*, 1977; Woods *et al.*, 1987). Secondly the light output is corrected for photoprotein consumption by converting the light emission to rate constants, k (s^{-1}) (Campbell, 1988). The light emission of aequorin is obtained by incubating *in vitro* the photoprotein in a series of known Ca^{2+} concentrations. Subsequently, there are two procedures to calculate the rate constants, both of which account for aequorin consumption: rate of aequorin consumption (Campbell *et al.*, 1981) and fractional luminous intensity (L/L_{max}). In the first one the total counts in a specific time are divided by the total number of counts remaining, after the subtraction of background. Since the decay of the light emission is exponential, plotting $\log_e I$ (I = light intensity) versus time and calculating the slope of the plot gives the rate constant (Campbell, 1988). The second method uses the peak height (L) on addition of Ca^{2+} and the maximal peak height (L_{max}) at saturating

Ca^{2+} concentration to calculate the rate constant (L/L_{max}). The first method is considered to be more precise (for a detailed explanation, see Campbell, 1988). Therefore, the rate of aequorin consumption was the approach of choice in this thesis.

The concentrations of free Ca^{2+} ions within living cells are measured by monitoring the light emission during the length of the experiment and the remaining light signal at the end of the experiment. This is achieved by lysing the cells in a hyposmotic solution containing a high Ca^{2+} concentration. This methodology allows to effectively measure Ca^{2+} concentrations between 100 nM to 10 μM (Cobbold & Rink, 1987).

1.5.1.4. Aequorin as a Ca^{2+} reporter.

Aequorin has several advantages which make it ideal as a Ca^{2+} reporter. It has a high selectivity for free calcium, a wide dynamic range for measuring calcium (i.e. 0.1-100 μM Ca^{2+}), a very low background and excellent signal-noise ratio (Campbell, 1988). In addition, aequorin does not disturb the Ca^{2+} homeostasis of the cell, is relatively insensitive to changes in pH in the physiological range and exhibits an excellent stability during long-term recordings. Furthermore, aequorin light emission can be easily and inexpensively detected with a luminometer. On the minor side, it requires a substrate (coelenterazine), produces a low signal and does not allow single-cell imaging. Overall, the low cost, robustness and simplicity of bioluminescent probes make them the first choice in high-throughout screening and research kits.

The use of aequorin to detect localised Ca^{2+} concentrations is probably one of its major advantages. Since the isolation and cloning of its DNA sequence (Inouye *et al.*, 1985), aequorin constructs have been used to monitor local Ca^{2+} concentrations within organelles including the nucleus (Badminton *et al.*, 1995), the endoplasmic reticulum (Kendall *et al.*, 1992) and the mitochondria (Rizzuto *et al.*, 1992). Additionally, it has been also employed to detect Ca^{2+} signal near to various proteins such as adenyl cyclase (Nakahashi *et al.*, 1997) and connexins (George *et al.*, 1998).

The advantages and disadvantages of aequorin in comparison to other techniques are further discussed in the next section.

1.6. MEASURING INTRACELLULAR CALCIUM

The methods used to monitor intracellular Ca^{2+} fall into two main categories: optical techniques and non-optical techniques, depending whether they use light emission to detect Ca^{2+} signals or a different approach such as variations in electrical properties. In this section the most prevalent techniques to monitor Ca^{2+} are discussed with a special focus on their advantages and disadvantages.

1.6.1. Optical Techniques.

1.6.1.1. Fluorescence indicators.

The use of fura-2 and its relatives to monitor cellular Ca^{2+} have greatly expanded in the last 20 years. The prime advantage of fluorescent indicators is the ease with which these dyes can be introduced into cells. Apart from their convenience, they also exhibit other advantages such as high Ca^{2+} affinity, fast kinetics and a wide dynamic range (Tsien, 1980; Grynkiewicz *et al.*, 1985). They also allow Ca^{2+} imaging at a single-cell level due to their strong fluorescent signal.

On the other hand, the rapid adoption of fluorescent indicators, and the experience gained in using them also quickly revealed several problems associated with their use such as leakage, compartmentalization and unwanted binding to cellular constituents (Roe *et al.*, 1990; Haugland, 1993). The addition of AM esters turns the fluorescent indicators into membrane-permeable entities gaining access to the interior of the cells. Nevertheless, this is not a selective process and part of the dye will be retained in other intracellular compartments such as ER, mitochondria and nucleus (Putney, 2000). Since many Ca^{2+} processes are coupled to these organelles, it is difficult to determine whether these compartments are involved in the Ca^{2+} transients detected. Furthermore, the hydrolysis of the AM esters results in the generation of byproducts which may be potentially cytotoxic or interfere with the Ca^{2+} pathways. Dye leakage mainly due to anion transport proteins is an additional problem.

Intracellular dye binding to immobile proteins hinders drastically its diffusion and may alter its natural properties such as Ca^{2+} affinity or light emission (Harkins *et al.*, 1993). Another potential problem is the fact that they bind Ca^{2+} effectively and may act as a Ca^{2+} buffers, especially at high concentrations (McFadzean & Brownlee, 1995). Several techniques and methods may be employed to reduce these problems including dye loading by microinjection or at lower temperature; the use of anion protein transport inhibitors; the use of dextrans instead of AM esters and quantification of dye extrusion. All these factors introduce intrinsic inaccuracies which might well account for the discrepancies observed between diverse studies, in particular when different fluorescent dyes have been used (Alonso *et al.*, 2003).

These are the generic problems associated with the use of fluorescent dyes. However, there are two additional drawbacks of particular importance. Firstly, it has been shown that fluorescent dyes such as Fura-2 may mask or even antagonise Ca^{2+} release from the ER (Alonso *et al.*, 2003). Secondly, Ca^{2+} effectors such as caffeine have been reported to interact directly with several commonly used fluorescent dyes such as indo-1 (Donoso *et al.*, 1994), mag-fura-2, magnesium green, fura-2 and fluo-3 (Muschol *et al.*, 1999) largely modifying their intrinsic properties (absorbance or fluorescence spectra, wavelength, quantum yield and kinetics). Specific strategies for each dye had to be used to eliminate the resulting artifacts. These two effects could seriously distort the physiological measurements of specific Ca^{2+}

responses. Consequently, the study of particular Ca^{2+} signals may require careful assessment of the potential interactions of the fluorescent dye used with the Ca^{2+} response and also the effects of every single agonist employed on the fluorescent properties of the dye. Moreover, if the elicited Ca^{2+} signals depend on which fluorescent dye has been employed, this then seriously limits the comparison of results obtained from different groups. This greatly compromises the reliability of these dyes to monitor Ca^{2+} responses.

In conclusion, although in many cases the use of fluorescent dyes is quick, easy, fairly reproducible and cause no significant changes in the Ca^{2+} response, special care has to be taken when using specific agonists and comparing data detected using different dyes.

1.6.1.2. GFP-based Ca^{2+} indicators.

These indicators named chameleons were initially designed by Tsien and co-workers (Miyawaki *et al.*, 1997; Tsien, 1998). They consist of tandem fusions of a blue- or cyan- emitting mutant of the green fluorescent protein (GFP) and calmodulin Ca^{2+} -binding site. When Ca^{2+} binds, there are changes on the conformation of the complex, resulting in an increase in FRET. Changes in the Ca^{2+} can be determined by the variation of light emission. They provide a reasonable range of detection (50 nM – 1 μM), do not require specific co-factors, their kinetics are independent of the concentration of the indicators and can be expressed in intracellular compartments (Miyawaki *et al.*, 1999;

Takahashi *et al.*, 1999). On the minus side, their limited Ca sensitivity may miss large Ca^{2+} transients ($> 1 \mu\text{M}$), the fluorescence of GFP is partially pH sensitive, In contrast, and more importantly GFP has been proven to be cytotoxic in living cells as well as to disrupt cell processes and embryo development (Liu *et al.*, 1999; Agbulut *et al.*, 2006; Cheung *et al.*, 2006).

1.6.1.3. Aequorin.

The advantages of aequorin are a high selectivity for free calcium (Baker, 1972; Cobbold & Rink, 1987; Campbell, 1988), a wide dynamic range for measuring calcium (i.e. 50 nm – 100 μM Ca^{2+}), high signal to noise ratio, expression and retention in different intracellular compartments (mitochondria, ER, plasma membrane, cytoplasm...), can be stably expressed in mammalian cells and has been shown to be safe and well tolerated by cells (Cobbold & Lee, 1991). Aequorin also lacks the undesirable side-effects encountered with fluorescent probes such as buffering capacity, autofluorescence and photo-induced cytotoxicity when exposed to excitation light (Miller *et al.*, 1994). Fluorescent dyes are typically loaded at concentrations of 10-50 μM causing the detrimental Ca^{2+} buffering effect. In contrast, only moderate levels of aequorin expression (i.e. $<1 \mu\text{M}$) are required to obtain reliable Ca^{2+} measurements because of its excellent signal to noise ratio. The low buffering effect together with its wide dynamic range makes aequorin the ideal tool to accurately quantify the large Ca^{2+} transients

occurring within the cells. Since oxidation of coelenterazine does not depend on any optical excitation, aequorin does not display the problems associated with fluorescent excitation such as photo-induced cytotoxicity or autofluorescence.

A crucial advantage of aequorin is its ability to detect local Ca^{2+} signals. As previously mentioned in section 1.6.1.2., fluorescent dyes do not always faithfully report rapid changes in Ca^{2+} seen in some cells and may miss highly localised Ca^{2+} transients. In contrast, aequorin has been used to accurately monitor local Ca^{2+} concentrations near to specific proteins (Nakahashi *et al.*, 1997; George *et al.*, 1998). To investigate the effect of diverse events on local Ca^{2+} concentration, aequorin is definitely a superior tool.

Its disadvantages are the requirement of coelenterazine to reconstitute functional aequorin and the low intensity of the light emission. Regarding the use of coelenterazine it must be said that it is hydrophobic and can permeate almost every cell type, including bacteria, and cellular organelles (Xu *et al.*, 1999). The low signal is probably the major drawback because it does not allow single-cell imaging at least is highly overexpressed. Therefore other supporting technique has to be used to assess its localisation within the cell.

1.6.2. Non-optical techniques.

Two main non-optical techniques have been mainly used: Ca^{2+} -selective electrodes and electrophysiology.

1.6.2.1. Ca^{2+} -selective electrodes.

The Ca^{2+} -selective electrodes use a ligand contained in a liquid lipophilic membrane which separates two aqueous compartments. This ligand selectively extract ions from the solutions and transports them across the membrane generating an electric current. An unknown Ca^{2+} concentration can be calculated using the potential difference and a reference concentration. They exhibit a wider dynamic range (from 1 nM to 100 mM) , allow long term recordings, organelles are excluded, it is almost unaffected by ions or proteins in the intracellular milieu and does not interfere with intracellular Ca^{2+} . However, they require a great deal of manipulative skills, their response time is not very fast (~0.5 - 1 s), electrical interference may occur and some lipophilic drugs can affect their performance (Campbell, 1983; Voipio *et al.*, 1994; Takahashi *et al.*, 1999).

1.6.2.2. Electrophysiology.

The channel activity of membrane-bound Ca^{2+} -dependent ion channels can be used to estimate Ca^{2+} concentrations in the vicinity of the channel. Single channel activity of Ca^{2+} -activated Cl^- channels (Miledi & Parker, 1984; Parker & Yao, 1994) and Ca^{2+} -activated K^+ channels

(Barrett et al., 1982) have been used for this purpose. This allows fast resolution (ms) and long term recordings if a stable seal is obtained. However, it is an invasive technique, imposes changes on the natural membrane potential and can be only be applied to cells where GΩ seals can be achieved. In addition, their calibration strongly relies in excised patches in which many cellular components may be missing or the effects of cellular processes (i.e. phosphorylation) could be different resulting in discrepancies on channel activation between cell-attached and excised patches. Additionally, the use of mathematical models based on different assumptions has resulted on values of Ca^{2+} concentrations ranging from 0.3 μM (Franciolini *et al.*, 2001) to 150 μM (ZhuGe *et al.*, 2000).

Additional information on the different methods to measure Ca^{2+} can be found in Baker, 1972; Campbell, 1983 and Takahashi, 1999.

1.6.3. Use of luminescence techniques in ion channels.

Most studies in ion channels have been performed with fluorescent proteins instead of bioluminescent ones. The first reports using fluorescent fusion proteins to study ion channels (Marshall et al., 1995) go back more than 10 years ago. Since then, there has been a great deal of diverse methodologies used to study different channels. Among them, some of the most significant for the purpose of this research have been the GFP-Shaker fusion protein used to measure voltage-gated conformational changes (Siegel & Isacoff, 1997). However, in spite of

showing certain voltage dependence, the wide discrepancy between the kinetics of fluorescence and voltage-activated processes does not support the use of this probe as a consistent instrument for research. A similar approach was more successfully used in a sodium channel obtaining a fusion protein with faster kinetics in response to voltage changes. This method proved that GFP joined to a mobile part of a channel provides fluorescence variations as a result of conformational changes (Ataka & Pieribone, 2002). Sheridan and collaborators (Sheridan *et al.*, 2002) suggested that the insertion of GFP in transmembrane domains might give a functional channel. Nevertheless, there is some evidence to indicate that this is unlikely to happen in BK channels (Giraldez *et al.*, 2005). Indeed many of their randomly engineered recombinant constructs at the C-terminus also resulted in diminished cell surface expression and/or different Ca^{2+} sensitivity. This indicates that the addition of tags to the BK channel should be avoided in order to resemble the native properties of the channel.

Resonance Energy Transfer techniques have been also used to study ion channels. Fluorescence Resonance Energy Transfer (FRET) was effectively employed to study the stoichiometry of a heteromeric complex K^+ channel and to estimate the distance between subunits (Kerschensteiner *et al.*, 2005). The bioluminescent equivalent, Bioluminescence Resonance Energy Transfer (BRET), has been successfully used to determine the conformational changes in the insulin receptor (Boutem *et al.*, 2001) and the interactions in assembly

complexes such as circadian clock proteins (Xu *et al.*, 1999) and G-protein-coupled receptors (Gales *et al.*, 2005). For a more detailed introduction see Piston *et al.* (2006); for an extensive review see Tsien (1998) and Miyawaki & Tsien (2000).

In this thesis the robust capability of aequorin to measure confined Ca^{2+} concentrations is used for the first time to report local Ca^{2+} signals in the vicinity of a BK channel.

1.7. AIMS OF THE THESIS

The overall aim of this work was to investigate the regulation *in situ* of calcium signals in the vicinity of the BK channel in living cells in order to determine whether the local calcium concentration is capable of independently controlling BK channel activation. This involved developing a novel recombinant protein by combining the auxiliary $\beta 2$ subunit and aequorin targeted near to the channel.

The strategy used to achieve this was:

1. To clone the $\beta 2$ subunit from MG63 cells and subsequently attach the aequorin sequence to the C-terminus using splicing by overlapping extension.
2. To demonstrate the functionality, properties (i.e. light emission) and correct targeting of the new protein.

3. To assess the optimal conditions for aequorin expression and calcium imaging in two different cell lines (MG63 and HEK293) using a luminometer and a photon imaging camera.
4. To investigate the BK channel microdomain and cytosolic calcium signalling in HEK293 cells in response to several agonists (ATP, histamine, carbachol, caffeine) and non-agonists (extracellular calcium, TEA, tetrandrine and cyclopiazonic acid) stimuli using a photon imaging camera.

CHAPTER 2

MATERIALS AND METHODS

2.1 MATERIALS

2.1.1. GENERAL REAGENTS

2.1.1.1. Chemicals.

General laboratory chemicals were AnalaR grade reagents and obtained from Sigma-Aldrich Company Ltd. (Poole, UK). All eukaryotic cell culture reagents were obtained from Gibco/Invitrogen (Paisley, UK). Coelenterazine was a kind gift from Dr Bruce Bryan (ProLume Inc, Beverly Hills, CA, USA).

2.1.1.2. Enzymes and molecular biology reagents.

Bacterial media components were from Oxoid (Hampshire, UK) and JM109 competent cells from Promega (Hampshire, UK). ImProm-II RT-System, GoTaq polymerase, T7 promoter primer and pTarget Mammalian Expression system were also purchased from Promega. BIO-X-ACT Short DNA polymerase, DNA markers and nucleotides were from Bioline (Bioline, UK). DNA-free, Proteinscript II T7 linked transcription/translation system and ABI Prism Big Dye Sequencing kit were obtained from Applied Biosystems/Ambion (Warrington, UK). QIAprep Spin Miniprep Kit and plasmid Maxi kits were from Qiagen. All the buffers (P1, P2, P3, PE and EB) used in these experiments were also provided by Qiagen. The transfection reagents, Lipofectamine 200, LTX and Plus, were from Invitrogen (Paisley, UK) and Eugene HD from Roche (Hertfordshire, UK).

2.1.2. GENERAL SOLUTIONS

Aequorin assay buffer: was used for measuring aequorin light emission in the home-built luminometer and contained 200 mM Tris-HCl, 0.5 mM EDTA, pH= 7.4.

Aequorin resuspension buffer: consisted of 20 mM Tris-HCl, 1 mM EDTA and 5 mM Dithiothreitol).

Buffer O: contained 10 mM Tris HCl, 500 mM NaCl, 1 mM EDTA, 5 mM β -mercaptoethanol and 0.1% gelatine adjusted to pH 7.5.

EDTA: a 0.5 M stock solution was made from ethylenediaminetetraacetic acid disodium dihydrate pH 7.5 and stored at room temperature (RT).

EGTA: a 0.1 M stock solution of ethyleneglycolbis-(β -aminoethyether)-N,N,N',N' tetraacetic acid at pH 7.5 and stored at -4°C.

KRH- Modified Krebs-Ringer-Hepes buffer: contained 120 mM NaCl, 4.8 mM KCl, 1.2 mM KH_2PO_4 , 1.2 mM MgSO_4 , 25 mM Hepes adjusted to pH 7.4. When stated, KRH was supplement with either 1.3 mM CaCl_2 or 1 mM EGTA.

LB medium: 10 g of tryptone, 5 g yeast extract and 10 g NaCl were dissolved in 1l sterile water. pH adjusted to 7 with NaOH and autoclaved.

LB plates with ampicillin: 15 g bactero agar were added to 1L LB medium, autoclaved, cooled at 50°C, then 100 µg/ml of ampicillin supplemented and ~25 ml poured into 85 mm Petri dishes.

LB plates with ampicillin/IPTG/X-Gal: As above with additional 0.5mM IPTG and 80 µg/ml X-Gal.

Lysis Buffer: was used to extract apoaeguorin from culture cells and consisted of 20 mM Tris HCl, 0.5 mM EDTA and 5 mM β-mercaptoethanol pH 7.4.

M9+B1 plates: M9 minimal medium plates containing thiamine are employed to obtain healthy competent bacteria ready for blue/white screening. 6 g Na₂HPO₄, 3 g KH₂PO₄, 0.5 g NaCl, 1 g NH₄Cl, and 15 g agar were added to 1 litre of deionised water, autoclaved, cooled at 50°C and subsequently 2 ml of MgSO₄ (1M), 0.1 of CaCl₂ (1M), 10ml of 20% glucose and 1 ml of Thiamine-HCl were added and ~25 ml poured into 85 mm Petri dishes.

SOC medium: filtered medium with pH=7 and the following compounds: tryptone (20 g/l), yeast extract (5 g/l), NaCl 10 mM, KCl (250 mM), MgCl₂-MgSO₄ (10 mM, 45% w/w) and glucose (20 mM).

TAE: was used for running agarose gels diluted from a 50X concentrated stock containing 141 g Tris base, 28.55 ml glacial acetic acid, 50 ml 0.5 M EDTA (pH 8.0) and double sterile water made up to 0.5L, pH 8.3.

TE: buffer employed for rehydrate primers containing 10 mM Tris HCl, 1mM EDTA and double sterile water up to 100ml at pH 8.

TFB1: transformation buffer needed to prepare competent bacteria. It contains 30 mM potassium acetate, 10 mM CaCl_2 , 50mM MnCl_2 , 100mM RbCl and 15% glycerol. pH was adjusted to 5.8 with acetic acid and the final solution filtered (0.2 μm).

TFB2: second transformation buffer for preparation of competent bacteria containing 10 mM MOPS, 75 mM CaCl_2 , 101 mM RbCl and 15% glycerol, with pH = 6.5 and filtered.

2.1.2.1. Physiological solutions.

Physiological solutions were used in patch-clamp experiments. Solutions were prepared under sterile conditions and filtered with a sterile 0.2 μm syringe filters (Whatman). Physiological saline solutions used:

Locke: 150 mM NaCl, 3 mM KCl, 2 mM MgCl_2 , 2 mM CaCl_2 , 10 mM HEPES and 10 mM glucose. pH=7.4 (adjusted with NaOH or HCl).

High K^+ : 5 mM NaCl, 140 mM KCl, 1 mM MgCl_2 , 1 mM CaCl_2 , 10 mM HEPES, 11 mM EGTA. pH=7.2 (adjusted with KOH).

2.2. MOLECULAR BIOLOGY TECHNIQUES

2.2.1. POLYMERASE CHAIN REACTION

The following reagents were pipetted into a thin-walled PCR reaction tube: 5 µl 5xGreen GoTaq Flexi buffer, 1.5 µl MgCl₂ (25 mM), 1 µl of each primer (10 µM), 5 µl dNTPs (5 mM), 0.25 µl GoTaq polymerase (5 U/µl) and nuclease-free water was added up to 25 µl. Finally, a thin layer of mineral oil (50 µl) was added to each tube to prevent evaporation. Thermal cycling was carried out in either a Perkin Elmer Thermo (adding Mineral Oil to prevent evaporation) or Uno-Thermoblock (with heated lid, Biometra). The PCR cycle program was a first step (94°C 1min); 30 cycles each consisting of denaturation (94°C 1min), annealing (58°C 1min), extension (72°C 2 min plus a 5 second extension per cycle); and a final step (72°C, 10min) to allow completion of DNA synthesis.

2.2.1.1. High-fidelity PCR.

High-fidelity PCR was performed using BIO-X-ACT Short DNA polymerase possessing proof-reading capability. This proof-reading activity improves the accuracy of the enzyme up to 7 times when compared with a standard Taq polymerase which consequently reduces the incidence of mutations arising from misincorporation errors such as base substitutions, frameshifts and nonsense mutations

The DNA substrate was amplified as follows: 2.5 µl 10X OptiBuffer, 2.4 µl MgCl₂ (50 mM), 2.5 µl dNTPs (10 mM), 1 µl BIO-X-ACT™ Short DNA polymerase (4 u/µl), 1 µl of each primer (10 µl), the template DNA (amounts and concentrations differ between experiments) and nuclease-free water up to 25 µl.

Thermal cycling consisted of a first step (95 °C, 5 min) followed by 30 cycles comprising 30 s at 95 °C, 45 s at 55 °C and 1 min at 68 °C and a final step of 68 °C for 5 min.

2.2.1.2. Primer design.

Primers were designed using Primer3 software (Rozen & Skaletsky, 2000) taking special attention to all parameters to avoid mismatching, different melting temperature of the primers and primer dimerization. Target sequences were obtained from National Center for Biotechnology Information (NCBI) database. Specificity was confirmed by BLAST analysis. Primers were purchased from Invitrogen.

The oligonucleotide primers were purchased dehydrated from Invitrogen, resuspended in ~0.5ml TE and stored at -20°C.

2.2.1.3. DNA quantification.

This process is employed to quantify the DNA concentration (plasmids, PCR products) and additionally to assess the purity of the DNA.

A 1:10 DNA/TE solution was dispensed into a sterile cuvette and absorbance measured at 260, 280, 230 and 320nm wavelengths in a

biophotometer. High quality samples show $A_{280/260}$ ratio ~1.7-1.9 (280 nm-DNA & 260 nm-RNA) whereas high measurements at 230 (for aromatic moieties) and 320 (particles in solution) indicate potential impurities due to poor efficiency of the purification process or use of unclean cuvettes. When a poor quality measurement was obtained, the purification process was repeated.

2.2.1.4. DNA sequencing.

DNA was sequenced using a ABI Prism Big Dye Terminator Cycle Sequencing Ready Reaction kit. PCR was performed using T7 Promoter Primer as a forward primer, a specific one as a reverse primer and a purified pTarget vector with the appropriate insert as a template (see Polymerase Chain Reaction in section 2.2.1). The product was run in 1% agarose gel (see agarose gel electrophoresis), the band cut and incubated overnight with 250 μ l of sterile water. To assess the amount of DNA in solution, samples of 1 μ l, 3 μ l and 5 μ l were run in another gel. The sequencing reaction was performed with 2 μ l Big Dye Terminator sequencing premix, 1 μ l Sequencing Buffer, 3.82 pm primer, the appropriate amount of DNA mixture, sterile water up to 10 μ l and 40 μ l mineral oil to avoid evaporation. As the Big Dye Terminator sequencing premix is light-sensitive the appropriate measures were taken to avoid light exposure. A PCR was carried out in a Perkin Elmer Thermal Cycler with cycle program as follows: (96°C-30s/50°C-15s/60°C-4m)x25 cycles. The reaction mixture was carefully isolated from the mineral oil, transferred into a 0.5 ml tube containing 2 μ l 3M

NaAc pH= 4.6 and 50 µl 95% Ethanol, vortexed and left to stand at room temperature for 15 min. Subsequently, the sample was centrifuged at 13000 rpm for 20 min, the supernatant removed, 250 µl of EtOH (70%) added to wash the pellet, latter vortexed and centrifuged for 5min. The pellet was given an additional wash in 250 µl of EtOH, then vortexed, centrifuged for another 5 min and supernatant mostly removed leaving 10 µl to avoid dehydration. All PCR sequencing was performed using ABI Prism 3100 Genetic Analyzer which uses a polymer electrophoresis system at the School of Medicine, Cardiff.

2.2.2. AGAROSE GEL ELECTROPHORESIS

Double stranded DNA fragments were separated by agarose gel electrophoresis, which allowed characterisation of DNA according to size.

A 2% agarose gel was made by dissolving electrophoresis grade agarose in 75ml of TAE buffer, boiling, cooling to room temperature, adding 2 µl of Ethidium Bromide, then poured the mixture into a mini-gel tray and allowed to setting. Agarose gels were placed in a Pharmacia electrophoresis chamber, submerged under 1x TAE buffer, each well loaded with 5 µl of sample to which have markers have been added. An extra well was loaded with Hyperladder II to assess the band size and semiqualitatively the amount of DNA. The gel was, as a general rule, run at 100 volts for 30 min, then transferred to a UV gel documentation system (Gel Doc. 1000, Bio-Rad), photographed, and fragment sizes compared to the 2 kb ladder.

2.2.3. RNA ISOLATION

The medium of a 25 cm² culture flask containing MG63 (70 passage) was removed; 2.5 ml of Trizol added and spread over the whole surface. The cell lysate was passed through a pipette several times. The solution centrifuged at 12000xg for 10 min at room temperature and then the supernatant was carefully removed using a Pasteur pipette. The aqueous phase containing the RNA was transferred to a fresh tube, 1.5 ml of isopropyl alcohol added in order to precipitate the RNA and incubated at room temperature for 10min. The supernatant was removed again and 2.5 ml of 75% ethanol was added to wash the RNA. The sample was vortexed and subsequently centrifuged at 12000xg for 5min more. The remaining supernatant was removed with a normal pipette and the pellet was dried by leaving it at room temperature a few minutes. Finally, 150 µl of RNase-free water were added and the sample was incubated overnight at -80°C to rehydrate the RNA.

2.2.3.1. DNase treatment.

A DNase treatment was performed to increase the purity of the RNA obtained. 0.5 µl 10xDNaseI Buffer and 1 µl DNase1 were added to a 50 µl RNA sample and mixed gently. The mixture was incubated at 37°C for 30min. The DNase inactivation reagent was vortexed vigorously to avoid the loss of the fluid from the interstitial spaces. Then 0.5 µl of DNase inactivation reagent were added, incubated for 2min more and

mixed each minute. After centrifugation at 10000xg for 2 min, the supernatant was transferred into a fresh tube and stored at -80°C.

2.2.3.2. RNA quantification.

The amount of RNA collected was quantified by placing 2 µl RNA/ 70 µl sterile water solution into a cuvette and measured by light absorbance in a spectrophotometer (ThermoSpectronic - Genesys 10 Series) at two distinct wavelengths (260 nm - RNA & 280 nm - DNA). Good samples show $A_{260/280}$ ratio < 1.6.

2.2.4. REVERSE TRANSCRIPTION PCR

An initial RNA target and Primer mixture was prepared using RNA (1 µg), random primers (0.5 µg/µl) and nuclease-free water up to 5ul, incubated at 70°C for 5 min and then incubated in ice for 5 min more.

Using the ImProm-II RT-System (Promega), a 15 µl mixture (4 µl 5X Reaction Buffer, 2.4 µl $MgCl_2$ (25 mM), 1 µl dNTPs (40 mM), 0.5 µl RNasin, 1ul Reverse Transcriptase) was vortexed gently and mixed together with the previous template-primer mixture. The RT-PCR was performed in a Perkin Elmer Thermal Cycler with cycle program 25°C – 5 min (annealing), 42°C - 60 min (extension) and 70°C - 15 min (Reverse Transcriptase heat inactivation). A negative control (no Reverse Transcriptase) was prepared and checked subsequently with a standard PCR.

2.2.5. TA CLONING INTO pTARGET VECTOR

2.2.5.1. *Ligation of DNA insert into pTarget.*

The ligation reaction consisted of 1 µl T4 DNA ligase Buffer, 60 ng pTarget Vector, 1 µl T4 DNA ligase, insert (3:1 ratio, see formula below) and deionised water up to 10 µl. Simultaneously, a positive and background control ligation reaction were performed. The mixtures were incubated for 3 hours at room temperature.

2.2.5.2. *Preparation of competent bacteria.*

This method, commonly known as the RbCl method, allows preparing great amounts of high efficiency *E.Coli* JM109 competent cells capable of being transformed with a foreign vector or DNA. One single colony was inoculated from a M9+B1 plate into 2 ml SOC media and incubated overnight at 37°C with shaking (225 rpm). The culture was diluted into 200 ml LB media supplemented with 20 mM MgSO₄ and incubated at 37°C until OD₆₀₀ reached 0.5. Cells were centrifuged at 4500 rpm for 5 min at 4°C, supernatant removed and resuspended in 80 ml ice cold TFB1 for 5min. Then cells were centrifuged once more at 4500 rpm for 5 min at 4°C, supernatant removed, resuspended in 8 ml ice cold TFB2 and were kept on ice for 45 min. Finally, 200 µl aliquots of the cell suspension were stored at -70°C where the loss of competency is minimal. The transformation efficiency (ability to acquire free DNA from their environment) assessed using Competent Cells Control DNA (Promega) was always over 10⁷.

2.2.5.3. Transformation of competent cells.

The transformation is the process that allows the insertion of a plasmid into the bacteria cells in order to obtain a large quantity of this plasmid.

Competent Cells were removed from -70°C, placed on ice for 5 minutes, gently mixed and 50 µl were added into chilled sterile 17×100 mm polypropylene culture tubes. The plasmid or ligation reaction (2µl) was dispensed onto the competent cells, incubated on ice for 20 min, heat shocked at 42°C for 50 s and then returned on ice for 2 min. Subsequently 450 µl of SOC medium were added and the mixture was incubated for 1.5 h at 37°C with shaking (150 rpm). A 100 µl aliquot of this mixture was spread onto LB/ampicillin/IPTG/X-Gal plates under sterile conditions. The plates were left at room temperature for 20 min to dry, incubated upside down overnight at 37°C and then stored in the refrigerator.

2.2.5.4. Screening transformant colonies for DNA insert.

The pTARGET Vector contains a coding sequence which allows blue/white recombinant screening. Among white colonies, 10 were picked and resuspended in 20 µl sterile water in a 96-well plate. From each solution 5 µl was resuspended into 100 µl of LB with carbenicillin and incubated at 37°C for 4 h. With the purpose of confirming the correct orientation and size of the insert, the remaining 15 µl of each plasmid-containing solution were incubated at 100°C for 10 min, cooled to room temperature and then 10 µl used as a template for a PCR screening, T7 Promoter Primer as a forward primer and a specific one

as a reverse primer. Among the samples with the appropriate size, 4 were selected to consequently perform purification of plasmid DNA. From 96-well plate samples (after 4 h incubation), the previously selected ones were inoculated into 5 ml of LB with carbenicillin and left growing overnight at 37 °C in a shaker incubator (220 rpm). Finally, an aliquot (500 µl) of this cell medium after incubation was mixed with 500 µl of sterile Glycerol and stored at -80°C for later use. The remaining 4 ml was employed for isolation of their plasmid.

2.2.6. ISOLATION OF PLASMID DNA

This procedure was performed using the QIAprep Spin Miniprep Kit, following the manufacturer's procedure with slight modifications.

A solution of LB medium with carbenicillin containing the plasmid of interest after overnight incubation (See section 2.1.6.4 Screening transformant colonies for DNA insert) was centrifuged at 3000 rpm for 10 min. The resultant pellet was resuspended in 250 µl of P1 buffer (50 mM Tris-HCl, pH 9.0, 10 mM EDTA, 100 µg/ml RNase A), transferred into a microcentrifuge tube and lysed with 250 µl of Buffer P2 (0.2 NaOH, 1% SDS) by inversion 6 times. 350 µl of Buffer N3 (3M KAc, pH 5.5) were added, mixed by inversion 6 times and centrifuged at 13000 rpm for 10 min. The consequent supernatant was carefully decanted and pipetted into a QIAprep spin column, centrifuged (13000 rpm – 1 min) and the flow-through discarded. The column was washed by adding 0.5 ml of Buffer PB to remove nuclease activity, centrifuged (13000 rpm – 1 min) and the flow-through discarded. The column was

then washed with 0.75 ml of Buffer PE, centrifuged (13000 rpm – 1 min), flow-through discarded and centrifuged (13000 rpm – 1 min) for a second time to remove any residual wash buffer. Finally the column was introduced in a 1.5 ml Eppendorf tube, 30 µl of Buffer EB (10 mM Tris-Cl, pH 8.5) added to the centre of the column to elute the plasmid cDNA, left to stand for 1min and centrifuged once more at 13000rpm for 1min. The final plasmid solution was stored at -20° C.

2.2.6.1. Isolation of large quantities of plasmid DNA.

Large-scale isolations of plasmid DNA were prepared using Qiagen plasmid Maxi kits.

A single colony from a selective plate was picked and inoculated a starter culture of 5ml LB medium containing ampicillin. After approximately 6 h incubation at 37°C with vigorous shaking, the starter culture was diluted 1/50 to 1/100 selective LB medium and grown overnight at 37°C with shaking (160 rpm). At this point, for low copy plasmids like pMMB66EH-AEQ (Watkins *et al.*, 1995), chloramphenicol which inhibits protein synthesis but not plasmid replication was added to a final concentration of 180 mg/l and incubated for another 4 h. The bacteria were then pelleted by centrifugation at 6000 x g for 15 min. After harvesting, Qiagen plasmid purification protocol was followed. The bacterial pellet was resuspended in 10 ml of P1 buffer, lysed with 10 ml of P2 buffer for 5 min at room temperature after gentle inversion. 10 ml of ice-cold P3 buffer were mixed by inversion 6 times followed by 20 min incubation on ice. The mixture was centrifuged at 20000 x g for 30

min at 4°C and the supernatant was further centrifuged at 20000 x g for 15 min at 4°C. After 10 ml of QBT buffer were used to equilibrate the Qiagen-tip 500, the supernatant was added. The column was then washed twice with 30 ml of QC buffer (1 M NaCl, 50 mM MOPS, pH=7.0, 15% (v/v) ethanol) and the plasmid DNA retained in the column eluted with 15 ml of QF buffer (1.25 M NaCl, 50 mM Tris-HCl, pH 8.5, 15% (v/v) ethanol). DNA was precipitated with the addition of 10.5 ml of isopropanol and centrifuged at 15000 x g for 30 min at 4°C. The DNA pellet was washed with 70% ethanol and centrifuged at 15000 x g for 10 min at 4°C, air-dried and resuspended in 200 µl of TE buffer.

2.2.7. PROTEIN EXPRESSION

2.2.7.1. *In vitro* Protein transcription/translation.

In vitro transcription/translation was performed using the Proteinscript II T7 linked transcription/translation system. This standard rabbit reticulocyte lysate system allows the synthesis in vitro of circular DNA with the T7 RNA polymerase promoter. Following the manufacturer's instructions, a mixture of 1 µl 5X Transcription mix, 1 µl of enzyme mix, 0.5 µg of plasmid DNA and nuclease-free water up to 5 µl was prepared, mixed by pipetting up and down, centrifuged briefly and incubated at 30°C for 60 min. The resultant solutions were either used immediately or stored at -20°C for future translation reactions.

The translation reactions were composed of 17.5 µl of Retic Lysate, 2 µl of unlabeled Methionine (500 µM), 1.25 µl of 20X Translation mix

and 3.25 μ l of nuclease-free water and store at -80°C until required. For the final reaction step, 1 μ l of the transcription reaction was added to the translation mixture, incubated at 30°C for 60 min and the product stored at -20°C for future analysis.

The *in vitro* transcription/translation products were then assayed for aequorin activity as described later in this section.

2.2.7.2. Expression of recombinant proteins in living cells.

2.2.7.2.1. Lipid mediated transfection.

2.2.7.2.1.1. Cell seeding.

Unless otherwise stated, transfection experiments were performed as follows. HEK293 cells were seeded at the appropriate density 48 h prior to transfection in order to give 90-95% confluence in the day of transfection. MG63 cells were cultured just 24 h before transfection.

Transfection experiments were carried out in either 6 well-plates or 22x22 mm coverslips placed onto 6 well-plates. In 6 well-plates, HEK293 cells were seeded at a density of 10^6 cells/well and MG63 at 5×10^5 cells per well. For coverslips, 10^5 of HEK293 cells and 5×10^4 of MG63 cells were transferred in a final volume of 300 μ l. The next day, wells were replenished to 2 ml.

In the case of HEK293, coverslips were previously coated with 400 μ l of poly-L-lysine (0.01% w/v, Sigma-Aldrich) to enhance attachment. After 5

minutes, the treating solution was removed; coverslips rinsed twice in cell culture water and dried in air.

2.2.7.2.1.2. Lipofectamine 2000 transfection.

In the day of transfection, cells were transfected using the appropriate vector and Lipofectamine 2000 reagent according to the manufacturer's protocol. In brief, 1 µg of total DNA was transfected into each well using a Lipofectamine to DNA ratio of 3:1 in a volume of 1 ml of Opti-MEM reduced serum medium. The transfection mixture was removed after 6 h of incubation at 37°C and the transfected cells were washed with PBS and maintained with the appropriate medium (MEM or DMEM). Cells were assessed two days after transfection.

Lipofectamine 2000 was the standard reagent used for transient transfection. Other transfection reagents were used in the initial test experiments which are described in the following sections.

2.2.7.2.1.3. Lipofectamine LTX and PLUS transfection.

A similar transfection procedure to LIPOFECTAMINE 2000 was used with LIPOFECTAMINE LTX and LIPOFECTAMINE PLUS. The amount of transfection reagents was adjusted accordingly to the manufacturer's recommendations using 2.5 µl and 1 µl of LIPOFECTAMINE LTX and PLUS respectively.

2.2.7.2.1.4. FUGENE HD transfection.

Transient transfection was performed using FUGENE HD (Roche) transfection reagent. Briefly, 100 µl of cell medium were mixed with 3 µl

of FUGENE HD in a sterile tube, incubated for 5 min and 1 µg of DNA added and incubated at room temperature for 15 min. Medium was removed from the wells, the mixture added and medium added to a final volume of 1 ml. Cells were incubated at 37°C for 24 h with the transfection mixture, then the medium was removed, cells washed with PBS and incubated in normal culture medium for another 48 h.

2.2.8. AEQUORIN EXPRESSION AND EXTRACTION FROM BACTERIA

The plasmid pMMB66EH-AEQ (Watkins *et al.*, 1995) which contains the gene of the native aequorin was used to transform JM109 bacteria. Transformation was performed as described in section 2.1.7.1. After the overnight bacteria growth, 2.5 ml of the culture was added to 300 ml of LB with ampicillin, incubated at 37°C and 150 rpm shaking until OD₆₀₀ was approximately 0.3-0.6. The medium was then supplemented with IPTG to a final concentration of 1 mM and induction was carried out for 2 h at 37°C. Next the solution was centrifuged at 3000 rpm for 10 min and the medium removed. The pellet was washed with PBS, centrifuged at 3000 rpm for another 10 min, the supernatant decanted and the final pellet resuspended in aequorin resuspension buffer. For protein extraction, the solution was maintained in ice at all times and was subjected to 5 sonication pulses of 15 s allowing the sample to cool down between pulses. The sample was centrifuged at 3000xg for 30 min at 4°C; the supernatant with aequorin in solution was subsequently transferred to a new tube and stored at -20 °C until used.

2.2.9. PROTEIN EXTRACTION FROM EUKARYOTIC CELLS

Forty-eight hours after transfection, cells were detached by treatment with trypsin, centrifuged at 1000 xg for 2 min, washed first with ice-cold PBS, centrifuged again and then washed with ice-cold PBS with 1 mM EDTA to make sure any traces of calcium were removed. Subsequently, cells were centrifuged at 1000 xg for another 2 min, harvested in 500 µl of hypotonic lysis buffer and incubated in ice for 5 minutes. Cells were homogenized by two passages through a 27 gauge needle followed by three freeze-thawing cycles.

2.2.9.1. Subcellular fractionation.

From each sample of protein cell extract, an aliquot of 100 µl was taken for the light measurement of the total protein suspension. The remaining mixture was centrifuged at 30,000 xg for 30 min at 4 °C to separate the proteins in the cytosol from those in the membrane. 300 µl of the supernatant were transferred to a fresh tube taking care not to disturb the pellet. The residual supernatant was removed and the pellet resuspended in 300 µl of lysis buffer. Protein samples were kept on ice at all times.

2.3. CELL BIOLOGY TECHNIQUES

2.3.1. CELL CULTURE

Three cell lines were used during this work: the Human Embryonic Kidney 293 (HEK293), the osteoblast-like MG63 and the Human Bone Osteoblast (HBO) primary cells. MG63 and HBO cells were kindly supplied by Dr Bronwen Evans, Department of Child Health, School of Medicine, Cardiff University. HEK293 cells which stably express human brain BK channel α subunit (Ahring *et al.*, 1997) were kindly provided by Professor Paul Kemp, School of Biosciences, Cardiff University.

2.3.1.1. Cell husbandry of MG63 and HBO.

HBO and MG63 cells were cultured at 37°C in a humidified atmosphere of 5% CO₂ and 95% air in Dulbecco's modified Eagle medium (DMEM) that contained 100 U/ml penicillin, 100 µg/ml streptomycin, 250 µg/mL amphotericin B with 5% foetal bovine serum (FBS). The cell medium was changed each three or four days period to optimise growth and ~10⁶ cells were passaged into new flasks each seven days.

2.3.1.2. Cell husbandry of HEK293.

The HEK293 cell line was maintained under same conditions in Minimum Essential Medium with Earle's Salts and L-Glutamine (MEM), supplemented with 10% fetal bovine serum, 1% MEM Non-Essential Amino Acids, 0.35% NaOH (1M) and 1% Antibiotic/Antimycotic (100X) and 0.20% Gentamicin (50 mg/ml). All HEK293 cells used in this thesis

were stably transfected with the BK channel α subunit. To maintain only the transfected cells lines an additional supplement of 1% Genitacin selective antibiotic (100 mg/ml) was added.

2.3.2. Cell storage.

A number of either MG63 or HEK293 cells from 5 to 10 million per ml were resuspended in freezing medium (90% normal medium + 10% DMSO) and 1ml transferred into cryotubes, placed into a freezing container (Nalgene, cooling temperature $-1^{\circ}\text{C}/\text{min}$) and then into a -80°C freezer for a minimum period of 2 hours. Finally the cryotubes were placed indefinitely into a liquid nitrogen container (-196°C) for later use.

All reagents were purchased from Invitrogen. All cell culture techniques were carried out under sterile conditions (class II cabinet, protective clothes and gloves, sterile glassware, ethanol 70% sprayed before use, etc).

2.4. CALCIUM IMAGING TECHNIQUES

2.4.1. APOAEQUORIN RECONSTITUTION

2.4.1.1. Coelenterazine.

Coelenterazine is a very unstable substrate which will lose activity in a few days if exposed to light and air at room temperature. To prevent the oxidation during storage, coelenterazine powder was dissolved in small volumes of methanol, aliquots were dispensed and dried under argon

flow. All dried aliquots were stored at -20°C in the dark. On the day of the experiment individual aliquots were immediately redissolved in a small concentration of methanol (10-20 μl) and supplemented to the appropriate solution. For each set of experiments, when possible, the same coelenterazine solution was used to reconstitute all aequorin variants to minimise variability due to different coelenterazine concentrations. This is of particular importance when comparing total number of light counts.

2.4.1.2. Reconstitution of apoaequorin in translation products.

Following *in vitro* transcription/translation (section 2.1.8.1), the total volume (25 μl) of the mixture was incubated with 25 μl Buffer O containing 5 μM coelenterazine for 4 hours. The aequorin activity was assayed in the home built luminometer by adding the total volume (50 μl) of the mixture to 500 μl aequorin assay buffer in an LP3 test tube and measuring the bioluminescent counts after the addition of 500 μl of 50 mM CaCl_2 .

2.4.1.3. Reconstitution of apoaequorin in bacteria cell extracts.

Apoaequorin reconstitution was achieved by the addition of equal volumes of buffer O with coelenterazine (final concentration 5 μM). Aliquots (50 μl) of the total protein suspension, membrane proteins and cytosolic proteins, were assayed in the home built luminometer as described in the above section.

2.4.1.4. Reconstitution of apoaequorin in living cells.

Transfected cells in 6-well plates were detached with trypsin and reconstituted as a cell suspension. Cells on coverslips were held as monolayers at all times. The culture medium was removed, cells were washed twice with PBS and a minimal volume of KRH medium containing 2 μ M coelenterazine, sufficient to cover the cells, was added. Cells were incubated at 37°C for 1 hour prior to the start of the experiment. Cells in suspension were centrifuged at 1000 x g for 2 min, washed with warm KRH medium to remove the excess of coelenterazine, centrifuged again and resuspended in KRH medium. Aliquots of this mixture were transferred to a LP3 tube containing 500 μ l of KRH. Monolayers of cells on coverslips were washed twice with warmed KRH and maintained in KRH at 37°C prior to the start of the experiment.

2.4.2. Luminometers.

A luminometer is a sensitive device for measuring extremely low photon emission such as those emitted by bioluminescent reactions. The basic components of a luminometer are: a light-proof sample housing, a photomultiplier (PMT) and a signal processor couple to a recorder. The sample housing is designed to reduce the background light signal and to maximize the efficiency of the detection by placing the sample as close to the detector as possible. The PMT function is to multiply the signal produced by incident photons by several orders of magnitude, from which single photons can be resolved. The collected data is

normally processed using a computer software program. All these features ensure uniformity of light collection from even the smallest sample. The individual photon-detecting devices used in these experiments are described in detail below.

2.4.2.1. Home-built luminometer.

This luminometer (Fig. 2.1) was designed in Cardiff (Campbell, 1988) and used to detect bioluminescence from either a suspension of live cells expressing aequorin or aequorin proteins. All experiments were performed in a dark room. Phosphorescence was minimised by never exposing either the PMT or the sample tubes to light even when switched off. The sample housing consisted of a rotating brass cylinder designed to accommodate a 12 x 65 mm plastic LP3 test tube (Fisher Scientific UK Ltd.). Reagents were added through an injection port fitted above the sample. When sequential additions were made, light detected during the replacement of the syringe was removed at the processing stage. The PMT (Thorn EMI, 9757AM) was specifically chosen for low dark current and connected to an adjustable high voltage supply (500 - 2000V, PM20, electron tubes). The effect of thermal noise in the PMT was reduced by cooling using a FACT50 air-cooled thermoelectric housing (Thorn EMI) maintained at -20 °C.



Fig. 2.1. Picture of the home-built luminometer used in this thesis.

2.4.2.1.1 Optimisation of sensitivity of the home-built luminometer.

A luminometer is a sensitive instrument which requires optimisation to achieve the favourable conditions for sensitive and accurate results. In order to achieve a consistent performance during the experimental procedures, the main parameters must be accurately monitored and adjusted. A study was conducted to determine the optimal conditions prior to the initial experiments.

Instrumental voltage optimisation was performed by allowing external light to pass through the aperture of the sample cylinder and recording the number of counts for 10 s. Background noise was the number of counts prior to the light exposure. All readings were taken in triplicates.

To determine the aequorin signal-to-background ratio against voltage plot, first 10 μl of aequorin were added to 500 μl of assay buffer. Light emission was then measured over a period of 30 s immediately upon

the injection of 500 μl of the triggering solution containing calcium chloride. Aequorin was extracted from bacteria as described in section 2.1.9 and reconstituted for 1 hour in the presence of coelenterazine (5 μM). Background noise was the average of three readings previous to aequorin consumption. Experiments were repeated at three different temperature settings using a PMT cooler.

To establish the optimal conditions for experiments with aequorin, we first delimited the voltage range in which light signal is much higher than the background noise. The initial range was from 1400 to 1800 V based in previous experience in our group. When the luminometer was subjected to light exposure, a highest relative increase was observed in the range between 1700 and 1800 V.

Once the voltage range was established, the effect of the temperature on reducing the thermal noise in the PMT was studied at three different temperature settings. At high voltages (1800-1850 V) the effects of cooling the PMT were quite noticeable (Fig 2.2, B) whereas below 1700 V were almost indistinguishable (Fig 2.2, B & C).

When aequorin signal was compared to the background noise at different voltages and cooler temperatures, the best performance was obtained by setting the high voltage power supply at 1700 V and the temperature of the cooler at -20°C . Under these conditions, the signal-to-noise ratio was improved by a factor of 30 compared to the other settings. Quite remarkable is the improvement achieved by cooling the PMT in order to reduce the thermal background noise (Fig 2.2, D).

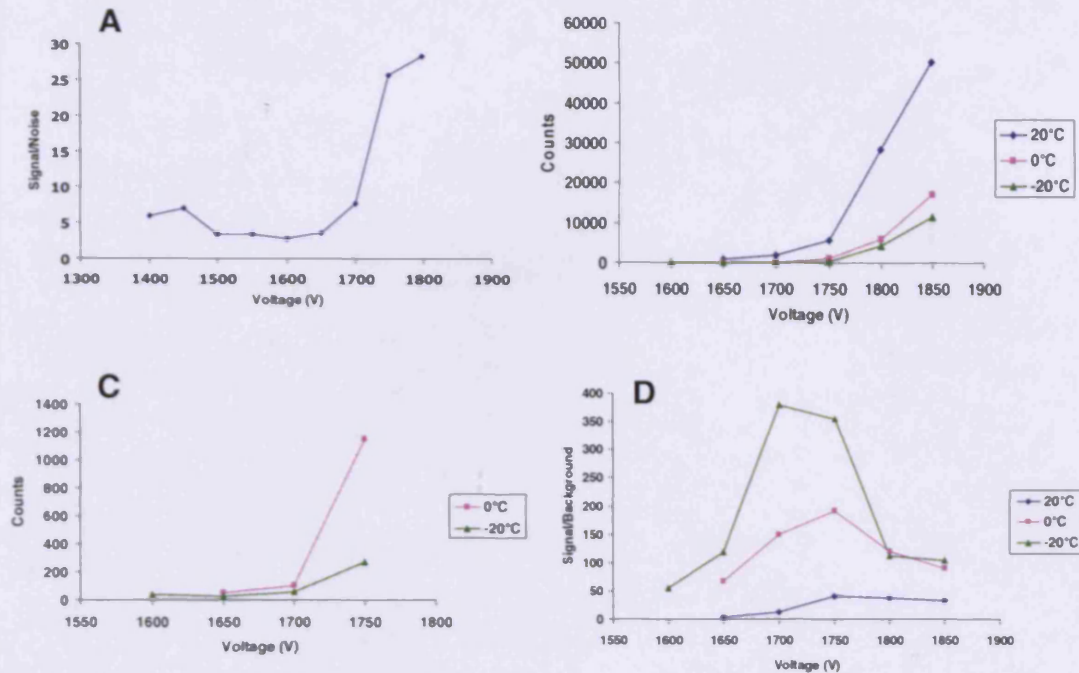


Fig 2.2. Optimisation of sensitivity of the home-built luminometer. (A) The optimal voltage range assessed by instrumental calibration was between 1700-1800 V. (B and C) illustrate the reduction of noise background by reducing the temperature. (D) The optimisation curves obtained with aequorin at different temperatures were employed to determine the optimal voltage (1700 V).

When dealing with an instrument as sensitive as a luminometer, calibration is an area of critical concern. As a result of the optimisation process, the aequorin signal-to noise ratio was improved by the factor of 30 to the initial experiments. This improved sensitivity of the system permitted the use of smaller samples and the detection of minor variations in aequorin signal.

2.4.2.2. ICCD camera.

An image intensified charge-coupled device (ICCD) camera is a sensitive and quantitative device which also exhibits a fast response time, good spatial resolution and low level signal detection. All these features are required to detect events such as Ca^{2+} signalling in individual cells and to investigate the complex spatial and temporal patterns of these processes. The basic principle relies on converting the light output to an electrical signal which is then amplified several orders of magnitude.

The bioluminescent imaging system used in this work was a 25 mm three stage microchannel image intensifier coupled to a CCD camera (Photek Ltd, Hastings, UK) via a reducing fibre optic taper and connected to an external high voltage power supply (Fig 2.3). When photons generated by the sample strikes the photocathode connected to a high voltage power supply unit, a portion of them causes electrons to be released via the photoelectric effect. These electrons are attracted towards the wall of the Multi Channel Plate (MCP) which, while maintaining the spatial resolution of the signal, amplifies it by generating a shower of secondary electrons. This process occurs three times resulting in a gain of 10^6 - 10^7 electrons per photon event. The electrons are then accelerated towards the phosphor screen, where they strike the output phosphor coating and cause it to release light. This final intensified light signal was transmitted onto the CCD camera via the fibre optic taper. The camera operates with a resolution of 512 x 512

non-interlaced pixels and at a frame rate of 60 Hz, giving a time resolution of 20 ms. The dark counts at room temperature for the whole field of view was approximately 40 counts/s.

The imaging equipment was located inside a dark box (Fig 2.4). Experiments were also carried out in a dark room with an air-conditioning system set at 22°C. This system was designed to allow continuous measurements of calcium signals from small populations of attached cells and to deliver solutions by means of a perfusion system.

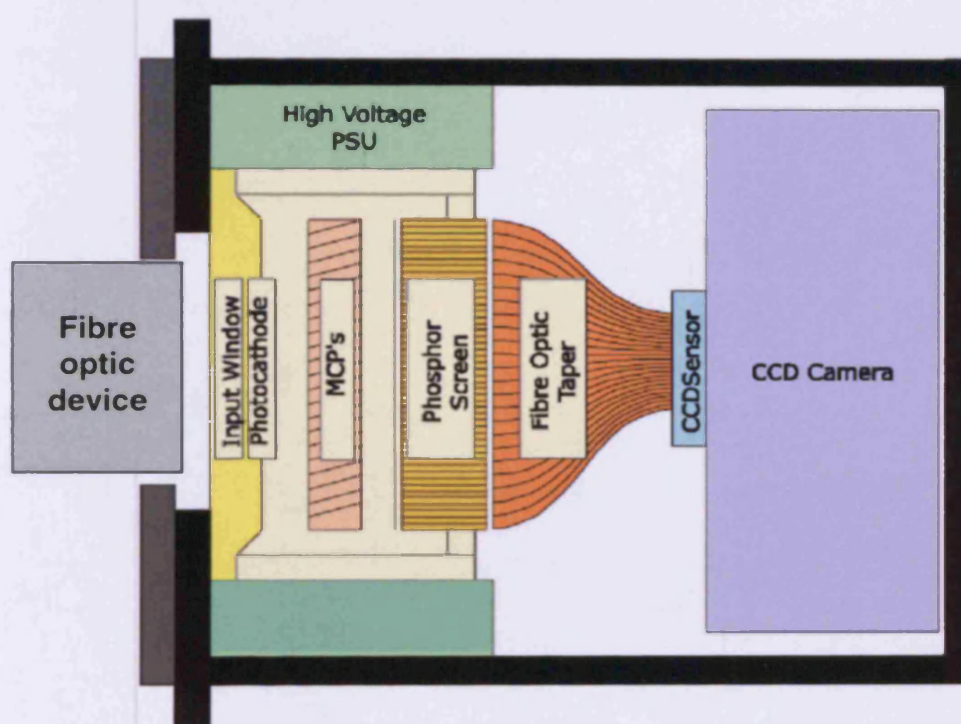


Figure 2.3. Schematic representation of the ICCD325 camera from Photek Ltd. Light is collected via a fibre optic device onto the front of the camera, intensified and imaged as described above (section 2.3.3.2). PSU stands for power supply unit.

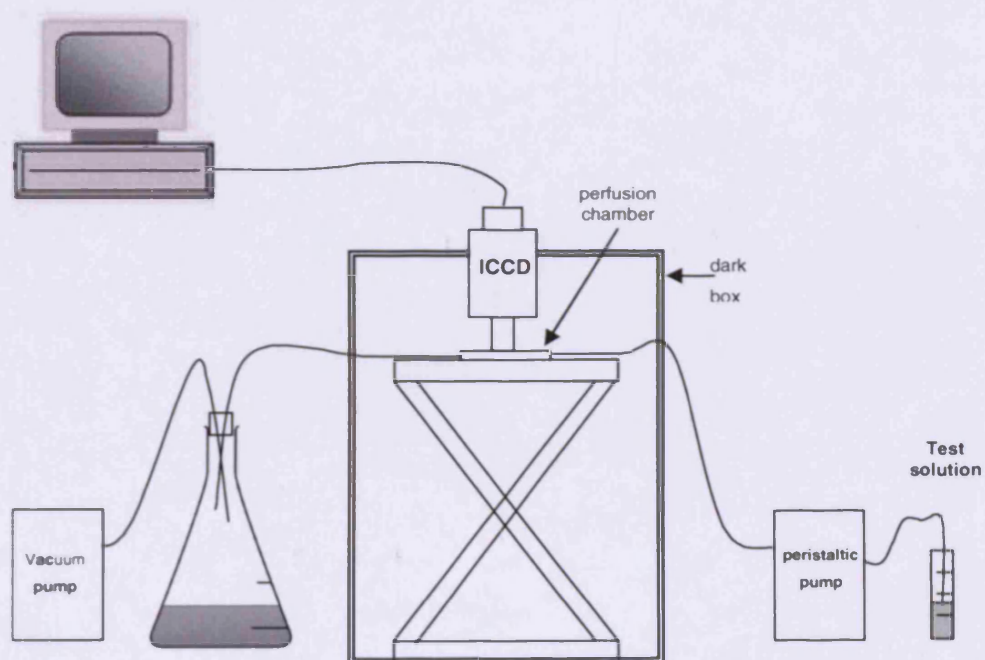
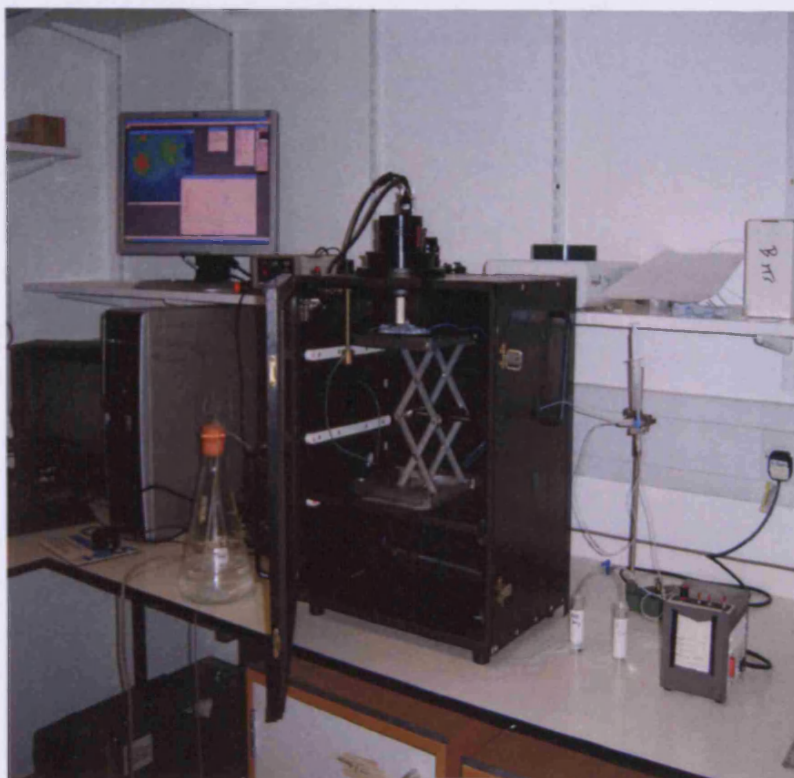


Fig 2.4 A picture (top) and a schematic representation (bottom) of the components of the ICCD camera system used in this thesis.

2.4.2.2.1. Sample handling.

Cells growing on a coverslip (22 x 22 mm) were inverted over the reservoir of a plastic perfusion chamber and secured into position. The perfused chamber was immediately brought into contact with the fibre optics bundle attached to the photocathode and sealed with microscope oil (Fig 2.4). Cells were perfused for at least 3 min in KRH solution.

2.4.2.2.1. Perfusion system.

Initial experiments were carried out using stop-flow perfusion. During the course of these experiments, a series of light signals often appeared which were not caused by the addition of an stimuli. These artefacts have been previously reported as being instigated by stop-flow medium changes (Tong *et al.*, 1999). Additionally, this method of perfusion increased the incidence of bubbles during the experiments. Some of these bubbles reached the chamber producing the lysis of the cells in the coverslip resulting in aequorin release and a high light signal. Therefore, a different approach was adopted to reduce these potential artefacts. Firstly, a two way valve was incorporated to enable the exchange of solutions and the use of over-flow perfusion. Secondly, a syringe was mounted on the perfusion system to act as a bubble trap. As a result, the incidence of these artefacts was significantly reduced.

All experiments performed during this work used over-flow perfusion to add solutions. The flow rate of the perfusion system was experimentally assessed using a coloured dye. The first drop of dye arrived at the cell

chamber after 32 s and full colour was reached at 48 s. Before and after each set of experiments, the tubing was fully cleaned by the perfusion of sterile water for 10 min in order to minimise the growth of bacteria which can release toxins into the solutions employed. In addition, the unclean parts of the tubing system were replaced when required.

2.4.2.2.3. Data Analysis.

The IFS32 Data Acquisition and Image Processing Software (Photek Ltd, U.K.) were used to analyse the data obtained. The system only records the xy coordinate for each pixel which is exposed to a positive photon event, saving large amounts of negative data. However, this may give rise to a coincident loss when two or more events occur on one pixel in less than 20 ms. A neutral density filter can be used to overcome this issue. Nevertheless, this potential problem was not observed in the course of all the experiments performed in this work.

The data acquired during the experiment was subjected to an analysis as follows: a variable number (5 - 20 on average) of Odd Area Sets (OAS) was drawn around the sections which emitted a substantial number of counts when lysed (Fig. 2.5); a 10 s frame video sequence was generated for the whole duration of the experiment; the cumulative counts during each frame were then extracted from the sequence and transferred to Microsoft Excel; finally graphs were plotted according to this numerical data. Background noise was obtained using a short video sequence with a cell-free coverslip, calculated using the average counts of similar OAS to each experiment and subsequently subtracted from

the initial readings. The average number of HEK293 cells on each cell cluster was estimated to be between 2000 cells. This estimation was based on an average cell diameter of 30 μM and under the assumption that cells were fully confluent and uniformly distributed throughout the monolayer.

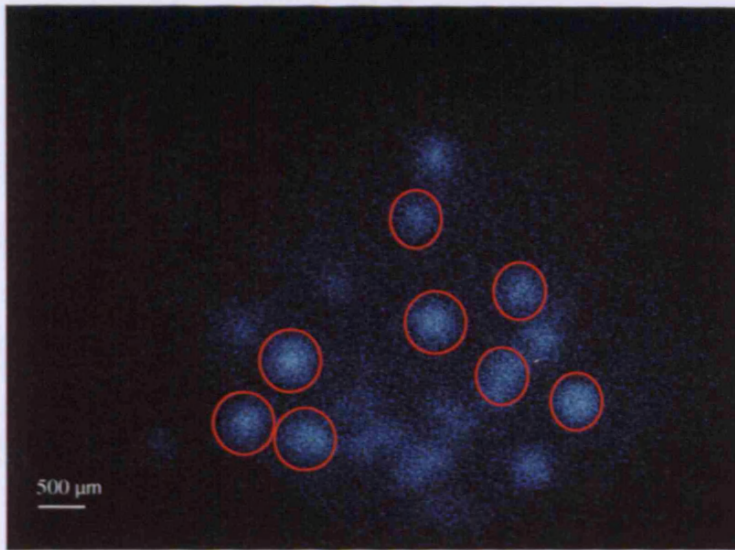


Fig 2.5. Light emission of cell clusters following the addition of a high Ca^{2+} lysis solution. The addition of a high Ca^{2+} hypotonic solution resulted in clusters of cells firing. A number of cell clusters (OAS, in red) was selected in different regions of the chamber for the subsequent data analysis. Each cell cluster contained approximately 2000 HEK293 cells on average. HEK293 cells were transfected with Luc-Aeq and incubated for 1 h in the presence of EGTA and coelenterazine (2 μM).

2.4.3. Converting aequorin light emission into calcium.

All experiments were performed at room temperature (22°C). Unconsumed aequorin was determined at the end of each experiment by exposing the cells to hypotonic buffer containing 10 mM CaCl_2 (which caused the cells to lyse slowly and thus avoid the use of

detergents). There is a great deal of evidence showing that Ca^{2+} –dependence remained unchanged after the fusion of an additional protein sequence (Kendall *et al.*, 1992; Badminton *et al.*, 1995; Nakahashi *et al.*, 1997; George *et al.*, 1998; Lin *et al.*, 2000). Conversion of light emission to Ca^{2+} concentration was calculated using two empirically determined equations previously employed in our laboratory, one for Luc-Aeq (Badminton *et al.*, 1996) and other for $\beta 2$ -Aeq based on a membrane-bound aequorin construct (George *et al.*, 1998). Aequorin consumption is reduced at lower temperatures than 37°C (Brini *et al.* 1995). Accordingly, the equations were modified to account for the difference in temperature according to Brini (1995). The final equations used to calculate the absolute free Ca^{2+} concentrations were as follows:

	Range of pCa
$\text{pCa} = 0.403 (-\log k) + 4.8727$ (Luc-Aeq)	8.5 – 4.5
$\text{pCa} = 0.41 (-\log k) + 4.843$ ($\beta 2$ -Aeq)	7.8 – 4.8

Each equation is valid between the range of pCa indicated. Unless otherwise stated, the rate constants for decay of the bioluminescence, k (s^{-1}), were determined as the mean counts per second divided by the remaining counts (Chapter 1, section 1.5.1.3.).

2.5. ELECTROPHYSIOLOGICAL TECHNIQUES

2.5.1. The patch-clamp technique

Patch-clamp is a powerful technique that allows the electrophysiological study of individual cells or even individual ion channels within a patch of membrane. This technique was first introduced by Neher and Sakmann (Neher & Sakmann, 1976) and subsequently improved by Hamill and collaborators (Hamill *et al.*, 1981).

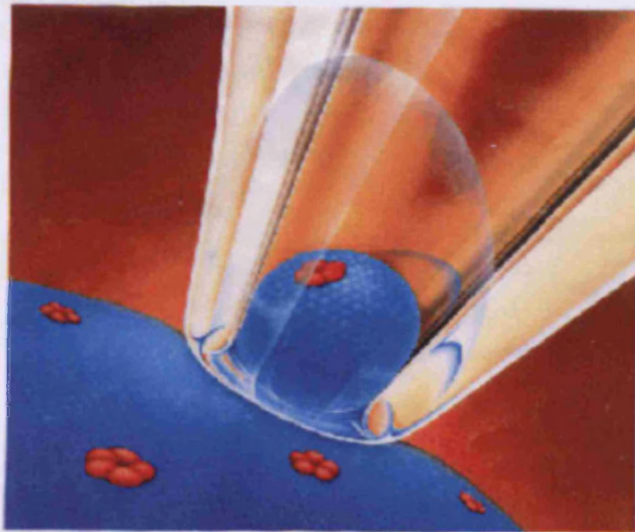


Fig. 2.6. Schematic representation of a single ion channel being recorded within the patch pipette (Neher & Sakmann, 1992).

The basic working principle involves the use of a glass pipette microelectrode with a tip diameter of $\sim 1 \mu\text{m}$. The microelectrode is pressed against the cell membrane and suction is applied inside of the glass pipette (known as 'blow-and-seal' method also used in brain slices, Stuart *et al.*, 1993). The small patch of the membrane is subsequently pulled into the pipette tip and a tight seal is formed with

an electrical resistance over 1 Giga-Ohm. This little patch, which is electrically isolated from the rest of the cell, allows the measurement of incredibly small electrical currents (~ 1 pA) produced by the ion flow through individual ion channels in the patch.

There are four main configurations which are called 'cell-attached', 'inside-out', 'outside-out' and 'whole-cell' recordings. In this thesis, the 'cell-attached' configuration, which is the least invasive of all, was employed in this thesis to record single-channel activity.

2.5.2. Seeding on to glass coverslips.

This process was performed in order to carry out electrophysiological recordings. Cells were carefully counted using a haemocytometer. From 1000 to 3000 cells were seeded on to sterile coverslips (16 mm diameter) uncoated and placed in 6 well plates. After 1 - 1.5 h incubation at 37°C (5% CO₂), 2 ml were added to each well and incubated at 37°C (5% CO₂) until used.

2.5.3. Patch-electrodes production.

A DMZ Universal Puller (Dagan Corporation) was employed to pull and heat-polish borosilicate glass capillaries (GC150-F10, Harvard Apparatus Ltd.) of dimensions 1.5 mm outside diameter and 0.86 mm inside diameter. Patch-electrodes with electrical resistances of 4-7 M Ω were produced by this method. The patch-electrodes for patch clamp were backfilled with the above high K⁺ saline. All solutions were filtered on application through 0.2 μ m syringe filters (Whatman).

2.5.4. Electrophysiological Recording.

Glass coverslips with cells attached were transferred inside a laminar flow cabinet to a glass recording chamber. The slip bring held in place by a tiny amount of vaseline to secure. Approximately 500 μ l of Locke solution was added carefully over the coverslip. Coverslips were scanned visually to select cells that appeared healthy and isolated. Recordings were made using the cell-attached patch clamp technique. The recording electrode tip was placed into the bathing solution by means of the coarse manipulator and positive pressure applied. Any junction potential was set to zero by adjusting the DC offset on the amplifier (Axopatch 1D, Axon Instruments).

Using a hydraulic micromanipulator the microelectrode was advanced toward the cell in solution. When microelectrode tip and cell were seen at the same time and a slight decrease in amplitude of the square-wave pulse detected on the oscilloscope, slight negative pressure was applied by suction to reach a membrane-electrode seal of 1 Giga-Ohm or more. Both the electrode and the seal resistance were computed by dividing the command pulse of 20 mV through the electrode, by the deflection measured from the oscilloscope display taking into account the amplifier gain (i.e. mV / pA).

2.5.5. Data analysis.

WinEDR Electrophysiology Data Recorder v2.5.8 Software (Dempster, 2003) was employed to perform the data analysis. Distributions of

current amplitude histograms were constructed by the software for each holding potential and the peaks were fitted with either a Gaussian distribution curve whenever possible or a 'Patlak average' plot. The amplitude of the current was derived from the mean current value of each peak.

2.7. STATISTICAL ANALYSIS

Data are reported as means \pm SEM for the indicated number of experiments.

$$SD = \sqrt{\frac{\sum (x - \bar{x})^2}{n - 1}} \quad SEM = \frac{SD}{\sqrt{n}}$$

Where x = sample value, \bar{x} = mean value and n = the sample number.

Statistical significance was determined using the independent two sample Student's t -test. The criterion used for significance was $p < 0.05$.

The coefficient of variation is reported as a percentage and calculated from the average and standard deviation as follows

The coefficient of variation (CV) is a statistical method to standardise the variability of a number of samples. It is reported as a percentage and calculated from the mean and standard deviation as follows:

$$CV = \frac{SD}{\bar{x}} \times 100$$

CHAPTER 3

ENGINEERING AND CHARACTERISATION OF A β 2-AEQUORIN CHIMERA TARGETING THE BK CHANNEL

3.1. INTRODUCTION

Aims:

- To develop a novel recombinant protein as a result of combining the $\beta 2$ subunit and the Aequorin sequences.
- To assess the functionality of the new protein.
- To determine the optimal conditions for aequorin reconstitution.

Strategy:

To obtain this protein, several possibilities were available about how to combine $\beta 2$ subunit and Aequorin. Since both N-terminus and C-terminus face the cytosol (Tseng-Crank *et al.*, 1994), either can be combined with aequorin in order to monitor intracellular calcium. Recent studies have shown that the N-terminus of the $\beta 2$ subunit possesses an inactivating particle and is involved in the trafficking mechanism of the protein (Wallner *et al.*, 1999; Lv *et al.*, 2008). Production of recombinant proteins using aequorin has been so far limited to its N-terminus. Literature reports have shown that modifications of the N-terminus of aequorin have no adverse effects on its luminescent activity (Badminton *et al.*, 1995; Brini *et al.*, 1999). Conversely several studies have reported a complete or significant lost of aequorin activity when modifications were introduced at the C-terminus (Tsuji *et al.*, 1986; Nomura *et al.*, 1991; Watkins NJ & Campbell AK, 1993). Consequently,

the C-terminus of $\beta 2$ was selected to be connected to the N-terminus of the Aequorin sequence.

Two cell lines were used in this work, HEK293 α as a model cell line and MG63 as a native cell line. The term 'model cell line' refers to the feature of these cells in which many proteins are either absent or expressed at low levels. In contrast, the term 'native cell line' applies here to those cells in which the patterns of protein expression are analogous or very similar to primary cells and therefore to real tissue. HEK293 is commonly used as a model cell line. HEK293 α has been steadily transfected with the BK channel α subunit and is well characterised (Lippiat *et al.*, 2003). The MG63 cell line was selected because it exhibits an unusual high density of BK channels and has been also well characterised (Li *et al.*, 2007). In order to correctly evaluate the effects of $\beta 2$ Aeq in MG63, a PCR study was carried out to detect the presence of α and $\beta 1-4$ subunits and obtain the complete sequence of the $\beta 2$ subunit.

The first goal was to obtain and clone the full coding sequence (CDS) of the $\beta 2$ subunit. This was achieved using Retro Transcription PCR with two primers flanking the sequence using mRNA extracted from MG63. PCR was carried out using a standard polymerase which adds a 3'-A overhang to the final product facilitating the subsequently TA cloning in the mammalian vector.

The second step was to join both sequences together with the removal of the stop codon from the first sequence. To accomplish this, the splicing by overlapping extension (SOE) PCR methodology was used. This is a method of recombining DNA sequences which relies on carefully designed primers and various consecutive PCR steps (Horton et al., 1990). The initial templates were the $\beta 2$ subunit previously inserted into a vector and a plasmid designed in our group containing the aequorin sequence (Watkins, 1995). Since a number of PCR reactions are needed, a high fidelity polymerase was employed during this process to reduce the incorporation of errors in the final products. This polymerase also displays the ability to add 3'-A overhangs enabling the final TA cloning procedure.

Once the correct sequence of the DNA sequence was confirmed, a subsequent experimental investigation was carried out to assess the properties of the new recombinant protein. Following the initial adjustment of the instrumental conditions, a cell-free system and living cells (HEK293 α and MG63) were used to study the functional aspects of the protein. Finally, the optimal conditions for aequorin reconstitution were determined.

3.2. METHODS

3.2.1. Primer design.

Primers for the housekeeping gene beta actin, the BK channel α subunit (KCNMA1) and β 1-4 subunits (KCNMB1-4) were designed in order to verify the presence of these genes in osteoblasts (Table 3.1).

Two gene-flanking primers were specifically designed to be up and downstream of the KCNMB2 CDS sequence to ensure that the whole sequence was obtained (Fig 3.1).

GENE	Genbank Access number	Sequence	Locus	Product Size
<i>Beta Actin</i>	NM_001101	cccagccatgtacgttgcta	387	125 bp
		agggcataccccctcgtagatg	512	
<i>KCNMA1</i>	NM_002247	acgcaatctgcctcgcagagttg	1640	407 bp
		catcatgacaggccttgacag	2047	
<i>KCNMB1</i>	NM_004137	ctgtaccacacggaggacact	268	188 bp
		gtagaggcgctggaataggac	456	
<i>KCNMB2</i>	NM_181361	catgtccctggtgaatgttg	465	236 bp
		ttgatccgttgatcctctc	701	
		gagaccctggaccaacattct	318	823 bp
		agaaccttaagttgtaacgtgcag	1141	
<i>KCNMB3</i>	NM_171830	aacccccctttcatgcttct	537	276 bp
		tcttccttgctcctcctca	813	
<i>KCNMB4</i>	NM_014505	gttcgagtgcaccttcacct	195	245 bp
		taaatggctgggaaccaatc	439	

Table 3.1. List of the primers used to confirm the presence of BK α and four β subunits. KCNMB2 primers located at 318 and 1141 were designed to obtain the whole sequence of the β 2 subunit.

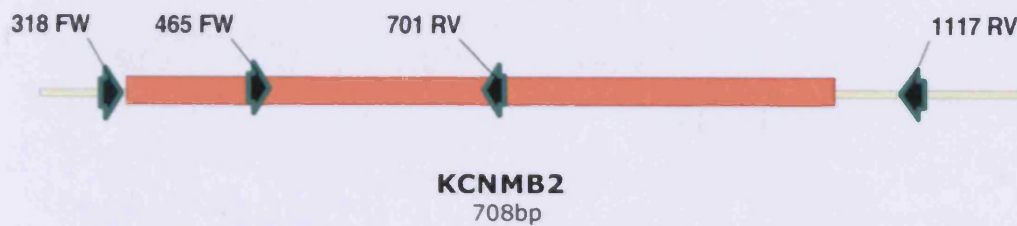


Fig 3.1. Diagram of the two of the primers are located within the DNA sequence corresponding to the protein sequence (in orange) and the other two up/downstream of the sequence, within the mRNA sequence (in yellow).

3.2.2. Polymerase Chain Reaction.

RNA extraction and standard PCR were in MG63 performed as described previously (See Material & Methods) and the products confirmed by sequencing. PCR conditions were in all cases GoTaq, 40 cycles and 58°C as melting temperature. Primers are listed in table 3.1.

3.2.3. Cloning of the $\beta 2$ subunit.

The complete $\beta 2$ subunit sequence extracted from MG63 was used for cloning into the Mammalian Vector pTarget. Following the bacteria transformation and the PCR screening of the resulting bacterial colonies, the plasmids showing the correct size and orientation were selected for maxiplasmid preparations. The entire sequence of the insert was confirmed by PCR amplification and subsequent sequencing of the band.

3.2.4. Engineering and cloning of $\beta 2$ -Aequorin.

The method known as Splicing by Overlap Extension (SOE) was performed to join the aequorin sequence (573 bp) to the BK $\beta 2$ subunit

(708 bp). The first step requires obtaining the sequences of interest sharing a common fragment. To achieve this, a $\beta 2$ reverse primer with 24 extra nucleotides overlapping the initial sequence at the N-terminus of aequorin was designed together with an aequorin forward primer with the last 24 bp at the C-terminus of the $\beta 2$ subunit sequence. When designing these primers, special care was taken to remove the stop codon from the end of the $\beta 2$ subunit and maintain the sequences in frame. This step is crucial to ensure that the correct fusion protein sequence is achieved.

High-fidelity PCR amplification was carried out with these primers using as templates the $\beta 2$ sequence in pTarget plasmid mentioned before and the pMMB66EH-AEQ plasmid previously constructed by Watkins (1995). To obtain enough amounts of both DNA products, a stepwise PCR optimisation process was conducted involving the use of different amounts of templates, increasing of the $MgCl_2$ concentration and the addition of enhancing agents (DMSO). The PCR products were run on 1% agarose gels, purified and the concentration of the purified product assessed. Equal amounts of either fragment were mixed and amplified using the outer primers resulting in the fusion of both DNA sequences.

In order to successfully generate the fusion construct, firstly it is required to obtain enough amount of appropriate band size. To accomplish this, a PCR optimisation was performed, the final product

run in a gel to avoid any unspecific band, the band cut and the product purified.

The fusion PCR product was loaded on 1% agarose gel, purified and cloned into the pTarget vector. PCR screening was performed in the bacteria colonies in order to detect the presence of the correct fusion sequence within the plasmids and confirm their appropriate orientation. After the screening, the exact DNA composition of the inserts was verified by sequencing.

3.2.5. Cell-free protein expression.

In vitro transcription/translation was performed using the Proteinscript II T7 linked transcription/translation system as described in Material & Methods, section 2.2.7.1. Equal amounts (0.5 µg) of three pTarget vectors containing β2, β2-Aeq and Luc-aeq were employed. The total volume was assessed for aequorin activity was carried out using the home-built luminometer as described in Material & Methods, section 2.4.1.2.

3.2.6. MTS Cell proliferation assay.

The MTS assay is a simple and accurate method to examine cell viability. This assay is based on the ability of the mitochondrial dehydrogenases of living cells to reduce the yellowish coloured 3-(4,5-dimethylthiazol-2-yl)-5-(3-carboxymethoxyphenyl)-2-(4-sulfophenyl)-2H-tetrazolium (MTS) into the purple crystals of formazan. The latter can be

measured by colorimetric assay and is proportional to the number of viable cells.

The effects of the transfection process on cell growth were quantified by means of a CellTiter 96 Aqueous Cell Proliferation Assay (MTS assay). Cells were plated at 3000 cells per well in a 96-well plate. Two days later, the cells were subjected to transfection with Lipofectamine 2000 using pTarget plasmids containing one of the following inserts: Luc-Aeq, $\beta 2$ -Aeq or $\beta 2$ (1 $\mu\text{g/ml}$). Following 6 hours incubation in OptiMEM medium in the presence of these constructs, the medium was replaced with normal medium for 48 hours. Following addition of 20 μl of a PMS/MTS (1:20) solution to each well and incubation for 1 h, the absorbance of each well was measured at 490 nm using an ELISA plate reader. Two control sets were conducted using normal cell culture medium instead of OptiMEM medium and Lipofectamine with no DNA added. Background absorbance was calculated as the mean of three wells containing no cells and subtracted from the values of the sample wells. Data values from three different experiments were converted to percent of control and pooled for statistical analysis.

3.2.7. Assessment of aequorin reconstitution.

The home-built luminometer was used to measure the light counts of HEK293 α cells in suspension. Cells were transfected with either Luc-Aeq or $\beta 2$ -Aeq for 48 hours. Each sample contained 50000 cells. Unless otherwise stated, coelenterazine concentration was 2 μM . For



the time-course experiment, aequorin activity was assayed at four intervals of 1 hour. All data were extracted from three different experiments.

3.3. RESULTS

Following the assessment of the cell lines selected, the $\beta 2$ was cloned into a vector and subsequently joined to the Aequorin sequence by means of genetic engineering techniques. The properties of the protein were then evaluated and the optimal conditions for cell work determined.

3.3.1. *MG63 and HEK293 α cell assessment.*

In order to detect the presence of the α and $\beta 1-4$ subunits RT-PCR was carried out in MG63. Additionally, the same study was performed in Human Primary Osteoblast (HBO) with the purpose of using the aequorin probes in a primary cell line. HEK293 α was also subjected to RT-PCR to verify whether the α subunit was still expressed in these cells.

The presence of BK α subunit and all four β subunits was detected in both MG63 and HBO cells at mRNA level (Fig 3.2). This is consistent with previous reports using patch-clamp techniques showing that BK channels are present in MG63 (Li *et al.*, 2007). The α subunit exhibits significantly higher expression levels than those observed for each individual β subunit. Understandably, this is probably due to the fact that

the α subunit primers target a shared sequence of the four subunits required to form the channel while the β subunit primers aim at four different sequences. However, this is only a qualitative indication. For a true comparison between mRNA expression levels, Real Time PCR should be performed.

One sole band was detected for α subunit with our primers. These primers targeted a site where splice variants has been located in other tissues. At this site, named site 1 in (Tseng-Crank et al., 1994), 0 aa were found during the sequencing process ruling out the presence of the transcript variant 1 (Genbank NM_001014797) (Pallanck L & B., 1994) and isoforms hbr2, hbr3, hbr4, hbr6 and hbr7 (Tseng-Crank et al., 1994). While in brain three difference sequences have been discovered in this site, only one appears in bone. Other splice variants may be present but further investigation will be required. These data indicate that not all isoforms are expressed in MG63, the isoform corresponding to GeneBank U11717 being the most probable one. Sequencing however must be performed to confirm this.

RT-PCR amplification was also carried out in HEK293 α (cell passage 40) confirming the presence of the α in this stable transfected cell line. In addition, patch-clamp recordings also showed at least three channels with a high current (~ 13 pA, Fig 3.3.) similar to that reported in previous studies (Tseng-Crank et al., 1994). This high conductance is characteristic of the BK channel indicating that the channels recorded

were probably BK channels. Since these patches were generally unstable and only lasted for a few minutes, the number of successful recordings achieved was insufficient to confirm that the channels recorded were BK channels. Nevertheless, other researchers in our group have performed a more extensive patch-clamp analysis of these HEK293 α cells confirming that BK channels (~ 240 pS) are still expressed in the plasma membrane (Li Bo, personal communication, 2008).

PCR confirmed that both MG63 and HBO cells express BK α subunit and β 1-4 subunits at mRNA level making them ideal candidates for cell transfection. Since HEK293 α cells were still capable of expressing the α subunit, they can also be used as a model cell line to express β 2 constructs.

3.3.2. β 2 subunit cloning.

With the purpose of facilitate the genetic engineering process of combining β 2 and Aequorin, the complete CDS of the β 2 subunit was first cloned into a DNA vector.

The PCR amplification of the whole sequence of the β 2 with the gene flanking primers generated a DNA band corresponding to the correct size (Fig 3.5 A). The PCR product was then inserted into the Mammalian Vector pTarget by TA cloning. The bacterial colonies were subsequently screened by PCR to identify those plasmids with the

appropriate insert and orientation (Fig 3.5 B). Finally, a plasmid was selected, amplified by PCR (Fig 3.5 C), the resultant band purified and used as a template for sequencing to verify the gene identity (Table 3.2).

Published $\beta 2$ sequence (NM_181361 GenBank) and the one obtained from the pTarget plasmid were compared. Three single nucleotide changes were detected along the whole sequence (See Table 3.2). These three point mutations are silent which means that the amino acid sequence remains unaltered and therefore will not interfere when expressed.

The whole $\beta 2$ sequence was successfully inserted into pTarget with a 100% identity in the AA sequence.

Fig 3.2. Subunit composition of the BK channel in human osteoblast.

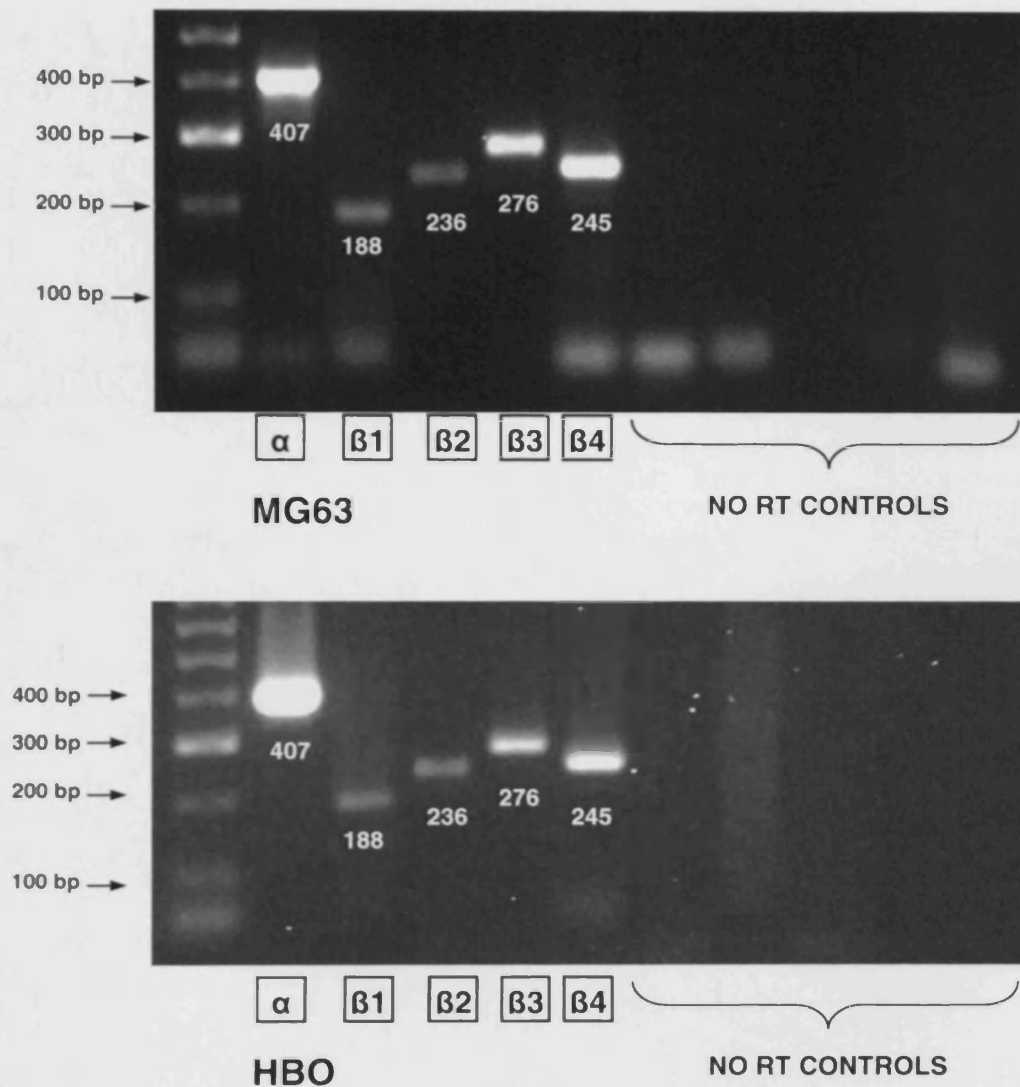


Fig 3.2. Subunit composition of the BK channel in human osteoblast. Gel electrophoresis shows bands equivalent to the predicted size of the BK channel subunits α , $\beta 1$, $\beta 2$, $\beta 3$ and $\beta 4$ in MG63 (A) and Human Primary Osteoblast (B) cell lines. Bands were compared to Hyperladder II.

Fig. 3.3. Single channel recording of BK channels in HEK293 α cells in a cell-attached patch.

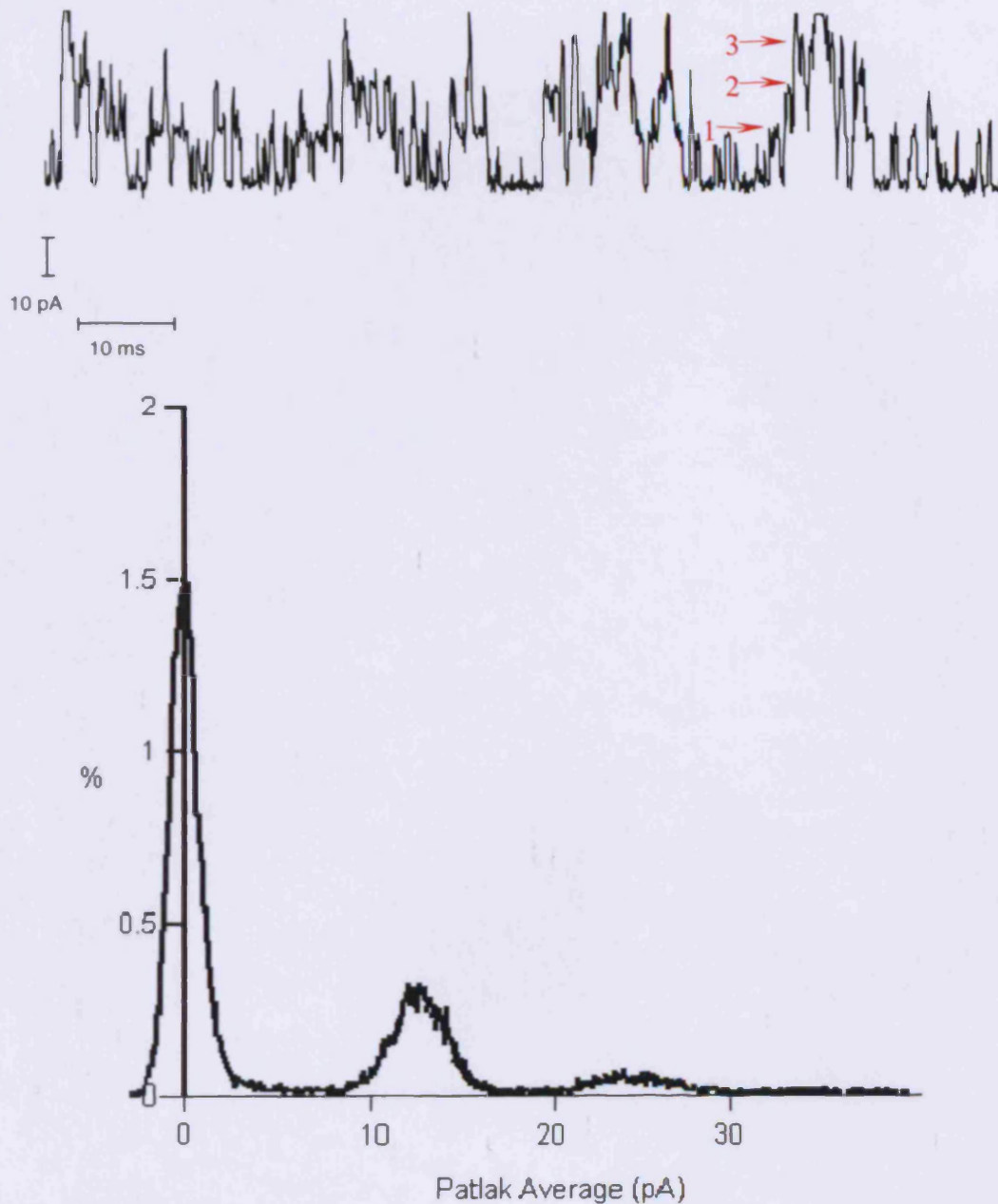


Fig. 3.3. Single channel recording of BK channels in HEK293 α cells in a cell-attached patch. (A) Raw data showing high activity in this patch at 120 mM with at least 3 channel openings (arrows). (B) The Patlak average distribution of current histogram from the whole 30 s recording period showing peaks at 12.97 and 24.05 pA indicating that at least three channels were present in this patch.

Fig 3.4 PCR amplification of the BK α subunit in HEK293 α .

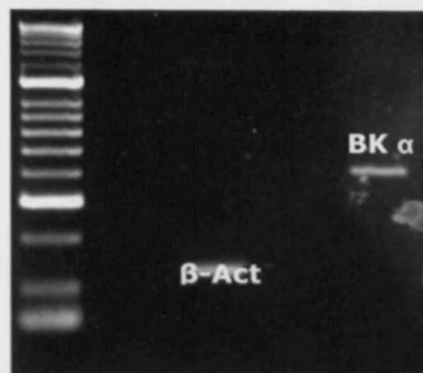


Fig 3.4. PCR amplification of the BK α subunit in HEK293 α . Gel analysis of the RT-PCR product obtained from HEK293 α mRNA confirmed the presence of the α subunit in the stable transfected cell line. DNA marker was Hyperladder II.

Fig 3.5 Cloning of the $\beta 2$ subunit.

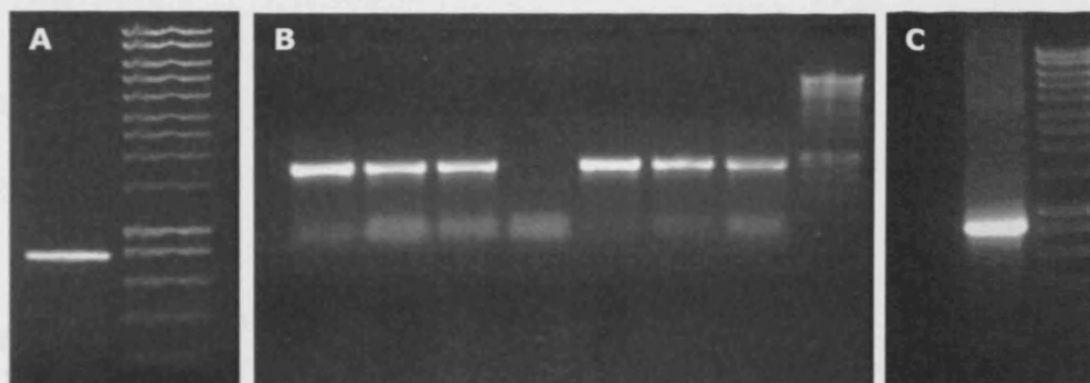


Fig 3.5 Cloning of the $\beta 2$ subunit. (A) Whole sequence of $\beta 2$ subunit (823 bp) obtained by RT-PCR from MG63 using gene-flanking primers. (B) PCR screening to determine the plasmids with the correct insert and orientation. (C) PCR amplification of the insert of a pTarget vector for sequencing. Hyperladder I was the marker of choice to compare the band length.

Sequencing result for $\beta 2$ insert in pTarget

```

atgtttatatggaccagtggccggacctcttcatcttatagacatgatgaaaaaagaaat
M F I W T S G R T S S S Y R H D E K R N
atttaccagaaaaatcagggaccatgacctcctggacaaaaggaaaacagtcacagcactg
I Y Q K I R D H D L L D K R K T V T A L
aaggcaggagaggaccgagctattctcctgggactggctatgatgggtgtgctccatcatg
K A G E D R A I L L G L A M M V C S I M
atgtattttctgctgggaatcacactcctgcgctcatacatgcagagcgtgtggaccgaa
M Y F L L G I T L L R S Y M Q S V W T E
gagtctcaatgcaccttgctgaatgcgtccatcacggaaacatttaaCtgtctccttcagc
E S Q C T L L N A S I T E T F N C S F S
tgtgggtccagactgctggaaactttctcagtaccctgcctccaggtgtacgttaacctg
C G P D C W K L S Q Y P C L Q V Y V N L
acttcttccgggggaaaagctcctcctctaccacacagaagagacaataaaaaatcaatcag
T S S G E K L L L Y H T E E T I K I N Q
aagtgtccttaCatacctaaatgtggaaaaaattttgaagaatccatgtccctgggtgaat
K C S Y I P K C G K N F E E S M S L V N
gttgtcatggaaaacttcaggaagtatcaacacttctcctgctattctgaccagaagga
V V M E N F R K Y Q H F S C Y S D P E G
aaccagaagagtgttatcctaacCaaactctacagttccaacgtgctgttccattcactc
N Q K S V I L T K L Y S S N V L F H S L
ttctggccaacctgtatgatggctgggggtgtggcaattgttgccatggtgaaacttaca
F W P T C M M A G G V A I V A M V K L T
cagtacctctccctactatgtgagaggatccaacggatcaatagataa
Q Y L S L L C E R I Q R I N R -

```

Published $\beta 2$ sequence Access Number NM_181361 (GenBank)

```

atgtttatatggaccagtggccggacctcttcatcttatagacatgatgaaaaaagaaat
M F I W T S G R T S S S Y R H D E K R N
atttaccagaaaaatcagggaccatgacctcctggacaaaaggaaaacagtcacagcactg
I Y Q K I R D H D L L D K R K T V T A L
aaggcaggagaggaccgagctattctcctgggactggctatgatgggtgtgctccatcatg
K A G E D R A I L L G L A M M V C S I M
atgtattttctgctgggaatcacactcctgcgctcatacatgcagagcgtgtggaccgaa
M Y F L L G I T L L R S Y M Q S V W T E
gagtctcaatgcaccttgctgaatgcgtccatcacggaaacatttaaTtgtctccttcagc
E S Q C T L L N A S I T E T F N C S F S
tgtgggtccagactgctggaaactttctcagtaccctgcctccaggtgtacgttaacctg
C G P D C W K L S Q Y P C L Q V Y V N L
acttcttccgggggaaaagctcctcctctaccacacagaagagacaataaaaaatcaatcag
T S S G E K L L L Y H T E E T I K I N Q
aagtgtccttaTatacctaaatgtggaaaaaattttgaagaatccatgtccctgggtgaat
K C S Y I P K C G K N F E E S M S L V N
gttgtcatggaaaacttcaggaagtatcaacacttctcctgctattctgaccagaagga
V V M E N F R K Y Q H F S C Y S D P E G
aaccagaagagtgttatcctaacAaaactctacagttccaacgtgctgttccattcactc
N Q K S V I L T K L Y S S N V L F H S L
ttctggccaacctgtatgatggctgggggtgtggcaattgttgccatggtgaaacttaca
F W P T C M M A G G V A I V A M V K L T
cagtacctctccctactatgtgagaggatccaacggatcaatagataa
Q Y L S L L C E R I Q R I N R -

```

Table 3.2 $\beta 2$ nucleotide and protein sequence comparisons: 3 point mutations (in red) which are silent and therefore not alter the protein sequence.

3.3.3. Engineering and cloning of $\beta 2$ -Aequorin.

Following the cloning of the $\beta 2$ subunit, SOE method was employed to combine $\beta 2$ and Aequorin sequences.

Initially, two complementary sequences were successfully joined to both whole sequences of $\beta 2$ subunit and Aequorin (Fig 3.6 A & B) obtaining enough to perform the next step. After a process of PCR optimisation, these products sharing complementary sequences were able to generate a good yield of the final $\beta 2$ -Aequorin protein (Fig 3.6 C). The upper band was cut, purified and inserted into pTarget. PCR screening of the vector after ligation with $\beta 2$ -Aequorin insert reveals which plasmids possess the correct sequence and orientation (Fig 3.6 D). Several vectors were sequenced giving in some cases frame-shift mutations or early stop codons. Among those, one of them originated with the full coding sequence, although with three point mutations.

Sequencing analysis showed three point mutations, one of them being silent. The other two produced amino acid modifications (Table 3.3) in positions 180 and 227 of the protein sequence (Table 3.4).

The hydrophobic character of the protein was assessed using the Kyte-Doolittle scale by means of the software *Molecular Toolkit* developed by Colorado State University. Analysis of the secondary structure and the hydrophobic prediction for the entire protein obtained (Fig 3.7 A) and the potential predicted structure (Fig 3.7 B) did not exhibit major

modifications as a result of these substitutions. A more detailed image (Fig 3.7 C) clearly shows the little impact of these modifications on the protein structure. Furthermore, no significant variations were noticed between the secondary structures of each individual protein and the fusion protein (Fig 3.7 A).

To summarise, $\beta 2$ and Aequorin sequences have been combined using genetic engineering techniques. The DNA sequencing analysis demonstrated that the resulting sequence was in frame with only two point mutations in the $\beta 2$ -part of the sequence. No major structural changes were detected in the AA sequence by the hydrophobic analysis.

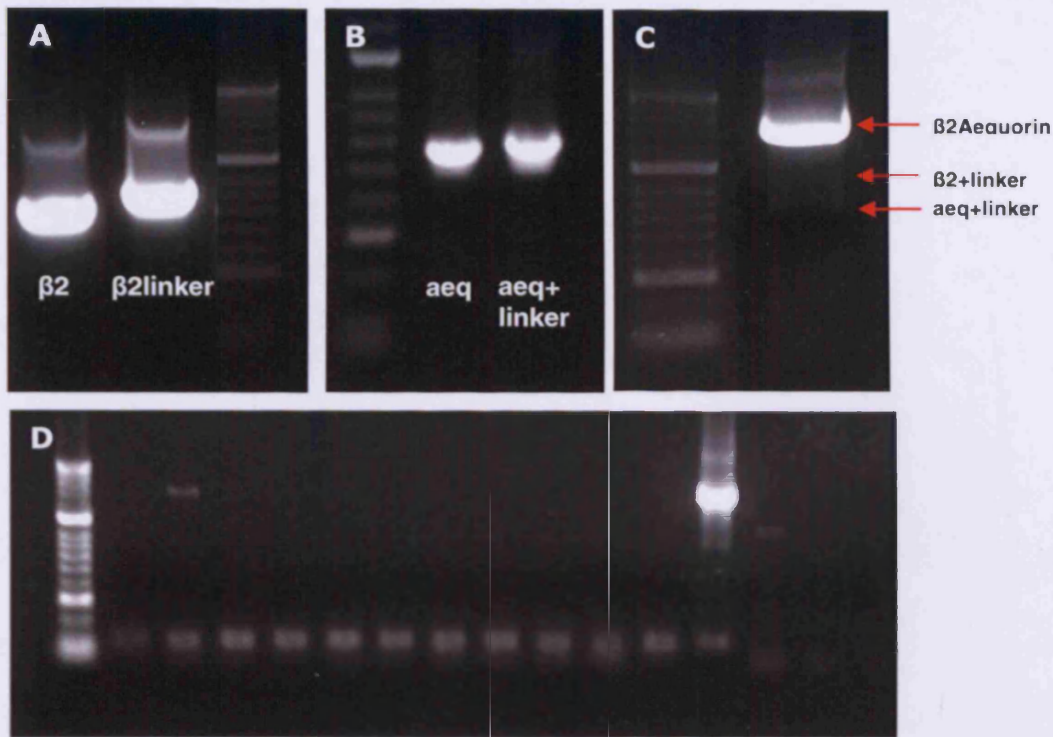
Fig 3.6. Engineering and cloning of $\beta 2$ -Aequorin.

Fig 3.6. Engineering and cloning of $\beta 2$ -Aequorin. (A & B) PCR bands showing the joint of the complementary extra sequence to both $\beta 2$ and Aequorin sequences. (C) SOE PCR product illustrates the successful fusion of both sequences and the starting templates remaining. (D) PCR screening of several colonies reveals two plasmids with the appropriate sequence length and orientation. Bands were compared to Hyperladder II.

Table 3.3 Amino acid modifications in the β 2-Aeq protein sequence.

AMINO ACID MODIFICATION

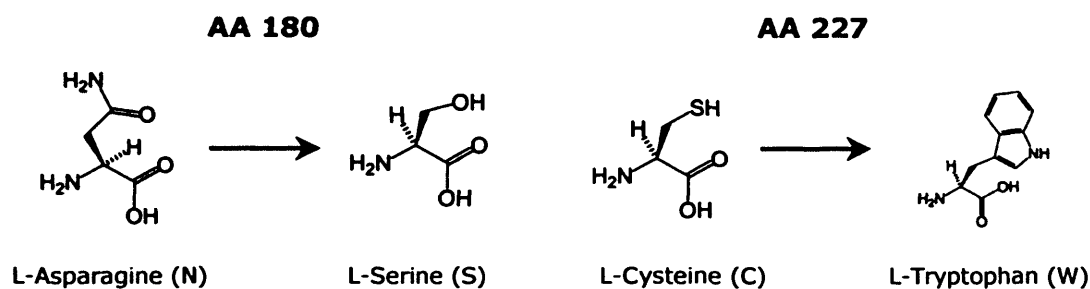


Table 3.3 The diagram above illustrates two amino acid modifications originated during the engineering and cloning procedure. The alteration from Asparagine to Serine maintains the polarity of the amino acid while the change between Cysteine and Tryptophan has altered partly the individual polarity of the amino acid from polar to non-polar respectively.

Table 3.4 β 2-Aequorin nucleotide/protein sequence comparisons

Sequencing result for β 2-Aequorin insert in pTarget

```

atgtttatatggaccagtggccggacctcttcatcttatagacatgatgaaaaaagaaat
M F I W T S G R T S S S Y R H D E K R N
atttaccagaaaatcagggacatgacctcctggacaaaaggaaaacagtcacagcactg
I Y Q K I R D H D L L D K R K T V T A L
aaggcaggagaggaccgagctattctcctgggactggctatgatgggtgtgctccatcatg
K A G E D R A I L L G L A M M V C S I M
atgtatcttctgctgggaatcacactcctgcgctcatacatgcagagcgtgtggaccgaa
M Y F L L G I T L L R S Y M Q S V W T E
gagtctcaatgcaccttgctgaatgctccatcacggaaacatttaattgctccttcagc
E S Q C T L L N A S I T E T F N C S F S
tgtgttcagactgctggaaactttctcagtaccctgcctccaggtgtacgttaacctg
C G P D C W K L S Q Y P C L Q V Y V N L
acttcttccggggaaaagctcctcctctaccacacagaagagacaataaaaaatcaatcag
T S S G E K L L L Y H T E E T I K I N Q
aagtgtcctatatacctaaatgtggaaaaaattttgaagaatccatgtccctgggtgaat
K C S Y I P K C G K N F E E S M S L V N
gttgtcatggaaaacttcaggaagtatcaacacttctcctgctattctgacctcagaagga
V V M E N F R K Y Q H F S C Y S D P E G
aGccagaagagtgttatcctaacaaaactctacagttccaacgtgctgttccattcactc
S Q K S V I L T K L Y S S N V L F H S L
ttctggccaacctgtatgatggctgggggtgtggcaattgttgccatgggtgaaacttaca
F W P T C M M A G G V A I V A M V K L T
cagtacctctccctactatgGgagaggatccaacggatcaatagaatgggtcaagcttaca
Q Y L S L L W E R I Q R I N R M V K L T
tcagacttcgacaacccaaaatggattggacgacacaagcacatgtttaattttcttgat
S D F D N P K W I G R H K H M F N F L D
gtcaaccacaatggaaggatctctcttgacgagatgggtctacaaggcgtccgatattgtt
V N H N G R I S L D E M V Y K A S D I V
ataaacaatcttgaggaacacctgaacaagccaaacgtcacaaagatgctgtagaagcc
I N N L G A T P E Q A K R H K D A V E A
ttcttcggaggagctggaatgaaatattggtgtagaaactgaatggcctgaatacatcgaa
F F G G A G M K Y G V E T E W P E Y I E
ggatggaaaagactggcttccgaggaattgaaaaggattcaaaaaaccaaatacacactt
G W K R L A S E E L K R Y S K N Q I T L
attcgtttatgggggtgatgcattgttcgatatcattgacaaaagaccaaataaggagctatt
I R L W G D A L F D I I D K D Q N G A I
tcaactggatgaatggaaagcatacaccaaatactgctggcatcatccaatcgtcagaagat
S L D E W K A Y T K S A G I I Q S S E D
tgcgaggaaacattcagagtgtgcgatattgatgaaagtggacagctcgatgttgatgag
C E E T F R V C D I D E S G Q L D V D E
atgacaagacaacatttaggattttggtacaccatggaCctgcttgcgaaaagctctac
M T R Q H L G F W Y T M D P A C E K L Y
ggaggagctgtcccctaa
G G A V P -

```


Theoretical $\beta 2$ -Aequorin sequence

```

atgtttatatggaccagtggccggacctcttcatcttatagacatgatgaaaaaagaaat
M F I W T S G R T S S S Y R H D E K R N
atttaccagaaaaatcagggaccatgacctcctggacaaaaggaaaacagtcacagcactg
I Y Q K I R D H D L L D K R K T V T A L
aaggcaggagaggaccgagctattctcctgggactggctatgatgggtgtgctccatcatg
K A G E D R A I L L G L A M M V C S I M
atgtattttctgctgggaatcacactcctgctgcatacatgcagagcgtgtggaccgaa
M Y F L L G I T L L R S Y M Q S V W T E
gagtctcaatgcaccttgctgaatgctccatcacggaaacatttaattgctccttcagc
E S Q C T L L N A S I T E T F N C S F S
tgtggtccagactgctggaaactttctcagtaccctgcctccaggtgtacgttaacctg
C G P D C W K L S Q Y P C L Q V Y V N L
acttcttcgggggaaagctcctcctaccacacagaagagacaataaaaaatcaatcag
T S S G E K L L L Y H T E E T I K I N Q
aagtgtcctatatacctaataatgtggaaaaaattttgaagaatccatgtccctgggtgaat
K C S Y I P K C G K N F E E S M S L V N
gttgtcatggaaaacttcaggaagtatcaacacttctcctgctattctgaccagaagga
V V M E N F R K Y Q H F S C Y S D P E G
aAccagaagagtgttatcctaacaaaactctacagttccaacgtgctgttccattcactc
N Q K S V I L T K L Y S S N V L F H S L
ttctggccaacctgtatgatggctgggggtgtggcaattgttgccatgggtgaaacttaca
F W P T C M M A G G V A I V A M V K L T
cagtacctctcctactatgTgagaggatccaacggatcaatagaatgggtcaagcttaca
Q Y L S L L C E R I Q R I N R M V K L T
tcagacttcgacaacccaaaatggattggacgacacaagcatatgttcaattttcttgat
S D F D N P K W I G R H K H M F N F L D
gtcaatcacaatggaagaatctccttgacgagatgggtctacaaggcgtctgatattgtt
V N H N G R I S L D E M V Y K A S D I V
ataaacaatcttggagcaacacctgaacaagccaaacgacacaaaagacgtgtagaagct
I N N L G A T P E Q A K R H K D A V E A
ttcttttggaggagctggaatgaaatatgggtgtagaaactgaatggcctgaatacatcgaa
F F G G A G M K Y G V E T E W P E Y I E
ggatggaaaagactggctaccgaagaattggaaaggtattcaaaaaaccaaattcacactt
G W K R L A T E E L E R Y S K N Q I T L
attcgtttatgggggtgatgcattgttcgatatcattgacaaagacccaaaatggagctatt
I R L W G D A L F D I I D K D Q N G A I
acactcgatgaatggaaagcatataccaaatctgctggcatcatccaatcgtcagaagat
T L D E W K A Y T K S A G I I Q S S E D
tgcgaggaaacattcagagtgtgcatattgatgaaagtggacagctcgatgttgatgaa
C E E T F R V C D I D E S G Q L D V D E
atgacaagacaacatttaggattttggtacaccatggaTcctgcttgcgaaaagctctac
M T R Q H L G F W Y T M D P A C E K L Y
ggaggagctgtcccctaa
G G A V P -

```

Table 3.4 $\beta 2$ -Aequorin nucleotide and protein sequence comparisons: 3 point mutations (in red), two of which are point mutations causing an aminoacid change and the third is a silent mutation which maintains the aminoacid unmodified.

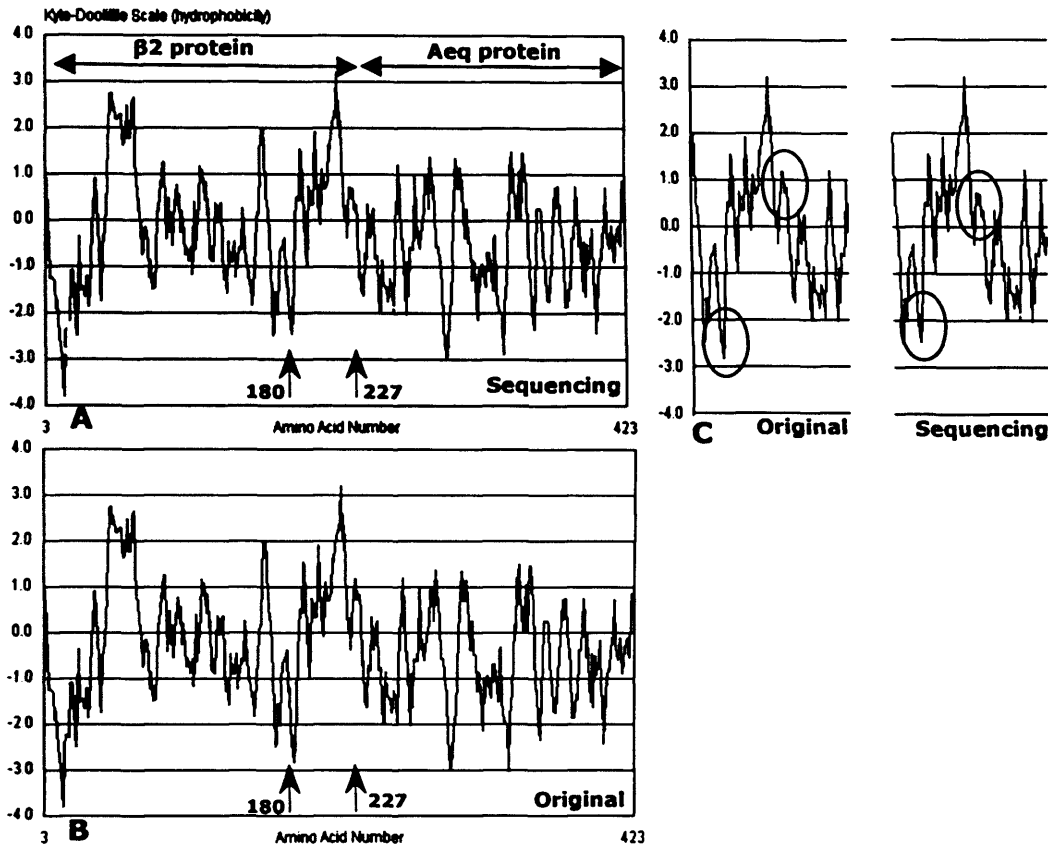
Fig 3.7 Hydropathy analysis of the $\beta 2$ subunit.

Fig 3.7 Hydropathy analysis of the $\beta 2$ subunit. (A & B) represent hydropathy plots of the entire amino acid sequence of the protein experimentally obtained and the theoretically predicted one respectively. Arrows indicate where amino acid modifications (180 & 227) occurred. (C) shows the differences found (indicated with circles) between both in more detail. All plots were determined according to Kite-Doolittle algorithm with a window size of seven. Regions with values above 0 are hydrophobic in character.

3.3.4. Expression of $\beta 2$ -Aequorin in a cell-free system.

A cell-free system was employed to determine whether $\beta 2$ -Aeq was capable of emitting light in response to calcium.

In vitro transcription/translation was performed using the TNT Protein script II T7 system and activity was determined as the total number of counts emitted in the presence of coelenterazine when exposed to calcium as described in Materials & Methods 2, section 2.4.1.2. Experiments for each construct were performed in triplicates.

$\beta 2$ -Aeq emitted thousands of light counts when it was exposed to calcium. The cytosolic Luciferase-Aequorin which produces similar count response to aequorin was used as a positive control. The number of photons generated by $\beta 2$ -Aeq was ten times lower than those obtained from Luciferase-Aequorin (Fig 3.8).

The light emitted by $\beta 2$ -Aequorin using the cell-free system demonstrated that the aequorin moiety of the construct was functional at a protein level.

The precise detection of Ca^{2+} responses requires that aequorin constructs emit sufficient counts to discriminate between Ca^{2+} signals and variations in background noise. Since $\beta 2$ -Aequorin exhibited less light emission than Luc-Aeq, it was vital to maximise the number of counts obtained. The conditions of Aequorin reconstitution may significantly increase the number of counts emitted by these constructs.

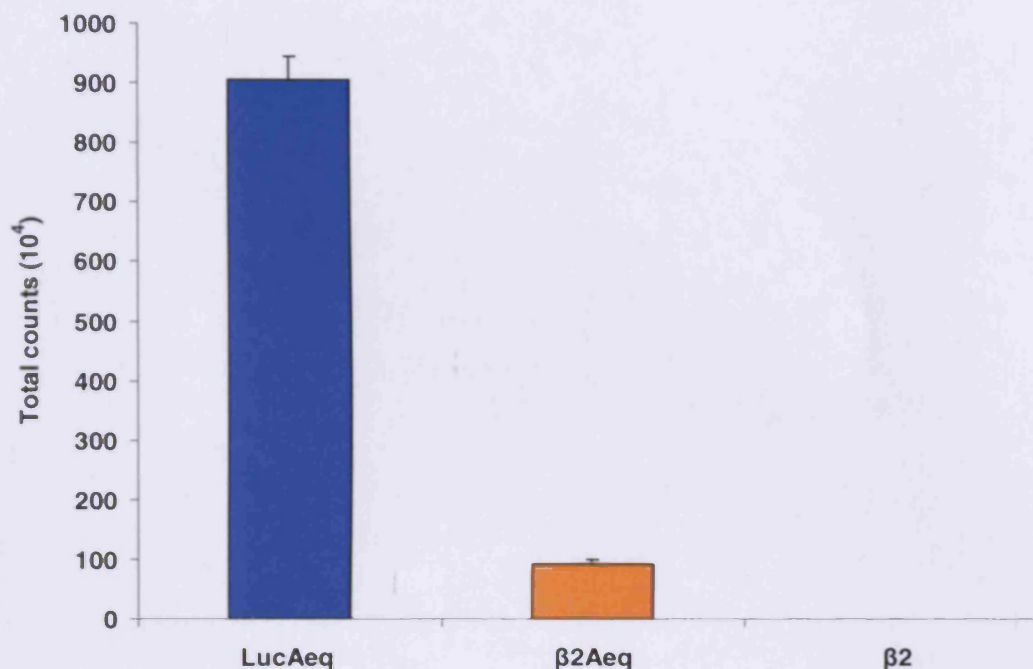
Fig 3.8. Cell-free expression of β 2Aeq and LucAeq.

Fig 3.8. Cell-free expression of β 2Aeq and LucAeq. Expression of β 2Aeq using a transcription/translation system (TNT Protein Script II) confirms emission of light when exposed to calcium proving that β 2 and Aequorin has been successfully assembled. LucAeq exhibits a light emission 10 times higher than β 2Aeq in a cell-free system. β 2 subunit was used as a control. Mean and SEMs were extracted from three experiments. Data from two sets of experiments (LucAeq/ β 2Aeq & β 2Aeq/ β 2) have been normalised.

Consequently, the best conditions for aequorin reconstitution were then assessed.

3.3.5. Evaluation of reconstitution conditions for $\beta 2$ -Aeq.

The number of counts emitted during a complete experiment depends on the conditions in which aequorin has been reconstituted. A high number of counts enables the accurate measurement of minor variations during the course of the experiment. On the contrary, a low level of counts may cause difficulties to distinguish between Ca^{2+} signals and background noise. Therefore, the optimal conditions for aequorin reconstitution were assessed in this set of experiments.

The best conditions for aequorin reconstitution were experimentally evaluated using three different parameters: coelenterazine concentration, Ca^{2+} concentration in the medium and time-course. Both constructs were also compared to determine whether differences in light emission were dependent of these factors.

HEK293 α cells in suspension expressing either Luc-Aeq or $\beta 2$ -Aeq were incubated for periods between 1 to 4 hours in different medium (1 mM EGTA, normal medium or 1.3 mM Ca^{2+} medium) containing 2 μM coelenterazine as described in Section 3.2.7. Similarly, the effects of different coelenterazine concentrations ranging from 1 to 10 μM was evaluated each hour during a 4 h period. The total light counts were acquired using the home-built luminometer after addition of NP40 lysis

solution. The results are the mean and SEMs of three different experiments.

After one hour incubation with coelenterazine, the number of light counts generated by the $\beta 2$ -Aeq construct decreased over the course of time independently of the type of medium used (Fig 3.9 A). Understandably, a greater reduction was observed when calcium was present in the medium whereas no significant difference was noticed between EGTA and normal medium. In the case of Luc-Aeq, a decline of light emission was obtained only in medium with calcium added. Counts remained barely unchanged when cells were suspended in EGTA or normal medium (Fig 3.9 B). The differences in aequorin reconstitution between the EGTA-medium and the Ca^{2+} -medium incubation were, for both constructs, significant only after 3-4 hours incubation. One hour incubation time was chosen as the best option because the maximal light emission was obtained during that period. Incubation in EGTA-medium also maximised the number of counts generated by the aequorin constructs (Fig 3.9 C).

A trend of coelenterazine dependency was observed following a similar pattern for both proteins: maximum light emission reached at 5 μM followed by a decrease at 10 μM for both proteins (Fig 3.11 A & B). Since this difference was no significant for both constructs, a coelenterazine concentration of 2 μM was selected to perform

Fig 3.9 Reconstitution efficiency of aequorin constructs in HEK293 in different media in the presence of coelenterazine.

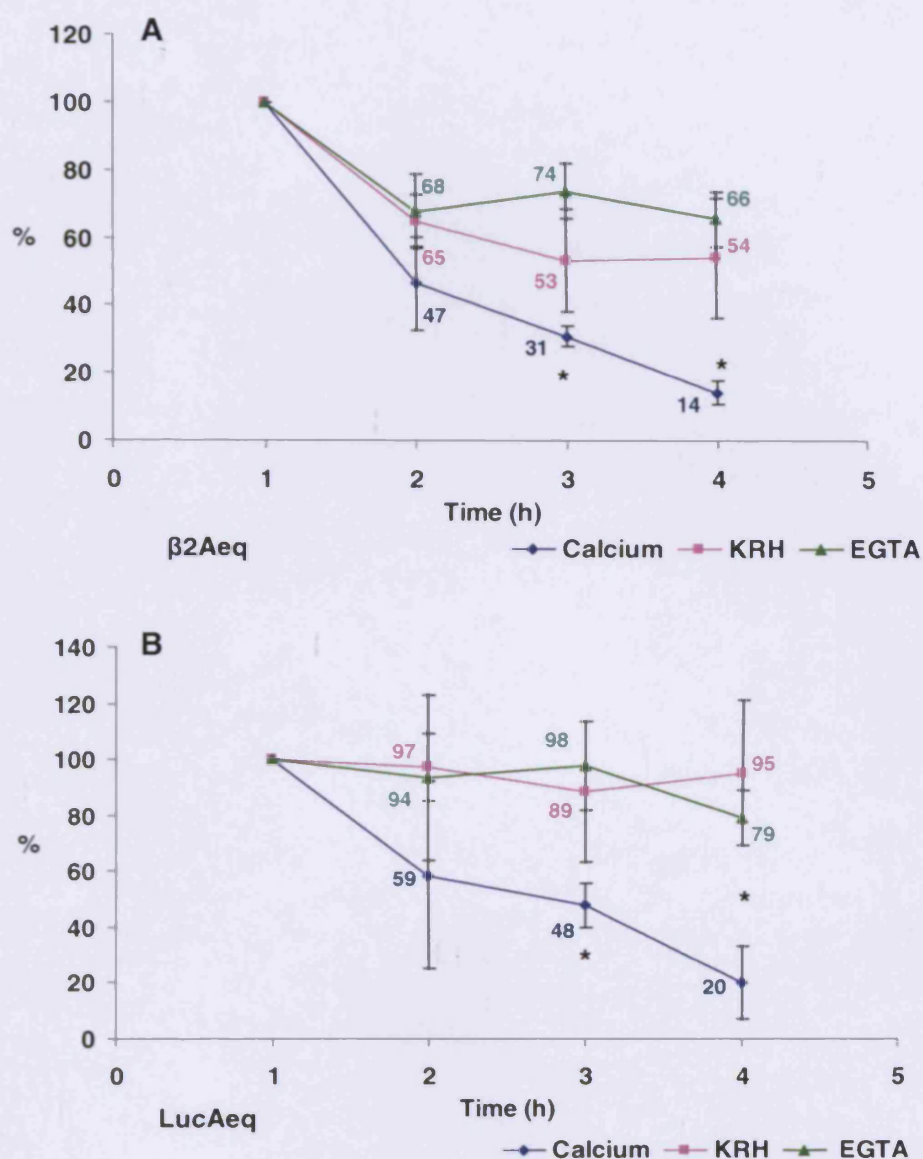


Fig 3.9 Reconstitution efficiency of aequorin constructs in HEK293 in different media in the presence of coelenterazine.

Time course reconstitution of $\beta 2\text{Aeq}$ (A) and LucAeq (B) is expressed as percentage of that obtained after 1 hour in the same medium. Efficiency of reconstitution of each chimera is expressed as percentage of the value obtained in Ca^{2+} -free medium. A major declined is observed for $\beta 2\text{Aeq}$ in all mediums while for LucAeq only occurred in Ca^{2+} medium. Subsequently, both constructs followed similar trend. Concentration of coelenterazine was 2 μM . * statistically significant in comparison to EGTA.

Fig 3.10 Reconstitution efficiency of aequorin constructs in HEK293 in different media in the presence of coelenterazine.

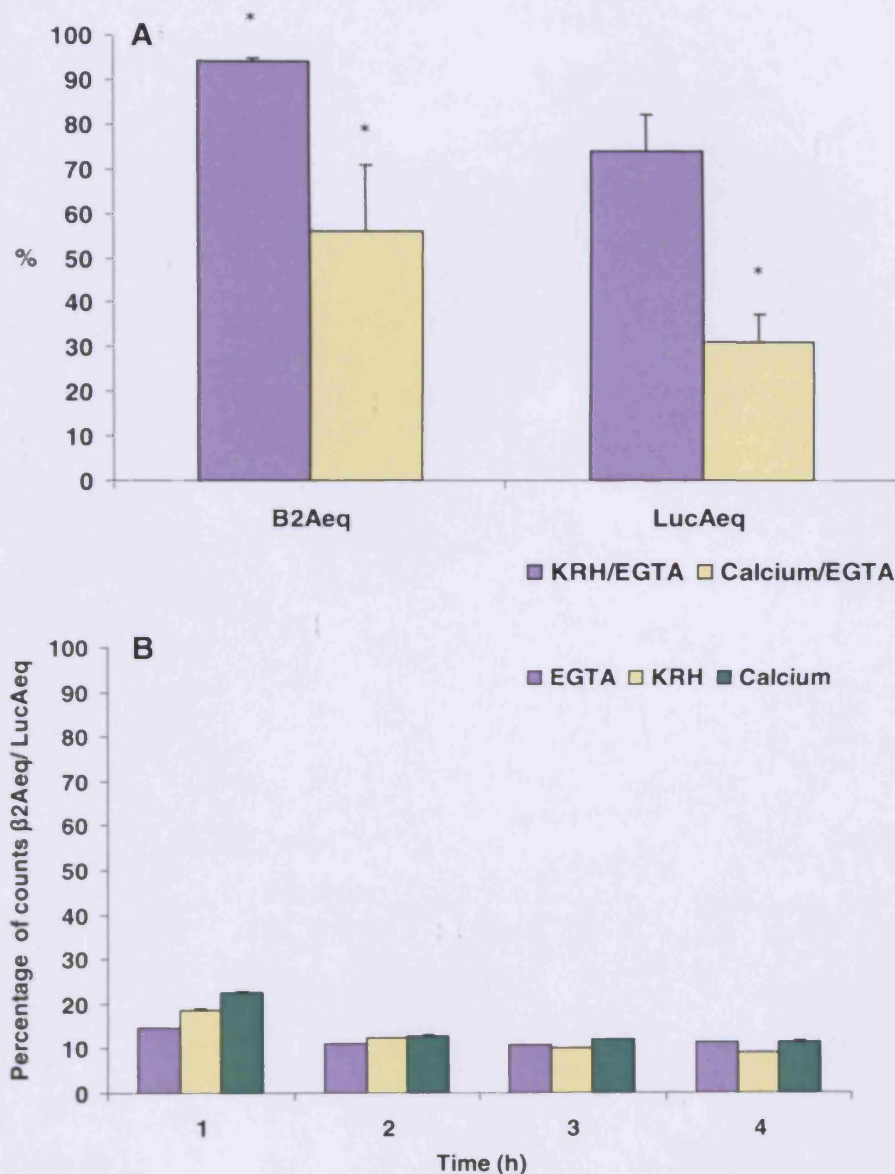


Fig 3.10 Relative reconstitution efficiency of aequorin constructs in HEK293 in different media in the presence of coelenterazine.

(A) Relative efficiency of reconstitution of each chimera is expressed as percentage of the value obtained in Ca^{2+} -free medium after 1 h (B). Relative efficiency of both chimeras reconstituted in media containing Ca^{2+} (1.3 mM), EGTA (1 mM) or with nothing added at different time points in the presence of coelenterazine (2 μM). * significant ($p < 0.05$) when compared to EGTA/EGTA (100 %).

Fig 3.11 Effects of coelenterazine concentration in the reconstitution efficiency of aequorin constructs in HEK293.

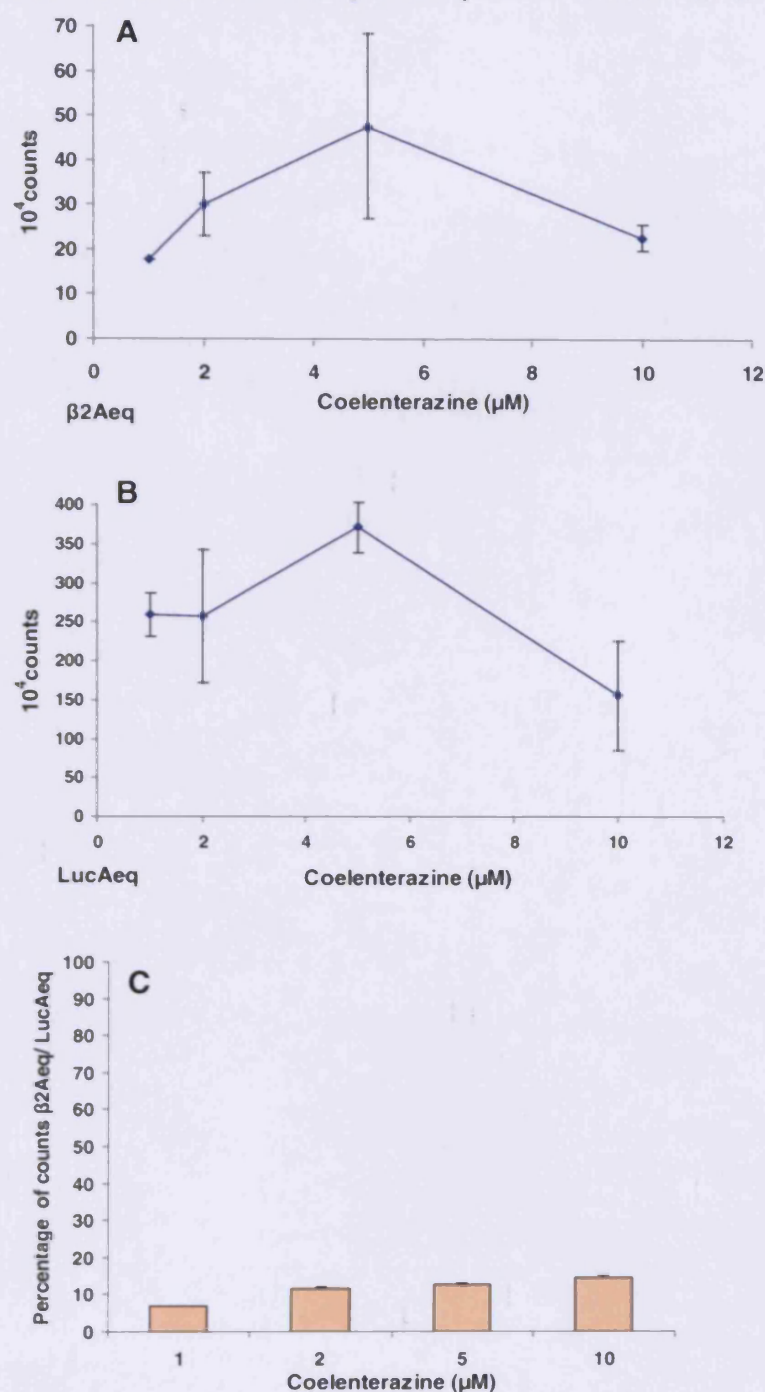


Fig 3.11 Effects of coelenterazine concentration in the reconstitution efficiency of aequorin constructs in HEK293.

Aequorin reconstitution in both $\beta 2Aeq$ and LucAeq was dependant of coelenterazine showing a maximum light emission peak at 5 μM concentration (A & B). Additionally, both exhibited a decline at 10 μM coelenterazine concentration. Relative light counts of both chimeras reconstituted showed little variation with the concentration at values above 2 μM (C). Graphs represent mean values and SEMs of three experiments.

reconstitution of aequorin in living cells enabling us to compare our data with previous research using Luc-Aeq (George *et al.*, 1998).

When the reconstitutions of Luc-Aeq and $\beta 2$ -Aeq were compared, Luc-Aeq showed a greater reduction of light emission than $\beta 2$ -Aeq in either normal or Ca^{2+} medium (Fig 3.10 A). The relative light emission amounts for the respective proteins remained at the same level (~10 %) for the whole period regardless of the medium used (Fig 3.10 B). There was little change for the average of the relative light emission for values of coelenterazine concentration higher than 1 μM (Fig 3.11 C).

The experimental conditions for Aequorin reconstitution were determined as follows: incubation in EGTA-medium for 1 hour in the presence of 2 μM coelenterazine.

3.3.6. Subcellular distribution of recombinant aequorin.

On occasions, the addition of a foreign protein sequence may alter the innate features of the native protein such as the correct targeting (Myers *et al.*, 1999). To determine whether $\beta 2$ -Aeq protein remains bound to the plasma membrane, a subcellular fractionation methodology was performed.

The subcellular fractionation approach adopted in this work involved the centrifugation of the cell lysate at a high speed. Following the lysis of the cells, the cell suspension was subjected to centrifugation at 30,000 $\times g$ for 30 min at 4 °C in order to separate the proteins in the

cytosol from those in the membrane. Cytosolic proteins are mainly in the supernatant while the pellet contains proteins from cellular membranes and other organelles such as nucleus, ER, Golgi and lysosomes.

The cytosolic vector Luc-Aeq served as a positive control to evaluate the efficacy of this method to separate the membrane proteins from the cytosolic ones. Initial experiments were performed by only lysing the cells with three freeze-thaw cycles. This simple approach showed low efficiency. The membrane fraction of the Luc-Aeq protein was above 30 % for HEK293 cells, indicating a poor cell lysis.

An additional step, which involved the passage of the cell suspension through a narrow-gauge syringe, was introduced to improve efficiency. As a result, only a residual proportion of Luc-Aeq was found in the membrane fraction demonstrating the effectiveness of the improved method. Furthermore, β 2-Aeq was recovered almost exclusively in the membrane fraction supporting the correct targeting of the recombinant protein (Fig 3.12).

Our data proved that the β 2-Aeq protein successfully targeted the membrane.

Fig 3.12 Subcellular fractionation of HEK 293 transfected with either β 2Aeq or LucAeq.

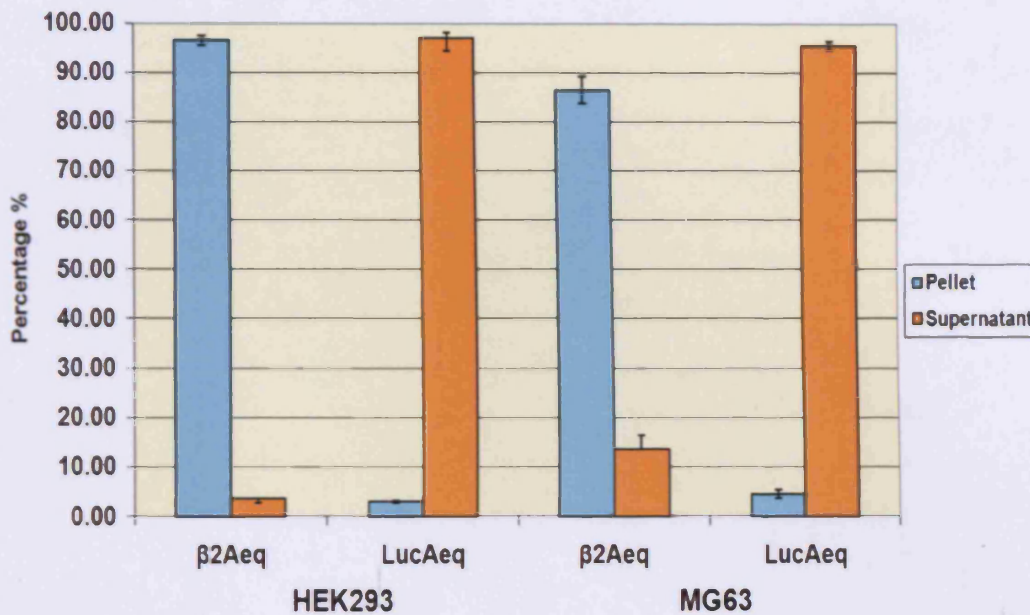


Fig 3.12 Relative proportion of protein in membrane vs. cytosol. Assessment of the relative proportion of the β 2Aeq and LucAeq in HEK293 and MG63 cell lines was estimated as the percentage of the total counts obtained in each fraction divided by the sum of the counts from the two fractions. The total counts from untransfected cells used as a control were subtracted from the sample values. Values and standard error were extracted from three different experiments.

3.3.7. Effects of $\beta 2$ -Aeq in cell growth.

Expression of foreign proteins may modify cell functions such as growth; i.e. GFP seems to instigate apoptosis in eukaryotic cells (Liu *et al.*, 1999). In order to assess if $\beta 2$ -Aeq produced cell toxicity or an impairment of cell growth, an MTS proliferation assay was carried out in HEK293 cells.

The effects of $\beta 2$ -Aeq on cell viability were evaluated using a MTS assay. In the MTS proliferation assay, HEK293 cells expressing pTarget vectors showed significantly lower growth rate than control cells (Fig. 3.13). All three vectors tested showed the same decline. No significant effects were observed by only using the transfection reagent Lipofectamine. Similar decrease was detected by simple observation on flasks expressing $\beta 2$ -Aeq when compared to normal cells. These evidence indicate that the decrease in cell number is probably caused uniquely by the expression of foreign DNA and not because of the lipid-mediated transfection process.

The MTS assay revealed that the transfection of the $\beta 2$ -Aeq vector reduced cell number in a similar manner to the $\beta 2$ plasmid.

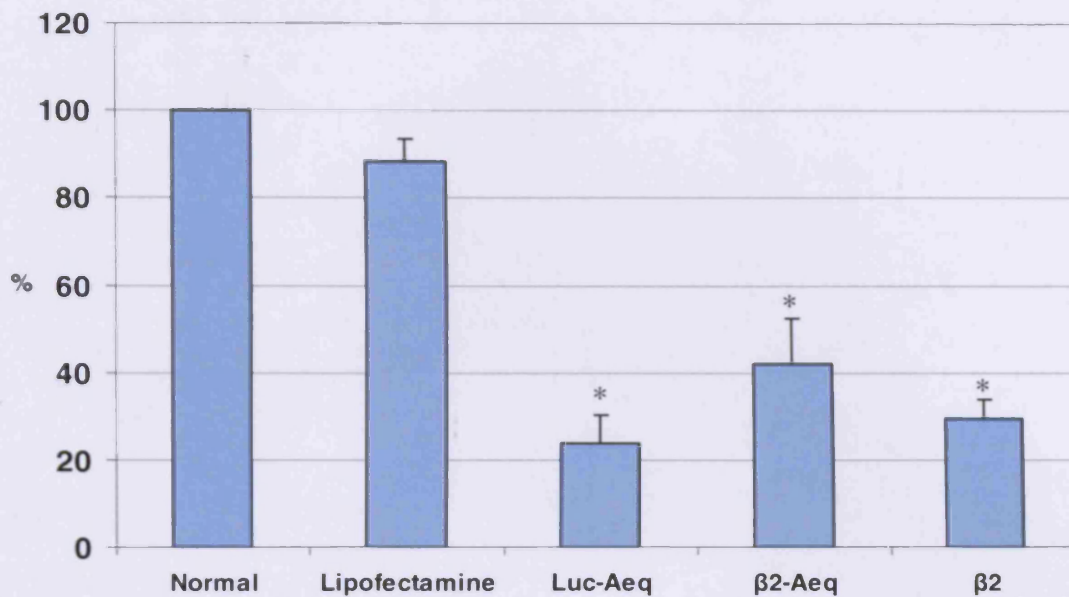
Fig 3.13 Effects of $\beta 2$ -Aeq transfection on cell number.

Fig 3.13 Effects of $\beta 2$ -Aeq transfection on cell number. MTS assay of cell proliferation shows decrease in HEK293 cell number by incubation with Luc-Aeq, $\beta 2$ -Aeq or $\beta 2$ subunit constructs. Differences between these plasmids are statistically insignificant. Lipid mediated transfection in the absence of DNA reveals a small non-significant decrease in cell number. Data represents mean \pm SEM of five experiments performed in triplicate. *- significant difference $p < 0.05$ compared to Normal Medium and Lipofectamine controls.

3.4 DISCUSION

3.4.1. Cell Assessment.

The different BK channel properties such as channel activation, response to blockers and activators, surface expression and calcium sensitivity are greatly influenced by the exact α subunit isoform present and its assembly with the accessory beta subunits. Therefore, it is crucial to know the exact subunit composition of the cell lines in order to establish whether $\beta 2$ -Aeq expression may be altered by other subunits or remain unaffected. In addition, the presence of certain subunits may modify the pharmacology and response of the BK channel which in turn may cause changes on cell function including Ca^{2+} signalling (Meera *et al.*, 1996 & 2000).

The results presented here provide evidence for the first time of the presence of the all four BK β subunits in MG63. These data also indicate that not all isoforms of the α subunit are expressed in MG63, isoform corresponding to GeneBank U11717 being the most probable one. Sequencing however must be performed to confirm this. It has been reported that α subunit splice variants may impede the normal expression of the β subunits (Zarei *et al.*, 2001). Since this splice variant coincides with the one already verified using RT-PCR and electrophysiological techniques in the stable-transfected HEK293 cell line, the α and $\beta 2$ subunits should express and co-assemble in a similar

manner. Therefore, both cell lines were suitable to be transfected with $\beta 2$ constructs.

In addition, this study gives new insights into the subunit composition of BK channels in osteoblasts. These findings, together with the determination of the splice variant form, contribute to gaining a better understanding of the phenomenology and pharmacology of the channel.

3.4.2. Engineering of $\beta 2$ -Aeq and functional evaluation.

Following the acquisition and cloning of the whole coding sequence of the $\beta 2$ subunit, a novel recombinant protein was successfully created comprising the $\beta 2$ subunit and Aequorin. A protein prediction analysis found no major differences due to the point mutations introduced in the $\beta 2$ subunit part of the sequence during the production of this construct. The aequorin part of the protein remained unchanged.

When two heterogeneous proteins are combined to create a new recombinant protein, functional differences may be expected as a result. Therefore, a subsequent experimental investigation was conducted to assess the properties and functionality of the new recombinant protein.

The study of the functional aspects of the bioluminescent part was carried out using a cell-free system. The *in vitro* transcription/translation system demonstrated that the main properties of aequorin were conserved in the $\beta 2$ -Aequorin protein. Like aequorin, light emission was

obtained when $\beta 2$ -Aequorin was exposed to calcium. The new protein showed low light emission efficiency when compared to Luc-Aeq which exhibits bioluminescent activity similar to the native aequorin (Badminton *et al.*, 1995).

Maintenance of correct protein targeting is crucial for cell function. The targeting of transmembrane proteins like the $\beta 2$ subunit occurs by means of the hydrophobic membrane-spanning domains which anchor it within the cell membrane. Based on the analysis of its hydrophobic character, neither the addition of the aequorin protein nor the amino acid modifications had a significant impact on the overall hydrophobicity pattern of the $\beta 2$ section of the protein. Therefore, the targeting properties of the protein should remain unchanged.

This prediction was experimentally assessed by means of a subcellular fractionation methodology. This approach produced a high ratio of the cytosolic aequorin protein in the expected fraction proving the effectiveness of the adopted methodology. The cellular location of the $\beta 2$ -Aeq in the membrane was also confirmed with only a minimum amount been found in the cytosolic fraction (Fig. 3.10). The study was performed in two different cell lines, HEK293 and MG63, demonstrating that the cellular location of the $\beta 2$ subunit is probably tissue independent.

These results provide strong evidence in favour of the localisation of the $\beta 2$ -Aeq protein in the plasma membrane. Nevertheless, it must be

mentioned that they do not discriminate whether $\beta 2$ -Aeq is located in the plasma membrane or other intracellular compartments such as ER, Golgi or lysosomes. The $\beta 1$ subunit, which maintains 82 % homology with the $\beta 2$, has been reported to be expressed primarily in conjunction with the α subunit (Hartness *et al.*, 2003; Morrow *et al.*, 2006), in particular the QEERL splice variant (Kim *et al.*, 2007). The α subunit used in this thesis contains this amino acid sequence which is mostly expressed in the plasma membrane (Kim *et al.*, 2007). Moreover, $\beta 1$ subunit tagged with GFP in the C-terminus exhibited similar pattern of expression and electrophysiological properties. In recent studies using co-immunofluorescence, it has been shown that the $\beta 2$ subunit expressed alone was mostly retained in the ER (Lv *et al.*, 2008). On the other hand, if the α subunit was present, the $\beta 2$ subunit could successfully reach the plasma membrane. The values obtained in this study (~90%) for localisation of the native $\beta 2$ subunit in the plasma membrane were consistent with our results. Moreover, only modifications in the N-terminus of the subunit seemed to alter its targeting to the plasma membrane.

The MTS assay carried out in transfected HEK293 cells revealed a significant decrease in cell number. Since incubation with Lipofectamine showed only a marginal decline, the lower number of cells is probably due to the expression of foreign DNA. Similar results were observed using three different vectors: the cytosolic Luc-Aeq, the native $\beta 2$ subunit and the recombinant $\beta 2$ -Aeq. Two of the vectors targeted

different subcellular compartments (Luc-Aeq, cytosol & $\beta 2$ -Aeq, membrane) suggesting that this effect was not produced by either cytotoxicity of protein overexpression in the cytosol or structural changes in the cell membrane. The native $\beta 2$ protein generated the same result indicating that this was probably not caused by the expression of artificially modified proteins. A reason for the difference in cell growth may be that the overexpression of any foreign DNA in the cells may impair or slow down cellular processes. All experiments in this work were expressed as percentage of the total or normalised to the cell number. Consequently, the reduction in cell number should not compromise the results obtained.

Since no significant difference was observed between $\beta 2$ -Aeq and $\beta 2$ transfected HEK293 cells, our data demonstrate that the incorporation of the Aequorin sequence to the $\beta 2$ subunit has not altered cellular functions such as cell growth.

3.4.3. Assessment of best conditions for aequorin reconstitution.

The conditions to achieve the maximum light output from the aequorin vectors were also experimentally evaluated. Time-course assessment showed that after the first hour, counts remained similar in the case of Luc-Aeq for EGTA and normal medium and decreased in Ca^{2+} medium. $\beta 2$ -Aeq presented a decline in all mediums, greater with Ca^{2+} medium. Although a potential loss of aequorin stability or protein degradation may partly for these differences, a more probable explanation is that the

rate of aequorin consumption surpassed the rate of aequorin reconstitution after the first hour. In the first hour, both constructs emitted significantly more counts when incubated in EGTA. Since coelenterazine concentrations did not exhibit a significant impact in the number of counts, 2 μ M was selected as the best option in order to be able to compare with previous studies using Luc-Aeq (George *et al.*, 1998). Consequently, the optimal conditions for both proteins were incubation in EGTA medium for 1 hour in the presence of 2 μ M.

3.4.4. Differences between β 2-Aeq and Luc-Aeq.

The main difference noticed between both proteins was a 10-fold lower light emission obtained from β 2-Aeq than from Luc-Aeq. Amino acid modifications have previously reported to cause this type of alterations (Watkins NJ & Campbell AK, 1993). However, since the amino acid sequence of the aequorin section remained unchanged, the difference was not attributed to amino acid variations.

Protein degradation may account for this difference because proteolysis activity depends on the organelle location of the protein (Badminton *et al.*, 1995; Jeffery *et al.*, 2000). However, since proteases are generally induced by Ca^{2+} and incubation in different Ca^{2+} concentration showed little effect on the relative light emission obtained (Fig. 3.7 B), proteolysis was probably not an important factor on this difference in light emission. Similarly, the stability of the two photoproteins may have been different resulting in a greater decrease of the active protein of

one of the constructs over the other (Badminton *et al.*, 1995). Nevertheless, no important change was detected in the relative light emission during the four hour period (Fig. 3.7 B) indicating that the stability of both photoproteins was analogous.

Different patterns of protein expression may also produce the difference in light emission detected. Nevertheless, similar results (10 times higher number of counts) have been obtained in three very distinct circumstances: a cell-free system, isolated proteins and living cells (See Chapter 3, sections 3.4.4 and 3.4.5). It is unlikely that proteins are expressed in the same manner in such heterologous systems.

One feasible explanation might be that the cytosolic carboxyl terminus of the $\beta 2$ subunit is only 20 amino acids long, based on the predicted structure (UniProtKB / Swiss-Prot entry Q9Y691). This cytosolic domain which is normally the flexible part of the protein might not be long enough to confer sufficient freedom to the aequorin structure to fold appropriately. Previous studies showed that when connexin26, a plasma membrane protein with 26 aa cytosolic tail, was linked to aequorin, the resulting protein lost most of the chemiluminescent activity (Martin *et al.*, 1998). In this case, the addition of a larger tail to combine both proteins restored the chemiluminescent emission of the aequorin moiety (George *et al.*, 1998). Interestingly, the opposite effect was detected working with EGFP and aequorin targeted to the cytosol: a spacer of 36 aa between sequence completely abolished the light

emission which did not occur with only 18 aa (Bermudez-Fajardo, 2002). One possible reason might be that the proper folding of the aequorin protein was impeded by a lack of flexibility in connection with its correct assembly into the plasma membrane.

To better understand the differences between both constructs, a comparison between reconstitution of $\beta 2$ -Aeq and Luc-Aeq was also conducted providing the following results. The effects of the medium used during aequorin reconstitution (EGTA, Ca^{2+} or nothing added) between $\beta 2$ -Aeq and Luc-Aeq differ. The main difference between both proteins was the reduction of light counts of $\beta 2$ -Aeq in all different media which did only occur in the presence of Ca^{2+} for Luc-Aeq. This result may be explained by either a lower reconstitution of $\beta 2$ -Aeq in EGTA medium or a higher consumption of Luc-Aeq in the absence of EGTA. This fact may be attributed to one being located in the cytosol and the other embedded in the plasma membrane.

Aequorin reconstitution of both $\beta 2$ -Aeq and Luc-Aeq displayed a similar pattern of behaviour when the respective average readings were compared under different conditions of media, incubation times and coelenterazine concentration. Our data indicate that the rate of aequorin reconstitution/consumption under the same conditions is very similar for both recombinant proteins. Through these results, it is clear that the modifications of the aequorin moiety causing the 10 fold reduction of $\beta 2$ -Aeq light emission have no evident effect on the speed rate of

aequorin regeneration from apoaequorin, or its ability to bind coelenterazine. If a potential loss of aequorin stability or protein degradation occurred during the length of the experiments, they produced similar effects on both constructs.

3.4.4. Conclusions.

In summary, a novel recombinant protein has been obtained by combining the BK channel $\beta 2$ subunit and the aequorin sequences. The fusion protein exhibits the inherent properties of both individual proteins: Ca^{2+} -dependent light emission, binding to coelenterazine and reconstitution rates as aequorin; plasma membrane targeting and cell growth patterns similar to the $\beta 2$ subunit. The optimal conditions for $\beta 2$ -Aeq reconstitution have also been determined in order to carry out the following cell transfection experiments. In addition, the differences between two aequorin-linked recombinant proteins have been assessed. This study brings new insights into the extent that aequorin properties are retained when it is combined with other proteins.

CHAPTER 4

EVIDENCE FOR LOCAL REGULATION OF THE CALCIUM SIGNALS IN THE PROXIMITY OF THE BK CHANNEL IN LIVING CELLS

4.1 INTRODUCTION

Since the first studies conducted by Ringer (1883), an enormous amount of evidence has demonstrated the essential role of calcium in controlling a multitude of cellular functions. Indeed minor variations of intracellular Ca^{2+} signals can initiate or modulate many cellular processes including neurotransmitter release, apoptosis and ion channel modulation (See Chapter 1, sections 1.1.2. & 1.1.3.). These Ca^{2+} signals are normally generated in response to extracellular stimuli such as hormones, neurotransmitters, agonists and temperature. Numerous proteins operate in conjunction with intracellular organelles to accurately control Ca^{2+} signals across the cell. The Ca^{2+} concentration is not homogeneously distributed within the cell and high calcium cell compartments exist such as ER, mitochondria and sub-plasma membrane domains (Button & Eidsath, 1996; Golovina & Blaustein, 1997). Consequently, the intracellular Ca^{2+} responses are not uniform and vary widely in strength and range. They may also be repetitive (Ca^{2+} oscillations) or localised. Local Ca^{2+} transients may either be concealed or propagate gradually to the rest of the cell.

Aequorin has been a fundamental tool for studying the complex mechanism of Ca^{2+} signalling. Since the isolation and cloning of its DNA sequence (Inouye *et al.*, 1985), several recombinant photoproteins have been engineered using the aequorin moiety. They have been primarily employed to target defined intracellular locations such as the nucleus

(Badminton *et al.*, 1995), the endoplasmic reticulum (Kendall *et al.*, 1992), the Golgi apparatus (Pinton *et al.*, 1998) and the mitochondria (Rizzuto *et al.*, 1992). Of particular interest to our research are those studies in which aequorin was connected to plasma membrane-bound proteins. For this purpose, aequorin has been fused to the following partners: a serotonin 5-HT receptor (Daguzan *et al.*, 1995), an adenylyl cyclase (Nakahashi *et al.*, 1997), the neural synaptosome-associated protein SNAP-25 (Marsault *et al.*, 1997), various connexins (George *et al.*, 1998) and endothelial nitric-oxide synthase (eNOS) (Lin *et al.*, 2000). All these studies have revealed the presence of a wide range of heterogeneous Ca^{2+} environments within the cell. These findings have been also supported by complementary studies using fluorescent Ca^{2+} sensitive dyes (Golovina and Blaustein, 1997; Graier *et al.*, 1998).

All this evidence emphasises the remarkable versatility of cellular Ca^{2+} signalling. However, cells also need to trigger selective responses. The importance of creating local Ca^{2+} microdomains to control specific cellular responses has been highlighted by recent reports (Rizzuto & Pozzan, 2006; Clapham, 2007; Parekh, 2008). These local Ca^{2+} microdomains provide a means for rapid and selective activation of specific cellular processes. The BK channel also needs this tight Ca^{2+} regulation to modulate its precise mechanism of activation. Therefore, new tools to measure the local Ca^{2+} concentration affecting the channel such as the $\beta 2$ -Aeq chimera developed in this thesis are required.

This chapter aims to examine the local regulation of Ca^{2+} signals in the vicinity of the BK channel in cultured cells using the $\beta 2$ -Aequorin construct developed and characterised in this thesis. The first step was to evaluate the light emission obtained from cells using either an ICCD camera or a luminometer. Two cell lines were tested and transfection efficiency was measured at this stage. The second step was to determine whether Ca^{2+} transients detected with our new probe were significantly different from those in the cytosol in support of a potential local regulation of Ca^{2+} near the BK channel. The Ca^{2+} signals were investigated at rest and in response to the addition of extracellular Ca^{2+} . The specific characteristics of the Ca^{2+} signals elicited were also studied.

4.2 METHODS

4.2.1 *Transfection efficiency.*

Transfection efficiency is the ratio of successfully transfected cells to the total number of cells. Transfection is a process that depends on external parameters such as the amount of DNA, the method of transfection, the number and type of cells as well as internal parameters such as the different processes occurring inside the cells. Under similar conditions, it is assumed that transfection efficiency remains equal for each plasmid if the gene operates under the control of the same promoter. Therefore, to determine the transfection efficiency of a given vector, a reporter gene like GFP may be used as long as both vectors

are under the control of the same promoter, the CMV promoter in our case. Transfection efficiency was assessed in MG63 and HEK293 cells using Fluorescence-activated cell sorting analysis.

4.2.2 Fluorescence-activated cell sorting.

Fluorescence-activated cell sorting (FACS) is a reliable method which enables rapid separation of cells in a suspension on the basis of size and the colour of their fluorescence. Cells in suspension pass in single file through a thin stream where a laser beam is applied. As each cell passes through the beam, the resulting fluorescence signal of cells expressing EGFP is detected by a photocell. When the signal meets either of the criteria set for size and fluorescence, an electrical charge is given to the cell which is subsequently sorted by passing between a pair of charged metal plates.

FACS analysis was performed to determine the transfection efficiency of the cell lines used in this project. Cells were subject to transfection with a vector (Waud *et al.*, 2001) carrying the EGFP reporter gene under control of CMV promoter prior to FACS assessment. Following 48 h transfection, cells were detached with trypsin, collected, washed twice with PBS, resuspended in medium and incubated in ice until analysis. Measuring was done by placing a gate round the EGFP-positive cells in the viable cell population. The viable cell population was determined using the forward and side scatter characteristics of the cells. A total of 10,000 events per cell sample were recorded using a

FACScalibur flow cytometer (BD Biosciences, Oxford, UK). FACS data were analysed with WinMDI software. The efficiency was expressed as percentage of cells expressing EGFP. Untransfected cells were used as the negative control. Transfection efficiency was calculated after subtracting the control values from experimental values.

4.2.3 Calcium-dependent signal from living cells.

HEK293 and MG63 cells were transfected with either β 2-Aeq or Luc-Aeq for 48 h as described in Chapter 2, 2.2.7.2. Cells were seeded on either 6 well plates or coverslips for Ca^{2+} imaging experiments using the home-built luminometer or the ICCD camera respectively. Cells expressing apoaequorin were washed twice with Ca^{2+} -free KRH to remove all traces of calcium and incubated in this medium for 1 h at 37°C in the presence of coelenterazine (2 μM). Light emission was converted into Ca^{2+} concentrations using the equations described in Chapter 2, 2.4.3. All Ca^{2+} imaging experiments were carried out at room temperature (22°C).

4.2.3.1. Effects of the addition of an isosmotic solution on intracellular free Ca^{2+} detected using a home-built luminometer.

Transfected HEK293 cells in 6-well plates were detached with trypsin and reconstituted at 37°C as a cell suspension using a minimum volume of EGTA (1 mM) medium (coelenterazine 5 μM). Subsequently, cells were washed twice with warm KRH medium to remove the excess of coelenterazine and resuspended in a final volume of 500 μl of Ca^{2+} -

free KRH. Aliquots of 20 μ l were added to a LP3 tube containing 500 μ l of the same medium and transferred to the sample housing of the home-built luminometer. A solution containing 500 μ l of identical medium was injected after 20 s and the remaining counts were obtained by addition of a solution containing 50 mM CaCl_2 and 3 % of the detergent Nonidet 40. The experiments were performed in triplicates.

4.2.3.2 Effects of addition of extracellular Ca^{2+} on intracellular free Ca^{2+} recorded using an ICCD camera.

Ca^{2+} imaging experiments using the ICCD camera (Photek, UK) were performed as described in 2.3.3.2. In brief, following the reconstitution of aequorin, the cells were washed twice with Ca^{2+} -free (1 mM EGTA) KRH medium to remove coelenterazine. The cells were then transferred to the chamber and brought into contact with the fibre optics. A continuous flow perfusion system was employed to change solutions. The imaging protocol was as follows: 10 min Ca^{2+} -free KRH; 10 min Ca^{2+} (1.3 mM) KRH; 5 min Ca^{2+} -free KRH; 5 min Ca^{2+} KRH and 20 min lysis solution.

IFS32 Software (Photek, UK) was employed to analyse the data acquired. The complete imaging experiment was converted into a 10 s frame video sequence and a number of cell clusters (OAS) selected as described in Chapter 2, 2.4.2.2. The means \pm SEM were obtained from all the cell clusters selected from three different coverslips.

4.2.3.3 Analysis of individual Ca^{2+} signals.

Each cell cluster from the previous experiments was individually analysed using IFS32 software. Aequorin consumption was calculated as the total number of light counts recorded during the period studied divided by the total light counts obtained at the end of the experiment. The total aequorin expression per cell cluster was expressed as the total light counts during the whole experiment divided by the number of pixels of the OAS.

4.3 RESULTS

In this chapter, a series of initial experiments was carried out to determine the suitability for Ca^{2+} imaging of the two cell lines, HEK293 and MG63, employed. Similarly, experiments were performed to examine if Ca^{2+} signals of cells in suspension could be detected appropriately. Once the correct conditions were determined, the Ca^{2+} signals of cells expressing either $\beta 2\text{-Aeq}$ or Luc-Aeq were investigated at rest and in response to the addition of extracellular Ca^{2+} . Finally, the particular characteristics of the Ca^{2+} transients were assessed.

4.3.1. Transfection efficiency.

The initial Ca^{2+} imaging experiments showed that low light emission was obtained from MG63 cells (Fig. 4.4). In contrast, HEK293 cells generated sufficient light counts (Fig. 4.6). One factor contributing to the total light emission is the transfection efficiency. The total amount of

aequorin present in a given sample is dependent on the number of cells successfully transfected. To evaluate whether this difference in light emission was due to the transfection efficiency, a series of experiments was undertaken to determine the effects of different transfection reagents and the transfection efficiency in HEK293 and MG63 cells.

Qualitative studies on transfection efficiency were carried out using various transfection reagents (Lipofectamine 2000, Lipofectamine Plus, Lipofectamine LTX and Eugene HD). From simple observation of the GFP signal under the fluorescent microscope, there was no noticeable differences between the numbers of successful GFP-transfected cells employing different reagents (Fig 4.1). Nevertheless, at first sight, the much lower transfection efficiency achieved in MG63 (Fig 4.1 F) than in HEK293 cells (Fig 4.1 A) was clear. The qualitative estimation by simple observation of the transfection efficiencies was in line with the subsequent assessment via FACS analysis.

The assessment of transfection efficiency via flow cytometry was performed in HEK293 and MG63 cell lines. The value of transfection efficiency achieved in HEK293 cells after 48 h was around 20 % whereas a much lower rate, below 1 %, was achieved for MG63 (Table 4.1). Figs 4.2 & 4.3 illustrate representative histograms for HEK293 and MG63 cell lines respectively. When plotting the number of cells (events) against the fluorescence intensity (FL1-H), EGFP-transfected HEK293 cells exhibited a higher fluorescence signal (Fig 4.2 B) in contrast to the

native cells (Fig 4.2 A). In MG63, no noticeable difference was observed between EGFP transfected (B) and control cells (A) indicating the low transfection efficiency (Table 4.1) achieved in these cells. The populations of viable cells selected for each cell line are also shown (Fig 4.2 C & Fig 4.3 C).

Since very low transfection efficiency was observed in MG63 cells, a set of experiments using selective medium was carried out to generate two stable transfected MG63 cell lines with either β 2-Aeq or Luc-Aeq plasmids. In a stable cell line, a selective antibiotic is used to make sure that only the cells containing the appropriate plasmid survive. This leads to 100% of successfully transfected cells. Following the two weeks incubation in gentamicin-selective medium, most of the MG63 cells died as expected. However, the growth rate of the surviving cells was surprisingly low taking almost 2 weeks to reach confluence in comparison to the native MG63 cells (3 – 4 days on average). This was consistent with our previous cell proliferation experiments showing this reduction in cell growth in transfected HEK293 cells (Fig. 3.9). A sample containing 20000 of the surviving MG63 cells was subjected to aequorin assay using the luminometer. The mean values of Luc-Aeq transfected MG63 cells after cell lysis were very low, especially in comparison to those obtained in transient transfected HEK293 cells (3820 and 465114 counts, respectively). An explanation may be that a few untransfected cells developed resistance to the antibiotic and they overgrow the transfected cells, which were shown to grow more slowly (Fig. 3.9).

There is also evidence that aequorin activity is lost during the creation of stable cell lines (George, 1998). This may have also caused the low light emission observed in the stable MG63 cell line.

Our data showed that adequate transfection efficiency was achieved in HEK293 but not in MG63 cells.

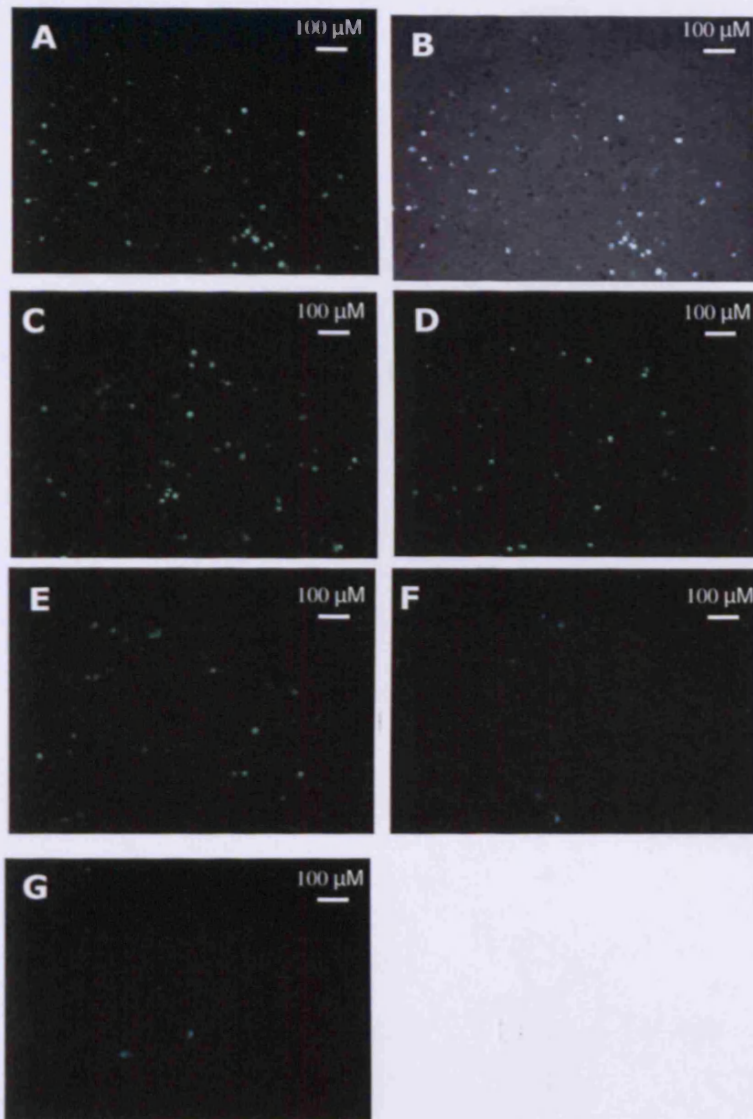
Fig 4.1. Comparative analysis of different transfection reagents.

Fig 4.1. Comparative analysis of cells expressing GFP using different transfection reagents. HEK293 α transfected with Lipofectamine 2000 (A), previous image with cells (B), Lipofectamine Plus (C), Lipofectamine LTX (D), Eugene HD (E) and MG63 cells transfected with Lipofectamine 2000 (F) and Eugene HD (G) as described in Chapter 2, 2.2.7.2. Cells were transfected with a EGFP vector for 48 hours and fully confluent at the time of the image capture. Images were attained 48 hours after transfection using a fluorescent microscope. Image (B) combines fluorescence and bright field. Pictures were taken on a Zeiss Axiovert microscope at X100 magnification with GFP-specific filters (excitation 480/30, dichromic 505/40 nm and emission 535/40 nm).

Table 4.1. Transfection efficiency in HEK293 and MG63 cells.

Transfection efficiency	
Cell line	Cells showing Fluorescence (%)
HEK293	19.25± 0.18
MG63	0.48± 0.20

Table 4.1. Transfection efficiency in HEK293 and MG63 cells. The table shows the percentage of cells showing GFP associated fluorescence. Experiments were made in triplicates and the means \pm SEM are shown.

Fig. 4.2. FACS analysis of transfection efficiency in HEK293.

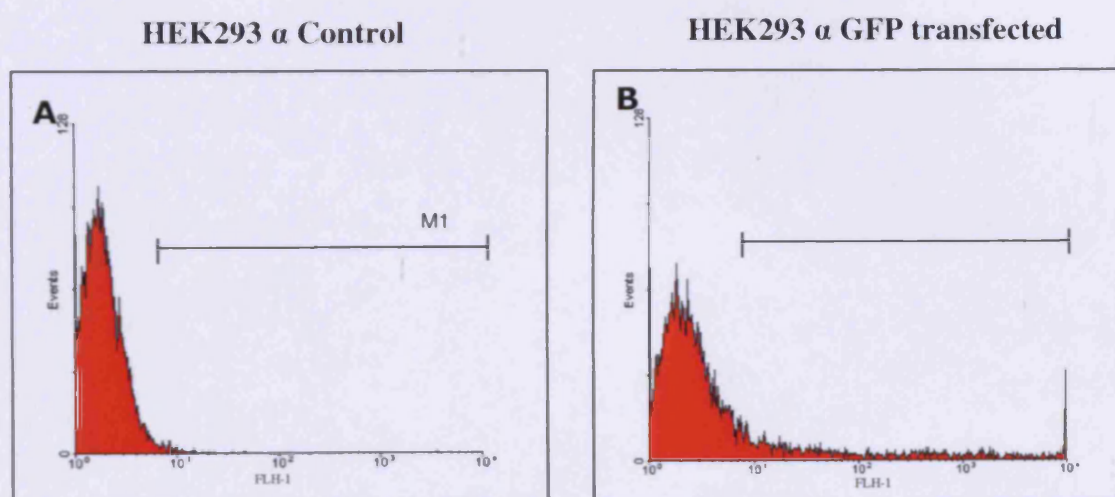


Fig. 4.2. FACS analysis of transfection efficiency in HEK293 cells.

In histograms A & B the number of cells (events) is plotted against the fluorescence intensity (FL1-H). Histogram (B) exhibits a long tail characteristic of GFP-tagged cells emitting a fluorescence signal in contrast to the native cells (A). A population of viable cells (in red) was selected using a FSC-SSC dot plot within 10,000 cells. A marked region (M1) was established containing 1 % of the control cells and the percentage of cells moving into this marked region calculated as described in section 4.2.1.

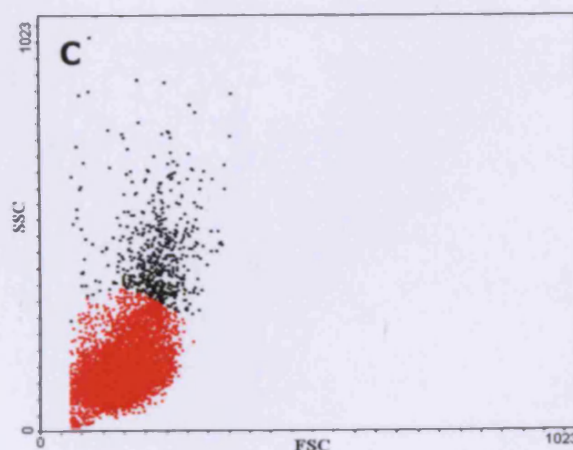
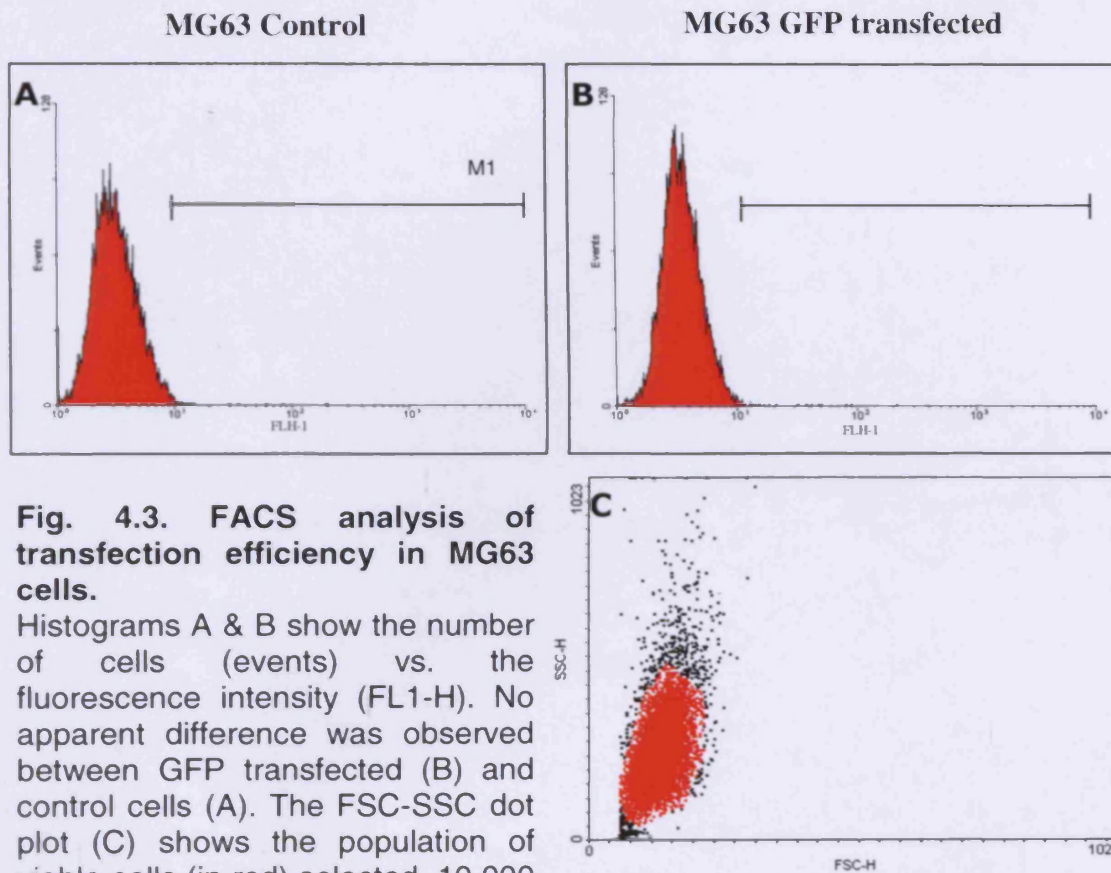


Fig. 4.3. FACS analysis of transfection efficiency in MG63.**Fig. 4.3. FACS analysis of transfection efficiency in MG63 cells.**

Histograms A & B show the number of cells (events) vs. the fluorescence intensity (FL1-H). No apparent difference was observed between GFP transfected (B) and control cells (A). The FSC-SSC dot plot (C) shows the population of viable cells (in red) selected. 10.000 cells were analysed. A marked region (M1) was established containing 1 % of the control cells and the percentage of cells moving into this marked region calculated as described in section 4.2.1.

Fig. 4.4. Light emission of MG63 cells transfected with Luc-Aeq.

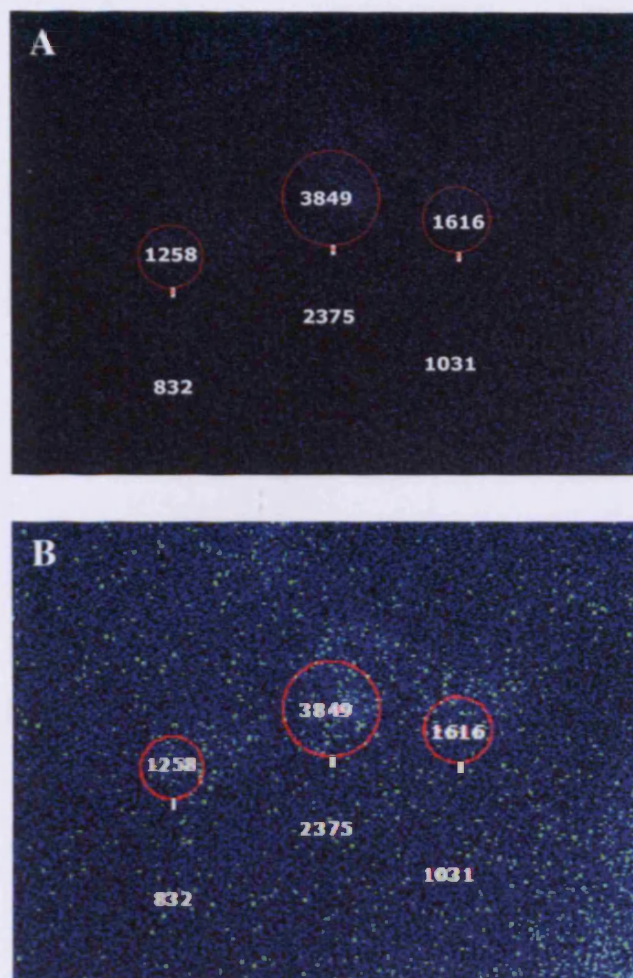


Fig 4.4. Light emission of MG63 cells transfected with Luc-Aeq. A: Unmodified image of the cumulative counts obtained from confluent MG63 cells after hypotonic treatment. Red circles delimit the areas with slightly higher light emission probably accounting for the few cells expressing aequorin. The total counts within each area are indicated. Below each area are the counts obtained in a non-light emission zone using similar area. This image was acquired using an ICCD camera (Photek) as described in Chapter 2, 2.4.2.2. This image was subsequently modified (B) by a fade correction of 80 using Corel Paint Shop Pro X Software to allow a better visualisation of the counts in the different areas.

4.3.2. Effects of the addition of an isosmotic solution on intracellular free Ca^{2+} in transfected HEK293 cells in suspension.

A series of initial experiments were conducted to assess the effects of different agonists on intracellular Ca^{2+} in transfected HEK293 cells in suspension using the home-built luminometer. The preliminary data quickly revealed substantial variations between experiments. A possible cause may have been that Ca^{2+} responses in HEK293 cells were susceptible to mechanical stimuli (Campbell AK, personal communication, 1996). This set of experiments was undertaken to examine whether the intracellular Ca^{2+} concentrations of cells in suspension may vary as a consequence of a mechanical disturbance.

Following 1 h aequorin reconstitution in Ca^{2+} -free medium (1 mM EGTA) of HEK293 cells in suspension and coelenterazine removal, a LP3 tube containing 500 μl of Ca^{2+} -free medium was supplemented with 20 μl of the cell suspension. Once light output reached stability, mechanical stimuli were administered via fast injection (over 1 sec) of 500 μl of identical Ca^{2+} -free medium resulting in a major increase in intracellular free Ca^{2+} (BK: $9.48 \pm 3.37 \mu\text{M}$ & Luc-Aeq: $6.27 \pm 2.98 \mu\text{M}$, Fig. 4.5) that lasted for a period of 3-5 s and then Ca^{2+} returned to basal levels. It should be noted that Ca^{2+} levels above 5 μM represent the limit of accuracy when measuring Ca^{2+} using aequorin (George *et al.*, 1998). Therefore, the resulting Ca^{2+} concentrations were probably underestimated. Nevertheless, it is evident that a prominent Ca^{2+}

response was obtained as a result of the addition of an isosmotic solution. Since these experiments were performed in the presence of EGTA, this Ca^{2+} response must have been produced by Ca^{2+} release from intracellular stores.

The results presented in this section indicate the possible existence of intracellular Ca^{2+} channels triggered by mechanical stimuli in HEK293 cells.

4.3.3. Effects of the addition of extracellular calcium on intracellular free Ca^{2+} .

To investigate whether $\beta 2\text{-Aeq}$ could report changes in intracellular Ca^{2+} concentrations in HEK293 cells, HEK293 cells expressing $\beta 2\text{-Aeq}$ were exposed to a Ca^{2+} challenge. The cells were also transfected with Luc-Aeq in order to compare the regulation of Ca^{2+} signals detected in either the BK channel or cytosolic domains. The basal intracellular free Ca^{2+} in both domains in either the presence or absence of extracellular Ca^{2+} were also studied.

HEK293 cells on coverslips expressing either $\beta 2\text{-Aeq}$ or Luc-Aeq were used to measure by luminescence the intracellular free Ca^{2+} concentration. When aequorin was reconstituted *in situ* in cells exposed to calcium-deficient medium containing EGTA (1 mM), and calcium (1.3 mM) was then added back to the medium, a rapid increase in the intracellular free Ca^{2+} reaching a maximum of 4.56 μM was observed

(Fig. 4.5). A lower peak (1.81 μM) was detected in the cytosol. The Ca^{2+} transients declined to basal Ca^{2+} levels after approximately 5 min near the BK channel and 10 min in the cytosol. These high calcium domains are reflected by visual comparison of cells expressing either Luc-Aeq or $\beta 2$ -Aeq (Fig. 4.4. B & F, respectively).

Following the first addition of extracellular Ca^{2+} for 10 min, cells were perfused with Ca^{2+} -free medium EGTA (1 mM) for 5 min and then Ca^{2+} -containing medium was re-perfused for another 5 min prior to the cell lysis. This subsequent addition of extracellular Ca^{2+} was intended to determine whether the marked Ca^{2+} transients induced in first instance were only dependent of extracellular Ca^{2+} . The second Ca^{2+} challenge induced a small increase from 0.35 to 0.50 μM in cytosolic free Ca^{2+} (Fig. 4.5). No change in intracellular free Ca^{2+} was observed near the BK channel. This indicates that the large Ca^{2+} transients triggered after the first addition of extracellular Ca^{2+} were mainly produced by SOC entry. The initial long-term exposure to EGTA during the incubation period probably caused the emptying of the ER Ca^{2+} stores.

The basal intracellular free Ca^{2+} levels detected by the $\beta 2$ -Aeq chimera were higher than those reported by the cytosolic Luc-Aeq (Fig. 4.7 & Table 4.2). Previous studies of plasma membrane bound proteins have reported Ca^{2+} levels within the same range (Martin *et al.*, 1998).

Fig. 4.5 Effect of mechanical stimuli on free Ca^{2+} in the cytosolic and BK microdomains of HEK293 cells in suspension expressing either $\beta 2$ -Aeq or Luc-Aeq.

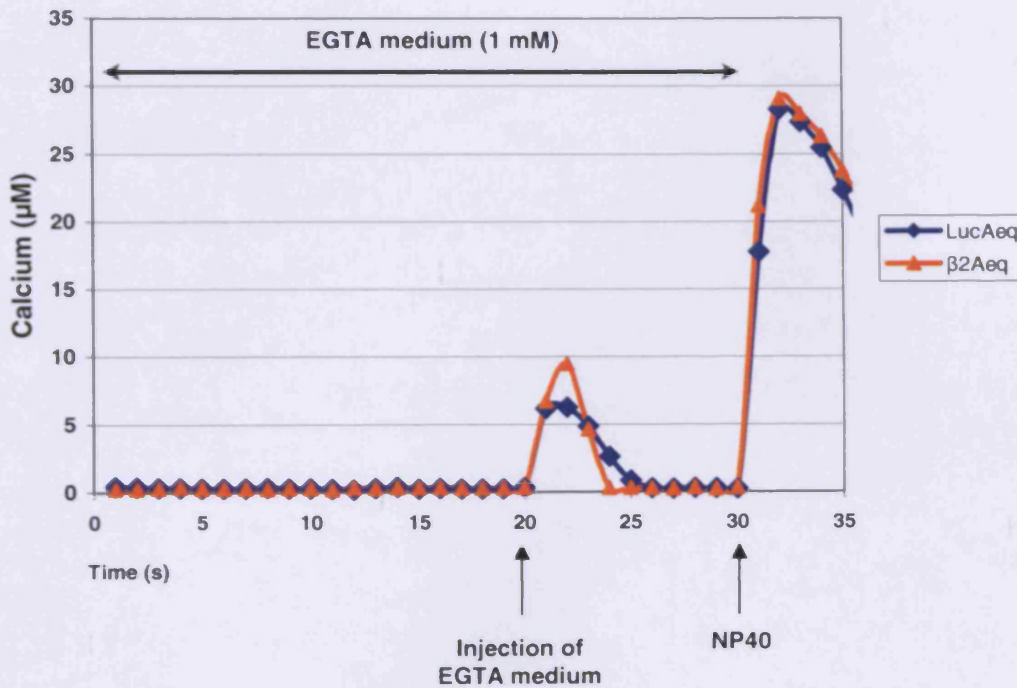


Fig. 4.5 Effect of mechanical stimuli on free Ca^{2+} in the cytosolic and BK microdomains of HEK293 cells in suspension. HEK293 cells containing either Luc-Aeq or $\beta 2$ -Aeq were suspended in Ca^{2+} -free medium (1 mM EGTA) prior to challenge with an equal volume of identical medium. Addition of an equal volume of similar medium generated a mechanical disturbance resulting in a fast rise in the free Ca^{2+} near the channel to approximately 9.48 μM and also in cytosolic Ca^{2+} (6.27 μM). Intracellular free Ca^{2+} in both domains returned to basal levels after approximately 3-5 s. The remaining aequorin was estimated after the addition of 3% NP40 in a high Ca^{2+} solution. Cells were incubated in Ca^{2+} -free medium for 1 h (coelenterazine 5 μM). Light counts were recorded every second using a home-built luminometer. The data are expressed as mean \pm SEM and are representative of three separate experiments.

The initial Ca^{2+} concentrations at rest in the BK channel microdomain in Ca^{2+} -free medium were 3 times higher than in the cytosol (0.79 & 0.26 μM , respectively, Table 4.2, region 1). In regions 2, 3 and 4 (Fig. 4.7) this difference dropped to around twice the cytosolic resting Ca^{2+} level in either the presence or absence of Ca^{2+} in the medium. In both domains, the Ca^{2+} concentrations prior to the first Ca^{2+} addition (BK domain: 0.79 μM , cytosol: 0.26 μM) were significantly lower than those subsequently detected (BK domain: 0.86 in EGTA & 0.88 μM with Ca^{2+} ; cytosol: 0.38 in EGTA & 0.42 μM with Ca^{2+}). These initial reduced levels were probably caused by the long-term incubation in EGTA.

The basal intracellular free Ca^{2+} levels detected by the $\beta 2$ -Aeq chimera were higher than those reported by the cytosolic Luc-Aeq (Fig. 4.7 & Table 4.2). This is consistent with previous studies of plasma membrane bound proteins that showed levels within the same range (Martin *et al.*, 1998). The initial Ca^{2+} concentrations at rest in the BK channel microdomain in Ca^{2+} -free medium were 3 times higher than in the cytosol (0.79 & 0.26 μM , respectively, Table 4.2, region 1). In regions 2, 3 and 4 (Fig. 4.7) this difference dropped to around twice the cytosolic resting Ca^{2+} level in either the presence or absence of Ca^{2+} in the medium. In both domains, the Ca^{2+} concentrations prior to the first Ca^{2+} addition (BK domain: 0.79 μM , cytosol: 0.26 μM) were significantly lower than those subsequently detected (BK domain: 0.86 in EGTA & 0.88 μM with Ca^{2+} ; cytosol: 0.38 in EGTA & 0.42 μM with Ca^{2+}).

These differences in Ca^{2+} signals may have been induced by a bias caused by either the use of two difference Ca^{2+} -conversion equations or the contribution of the background counts to the low light signal produced by the $\beta 2\text{-Aeq}$ construct. This possibility was appropriately addressed first by interchanging the equations in two representative experiments with each construct. In this case, only a 2.5-3 % difference was noticed between the initial data and the values generated using the other equation. Secondly, a series of surrogate background levels was artificially created to determine the effect of the background counts on both constructs. The initial counts obtained in the first 10 seconds were used to create background levels ranging from 0 to 90% of the raw signal. In all cases, $\beta 2\text{-Aeq}$ detected higher levels of Ca^{2+} than those revealed by Luc-Aeq . Nonetheless, a higher difference between the Ca^{2+} levels of the $\beta 2\text{-Aeq}$ and Luc-Aeq was appreciated when the background counts raised to 90 % of the raw signal. The difference between Ca^{2+} levels increased from 3.37 fold at 0 % of background counts to 5.14 fold at 90 %. This may have been mainly produced by the decrease of Luc-Aeq levels from 0.26 to 0.17. These observations indicated that the higher Ca^{2+} signals detected by $\beta 2\text{-Aeq}$ were genuine. This also indicated that the qualitative comparison of membrane and cytosolic Ca^{2+} levels shown here was correct but the attempts of quantify this Ca^{2+} values should be taken carefully.

Fig 4.6. Visual evaluation of the effects of extracellular calcium on the light emission of HEK293 cells expressing either Luc-Aeq or β 2-Aeq.

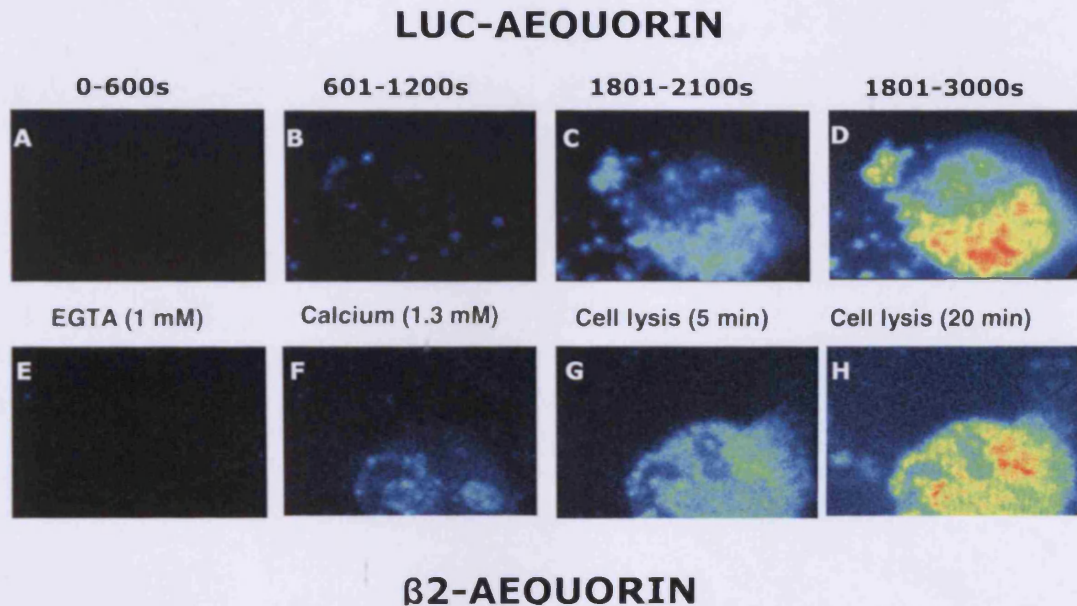


Fig 4.6. Visual evaluation of the effects of extracellular calcium on the light emission of HEK293 cells expressing either Luc-Aeq or β 2-Aeq. These images illustrate the different light outputs exhibited by Luc-Aeq (top) and β 2-Aeq (bottom) in response to extracellular Ca^{2+} . A higher increase in light emission was observed near the BK channel (F) than in the cytosol (B) as a result of the addition of extracellular Ca^{2+} . No difference was noticed when constructs were exposed to Ca^{2+} -free medium (A & E). Cell lysis images (C, D, G & H) show the circular area where the ICCD camera was located. Images represent the cumulative light counts obtained during the indicated periods and were acquired using an ICCD system (Photek, UK) as described in Chapter 2, section 2.4.2.2. To allow image comparison, the total number of light counts was employed to normalise the brightness of the pictures using IFS32 Software (Photek, UK).

Fig 4.7. Effects of extracellular calcium on intracellular free Ca^{2+} from HEK293 cells transfected with Luc-Aeq or $\beta 2$ -Aeq.

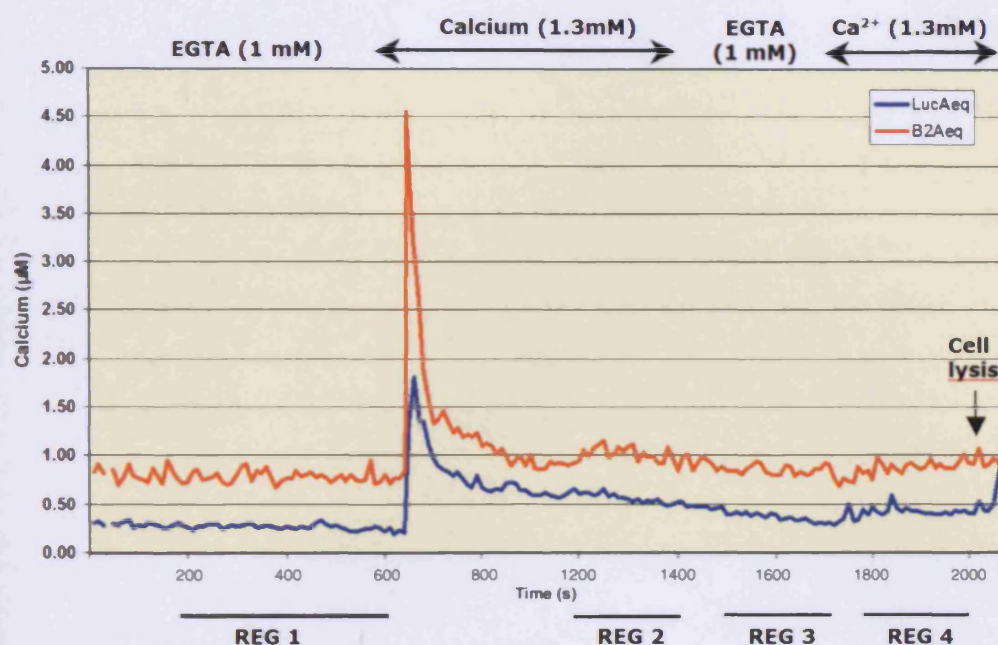
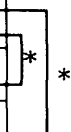


Fig 4.7. Effects of extracellular calcium on intracellular free Ca^{2+} from HEK293 cells transfected with Luc-Aeq or $\beta 2$ -Aeq. Following 1 h incubation in Ca^{2+} -free medium (1 mM EGTA), HEK293 cells in coverslips transfected with either Luc-Aeq or $\beta 2$ -Aeq were exposed to cell medium with either EGTA (1 mM) or Ca^{2+} (1.3 mM) during the periods indicated on the top. The *upper trace* is the calcium response in $\beta 2$ -Aeq transfected cells, and the *lower trace* is the response monitored with Luc-Aeq. The Ca^{2+} transient induced near the BK channel reached a peak of approximately 4.5 μM and then decayed to basal Ca^{2+} levels after approximately 5 min. A Ca^{2+} transient was also triggered in the cytosol reaching a peak at around 1.8 μM and then returning to basal Ca^{2+} after 10 min. The traces shown are the means from between 30 to 40 cell clusters recorded during three separate experiments. The remaining counts were obtained after the cell lysis and luminescence was converted to Ca^{2+} concentration as described in Chapter 2, 2.4.3. Light output was acquired using an ICCD camera (Photek, UK). Ca^{2+} imaging experiments were performed as described in Chapter 2, 2.4.2.2. The bottom lines Reg 1-4 indicate the regions selected to assess the basal Ca^{2+} levels (Table 4.2).

Table 4.2. Comparison of basal intracellular free Ca^{2+} concentrations in HEK293 cells expressing either Luc-Aeq or $\beta 2$ -Aeq.

BK microdomain	
Regions	Ca^{2+} (μM)
1 (EGTA)	0.79 ± 0.00
2 (Ca^{2+})	0.98 ± 0.02
3 (EGTA)	0.86 ± 0.01
4 (Ca^{2+})	0.88 ± 0.01



Cytosolic	
Regions	Ca^{2+} (μM)
1 (EGTA)	0.26 ± 0.00
2 (Ca^{2+})	0.57 ± 0.01
3 (EGTA)	0.38 ± 0.01
4 (Ca^{2+})	0.42 ± 0.01



Table 4.2. Comparison of basal intracellular free Ca^{2+} concentrations in HEK293 cells expressing either Luc-Aeq or $\beta 2$ -Aeq. The resting Ca^{2+} levels in the BK channel and cytosolic domains were significantly lower prior to the addition of Ca^{2+} medium (reg 1, Fig. 4.7) than those subsequently recorded in regions 3 and 4. The second addition of extracellular Ca^{2+} (reg 4) also produced minor increases in resting Ca^{2+} in both domains, although this rise was only significant in the case of cytosolic aequorin. The table values are the mean \pm SEM and were calculated from the traces in Fig. 4.7 during the periods indicated. Periods where Ca^{2+} levels remained stable. Were selected to determine the regions (reg 1-4) used. *- represents statistical significance ($p < 0.05$).

These initial reduced levels were probably caused by the long-term incubation in EGTA. A significant increase from 0.38 to 0.42 μM in basal intracellular free Ca^{2+} in the cytosol was also observed following the second supplement of extracellular Ca^{2+} (Fig. 4.7 and Table 4.2). In contrast, the basal Ca^{2+} concentrations remained unchanged (0.86 μM vs. 0.88 μM) in the BK microdomain.

The addition of extracellular Ca^{2+} caused a distinctively high Ca^{2+} response in the BK channel microdomain of HEK293 cells, probably caused by SOC entry. In addition, basal intracellular Ca^{2+} levels recorded by $\beta 2\text{-Aeq}$ were higher than those in the cytosol irrespectively of the presence of extracellular Ca^{2+} .

4.3.4. Individual Ca^{2+} responses in HEK293 cells.

The addition of extracellular Ca^{2+} revealed differences in the Ca^{2+} responses of individual cell clusters in both BK channel and cytosolic domains. To determine the characteristics of the Ca^{2+} signals of individual cell clusters a more detailed analysis was performed.

The initial challenge with extracellular Ca^{2+} (1.3 mM) (Fig. 4.7) produced Ca^{2+} transients ranging from 2 to more than 10 % in aequorin consumption near the BK channel (Fig. 4.8. A). These values were between 0.75 and 6 % (Fig. 4.9. B) in the cytosol during the 10 min period analysed. Following the first Ca^{2+} challenge, addition of medium containing EGTA (1 mM) for 5 min and a second addition of extracellular Ca^{2+} , a new series of Ca^{2+} transients was obtained (Fig.

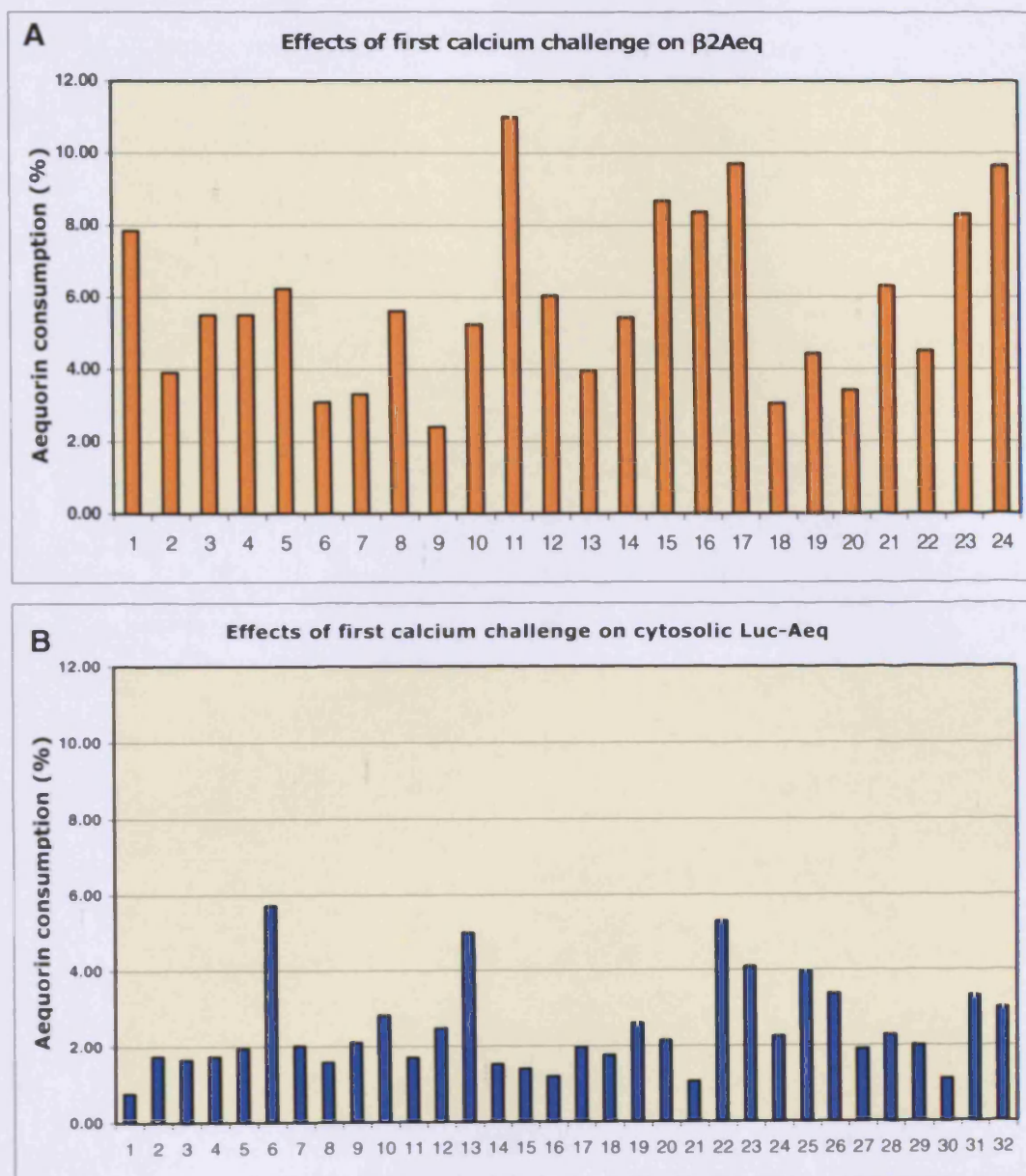
4.9). In this second Ca^{2+} challenge, the Ca^{2+} signal in the proximity of the BK channel varied from 0.13 to 1.8 % (Fig. 4.9. A) whereas in the cytosol were between 0.11 and 0.89 % (Fig. 4.9 B).

The initial challenge with extracellular Ca^{2+} (1.3 mM) (Fig. 4.7) produced Ca^{2+} transients ranging from 2 to more than 10 % in aequorin consumption near the BK channel (Fig. 4.8. A). These values were between 0.75 and 6 % (Fig. 4.9. B) in the cytosol during the 10 min period analysed. Following the first Ca^{2+} challenge, addition of medium containing EGTA (1 mM) for 5 min and a second addition of extracellular Ca^{2+} , a new series of Ca^{2+} transients was obtained (Fig. 4.9). In this second Ca^{2+} challenge, the Ca^{2+} signal in the proximity of the BK channel varied from 0.13 to 1.8 % (Fig. 4.9. A) whereas in the cytosol were between 0.11 and 0.89 % (Fig. 4.9 B). Accordingly, a higher degree of variability was detected in the vicinity of the BK channel ($\text{CV} = 2.36$ %, Table 4.3) than those induced in the cytosol ($\text{CV} = 1.26$ %, Table 4.3). The Ca^{2+} concentrations close to the BK channel exhibited a two-fold increase in variability when compared to the cytosol during both events, the first and the second Ca^{2+} challenges (Table 4.2).

It could be argued that a potential artefact generated by differences in aequorin expression between cell clusters may have caused the diversity of individual Ca^{2+} signals. To exclude this possibility, the Ca^{2+} responses were compared to the total aequorin for each individual cell

cluster. This study found that no correlation between the Ca^{2+} signals and the total aequorin expression of the cell cluster (Table 4.10). It could also be expected that an initial large and prolonged rise in intracellular free Ca^{2+} during the first Ca^{2+} challenge also induces a similar high Ca^{2+} signal during the subsequent Ca^{2+} challenge. Nevertheless, the data presented in these experiments showed that the first (Fig. 4.8) and second Ca^{2+} transients (Fig. 4.9) were also unrelated in the BK and cytosolic domains. In some occasions in the BK channel microdomain, a high Ca^{2+} signal during the first challenge (i.e. 6.31 %, cell cluster 21, Fig. 4.8 A) was followed by a second high Ca^{2+} signal (0.61 %, Fig. 4.9 A) while in other cases the secondary response was lower (0.48 %, cell cluster 1, Fig. 4.9 A) even when the first Ca^{2+} transient had been considerably high (7.83 %, Fig. 4.8 A). Similar results were observed in the cytosol (Fig. 4.8 B & 4.9 B).

These results have demonstrated the high degree of variability of the Ca^{2+} signals triggered in individual cell clusters. No association was found between the experimental conditions and the Ca^{2+} transients indicating that the diversity in the Ca^{2+} responses was probably due to the different biological features of each cell cluster.

Fig 4.8. Individual Ca^{2+} transients induced by addition of extracellular Ca^{2+} .Fig 4.8. Individual Ca^{2+} transients induced by addition of extracellular Ca^{2+} .

Individual clusters of HEK293 cells exhibited different Ca^{2+} signals in response to the addition of extracellular Ca^{2+} (1.3 mM) for 10 min (Fig. 4.7). Larger transients ranging from 2 to more than 10 % near the BK channel (A). Cytosolic Ca^{2+} responses varied 0.75 and 6 % (B). Each number in the x axis represents a individual cell cluster. Cell clusters were selected as described in Chapter 2, 2.3.3.2.3. from three separate experiments. HEK293 cells in coverslips were transfected with either $\beta 2\text{-Aeq}$ or Luc-Aeq, incubated for 1 hour in EGTA medium (2 μM coelenterazine) and perfused with EGTA medium prior to the Ca^{2+} challenge. Light counts were acquired using an ICCD camera (Photek, UK) as described in Chapter 2, 2.4.2.2. Bars show the percentage of aequorin consumed during a period of 10 min.

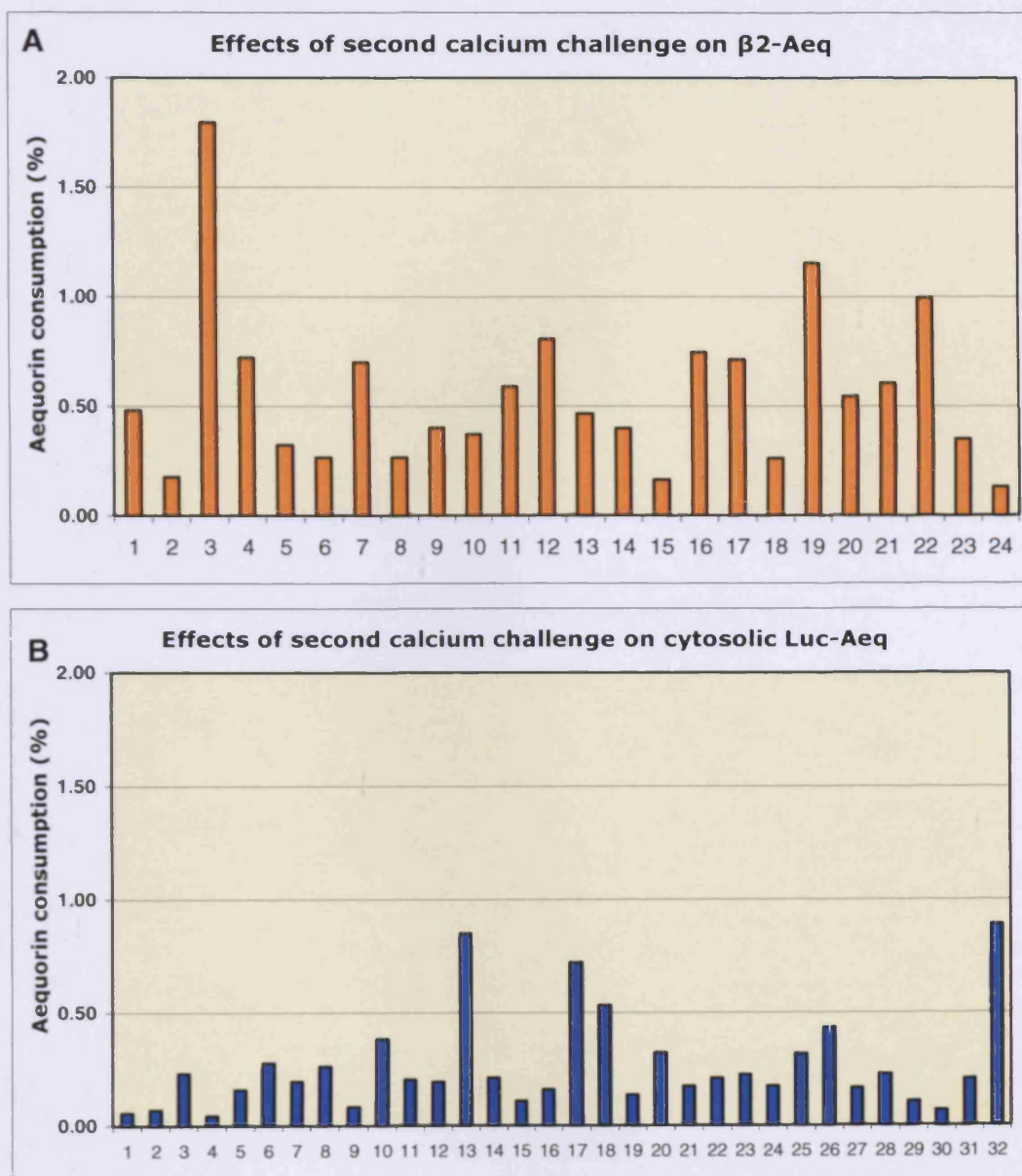
Fig 4.9. Individual Ca^{2+} transients induced by a second addition of extracellular Ca^{2+} .

Fig 4.9. Individual Ca^{2+} transients induced by a subsequent addition of extracellular Ca^{2+} in HEK293 cells. Different Ca^{2+} responses were observed in individual clusters of HEK293 cells during a second addition of extracellular Ca^{2+} (1.3 mM) (Fig. 4.7). $\beta 2$ -Aeq reported larger individual Ca^{2+} transients ranging from 0.13 to 1.8 % (A) than those in the cytosol (B). The individual Ca^{2+} signals induced in the cytosol varied between 0.11 and 0.89 % (B). Cell clusters were extracted from three different experiments and are indicated in the x axis. Experimental conditions were as follows: incubation in EGTA (1 mM, 1 h, 2 μM coelenterazine) and then perfusion with 10 min EGTA, 10 min Ca^{2+} (1.3 mM) medium, 5 min EGTA, 5 min Ca^{2+} (1.3 mM) and cell lysis solution (Fig 4.7). Ca^{2+} imaging experiments were carried out using an ICCD camera (Photek) as described in Chapter 2, 2.4.2.2. Bars show the percentage of aequorin consumed during the 5 min period corresponding to the second addition of extracellular Ca^{2+} .

Fig 4.10. Comparison of Ca^{2+} signals to the total expression of aequorin in individual cell clusters.

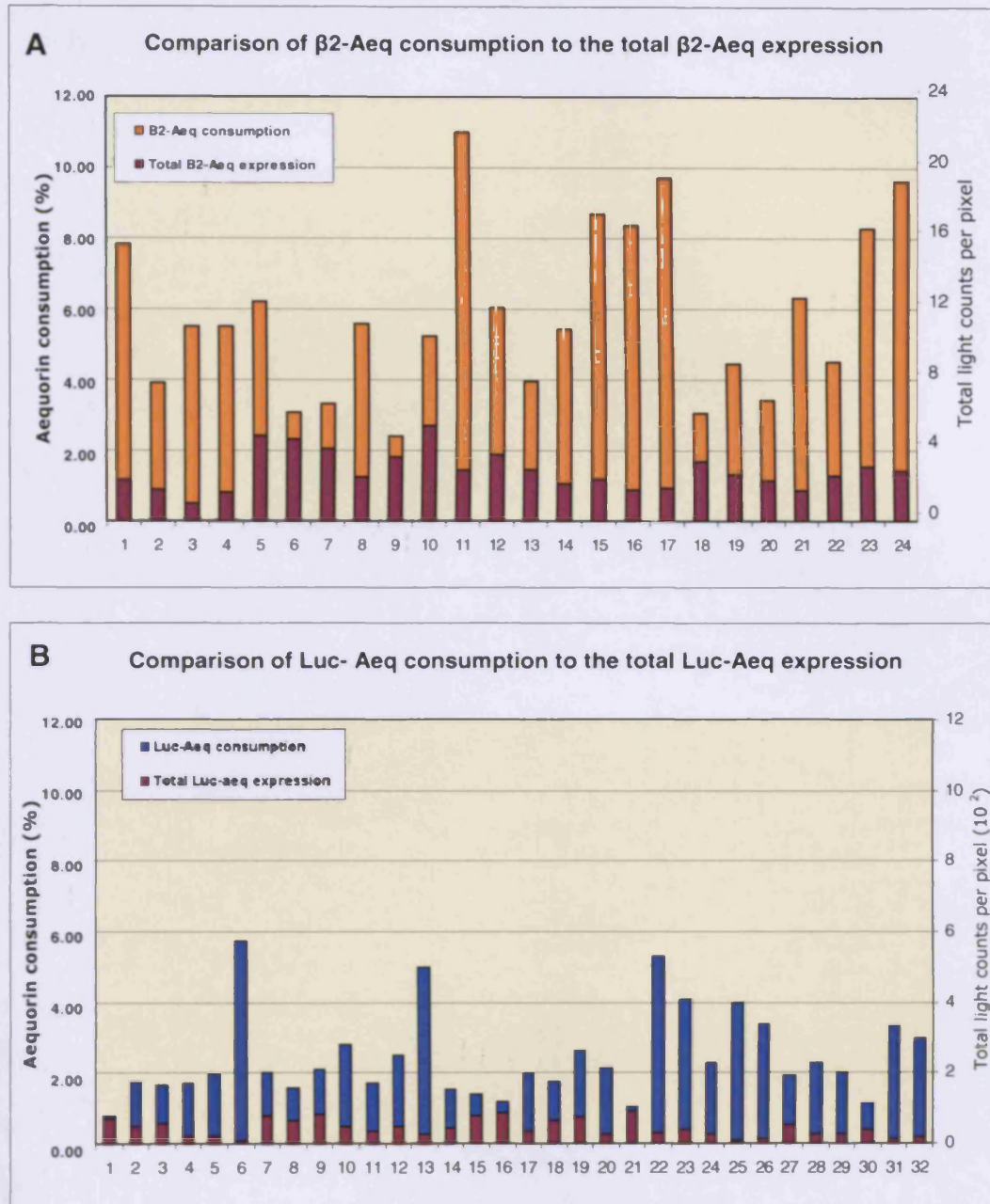


Fig 4.10. Comparison of Ca^{2+} signals to the total expression of aequorin in individual cell clusters. The differences of individual Ca^{2+} responses in both BK channel (A) and cytosolic (B) domains were independent of the total aequorin expressed in the individual cell cluster. This indicates that the difference in Ca^{2+} responses in individual HEK293 cell clusters was due to biological factors. Blue bars represent the aequorin consumed (left Y axis) after the first addition of extracellular Ca^{2+} as described in Fig. 4.8. Note that the units and scale of total light counts per pixel (right Y axis) were selected to facilitate the interpretation of each individual graph. The total aequorin expression (red bars) for individual cell clusters is expressed as the total light counts obtained for the same cell cluster at the end of the experiment divided by the total number of pixels of the specific OAS. The area of the OAS is proportional to the number of pixels. All data was obtained using a ICCD camera and IFS32 Software (Photek, UK).

Table 4.3. Variability of the individual Ca^{2+} responses.

	$\beta 2$-Aeq	Luc-Aeq
1 st Ca^{2+} challenge	2.36 %	1.26 %
2 nd Ca^{2+} challenge	0.37 %	0.19 %

Table 4.3. Variability of the individual Ca^{2+} responses. The higher degree of variability observed near the BK channel is indicated by the coefficient of variability. The coefficient of variability was higher than in the cytosol during both the first and the second Ca^{2+} challenges. The coefficients of variability are the percentage of the standard deviation divided by the mean and were calculated from the aequorin consumption data presented in figures 4.8 and 4.9.

4.4 DISCUSSION

The results in this chapter have demonstrated that Ca^{2+} concentrations in the proximity of the BK channel were locally regulated. A higher Ca^{2+} signal was detected near the channel at rest and in response to the addition of extracellular Ca^{2+} . The analysis of the Ca^{2+} responses induced showed important differences between individual cell clusters in both BK channel and cytosolic domains. In addition, evidence of the presence of intracellular mechanosensitive channels in HEK293 was found. Moreover, the assessment of aequorin light emission carried out in MG63 and HEK293 cells revealed that only the latter generated sufficient counts to enable the use of a CCD camera for Ca^{2+} imaging experiments.

4.4.1. Assessment of the best conditions for Ca^{2+} imaging in HEK293 and MG63 cells: evidence of mechanosensitive channels in HEK293.

The preliminary Ca^{2+} imaging experiments performed in HEK293 and MG63 cell lines using both the home-built luminometer and the CCD camera revealed that very low light emission was detected in MG63 cells (Fig. 4.4). Since an adequate light yield is required in order to distinguish the Ca^{2+} -induced signal from the background noise, a study was conducted to determine the causes of the differences in light emission between HEK293 and MG63. The number of counts emitted depends on the expression rate of aequorin and its inherent properties (i.e.: $\beta 2\text{-Aeq}$ displays a 10 times lower the quantum yield than Luc-

Aeq). Consequently, it is important to assess whether a sufficient amount of transfected cells are present.

The analysis of the transfection efficiency in HEK293 and MG63 cells was performed by two methods: qualitative, by simple observation of the visible signal and quantitative, via FACS analysis. Both methods delivered similar results revealing a much higher transfection rate in HEK293 cells (Table 4.1). This dramatic difference in transfection efficiency may be ascribed to the use of different cell lines. Indeed MG63 cells showed low transfection efficiency that was several orders of magnitude lower when compared to HEK293 (Table 4.1). Other studies have also reported the low transfection efficiency achieved in MG63 (Corsi *et al.*, 2003; Hantusch *et al.*, 2007). The comparison of light counts recorded in experiments carried out with aequorin vectors in either HEK293 or MG63 cells also corroborate the higher transfection rate observed in HEK293.

The transfection efficiency achieved by HEK293 (~20 %, Table 4.1) proved to be adequate to enable the calcium monitoring of these cells under a CCD camera. In contrast, the light emission recorded from MG63 cells was insufficient probably due to their low transfection efficiency (Fig 4.3). The area covered by the CCD camera is only a few square centimetres, which may allocate a few thousand of confluent HEK293 cells. One fifth of these cells can fire as a response to calcium giving a sufficient number of counts. In the case of MG63, the number

of cells under the camera is reduced due to the bigger size of these cells compared to HEK293 and from those merely 0.5% express aequorin. As a consequence, the low number of counts obtained makes the use of a CCD camera unreliable to examine Ca^{2+} signalling in MG63.

Aequorin assays were also undertaken using a home-built luminometer in order to study Ca^{2+} signalling in cells in suspension. Our findings showed that a marked increase in intracellular free Ca^{2+} in HEK293 cells was caused simply by the injection stimuli even in the presence of EGTA. These results concur with other studies showing Ca^{2+} transients monitored with aequorin in the presence of EGTA (Brown & Blinks, 1974) and also in quin-2 loaded cells after addition of EGTA (James-Kracke, 1986). This effect was probably due to a physical artefact that can be generated in a number of ways. One may appear as a result of physically disturbing the cells, especially when cells are in suspension. Another involves the mechanical stimulation of cells which initiates Ca^{2+} transients (Putney, 2000). Since this effect occurred in the absence of extracellular Ca^{2+} , these mechanical stimuli probably produced a Ca^{2+} release from intracellular stores. In support of this idea, the existence of stretch-activated Ca^{2+} channels triggering Ca^{2+} release from intracellular stores in the presence of EGTA has been reported (Fanchaouy *et al.*, 2007) and the presence of mechanosensitive TRP channels in the ER (O'Neil & Heller, 2005; Reaves & Wolstenholme, 2007). Furthermore, endogenous stretch-activated Ca^{2+} channels have

been recorded in HEK293 WT by means of electrophysiological techniques (Morita *et al.*, 2007).

These experiments made clear that MG63 cells elicited a low light signal and Ca^{2+} imaging could only be performed in HEK293 cells. Furthermore, the mechanical stimulation of HEK293 cells in suspension induced large Ca^{2+} transients in both the BK channel and the cytosol domains. The results presented here indicate that Ca^{2+} mobilised into both domains upon mechanical disturbance is entirely of intracellular origin.

4.4.2. Effects of extracellular calcium.

To investigate whether the Ca^{2+} responses detected by the $\beta 2\text{-Aeq}$ chimera were different from those produced in the cytosol, HEK293 cells were subjected to a Ca^{2+} challenge. There has been shown (George *et al.*, 1998) that the addition of extracellular Ca^{2+} to cells that have been exposed to EGTA for long periods results in considerable Ca^{2+} transients. The same approach was used in HEK293 cells. Following incubation in EGTA (1 mM) for a period of 1 h, cells were exposed to Ca^{2+} (1.3 mM) containing medium for 10 min, followed by 5 min of EGTA medium and re-addition of extracellular Ca^{2+} before cell lysis (Fig. 4.8). In these experiments, HEK293 cells expressing the plasma membrane-bound $\beta 2\text{-Aeq}$ revealed a rapid rise in Ca^{2+} concentration which was consistently higher than that detected by the cytosolic Luc-Aeq (4.56 μM vs. 1.81 μM , respectively). Long time

exposure to Ca^{2+} buffers such as EGTA or BAPTA can cause a fall in Ca^{2+} levels in the ER. Accordingly, these Ca^{2+} transients were probably caused by a combination of SOC channels and CICR from intracellular stores. Since the subsequent 5 min exposure to EGTA and re-addition of extracellular Ca^{2+} did not generate such a response (Fig. 4.8), it is likely that SOC entry was mainly responsible for the initial Ca^{2+} increase. Previous studies using plasma membrane-bound aequorin revealed that analogous Ca^{2+} transient occurred during addition of Ca^{2+} which quickly decayed to values proximal to those before Ca^{2+} influx occurred (Marsault *et al.*, 1997; Nakahashi *et al.*, 1997).

The key question now is whether the Ca^{2+} concentrations reached in response to stimuli beneath the plasma membrane, especially near the BK channel, are consistent with previous studies. Three techniques have been mainly used for this purpose: electrophysiology, bioluminescence and fluorescent dyes (Chapter 1, 1.6). Only the first one was specific for the BK channel microdomain. Aequorin light emission was used in other microdomains near the membrane and fluorescent dyes detected general Ca^{2+} responses beneath the membrane. These limitations should be considered when comparing these studies.

Single channel activity of Ca^{2+} -activated BK channels have been employed to calculate the Ca^{2+} concentrations affecting the channel (Chapter 1, 1.6). The Ca^{2+} transients reported here are similar to

previous subplasma membrane Ca^{2+} concentrations estimated using BK activation as a means of assessment (Muñoz *et al.*, 1998; Frieden *et al.*, 2002). In the first study, a high Hill coefficient was employed to account for the difference between Fura 2 measurements and BK activation as a result of ionomycin stimulation. A switch-off mechanism for BK activation was proposed at a level of around $1\ \mu\text{M}\ \text{Ca}^{2+}$. There is no other evidence supporting such hypothesis. This is probably because ionomycin does not release Ca^{2+} homogeneously within the cell (Dedkova *et al.*, 2000) as was assumed. The latter research (Frieden *et al.*, 2002) matches closely the Ca^{2+} concentrations reported in this thesis. In their study, the equation employed to calculate the Ca^{2+} concentrations was based on previous studies (Barrett *et al.*, 1982), which assumed that BK channels in a membrane patch had similar properties and acted independently. Barret and collaborators (Barrett *et al.*, 1982) reported a Hill coefficient of 2.7, which is consistent with the two high-affinity Ca^{2+} sites and other with lower affinity found in BK channels (Zeng *et al.*, 2005). This indicates that this approach is probably quite accurate. Nevertheless, other mathematical models using similar coefficients but different assumptions such as non-cooperative Ca^{2+} binding resulted in estimated Ca^{2+} concentrations beneath the membrane of $50\ \mu\text{M}$ (Markwardt & Isenberg, 1992) and $150\ \mu\text{M}$ (ZhuGe *et al.*, 2000). Other study (Franciolini *et al.*, 2001) showed very low ionomycin-induced Ca^{2+} transients ($0.3\ \mu\text{M}$) near the membrane. In this case, the assumption of Ba^{2+} contamination in the

solution resulted in long inactive periods (>2 s) being ignored in the analysis. These close states were not excluded in Barrett's studies (Barrett *et al.*, 1982) probably explaining the differences in estimated Ca^{2+} concentrations between both studies. The wide disparity among all these studies exposes the importance of making the correct assumptions. The use of aequorin probes like the one designed in this thesis may provide further evidence about the precise Ca^{2+} concentration affecting the BK channel and also to the suitability of the assumptions made in previous studies.

Imaging studies using plasma membrane-bound aequorin have also been undertaken to determine Ca^{2+} concentrations in these domains. Initial experiments using 5HT-Aeq indicated the existence of a high sub-plasma membrane domain (Marsault *et al.*, 1997). However, the use of other membrane-bound proteins fused to aequorin failed to reveal such domain (Nakahashi *et al.*, 1997; Martin *et al.*, 1998; Lin *et al.*, 2000). A potential explanation for their unique results may be the low expression of their construct obtained. Indeed, in some of our experiments using the low-transfected MG63 cell line, most of the $\beta 2$ -Aeq was completely consumed after the addition of extracellular Ca^{2+} . Only a small part of aequorin remained during the cell lysis. In addition, a posterior work with the 5HT-Aeq construct revealed Ca^{2+} rises within the micromolar range in a different cell line (Poburko *et al.*, 2006). The range of Ca^{2+} concentrations reported in this thesis is supported by other reports

using membrane-bound aequorin (Nakahashi *et al.*, 1997; Martin *et al.*, 1998; Lin *et al.*, 2000).

The series of Ca^{2+} -sensitive fluorescent dyes (C18-fura 2, FFP18, and FIP18) used to monitor Ca^{2+} near the plasma membrane have also indicated that the Ca^{2+} levels beneath the membrane could reach concentrations as high as 150 μM (Davies & Hallett, 1998). Following this brief massive increase, the Ca^{2+} levels go down to order of magnitude similar to ours (5 μM). The difficulty of the calibration of these fluorescent dyes is well documented because of the important differences between *in-vitro* and *in-vivo* properties of these compounds (Takahashi *et al.*, 1999). The majority of the following reports using these dyes only showed the variation in fluorescent emission at the appropriate wavelengths avoiding the use of Ca^{2+} concentrations. Furthermore, no other studies employing such dyes have reported a similar ratio increase of 50-150 times. Normally, the reported ratio increase was 3-4 times in response to stimuli (Graier *et al.*, 1998), which is consistent with our results.

During these experiments, the resting Ca^{2+} concentrations were also studied to determine whether there were differences between BK channel and cytosolic domains at rest (Fig. 4.8). Four regions (Fig. 4.7) where Ca^{2+} levels remained stable were compared under different conditions. The initial basal Ca^{2+} levels of HEK293 cells previously maintained in Ca^{2+} -free medium were significantly lower (BK: 0.79 μM ;

Cyt: 0.26 μM) than those obtained during the subsequent addition of Ca^{2+} -free medium (BK: 0.86 μM ; Cyt: 0.38 μM) and re-addition of extracellular Ca^{2+} (BK: 0.88 μM ; Cyt: 0.42 μM). These initial lower levels in both domains were probably caused by the long-term incubation in EGTA, which may have emptied the ER Ca^{2+} stores. When cells were supplemented with EGTA for 5 min and subsequently with Ca^{2+} medium for another 5 min, only a small increase in resting Ca^{2+} levels was observed. This increase was detected in both the BK and cytosolic domains (0.86 & 0.88 μM , 0.38 & 0.42 μM , respectively), although only in the case of the cytosolic aequorin was significant. The higher Ca^{2+} levels detected in the plasma membrane at rest shown in this work are also supported by previous reports using aequorin constructs (Martin *et al.*, 1998; Lin *et al.*, 2000) and Ca^{2+} -sensitive fluorescent dyes (Graier *et al.*, 1998). Moreover, it is known that BK channel activity at rest is low. These basal Ca^{2+} levels near the BK channel (0.79 & 0.88 μM) are also consistent with this. There is evidence that Ca^{2+} concentrations below 1 μM induced low BK channel activity at resting membrane potential (~ -60 mV) when the α subunit was co-expressed with either the $\beta 2$ (Orio & Latorre, 2005) or the $\beta 1$ subunit (Nimigean & Magleby, 2000; Bao & Cox, 2005). A potential hypothesis to explain the higher Ca^{2+} concentrations in the membrane is that zeta potential retains Ca^{2+} ions beneath the subplasma membrane creating the higher Ca^{2+} levels detected.

The data presented in this work have revealed higher Ca^{2+} signals near the BK channel in response to the addition of extracellular Ca^{2+} probably due to SOC entry. In addition, the basal Ca^{2+} levels near the BK channel were also higher than those in the cytosol in either the presence or absence of extracellular Ca^{2+} .

4.4.3. Individuality of Ca^{2+} responses in HEK293 cells.

The inherent nature of all cell systems entails a certain degree of biological variability. There are, however, many occasions in which the diversity of the cellular response cannot be attributed to this biological variability (Rao *et al.*, 2002). The term 'molecular noise' has been used to describe this apparently random range of variability. Sometimes even opposite cellular responses can be induced under similar conditions (Rommerts *et al.*, 2002). Single cell imaging usually reports the percentage of cells in which the specific Ca^{2+} transients were detected supporting cell individuality.

HEK293 cells transfected with either $\beta 2$ -Aeq or Luc-Aeq exhibited a wide range of different Ca^{2+} transients. To investigate whether there exists a pattern in these apparently random Ca^{2+} responses to the external stimulus, a detailed study of the individual Ca^{2+} signals in the context of the fluctuations of the biological and experimental conditions was conducted.

This individual variability has been previously reported using aequorin chimeras (Allen *et al.*, 1985; Baubet *et al.*, 2000) although no detailed study was performed. In this thesis, a comprehensive analysis of the experimental conditions was carried out to examine the characteristics of these Ca^{2+} signals. The Ca^{2+} concentrations were calculated using the percentage of aequorin consumption, which is proportional to the Ca^{2+} concentration. Consequently, the variability of the Ca^{2+} transients was not as a result of the total aequorin expression, the coelenterazine concentration or the total cell number. Furthermore, there was no pattern found when the individual Ca^{2+} signals were compared to the total aequorin expression in each cell cluster (Fig. 4.10). The cellular responses in well-characterised cell lines may also differ due to modification of the cell properties during the culture period. Nevertheless, in the experiments analysed, all cells originated from the same cell passage number and differences in Ca^{2+} responses were observed within each individual coverslip (Fig. 4.9 & 4.10). This latter result also suggests that the differences were not caused by either technical variations (i.e. position of the ICCD camera, manual manipulation of the coverslip prior to the experiment, etc) or experimental conditions (i.e. use of different drug solutions, delay in the perfusion of the initial solution, incubation time in EGTA, etc). Moreover, the same solutions were employed in all the experiments in both $\beta 2\text{-Aeq}$ and Luc-Aeq . In our experiments, HEK293 cells were completely confluent and Ca^{2+} signals of individual cell clusters were independent

of their actual position within the chamber. This indicates that the cell density or particular position of individual cells in the population had probably little influence on the cellular responses.

The variations of the cellular responses during the life-cycle (G1-Gap1; S-synthesis; G2-Gap2 and M-Mitosis) of individual cells may account for part of this variability on the individual Ca^{2+} responses. Alterations of intracellular Ca^{2+} concentrations during the cell cycle have been widely reported (Santella, 1998). Indeed, extracellular Ca^{2+} has been shown to be required to initiate the G1 phase; a rise in intracellular Ca^{2+} from 200 to 400 nM occurs during the breakdown of the nuclear envelope (Steinhardt & Alderton, 1988); the SOC entry decreases with cell cycle progression (Morimoto *et al.*, 2007) and IP_3 -induced Ca^{2+} release controls the timing of mitosis onset (Ciapa *et al.*, 1994). Additionally, local Ca^{2+} microdomains generated by the ER near the nucleus may also be involved (Whitaker, 2006). Ca^{2+} binding enzymes such as calmodulin and the proteolytic enzyme calpain probably mediate these effects of Ca^{2+} on the cell cycle (Santella, 1998). Furthermore, the expression, regulation and activity of ion channels also depends on the phase of the cell cycle. Ca^{2+} channels such as the T-type (Day *et al.*, 1998) and the CRAC channels (Tani *et al.*, 2007) showed different regulation during the cell cycle. Similar findings have been reported for voltage-dependent potassium channels (Chittajallu *et al.*, 2002) and Ca^{2+} -activated potassium channels such as the intermediate conductance potassium (IK) (Deng *et al.*, 2007) and small conductance

potassium (SK) channels (Morimoto *et al.*, 2007). The cell cycle state also alters the expression and activity of BK channels in embryos (Day *et al.*, 1998) and cell lines (Ouadid-Ahidouch *et al.*, 2004). Many of these variations during the cell cycle occur near or within the plasma membrane. This may account for the higher variability observed in the BK channel microdomain (CV = 2.36 %, Table 4.3) than in the cytosol (CV = 1.36 %). Considering the great deal of cellular events and processes modified during the cell cycle, the phase of the cell cycle of individual cells may have caused, to some extent, the wide diversity of Ca^{2+} signals.

This diversity could also be an example of the non-linear and chaotic properties of complex biological systems operating inside the cell (Coffey, 1998). The traditional deterministic approach is generally used in research studies in order to simplify the cause-effect relationship of the results obtained. However, deterministic models are mathematically convenient, but biologically unrealistic. The use of stochastic models that describe random process can be better suited to account for the variability encountered during these experiments. These models use probability distribution functions to describe the uncertainty of the cellular processes. This uncertainty is produced by multiple factors, often working interactively and synergistically. In particular, Ca^{2+} oscillations, which are also present in HEK293 cells (Bird & Putney, 2005), seem to follow stochastic models (Eichwald & Kaiser, 1993; Kummer *et al.*, 2005). The stimuli-induced cellular response in the

experiments probably triggers several intracellular pathways in addition to the increase in intracellular Ca^{2+} . Some of these biological cascades are also likely to generate specific positive or negative feedback in the Ca^{2+} responses. This in turn results in a very complex Ca^{2+} signalling process that triggers the myriad of different Ca^{2+} signals observed.

The experiments carried out in this thesis provided evidence that individual clusters of HEK293 cells produced different Ca^{2+} responses as a result of the addition of extracellular Ca^{2+} .

4.4.4. Conclusions.

The analysis of the transfection efficiency and light signals in HEK293 (Fig. 4.2) and MG63 (Fig. 4.3 & 4.4) cells revealed that a minimum level of protein expression must be achieved to accurately monitor Ca^{2+} concentrations. Only HEK293 cells exhibited sufficient aequorin expression to perform Ca^{2+} imaging experiments. There was also evidence that HEK293 cells possessed intracellular mechanosensitive Ca^{2+} channels (Fig. 4.5). In HEK293 cells expressing the $\beta 2$ -Aeq chimera, resting calcium levels below the plasma membrane were higher (0.79 μM) than those in the cytoplasm (0.26 μM). Similarly a larger Ca^{2+} transient (4.56 μM) in response to the addition of extracellular Ca^{2+} was detected near the BK channel than that in the cytosol (1.81 μM). These differences indicate that the intracellular free Ca^{2+} in the BK channel is locally regulated and significantly different of that detected in the cytosol. In both BK channel and cytosolic domains,

the study of these Ca^{2+} transients (Fig. 4.8 & 4.9) revealed significant differences in the Ca^{2+} signals between individual cell clusters demonstrating the individuality of Ca^{2+} responses in HEK293 cells.

CHAPTER 5

**REGULATION OF LOCAL CALCIUM SIGNALS
NEAR THE BK CHANNEL BY AGONISTS AND
INTRACELLULAR CALCIUM RELEASE**

5.1 INTRODUCTION

Intracellular free Ca^{2+} has been proposed to modulate the activation of the BK channel (Marty, 1981; Pallotta, *et al.*, 1981). These evidence, however, have been based on experiments using either electrophysiological techniques or fluorescent dyes targeted to the cytosol. As indicated in Chapter 1, section 1.6, these techniques are unable to provide the exact Ca^{2+} concentration affecting the BK channel *in situ* in living cells. Therefore, in order to test the hypothesis that local intracellular Ca^{2+} activate BK channels, the experiments in this chapter were undertaken.

Receptor-operated agonist such as carbachol (CCh), ATP and histamine trigger Ca^{2+} responses in many different cells, which can be effectively monitored using aequorin (Rembold *et al.*, 1995; Badminton *et al.*, 1996). It could be expected that agonist-induced Ca^{2+} responses may also mediate the activation of the BK channel. Indeed, the BK channel regulation by CCh and ATP has been reported to be mediated by intracellular Ca^{2+} changes (Trautmann & Marty, 1984; Strøbaek *et al.*, 1996). Similar findings have been reported for histamine (Frieden *et al.*, 2002) and caffeine (Chavis *et al.*, 1998). Consequently, these three agonists were selected to study the Ca^{2+} responses near the BK channel.

Intracellular Ca^{2+} signals can also be affected by the exposure to potassium channel blockers. These Ca^{2+} responses are mainly caused

by alterations of the cell membrane potential which lead to the activation of voltage-dependent Ca^{2+} channels. Voltage-dependent Ca^{2+} channels have been reported to co-express with BK channels (Berkefeld *et al.*, 2006). Consequently, a local increase in intracellular Ca^{2+} near the channel may well occur as a result of membrane depolarisation. Tetraethylammonium (TEA), a generic potassium channel blocker, has been reported to induce Ca^{2+} transients in fibroblasts in which a large conductance K^+ channel is involved (Bhagavan, *et al.*, 1998). Tetrandrine, a more specific BK channel blocker (Wang & Lemos, 1992), also produced modifications in intracellular Ca^{2+} concentrations (Chen *et al.*, 2000). Moreover, there is also evidence that iberiotoxin, a specific BK channel blocker (Candia *et al.*, 1992), alters the amplitude of Ca^{2+} spikes in neuronal cells (Haghdoust-Yazdi *et al.*, 2008). Nevertheless, it must be mentioned that the ability of these compounds to block BK channels has been shown to be independent of the intracellular free Ca^{2+} (Candia *et al.*, 1992; Wu *et al.*, 2000). The effects of changes in membrane potential induced by TEA and tetrandrine were studied in this chapter.

Ca^{2+} release from intracellular stores has been associated with BK channel activation (Sergeant *et al.*, 2001; Frieden *et al.*, 2002). The effects of ER Ca^{2+} release in other cellular processes have been investigated using compounds such as caffeine or cyclopiazonic acid (CPA) (Rembold *et al.*, 1995; Badminton *et al.*, 1996). Caffeine acts through ryanodine receptors, which induce Ca^{2+} release from the ER.

CPA is an potent inhibitor of ER Ca^{2+} -dependent ATPases (Seidler *et al.*, 1989). This compound in particular has been shown to produce activation of the BK channels by means of increasing intracellular Ca^{2+} (Ohi *et al.*, 2001). Experiments using CPA are normally performed in the absence of extracellular Ca^{2+} to ensure that any modification of intracellular free Ca^{2+} is due to Ca^{2+} release from intracellular stores. In this thesis, caffeine and CPA were employed to determine whether ER Ca^{2+} release produces specific regulation of the intracellular free Ca^{2+} affecting the BK channel.

The BK channel activation in response to agonists or blockers has been examined mainly by means of either patch-clamp studies or determination of cytosolic Ca^{2+} . As shown in the previous chapter higher Ca^{2+} signals occur near the BK channel than those detected in the cytosol. Therefore, to understand how the BK channel function is modulated by these compounds is essential to assess the local intracellular free Ca^{2+} affecting the channel. This chapter aims to determine the Ca^{2+} levels reached in the proximity of the BK channel in response to various receptor-operated agonists (CCh, ATP and histamine) and changes in membrane potential using K^{+} channel blockers (TEA and tetrandrine). The effects of ER Ca^{2+} release on Ca^{2+} signalling near the BK channel were also investigated using caffeine and the SERCA pump inhibitor, CPA. Furthermore, the effects of the Ca^{2+} responses obtained in these experiments are compared to the

estimated Ca^{2+} concentrations required to produce BK channel activation based on previous studies.

5.2 METHODS

5.2.1. Ca^{2+} monitoring in living cells in response to diverse agonists.

HEK293 cells seeded on coverslips were transfected with either $\beta 2$ -Aeq or Luc-Aeq for 48 h as described in Chapter 2, 2.2.7.2. Cells were then incubated in Krebs-Ringer-HEPES (KRH) medium containing either EGTA (1 mM) or Ca^{2+} (1.3 mM) for 1 h at 37°C in the presence of coelenterazine (2 μM). Following the reconstitution of aequorin, coelenterazine was eliminated by washing the cells twice with the same medium. The cells were then transferred to the chamber and carefully brought into contact with the fibre optic. Ca^{2+} imaging experiments using an ICCD camera (Photek, UK) were carried out as described in Chapter 2, 2.4.2.2. All experiments were performed at room temperature (22°C).

5.2.2. Ca^{2+} monitoring in living cells in response to diverse drugs.

The Ca^{2+} imaging protocols were as follows:

- Receptor-operated agonists.

CCh & ATP. Incubation (1 h) in Ca^{2+} (1.3 mM) KRH (2 μM coelenterazine): 3 min Ca^{2+} KRH; 5 min CCh (100 μM) in Ca^{2+} KRH; 3 min Ca^{2+} KRH; 5 min ATP (100 μM) in Ca^{2+} KRH and 20 min lysis solution.

ATP & histamine. Incubation (1 h) in Ca^{2+} (1.3 mM) KRH (2 μM coelenterazine): 3 min Ca^{2+} KRH; 5 min ATP (100 μM) in Ca^{2+} KRH; 3 min Ca^{2+} KRH; 5 min histamine (100 μM) in Ca^{2+} KRH and 20 min lysis solution.

- *K⁺ channel blockers.*

TEA & tetrandrine. Incubation (1 h) in Ca^{2+} (1.3 mM) KRH (2 μM coelenterazine): 3 min Ca^{2+} KRH; 5 min CCh (TEA 10 mM) in Ca^{2+} KRH; 3 min Ca^{2+} KRH; 5 min tetrandrine (10 μM) in Ca^{2+} KRH and 20 min lysis solution.

- *Caffeine.*

Caffeine (5 & 50 mM) in EGTA. Incubation (1 h) in Ca^{2+} -free KRH (1 mM EGTA) (2 μM coelenterazine): 3 min Ca^{2+} -free KRH; 5 min caffeine (5 mM) in Ca^{2+} -free KRH; 5 min caffeine (50 mM) in Ca^{2+} -free KRH and 20 min lysis solution.

Caffeine (5 & 50 mM) in Ca^{2+} (1.3 mM). Incubation (1 h) in Ca^{2+} (1.3 mM) KRH (2 μM coelenterazine): 3 min Ca^{2+} KRH; 5 min caffeine (5 mM) in Ca^{2+} KRH; 5 min caffeine (50 mM) in Ca^{2+} KRH and 20 min lysis solution.

- *Cyclopiazonic acid.*

CPA in EGTA. Incubation (1 h) in Ca^{2+} -free KRH (1 mM EGTA) (2 μM coelenterazine): 5 min Ca^{2+} -free KRH; 10 min CPA (10 μM) in Ca^{2+} -free KRH; 5 min Ca^{2+} KRH and 20 min lysis solution.

All compounds were dissolved in KRH medium in either the presence or absence Ca^{2+} . CPA was dissolved in DMSO for stock solutions (10 mM). It has been shown that low concentrations of DMSO (~0.1 % v/v) do not affect cellular Ca^{2+} during 10 min exposure (Leung *et al.*, 1994).

5.2.3. Data analysis.

IFS32 Software (Photek, UK) was employed to analyse the data acquired. The complete imaging experiment was converted into a 10 s frame video sequence and a number of cell clusters (OAS) selected as described in Chapter 2, 2.4.2.2.3. The means \pm SEM were obtained from all the cell clusters selected from three different coverslips. Light emission was converted to Ca^{2+} concentration using rate constants and the equations described in Chapter 2, 2.4.3.

Aequorin consumption is proportional to the intracellular free Ca^{2+} . Since small Ca^{2+} transients were detected in response to some of the compounds tested, the increase in aequorin consumption was employed to quantify these Ca^{2+} responses. There was also evidence that the Ca^{2+} concentrations near the BK channel were higher than those in the cytosol (see Chapter 4, Table 4.2). Therefore in a given time period, more aequorin is consumed near the BK channel than in the cytosol. In order to compare the Ca^{2+} responses between the BK channel and the cytosolic microdomains, the data were plot as the increase in aequorin consumption during the exposure to the stimuli. The mean of the aequorin consumption prior to the addition of the drug

was calculated and subtracted from the values obtained during the drug exposure. Since the resting values varied between individual cell clusters, the increase in aequorin consumption was determined for each individual cell cluster. The aequorin consumed was calculated by dividing the total light counts during the drug exposure by the total counts emitted during the experiment. The final graphs represent the means of the variation in aequorin consumption of all cell clusters studied.

5.3 RESULTS

Three different agonists (ATP, histamine and CCh) were employed to examine whether the agonist-induced Ca^{2+} signalling near the BK channel was (see Chapter 4) regulated by local intracellular Ca^{2+} signals. In addition, the effects of K^+ channel blockers (TEA and tetrandrine) on intracellular free Ca^{2+} were assessed. To mimic physiological conditions these experiments (agonists and K^+ channel blockers) were performed in the presence of extracellular Ca^{2+} . Moreover, Ca^{2+} transients induced by CCh and ATP have been reported to be inhibited in the presence of EGTA in other cell lines such as adrenal chromaffin cells (Castro *et al.*, 1995). Consequently, to ensure that Ca^{2+} transients were generated in HEK293 cells, the effects of these agonists were tested in the presence of extracellular Ca^{2+} .

To investigate whether ER Ca^{2+} release may affect Ca^{2+} signals in both BK channel and cytosolic domains, caffeine and CPA (SERCA pump inhibitor) were tested in the absence of extracellular Ca^{2+} .

5.3.1 Effects of agonist-induced Ca^{2+} responses in HEK293 cells.

To investigate the effects of agonist-induced Ca^{2+} responses on the BK channel microenvironment of HEK293 α cells, a series of receptor-operated agonist that modulates intracellular Ca^{2+} was tested.

Three different compounds were applied: ATP, histamine and CCh. Histamine (100 μM) showed no effect in either the cytosol or the BK channel microdomain (Fig. 5.2) indicating the absence of histamine receptors in HEK293 cells. In contrast, ATP (100 μM) and CCh (100 μM) generated Ca^{2+} transients in both cytosolic and BK channel domains (Fig. 5.2). This is consistent with previous studies reporting the presence of purinergic and muscarinic receptors in HEK293 cells (Schachter *et al.*, 1997; Luo *et al.*, 2001). The exposure to ATP produced on average a higher increase within the BK microdomain (Fig. 5.2). Nonetheless, no significant different was detected between both Ca^{2+} increases. In contrast, CCh caused a significantly higher Ca^{2+} increase in the BK channel microdomain (Fig. 5.2) indicating a potential specific effect of this drug on the modulation of the BK channel by Ca^{2+} . In the analysis of the individual Ca^{2+} responses of representative cell clusters (Fig 5.1), an increase in intracellular free Ca^{2+} from 1 to 2 μM was observed in the BK channel microdomain (Fig. 5.1 A).

Fig. 5.1. Effects of carbachol in individual clusters of HEK293 cells transfected with either $\beta 2$ -Aeq or Luc-Aeq.

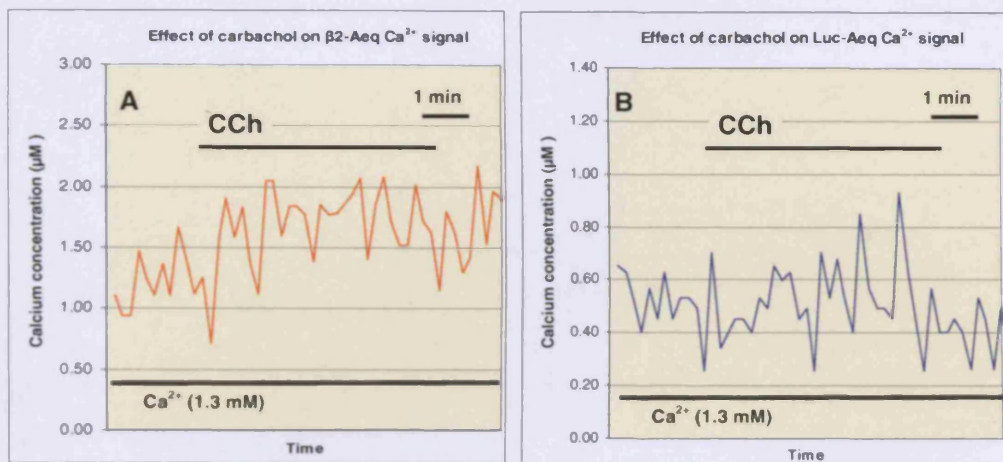


Fig. 5.1. Effects of carbachol in individual clusters of HEK293 cells transfected with either $\beta 2$ -Aeq or Luc-Aeq. Two representative experiments showing the effects of the exposure to CCh (100 μM) on intracellular free Ca^{2+} in either BK channel microdomain (A) or the cytosol (B). CCh induced a higher increase in the Ca^{2+} signal near the BK channel (A) than in the cytosol (B). The $\beta 2$ -Aeq chimera initially reported an intracellular free Ca^{2+} of around 1 μM which increased after exposure to CCh reaching peak values of approximately 2 μM . Following the addition of CCh, the cytosolic free Ca^{2+} also increased from a mean of approximately 0.5 μM to peaks of 0.8 μM . Several peaks can be observed in both domains during the CCh-induced Ca^{2+} transient. Cells were incubated for 1 h in the presence of medium containing Ca^{2+} (1.3 mM, 2 μM coelenterazine), perfused with similar medium for at least 3 min and supplemented with CCh (100 μM) for 5 min in the same medium. The remaining counts were obtained at the end of each experiment by the addition of an hyposmotic solution (10 mM CaCl_2). Light counts were acquired using an ICCD camera and IFS32 software (both from Photek, UK) as described in Chapter 2, 2.4.2.2. Light emission was converted to Ca^{2+} using rate constants as described in Chapter 2, 2.4.3.

Fig 5.2. Effects of intracellular Ca^{2+} modulators on Ca^{2+} responses in HEK293 cells transfected with Luc-Aeq or $\beta 2$ -Aeq.

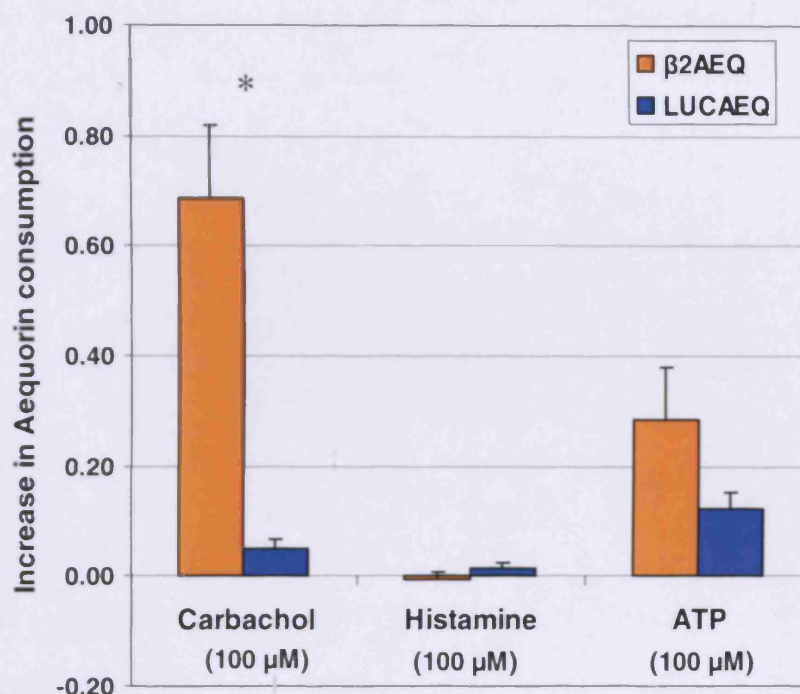


Fig 5.2. Effects of intracellular Ca^{2+} modulators in HEK293 cells transfected with Luc-Aeq or $\beta 2$ -Aeq. Cells were initially incubated in Ca^{2+} (1.3 mM) medium for 1 h, perfused with similar medium for at least 3 min and drugs supplemented for 5 min in Ca^{2+} -containing medium. Ca^{2+} rises in response to ATP (100 μM) and CCh (100 μM) were higher on the BK channel microdomain than in the cytosol. However, this increase was significant only in the case of CCh. Histamine (100 μM) produced no major increase in intracellular free Ca^{2+} in either domains. The remaining counts were obtained by addition of an hyposmotic 10 mM Ca^{2+} solution for 20 min. Data represent the means \pm SEM ($\beta 2$ -Aeq: CCh $n = 77$, histamine $n = 15$, ATP $n = 77$; Luc-Aeq: CCh $n = 97$, histamine $n = 35$, ATP $n = 97$) of aequorin consumption during 5 min exposure to the test solutions after subtracting the mean values obtained before drug addition. Data were obtained from at least 15 cell clusters recorded during three separate experiments. Data were acquired using an ICCD camera (Photek, UK) and analysed by means of IFS32 software (Photek, UK) as described in Chapter 2, 2.4.2.2. *- indicates that Luc-Aeq and $\beta 2$ -Aeq mean values are statistically different ($p < 0.05$)

Similarly, the initial cytosolic free Ca^{2+} (0.5 μM) reached peaks of approximately 0.8 μM after exposure to CCh.

Among the three agonists tested, only CCh (100 μM) showed a significant effect affecting the BK channel microdomain. Ca^{2+} oscillations were also recorded during the exposure to CCh.

5.3.2 Effects of K^+ channel blockers on intracellular free Ca^{2+} in HEK293 cells.

The effects of K^+ channel blockers on intracellular free Ca^{2+} were also assessed. The blocking of K^+ channels produce membrane depolarisation which then induce the activation of voltage-dependent Ca^{2+} channels. Since voltage-dependent Ca^{2+} channels such as L-type, P/Q-type and N-Type have been reported to co-express with BK channels (Berkefeld *et al.*, 2006), the possibility of a specific Ca^{2+} response induced by K^+ channel blockers close to the BK channel was studied. Two K^+ channel blockers were tested: TEA, a generic K^+ channel blocker and tetrandrine, which is specific for BK channels (Wang & Lemos, 1992).

Coverslips containing HEK293 α expressing either $\beta 2\text{-Aeq}$ or Luc-Aeq were perfused with either TEA (10 mM) or tetrandrine (10 μM) for 5 min. Neither TEA nor tetrandrine generated a significant modification in intracellular free Ca^{2+} in either domains (Fig. 5.4). A representative example is illustrated in Fig. 5.3 showing that intracellular free Ca^{2+} remained at approximately 0.7 and 0.3 μM in the BK channel (Fig. 5.3

A) and cytosolic (Fig. 5.3 B) domains respectively. The Ca^{2+} responses induced by TEA were found to be significantly different between $\beta 2\text{-Aeq}$ and Luc-Aeq (Fig. 5.4). However, the mean values obtained were very small indicating that these TEA-induced effects were probably negligible when compared to the basal levels prior to the exposure to TEA.

In summary, the K^+ channel blockers TEA (10 mM) and tetrandrine (10 μM) produced no significant changes in intracellular free Ca^{2+} in either the BK channel or the cytosolic domains.

5.3.2 Effects of caffeine.

To examine whether ER Ca^{2+} release can induce a specific local Ca^{2+} response in the proximity of the BK channel, various concentrations of caffeine were tested in either the presence or absence of extracellular Ca^{2+} .

Caffeine is used to trigger Ca^{2+} release from the ER (Smith *et al.*, 1988). The mechanism of action is through activation of ryanodine receptors. The doses of caffeine required to instigate this Ca^{2+} response are within the millimolar range (Karhapää & Törnquist, 1997). This latter study also reported that the caffeine-induced Ca^{2+} transients were dependent on extracellular Ca^{2+} because the Ca^{2+} increases detected were considerably reduced in the presence of Ca^{2+} chelators.

Fig. 5.3. Effects of TEA on intracellular free Ca^{2+} in individual clusters of HEK293 cells transfected with either $\beta 2$ -Aeq or Luc-Aeq.

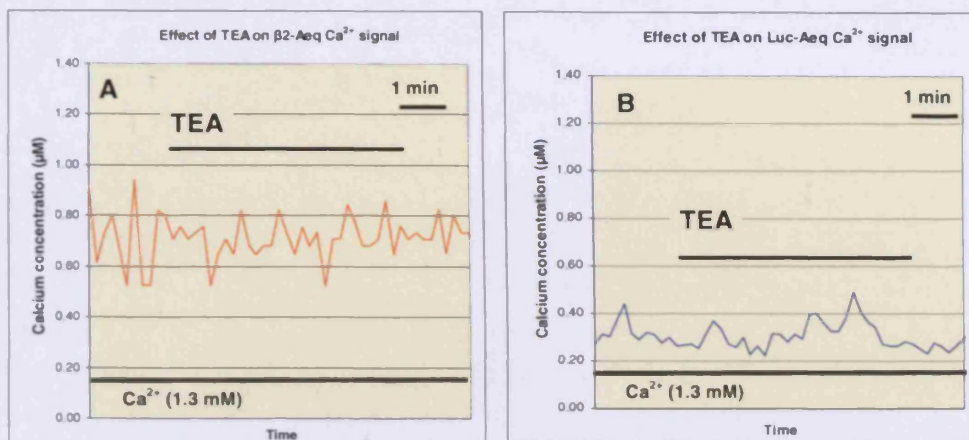


Fig. 5.3. Effects of TEA on intracellular free Ca^{2+} in individual clusters of HEK293 cells transfected with either $\beta 2$ -Aeq or Luc-Aeq. In these two representative experiments TEA (10 mM) induced no significant effect on intracellular free Ca^{2+} in either the BK channel microdomain (A) or the cytosol (B). The Ca^{2+} levels detected near the BK channel remained at approximately 0.7 μM (B) independently of the presence of TEA. Similarly the cytosolic basal Ca^{2+} of approximately 0.3 μM (B) did not change significantly as a result of TEA exposure. Cells were incubated in KRH medium (1.3 mM Ca^{2+} & 2 μM coelenterazine) for 1 h, perfused with Ca^{2+} medium for at least 3 min and TEA (10 mM) added for a 5 min period. At the end of experiments, the total remaining counts were obtained by 20 min exposure to an hyposmotic solution (10 mM CaCl_2). An ICCD camera and IFS32 software (both from Photek, UK) were used to acquire and analyse the aequorin signal as described in Chapter 2, 2.4.2.2. Intracellular free Ca^{2+} was calculated by converting the light emission to rate constants as described in Chapter 2, 2.4.3.

Fig 5.4. Effects of K⁺ channel blockers on intracellular free Ca²⁺ in HEK293 cells transfected with Luc-Aeq or β 2-Aeq.

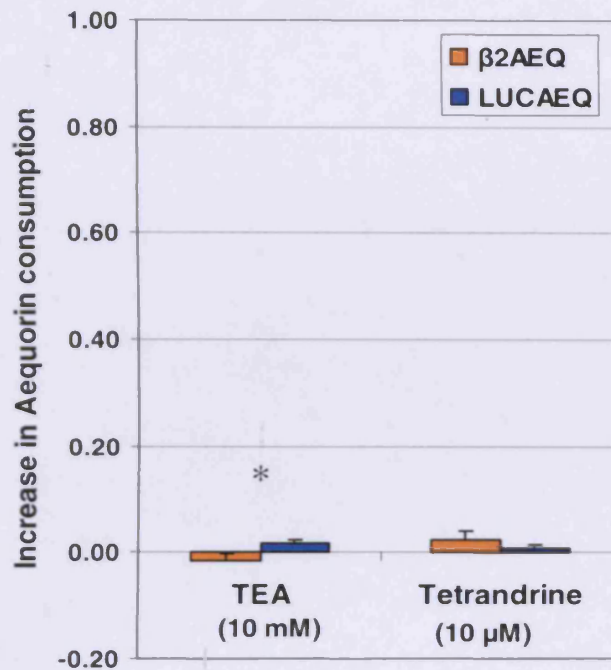


Fig 5.4. Effects of K⁺ channel blockers on intracellular free Ca²⁺ in HEK293 cells transfected with Luc-Aeq or β 2-Aeq. Cells in coverslips were incubated in medium containing 1.3 mM Ca²⁺ for 1 h in the presence of coelenterazine (2 μ M) and perfused with Ca²⁺ medium for at least 3 min before addition of the channel blockers. TEA (10 mM) and tetrandrine (10 μ M) were perfused for 5 min in Ca²⁺ medium. Minimum changes in intracellular free Ca²⁺ in either BK channel or cytosolic domains were induced by either TEA or tetrandrine. Although a statistical difference was detected in response to TEA between both domains, this is probably negligible due to the low Ca²⁺ signals generated. Cells expressing aequorin were exposed to a 10 mM Ca²⁺ solution in order to obtain the remaining light counts. The graph represents the means \pm SEM (β 2-Aeq: TEA n = 17, tetrandrine n = 17; Luc-Aeq: TEA n = 17, tetrandrine n = 27) of the aequorin consumed during the 5 min exposure to the channel blockers. Mean values calculated prior to the addition of the test solutions were subtracted. Data were obtained from at least 15 cell clusters recorded using an ICCD camera (Photek, UK) during three separate experiments and analysed using IFS32 software (Photek, UK) as described in Chapter 2, 2.4.2.2. * indicates that Luc-Aeq and β 2-Aeq mean values are statistically different

Experiments were conducted in either Ca^{2+} -free medium (1 mM EGTA) or Ca^{2+} (1.3 mM) medium following aequorin reconstitution in the same medium for 1 h. Cells were then perfused first with Caffeine (5 mM) for 5 min and then with caffeine (50 mM) for another 5 min, just before exposure to an hyposmotic solution to obtain the remaining light counts. The expected rise of intracellular Ca^{2+} was not observed in the experiments reported here indicating the absence of ryanodine receptor in HEK293 cells. In contrast, caffeine (5 & 50 mM) produced a steadily decrease in the BK microdomain (Fig. 5.5). In Ca^{2+} -free medium, this Ca^{2+} decline was only perceived at high concentrations (50 mM) (Fig. 5.6) while in the presence of extracellular Ca^{2+} was detected for both concentrations (5 & 50 mM). It must be noticed that a short Ca^{2+} increase from 0.2 to 0.3 μM lasting for 10 s was detected in the cytosol (Fig. 5.5. B) after addition of 5 mM caffeine in the presence of extracellular Ca^{2+} . This initial peak was only observed in a few cell clusters. Nonetheless, this may indicate the presence of endogenous ryanodine receptors in some individual cells.

A series of peaks were detected during these experiments, especially near the BK channel (Fig. 5.5 A & C). This effect may have been caused by Ca^{2+} oscillations which have been reported in HEK293 cells (Bird & Putney, 2005). Caffeine has also been reported to induce Ca^{2+} oscillations in other cell lines (Koopman *et al.*, 1997).

Fig. 5.5. Effects of caffeine in individual HEK293 cell clusters transfected with either $\beta 2$ -Aeq or Luc-Aeq.

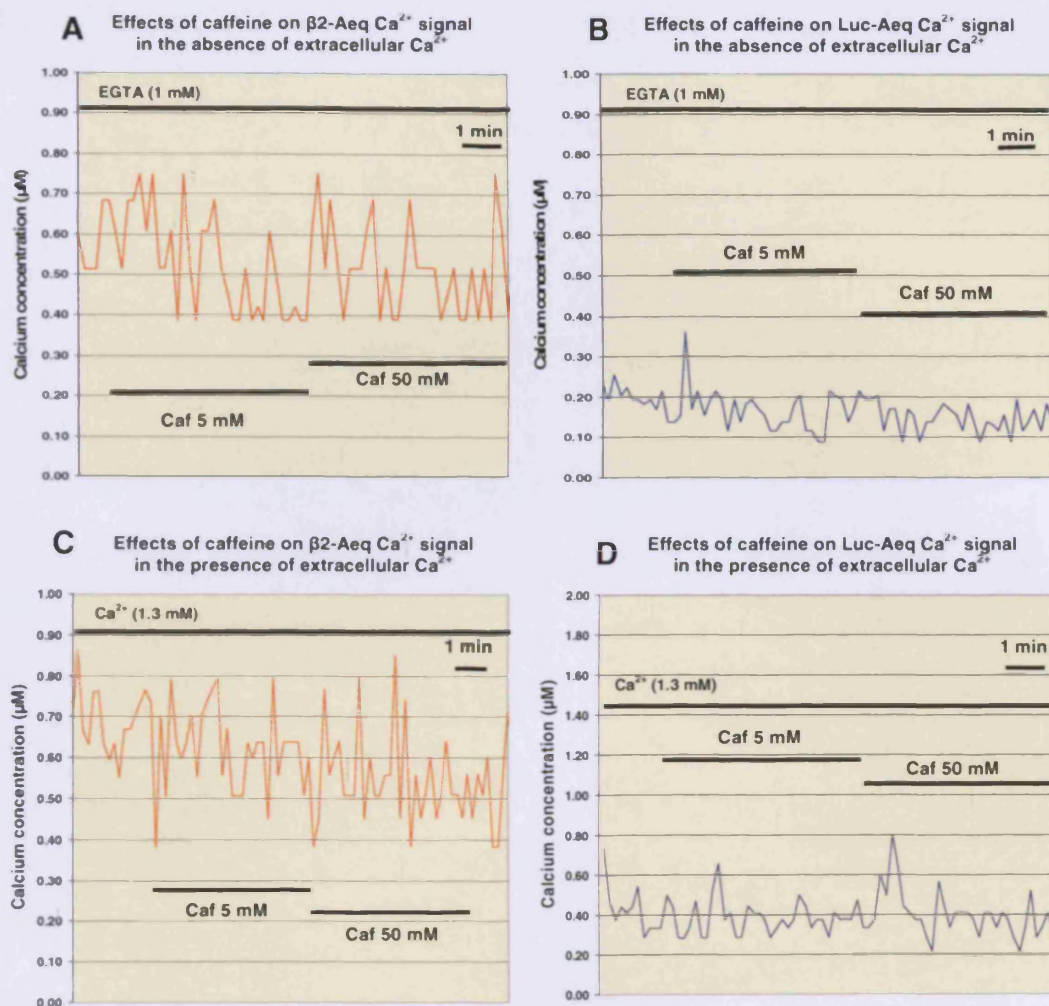


Fig. 5.5. Effects of caffeine on intracellular free Ca^{2+} of individual clusters of HEK293 cells transfected with either $\beta 2$ -Aeq or Luc-Aeq. The data plots illustrate four representative experiments showing the effects of caffeine addition (5 & 50 mM) on the intracellular free Ca^{2+} in either the absence (A & B) or presence (C & D) of extracellular Ca^{2+} . Caffeine (5 & 50 mM) induced a steady decay from approximately 0.60-0.65 to 0.5 μM on the average Ca^{2+} signal near the BK channel in either EGTA (1 mM) (A) or Ca^{2+} (1.3 mM) medium (C). A phenomenon similar to Ca^{2+} oscillations that ranged from 0.4 to 0.7 μM in the absence of Ca^{2+} (A) and from 0.4 to 0.8 μM (C) was observed in the BK channel microdomain during these experiments. Cells were incubated for 1 h in the presence of coelenterazine (2 μM) in medium either containing Ca^{2+} (1.3 mM) (C & D) or EGTA (1 mM) (A & B). Following 5 min perfusion with identical medium, coverslips were exposed first to caffeine (5 mM) for 5 min and subsequently to caffeine (50 mM) for another 5 min before adding an hyposmotic solution for 20 min to obtain the remaining counts. Data were acquired using an ICCD camera (Photek, UK) and analysed by means of IFS32 software (Photek, UK) as described in Chapter 2, 2.4.2.2. Light emission was converted to Ca^{2+} using rate constants as described in Chapter 2, 2.4.3.

Fig 5.6. Effects of caffeine on intracellular free Ca^{2+} in HEK293 cells transfected with Luc-Aeq or $\beta 2$ -Aeq.

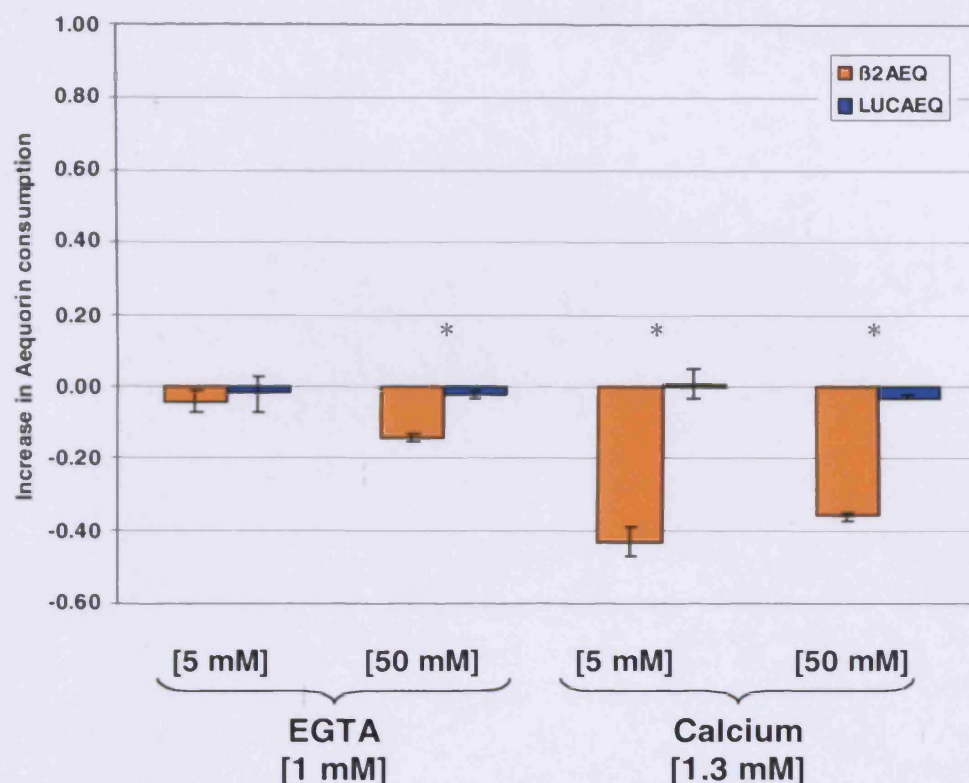


Fig 5.6. Effects of 5 min exposure to caffeine on intracellular free Ca^{2+} in HEK293 cells transfected with Luc-Aeq or $\beta 2$ -Aeq. Cells were incubated in either Ca^{2+} -free medium or medium with Ca^{2+} (1.3 mM) for 1 h (coelenterazine, 2 μM). Following 5 min perfusion with identical medium, coverslips were exposed first to caffeine (5 mM) for 5 min and subsequently to caffeine (50 mM) for another 5 min before lysing the cells. Data are the means \pm SEM ($\beta 2$ -Aeq: EGTA caffeine (5 & 50 mM) $n = 17$, Ca^{2+} caffeine (5 & 50 mM) $n = 21$; Luc-Aeq: EGTA caffeine (5 & 50 mM) $n = 34$, Ca^{2+} caffeine (5 & 50 mM) $n = 32$) of the variation of aequorin consumption during 5 min when compared to the consumption in the same medium prior to the addition of caffeine. Means and SEMs were obtained from between 15 to 30 cell clusters recorded during three separate experiments. Light counts were recorded using an ICCD camera (Photek, UK) and analysed using IFS32 software (Photek, UK) as described in Chapter 2, 2.4.2.2. * - indicates that Luc-Aeq and $\beta 2$ -Aeq mean values are statistically different ($p < 0.05$)

In conclusion, the addition of caffeine resulted in a reduction in intracellular free Ca^{2+} in the BK channel microdomain of HEK293 cells. This effect was dependent on the presence of extracellular Ca^{2+} . Ca^{2+} oscillations were observed in the proximity of the BK channel.

5.3.3. Effects of cyclopiazonic acid.

To investigate further the effects of Ca^{2+} release from intracellular stores on the BK channel microenvironment, CPA, a potent inhibitor of ER Ca^{2+} -dependent ATPases, was employed. In order to examine solely the effects of Ca^{2+} release from the ER, CPA was supplemented in Ca^{2+} -free medium (1 mM EGTA) preventing SOC entry.

Following incubation in EGTA (1 mM) for 1 h, the addition of CPA (10 μM) triggered a larger Ca^{2+} rise close to the BK channel than that observed in the cytosol (peaks: $1.88 \pm 0.09 \mu\text{M}$ & $0.65 \pm 0.05 \mu\text{M}$ respectively) (Fig. 5.7). The Ca^{2+} increase near the BK channel was also maintained for a longer period than in the cytosol (approx. 80 s & 10 s on average, respectively). This indicates that the inhibition of ER Ca^{2+} -dependent ATPases generated a local Ca^{2+} increase in the vicinity of the BK channel.

Perfusion of Ca^{2+} (1.3 mM) medium following the CPA treatment in EGTA elicited Ca^{2+} transients in both domains due to SOC entry from the extracellular milieu (Fig. 5.7). The slope of the Ca^{2+} transient detected in the cytosol reached a peak of 0.7 μM and then remained at 0.6 μM before exposure to the hypotonic solution.

Fig 5.7. Effects of cyclopiazonic acid on intracellular free Ca^{2+} in HEK293 cells transfected with Luc-Aeq or $\beta 2$ -Aeq.

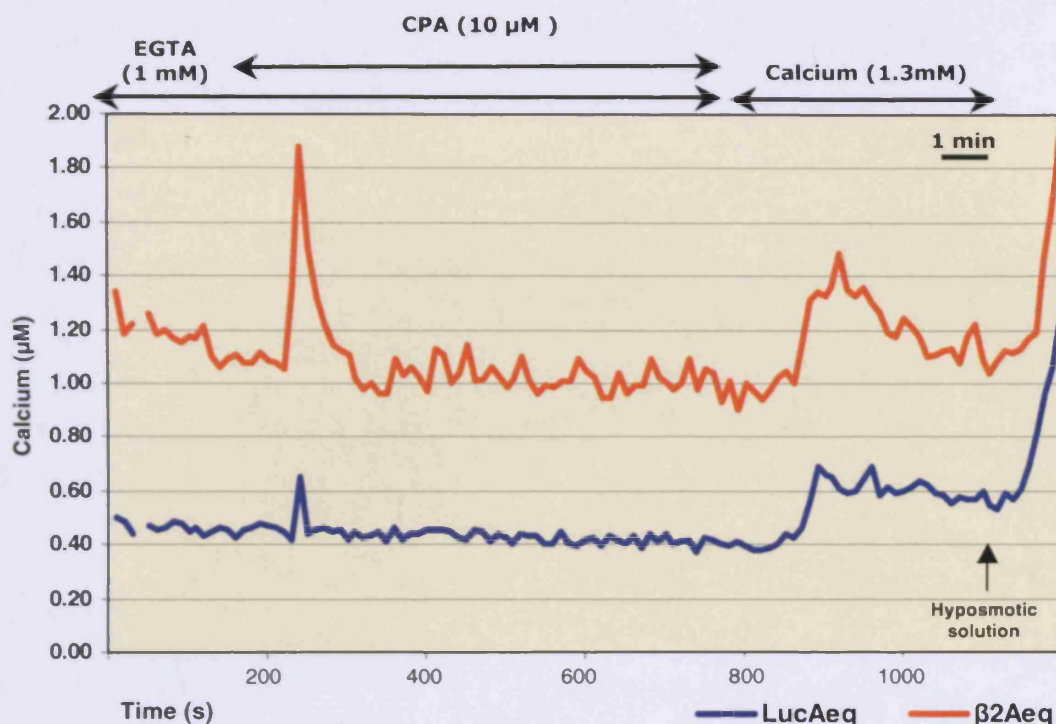


Fig 5.7. Effects of cyclopiazonic acid on intracellular free Ca^{2+} in HEK293 cells transfected with Luc-Aeq or $\beta 2$ -Aeq. Following 1 h incubation in Ca^{2+} -free medium (1 mM EGTA), HEK293 cells transfected with either Luc-Aeq or $\beta 2$ -Aeq were perfused with CPA (10 μM) in Ca^{2+} -free medium for 10 min. CPA induced a Ca^{2+} transient near the BK channel that reached at maximum of approximately 1.9 μM and decayed to basal Ca^{2+} levels after 70 s. In contrast, a short Ca^{2+} increase (0.65 μM) lasting only 10 s was detected in the cytosol. The subsequent addition of cell medium with Ca^{2+} (1.3 mM) for 5 min provoked Ca^{2+} transients in the BK channel and cytosolic domains reaching Ca^{2+} peaks of 1.5 and 0.7 μM respectively. Cells were then exposed to an hypotonic solution to obtain the remaining light counts. The traces illustrate the means of 39 ($\beta 2$ -Aeq) and 50 (Luc-Aeq) cell clusters obtained from at least three separate experiments. Light counts were converted to Ca^{2+} using rate constants as described in Chapter 2, 2.4.3. Ca^{2+} imaging experiments were performed using an ICCD camera and IFS32 software (both from Photek, UK) as described in Chapter 2, 2.4.2.2.

In the BK channel microdomain, the intracellular free Ca^{2+} increased from approximately 1 to 1.5 μM and subsequently decayed back to 1 μM after 5 min. Note that the central difference between the shapes of these Ca^{2+} transients detected near the BK channel and those previously obtained (Fig. 4.7) following long-term exposure to EGTA (1 mM) is the absence of the initial peak. This indicates that the initial peak (Fig. 4.7) was most likely promoted by Ca^{2+} -release from the ER, possibly by means of an initial CICR mechanism. The remaining component of this Ca^{2+} response (Fig 4.7) was similar to the one observed following exposure to CPA (10 μM) for 10 min and then to extracellular Ca^{2+} for 5 min (Fig. 5.7).

The $\beta 2$ -Aeq chimera reported a larger increase in intracellular free Ca^{2+} in response to CPA than that detected by the cytosolic Luc-Aeq. This provides evidence of a potential coupling between ER Ca^{2+} release and BK channel function.

5.4 DISCUSSION

The local free Ca^{2+} affecting the BK channel has been examined at rest and in response to a Ca^{2+} challenge (see Chapter 4) showing that in both cases was higher than cytosolic Ca^{2+} . In this chapter, the hypothesis that local intracellular free Ca^{2+} activates the BK channel was tested by using receptor-operated agonists (CCh, ATP and histamine) to induce Ca^{2+} responses in the plasma membrane and K^+ channel blockers (TEA and tetrandrine) to produce changes in the

membrane potential. The role of ER Ca^{2+} release was also studied by means of caffeine and CPA.

The results reported in this chapter showed that CCh and ATP produced Ca^{2+} transients in HEK293 cells in both the BK channel and cytosolic domains. The CCh-induced Ca^{2+} transient near the BK channel was significantly higher than that detected in the cytosol. Neither TEA nor tetrandrine generated a significant Ca^{2+} response in either domain. Caffeine caused a steady decay in intracellular free Ca^{2+} close to the BK channel. Unexpectedly CPA induced a larger Ca^{2+} transient in the BK channel microdomain. The effects of caffeine and CPA indicate that ER Ca^{2+} release can play a key role in controlling the local Ca^{2+} signals affecting the BK channel.

5.4.1 Effects of receptor-operated agonists.

To study the effects of receptor-operated agonists on intracellular free Ca^{2+} in either BK channel or cytosol, three different agonists (CCh, ATP and histamine) were tested. These agonists act through different receptors: muscarinic (CCh), purinergic (ATP) and histamine receptors. There is evidence of the presence of the purinergic (Schachter *et al.*, 1997), muscarinic (Luo *et al.*, 2001) and histamine receptors (Iwata *et al.*, 2005) in HEK293 cells. Although, CCh may also act through nicotinic acetylcholine receptors, these receptors are mainly expressed in the brain and have not been found in HEK293 cells (Gopalakrishnan

et al., 1996). These experiments were undertaken in the presence of extracellular Ca^{2+} (1.3 mM) in order to mimic physiological conditions.

Among the three agonists, only ATP and CCh induced a notable intracellular Ca^{2+} response (Fig. 5.2). Histamine (100 μM) exhibited a very small effect probably due to the absence or low expression of histamine receptors. However, endogenous histamine receptors in HEK293 cells have been reported (Iwata *et al.*, 2005) inducing minor increases (~50 nM) in cytosolic Ca^{2+} , which is probably similar to the data presented in this thesis. Nevertheless, no significant difference was found between the histamine-induced Ca^{2+} responses in the BK channel and cytosolic domains.

CCh (100 μM) generated a significant Ca^{2+} response in the BK channel microdomain (aeq consumption = 0.69). The Ca^{2+} levels above 1 μM observed after CCh exposure (Fig. 5.1) are consistent with previous reports showing that Ca^{2+} values above 1 μM produced an exponential increase in BK channel activation at resting membrane potential (~ -60 mV) when co-express with either the $\beta 2$ (Orio & Latorre, 2005) or the $\beta 1$ subunit (Nimigean & Magleby, 2000; Bao & Cox, 2005), which confers similar sensitivity to Ca^{2+} .

CCh activates muscarinic receptors inducing IP_3 production which causes Ca^{2+} -release from intracellular stores (White & McGeown, 2002). The empty of the ER also triggers SOC entry. These two Ca^{2+} effects probably participated in the response observed near the BK

channel. The activation of BK channels by CCh has been reported to remain even in the absence of extracellular Ca^{2+} (Trautmann and Marty, 1984). Since the effects of SOC entry were discussed in the previous chapter, this discussion is focused on the role of the Ca^{2+} -release from the ER produced by IP_3 .

Since IP_3 -induced Ca^{2+} -release produced a higher increase in intracellular free Ca^{2+} in the BK microdomain, a precise regulation of local Ca^{2+} near the channel by IP_3 might well have taken place (Fig. 5.8). Zeta potential may also be involved by attracting and maintaining the flow of Ca^{2+} ions released from the ER near the plasma membrane and consequently creating a local high Ca^{2+} concentration. The Ca^{2+} release is later diffused to the cytosol causing part of the increase observed in cytosolic Ca^{2+} . IP_3 -induced Ca^{2+} -release from other channels distant from the plasma membrane (Fig. 5.8 B) and SOC entry may account for the rest of this increase. It has also been suggested that CCh acts on BK channels through a pathway sensitive to the pertussis toxin and unrelated to the L-type Ca^{2+} channels (Chavis *et al.*, 1998). This pathway may be involved in CCh-induced Ca^{2+} response near the BK channel.

A series of peaks in intracellular free Ca^{2+} in response to CCh was also observed, especially in the BK microdomain (Fig. 5.1 A). These events resembled Ca^{2+} oscillations, although no further examination was undertaken. Mathematical models have suggested that IP_3 receptors

Fig. 5.8. Schematic representation of the effects of ER Ca release on the Ca^{2+} activation the BK channel.

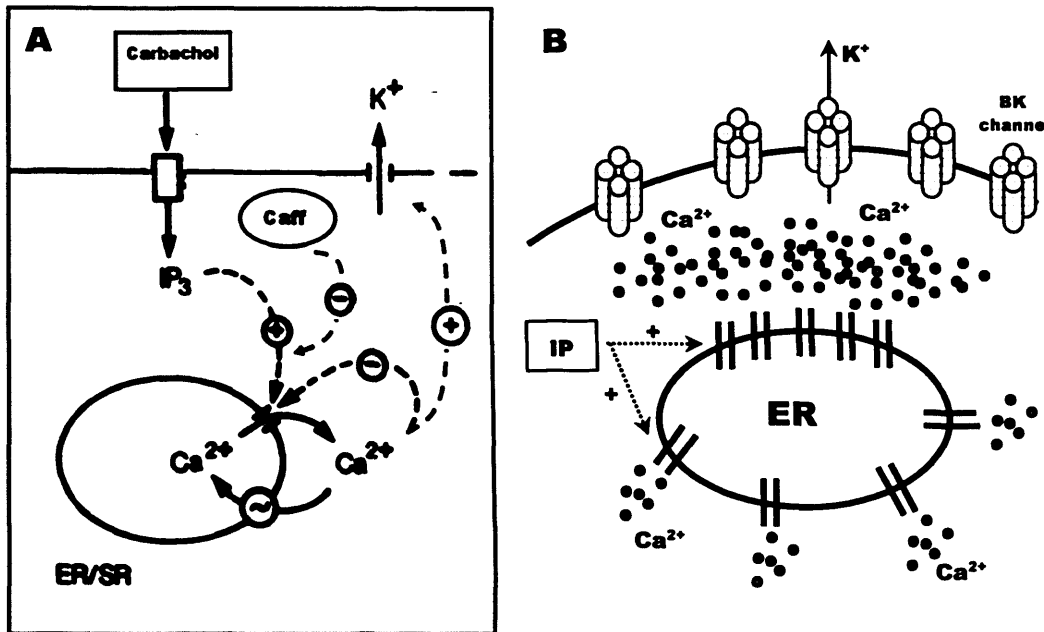


Fig. 5.8. Schematic representation of the effects of ER Ca release on the Ca^{2+} activation the BK channel. The diagram on the right (A) illustrates the production of IP_3 by the activation of muscarinic receptors by carbachol which subsequently activates IP_3 receptors causing the Ca^{2+} -release from intracellular stores. This Ca^{2+} -response is then detected by the BK channel triggering its activation. Caffeine induces an increase in the threshold of the IP_3 receptors inhibiting the ER Ca^{2+} -release. The hypothesis of IP_3 -triggered Ca^{2+} channels generating a larger Ca^{2+} -response near the membrane is shown in figure B. According to this hypothesis, an increase in IP_3 causes the Ca^{2+} -release from the ER which is larger close to the BK channel. This local Ca^{2+} -increase might be used to regulate locally the BK channel activation near the membrane. This is consistent with the greater Ca^{2+} signal detected near the BK channel in response to carbachol (See Fig. 5.2). In resting conditions, this considerable Ca^{2+} -response is normally compensated by the Ca^{2+} -ATPase pump. Cyclopiazonic acid produces the inhibition of this pump causing also a larger Ca^{2+} -increase near the BK channel (See also Fig. 5.7).

and the Ca-ATPase in the ER and plasma membrane play an essential role in the mechanism of the Ca^{2+} oscillations. Moreover, CCh-induced Ca^{2+} oscillations occur in HEK293 cells (Luo *et al.*, 2001). In this report performed in Ca^{2+} (1.5 mM) medium, the Ca^{2+} oscillations appeared in 50% of the cells examined and showed a frequency of around 0.5-1/min which also varied among the cells. This could explain the difficulties encountered in this thesis for the study of the Ca^{2+} responses in the presence of extracellular Ca^{2+} .

In contrast to the data shown in this research, other studies using membrane bound aequorin chimeras (Nakahashi *et al.*, 1997) have revealed that carbachol (200 μM) triggered a lower Ca^{2+} signal near the membrane than in the cytosol. Two are the main differences between this report and the work presented in here. Nakahashi and collaborators used a different method to supplement solutions to the cells which may produce a considerable difference between experiments (See section 4.3.3.). This idea is also supported by other reports (Tong *et al.*, 1999). More importantly in this research (Nakahashi *et al.*, 1997) aequorin was linked to the adenylyl cyclase protein. The fine tuning of Ca^{2+} signalling near the membrane controls many different cellular processes and must be tightly regulated (See section 1.1). Consequently, each particular protein is probably affected by a specific Ca^{2+} microdomain which may well differ from those having an effect on other proteins. The existence of these Ca^{2+} -microdomains has been previously proposed (Rizzuto and Pozzan, 2006) and would explain the different Ca^{2+} -transients

detected by either the adenylyl cyclase or $\beta 2$ -Aeq chimeras. The BK channels may require a large Ca^{2+} -transient to maintain the appropriate membrane potential while a lower Ca^{2+} concentration may be sufficient to trigger the signalling cascade of the the adenylyl cyclase.

The exposure to ATP (100 μM) caused Ca^{2+} transients in both the BK channel and the cytosol (Fig. 5.2). The mean of the Ca^{2+} response near the BK channel (0.28 ± 0.10 increase in aequorin consumption) was notably higher than that in the cytosol (0.12 ± 0.03). However, no significant difference in the ATP-induced Ca^{2+} response was found between the BK channel and cytosol domains. It is thought that the binding of extracellular ATP to P2Y receptors results in the production of intracellular IP_3 and consequently to an increase in intracellular free Ca^{2+} . Interestingly ATP failed to produce a statistically significant Ca^{2+} response near the BK channel as that caused by CCh. Following the hypothesis of an IP_3 mechanism, this discrepancy may be explained by the fact that IP_3 production by ATP is much lower than that by CCh (McMillian *et al.*, 1988). It may be also possible that the IP_3 -triggered Ca^{2+} channels in the intracellular stores close to the BK channel possess a higher threshold than those releasing Ca^{2+} to the cytosol. This would explain the differences observed between the Ca^{2+} responses in both domains.

The muscarinic-operated agonist, CCh, induced a significant increase in intracellular free Ca^{2+} near the BK channel. This compound also

triggered a phenomenon similar to Ca^{2+} oscillations. ATP caused a marked increase in the proximity of the channel although no significant difference was found in comparison to the Ca^{2+} response in the cytosol. Histamine failed to induce a significant Ca^{2+} transient.

5.4.2. Effects of K^+ channel blockers.

K^+ channel blockers can cause membrane depolarisation, which in turn activates voltage-dependent Ca^{2+} channels. Some of these channels such as L-type, P/Q-type and N-Type can co-express with the BK channel forming Ca^{2+} microdomains (Berkefeld et al., 2006). Consequently, K^+ channel blockers such as TEA or tetrandrine may induce specific regulation of Ca^{2+} signalling near the BK channel. Since the resting membrane potential of HEK293 cells is around -40 mV (Thomas & Smart, 2005), the concentrations of these blockers used in this work should be sufficient to depolarise the cell membrane which may cause Ca^{2+} influx.

Two K^+ channel blockers were used for this purpose: TEA and tetrandrine. Both blockers exhibit different kinetics indicating a different mechanism of inhibiting BK channel activity (Wang & Lemos, 1992). The generic K^+ channel blocker, TEA, is also capable of inducing Ca^{2+} oscillations (Tamarina et al., 2005) and Ca^{2+} increases in response to the alterations produced in membrane potential (Nilius et al., 1993; Brzyska et al., 2002). Tetrandrine is a more specific BK channel blocker (Wu et al., 2000). In addition, it also produces other effects which may

alter intracellular Ca^{2+} such as blockage of T-type and L-type Ca^{2+} channels (IC_{50} 9 μM and 30 μM , respectively) and inhibition of the Ca^{2+} ATPase pump similar to thapsigargin (Rossier *et al.*, 1993; Leung *et al.*, 1994). The inhibition of the Ca^{2+} ATPase pump by Tetrandrine in other cell lines has been reported to be much higher ($\text{IC}_{50} \sim 98 \mu\text{M}$) (Chen *et al.*, 2000).

Neither TEA (10 mM) nor tetrandrine (10 μM) had a major impact in intracellular Ca^{2+} (Fig. 5.4). TEA showed a statistically significant difference between the BK microenvironment and the cytosol. However, the effect recorded was too small to reliably establish this as a key factor in the distinctive Ca^{2+} modulation of the BK channel. No apparent Ca^{2+} oscillations were detected in the analysis of individual cell clusters (Fig. 5.3). The blocking activity of tetrandrine on Ca^{2+} channels did not cause any significant effect in the intracellular free Ca^{2+} in either the BK channel or cytosolic domains.

In summary, the changes in membrane potential caused by TEA and tetrandrine induced no significant modification of intracellular free Ca^{2+} in HEK293 cells.

5.4.3. ER and BK channel coupling: investigation using caffeine and cyclopiazonic acid.

There is evidence supporting the hypothesis of a potential coupling between local Ca^{2+} release and BK channel modulation (Sergeant *et al.*, 2001; Frieden *et al.*, 2002). The specific CCh-induced Ca^{2+}

response detected in the vicinity of the BK channel (see section 5.4.1) also indicates an possible IP_3 -mediated Ca^{2+} release from intracellular stores affecting the BK channel. To investigate this hypothesis, two compounds, caffeine and CPA, which affect the mechanism of ER Ca^{2+} release were employed.

5.4.3.1 *The effects of caffeine on intracellular free Ca^{2+} .*

Caffeine is widely used as a pharmacological tool to study the Ca^{2+} release from intracellular stores. The mechanism of action is through ryanodine receptors, which trigger ER Ca^{2+} release when activated. Caffeine also exhibits a variety of Ca^{2+} -independent actions such as inhibition of phosphodiesterase enzymes, activation of protein kinase A and increase of cytosolic cAMP (Butcher & Sutherland, 1962; Rousseau *et al.*, 1988; Lindaman *et al.*, 2002).

The results presented in this chapter showed that in HEK293 cells there was no increase in intracellular free Ca^{2+} induced by caffeine (Fig. 5.6) probably due to the absence of ryanodine receptors in these cells. Previous studies have reported the null effect of caffeine in HEK293 WT while a Ca^{2+} transient was detected in response to caffeine following transfection with ryanodine receptors (Brini *et al.*, 2005). Other cells are also devoid of both caffeine and ryanodine-sensitive Ca^{2+} channels and stores (Zimmermann & Walz, 1997), including an embryonic-type cell line (Scamps *et al.*, 1998). Although some studies have reported rises in intracellular calcium in HEK293, these effects were probably due to

an artefact caused by the perfusion system employed according to Tong and collaborators (Tong *et al.*, 1999). In the latter study, neither caffeine nor ryanodine generated a Ca^{2+} increase in HEK293 cells.

Interestingly, a notable decay ranging from 0.15 to 0.43 in aequorin consumption levels was detected with the $\beta 2$ -Aeq chimera (Fig. 5.5 & 5.6). A similar type of steadily decline but in basal calcium has been reported in previous studies (Cseresnyés *et al.*, 1997; Krizaj *et al.*, 1999). A common characteristic of all these studies is the biphasic effect of caffeine. An initial increase is observed immediately after caffeine addition and prior to the beginning of the Ca^{2+} decline. This increase was inhibited by ryanodine suggesting the presence of ryanodine receptors through which caffeine cause Ca^{2+} release from intracellular stores. The lack of Ca^{2+} response to ryanodine and the fact that it is routinely used as a model cell line to transfect ryanodine receptors support the idea that ryanodine receptors are not expressed in HEK293. Without these receptors, no initial Ca^{2+} increase was reported by either $\beta 2$ -Aeq or Luc-Aeq.

The Ca^{2+} decrease noticed by the $\beta 2$ -Aeq probe suggests a potential specific effect of caffeine in the BK channel microdomain. Caffeine has been shown to have a double effect on BK channels depending on the tissue, causing direct channel activation i.e. in arterial smooth muscle (McGahon *et al.*, 2007) or inhibition i.e. in portal vein (Xiong *et al.*, 1992). Activation of BK channels in HEK293 would produce membrane

hyperpolarisation causing the closure of voltage-dependent Ca^{2+} channels. Caffeine also produces direct inhibition of Ca^{2+} channels in the plasma membrane (Martin *et al.*, 1989), some of which co-assemble with the BK channel (Berkefeld *et al.*, 2006). The closure of Ca^{2+} channels in the plasma membrane by these two events may account for this Ca^{2+} decline near the BK channel and are consistent with the differences observed when caffeine was supplemented in either Ca^{2+} -containing or Ca^{2+} -free medium.

Another potential theory is based on the *two pool model* (Berridge & Galione, 1988). According to this model, there are two types of intracellular stores which maintain the equilibrium of intracellular calcium within the cell. The ER/SR one is triggered by IP_3 and the other is IP_3 -insensitive. Caffeine produces an augmentation of the IP_3 threshold which may partially reduce the IP_3 -induced calcium release (Parker & Ivorra, 1991). This inhibition might have caused the localised decrease in calcium detected in the BK channel microenvironment (Fig. 5.8 A). The higher threshold means that more IP_3 was free at basal levels which may have been sufficient to trigger the calcium release through other caffeine-insensitive Ca^{2+} channels with lower IP_3 affinity. These caffeine-insensitive channels have probably released Ca^{2+} in several areas no proximal to the BK channel in order to compensate the calcium decline detected near the BK channel. Ca^{2+} release from other sources such as the IP_3 -insensitive Ca^{2+} stores may have also been involved in this Ca^{2+} replenishment. Assuming an even distribution of

Luc-Aeq across the cell, the lower light signal emitted near to the BK channel would have been compensated by a higher signal in areas close to the caffeine-insensitive Ca^{2+} channels giving the overall equilibrium in Ca^{2+} signal detected by Luc-Aeq. If both events occur at low levels and simultaneously, no significant increase or decrease would be observed. The hypothesis of a confined Ca^{2+} fine-tune controlling BK channel activity is also supported by evidence showing a coupling between ER calcium release (Fig. 5.8 B) and BK channel modulation (Sergeant *et al.*, 2001; Frieden *et al.*, 2002). Furthermore, a recent report strengthens the idea of a close link between IP_3 -induced Ca^{2+} release and BK channel activation (Weaver *et al.*, 2007).

One last hypothesis involving the mitochondrial Ca^{2+} uptake as the mechanism behind the decline in Ca^{2+} concentration near the channel will be explained in the following section.

The caffeine effect has been shown to be dose-dependent and dependent on the presence of calcium in the extracellular milieu (Smith *et al.*, 1988; Missiaen *et al.*, 1994; Karhapää & Tömquist, 1997). Although there was no statistical difference between the mean values at concentrations of 5 mM (EGTA), 5 mM (Ca^{2+}) and 50 mM (Ca^{2+}), a clear trend towards lower aequorin consumption in the presence of Ca^{2+} could be observed (lower p values). There is also evidence that at low concentrations ($< 300 \mu\text{M}$) the caffeine-induced Ca^{2+} response is abolished in the absence of extracellular Ca^{2+} (Ahmed *et al.*, 1997)

which is coherent with the non significant difference noticed at a concentration of 5 mM in the presence of EGTA.

These experiments also revealed a series of Ca^{2+} peaks during the exposure to caffeine, especially in the BK channel microdomain Ca^{2+} (Fig. 5.5 A & C) and more frequently in the presence of extracellular Ca^{2+} . HEK293 cells generate Ca^{2+} oscillations in response to CCh (Luo *et al.*, 2001, see also section 5.4.1). Moreover, caffeine has been reported to induce Ca^{2+} oscillations in other cell lines (Koopman *et al.*, 1997) and also oscillations in the membrane potential (Komendantov & Kononenko, 2000). Consequently, Ca^{2+} oscillations may have well occurred during the course of these experiments. Nonetheless, the effects of these Ca^{2+} waves were difficult to assess during these experiments. Most studies in Ca^{2+} oscillations have been performed at a single cell level using fluorescent dyes. Aequorin has been also used (Berrie *et al.*, 1996) but mainly using microinjection in large cells which results in high light signals. Since these Ca^{2+} oscillations may vary temporally and spatially, they will normally appear as a very small light signals in the aequorin studies reported in this thesis (Allen *et al.*, 1985). In general, when individual Ca^{2+} peaks change little during the experiment, the mean Ca^{2+} peak may remain approximately constant. These Ca^{2+} waves can only be detected when firing simultaneously in various aequorin transfected cells or in single cells with a high expression of aequorin. Due to these difficulties, no further investigation

related to Ca^{2+} oscillations was carried out and the means of the Ca^{2+} signals were used to examine Ca^{2+} signalling.

In summary, a Ca^{2+} decay induced by caffeine occurred within the BK channel microenvironment. This effect may be explained by a co-operative combination of two effects: an inhibition of the IP_3 -triggered Ca^{2+} -release from intracellular stores and closure of voltage-activated Ca^{2+} channels in the plasma membrane. Caffeine-induced Ca^{2+} oscillations were also detected during the course of these experiments.

5.4.3.2 The effects of CPA on intracellular free Ca^{2+} .

Cyclopiazonic acid (10 μM), a well-known inhibitor of ER Ca^{2+} -dependent ATPases, induced surprisingly a significant Ca^{2+} -increase close to the BK channel (1.88 μM , Fig. 5.7) while only a small increase was detected in the cytosol (0.65 μM). Since these experiments were performed in the absence of extracellular Ca^{2+} , the Ca^{2+} transients could only be induced by Ca^{2+} release from intracellular stores. This larger increase near the membrane was unexpected because CPA is supposed to increase intracellular Ca^{2+} uniformly across the cytosol. In the presence of CPA, the Ca^{2+} leak from intracellular stores is not longer compensated by the CPA-inhibited Ca^{2+} re-uptake. Nonetheless, some studies have reported Ca^{2+} release from intracellular stores near the plasma membrane using membrane-bound fluorescent dyes (Davies *et al.*, 1997) and CPA-induced Ca^{2+} release resulting in the activation of Ca^{2+} dependent currents using patch-clamp techniques

(Wayman *et al.* 1996; Ohi *et al.*, 2001). Of particular interest is this latter work reporting BK channel activation following the addition of CPA in the presence of EGTA that lasted between 1-2 min. This time-frame is similar to the CPA-induced Ca^{2+} transients recorded in the proximity of the channel in this thesis. This research work (Ohi *et al.*, 2001) together with the results presented here indicate that the addition of CPA caused a local Ca^{2+} transient affecting the BK channel which also produced the activation of the channel.

The possibility of the $\beta 2$ -Aeq being trapped in the ER exists because the subcellular fractionation assessment (Fig. 3.12) only indicated that the $\beta 2$ -Aeq chimera targeted any of the cell membranes which includes the ER membrane. If this was the case, the aequorin moiety of the protein would be pointing to the cytosol and detecting directly the Ca^{2+} release from the ER. However, this is not probably the case because there is evidence that the $\beta 2$ subunit is mainly expressed in the cytosol if co-expressed with the α subunit (Lv *et al.*, 2008; see also Chapter 3, section 3.4.2). Furthermore, aequorin constructs retained in the ER and orientated to the cytosolic part have been reported to detect identical Ca^{2+} concentrations as those in the cytosol (Pinton *et al.*, 2004). These reports give support to the results presented in this thesis showing that $\beta 2$ -Aeq reports Ca^{2+} signals in the vicinity of the BK channel.

An hypothesis to explain this larger Ca^{2+} increase near the BK channel could be that the continuous mechanism of Ca^{2+} release and uptake

functioning in the proximity of the ER may have been altered by CPA. Consequently, the continuous Ca^{2+} leak from the stores could then be observed because the uptake into the stores was inhibited (Morgan & Jacob, 1994). If part of this Ca^{2+} release and uptake was specifically orientated towards the BK channel microenvironment (Fig. 5.8 B), then the disruption of the Ca^{2+} uptake would have resulted in a constant Ca^{2+} leak near the BK channel similar to that detected by the $\beta 2\text{-Aeq}$ chimera. This Ca^{2+} release would have not been compensated by the ER Ca^{2+} -dependent ATPase and lasted until this BK-orientated CPA-sensitive Ca^{2+} store in the ER was empty. This idea is consistent with the hypothesis that Ca^{2+} reuptake via the ER Ca^{2+} -dependent ATPase is the main mechanism for removal of Ca^{2+} from the subplasma membrane domain (Young & Zhang, 2004). Another potential hypothesis is based on the zeta potential playing a key role. As mentioned earlier (section 5.4.1), the zeta potential may have maintained the Ca^{2+} ions released from the ER near the membrane resulting in high local Ca^{2+} concentrations close to the BK channel.

The Ca^{2+} peak obtained in the cytosol in Ca^{2+} -free medium was similar to those previously reported in other cell lines (Hopf *et al.*, 1996). A simple mechanism of cellular diffusion may account for the diminution of the local Ca^{2+} signal induced in the BK channel and not detected in the cytosol. In addition, mitochondria may also be involved. Previous reports have suggested a buffering effect of mitochondria on the cytosol (Golovina & Blaustein, 1997; Varadi *et al.*, 2004). Indeed CPA also

induced an increase in mitochondrial Ca^{2+} uptake in smooth muscle (Szado *et al.*, 2003). Consequently, the large CPA-evoked Ca^{2+} response obtained near the membrane might have been buffered by mitochondria giving an attenuated rise in the cytosol. This hypothesis will be described later on.

CPA has been shown to deplete both caffeine and IP_3 -activated ER stores (Ziganshin *et al.*, 1994). Both CPA and CCh produced significant responses within the BK channel microenvironment. These results were consistent with previous evidence showing that CPA acts through IP_3 -sensitive intracellular stores also affected by CCh (Nakamura *et al.*, 2000; Molleman *et al.*, 2001). Ryanodine, which also activates these receptors, has been reported to induce large Ca^{2+} -transients beneath the plasma membrane producing the activation of BK channels in smooth muscle (Zhuge *et al.*, 2002).

As mentioned earlier, patch-clamp experiments have shown an increase of BK channel activity following the addition of CPA (Ohi *et al.*, 2001). In this research, concentrations of CPA within the same range to the experiments performed here triggered the activation of BK channels for a period of 1-2 min. The duration of the Ca^{2+} transients obtained in the experiments carried out in this thesis is similar to their results. In addition, the Ca^{2+} concentrations reached near the BK channel (1.88 μM) as a result of exposure to CPA were also consistent with those required to increase the activation of BK channels formed by α and

either $\beta 1$ or $\beta 2$ subunits (Nimigean & Magleby, 2000; Bao & Cox, 2005; Orio & Latorre, 2005). Furthermore, there is also evidence that a CPA-sensitive outward current promoted by CCh was selectively inhibited by iberiotoxin (Molleman *et al.*, 2001). This data demonstrates that BK channel activity and Ca^{2+} released elicited by CCh and CPA are two processes closely connected which is also corroborated by the results presented in this thesis.

CPA, caffeine and CCh can affect ER Ca^{2+} release. These three distinct compounds also modify Ca^{2+} concentration near the BK channel indicating the close link between ER Ca^{2+} release and BK channel activation.

5.4.4. The potential role of mitochondria in buffering calcium in the BK channel microdomain.

Mitochondria are recognised as the main sources of cellular energy. They are also deeply involved in the mechanisms of control of cellular calcium. There is a great deal of evidence showing their prominent role as a buffering constituent (Golovina & Blaustein, 1997; Szado *et al.*, 2003; Varadi *et al.*, 2004). Indeed it has been suggested that normal Ca^{2+} influx is maintained using a subset of mitochondria beneath the plasma membrane (Varadi *et al.*, 2004). A key role of mitochondria controlling Ca^{2+} modulation of BK channels has been proposed (Malli *et al.*, 2003) which may well explain most of the findings presented in this work.

In support of this hypothesis, there is evidence of mitochondrial Ca^{2+} uptake in response to CCh, ATP and caffeine (Rutter *et al.*, 1993; Button & Eidsath, 1996; Brini *et al.*, 1997; Montero *et al.*, 2002). These studies have demonstrated that CCh produced a higher Ca^{2+} uptake in mitochondria than ATP. In addition, there is evidence of a connexion between Ca^{2+} release mediated by ryanodine receptors and an increase in mitochondrial Ca^{2+} (Szado *et al.*, 2003). Caffeine also induced a large initial Ca^{2+} increase in mitochondria which was followed by a small plateau indicating a sustained Ca^{2+} uptake. This caffeine-induced effect may account for the initial Ca^{2+} rise caused by the activation of ryanodine receptors which are absent in HEK293 and the later steady decline in Ca^{2+} . The addition of CPA can also initiate Ca^{2+} transients in mitochondria (Szado *et al.*, 2003; Takei *et al.*, 2006) which also revealed a correlation with the ER Ca^{2+} release (Pinton *et al.*, 2001; Boehning *et al.*, 2003).

The effects of inhibitors of mitochondrial functions were shown to be dependent on extracellular Ca^{2+} (Nowicky & Duchen, 1998). In addition, a large Ca^{2+} transient has been detected in mitochondria as a result of extracellular Ca^{2+} which was reduced by inhibitors (Varadi *et al.*, 2004; Vandebrouck *et al.*, 2006). This data indicates that mitochondria are also involved in SOC entry. Furthermore, these inhibitors also generated a rise in cytosolic Ca^{2+} resulting in the activation of Ca^{2+} - dependent K^+ channels which were sensitive to charybdotoxin and TEA

(Varadi *et al.*, 2004) This latter study suggests a potential link between mitochondria Ca^{2+} uptake and BK channels.

Most of the findings presented in this thesis can be explained according to these reports. CCh and CPA induced considerable Ca^{2+} responses near the BK channel which may have been buffered by means of mitochondria buffering. In the case of ATP, the reduced buffering effect of mitochondria in the BK microdomain may have resulted in a higher increase in cytosolic Ca^{2+} . Consequently, no significant difference would have been detected between the BK channel and cytosolic domains. The caffeine-induced decay in intracellular free Ca^{2+} may have also been caused by mitochondrial Ca^{2+} uptake. Accordingly, mitochondria would have displayed a sustained Ca^{2+} increase as a result of the exposure to caffeine which would be consistent with the mentioned studies (Szado *et al.*, 2003). Similarly, the prominent Ca^{2+} buffering effect originated by mitochondria during the addition of extracellular Ca^{2+} would have probably been responsible for the lower Ca^{2+} increase recorded in the cytosol.

Finally, the most relevant work supporting this theory of mitochondrial buffering of the BK channel was undertaken by Malli and collaborators (Malli *et al.*, 2003). In this elegant approach using a combination of fluorescent dyes and whole-cell patch clamp analysis, they studied the effects of histamine-induced Ca^{2+} activation of the BK channel in three specific sub-plasma membrane locations: close to the ER, near

mitochondria and far from either. Their data revealed that in human umbilical vein endothelial cells there are three very distinctive Ca^{2+} concentrations beneath the plasma membrane depending on the presence of ER (6.33 μM), mitochondria (0.25 μM) or none of them (3.50 μM). Following the initial Ca^{2+} rise, the subsequent values of the Ca^{2+} plateau were 1.30, 0.10 and 1.18 respectively. All their experiments were carried out at room temperature. Electrophysiological recordings were performed simultaneously showing analogous increases in the channel open probability. This data indicate that mitochondria play a key role in buffering Ca^{2+} concentrations near the BK channel. In addition, the sub-plasma membrane Ca^{2+} measurements obtained in this work correlated well with theirs, even though they estimated Ca^{2+} concentrations near the membrane using an equation determined by BK channel activation in excised patches. The experiments presented in here showed that Ca^{2+} concentrations in the plasma membrane elicited in the presence of EGTA were in the order of 1.88 μM (Fig. 5.7) and 4.56 μM with Ca^{2+} medium (Fig. 4.7). It would be expected that histamine-induced Ca^{2+} transients in Ca^{2+} medium were between those values which are concordant with the findings of Malli and collaborators (Malli *et al.*, 2003). The close similarity between both results indicates that both approaches are equally valid.

The hypothesis proposed in this thesis is that BK channels together with the $\beta 2\text{-Aeq}$ chimera were distributed uniformly across the membrane of

each cell. Therefore, the three different possibilities (proximity to the ER, mitochondria or none of them) would have contributed to the mean values reported in this work.

The similarity found between the results in this thesis and those of previous reports provide support to the hypothesis of a potential role of mitochondria controlling the Ca^{2+} activation of BK channels.

5.4.5. Conclusions

To summarise, the results in this chapter provide support to the hypothesis that BK channels are activated by local Ca^{2+} signals. Indeed CCh, caffeine and CPA induced local Ca^{2+} responses near the channel. $\beta 2$ -Aeq chimera reported a specific Ca^{2+} regulation in the proximity of the BK channel in HEK293 cells as a result of exposure to CCh (100 μM) (Fig. 5.2). ATP (100 μM) produced Ca^{2+} transients of the same magnitude in the BK channel and cytosolic domains. Histamine (100 μM) caused no significant increase in intracellular free Ca^{2+} in both domains. Similarly, no significant Ca^{2+} response was triggered by changes in membrane potential following the addition of either TEA (10 mM) or tetrandrine (10 μM) (Fig. 5.4). Caffeine (5 & 50 mM) induced a sustained decay in intracellular free Ca^{2+} near the BK channel (Fig. 5.6). This effect was more prominent in the presence of extracellular Ca^{2+} . Ca^{2+} oscillations were detected near the BK channel in response to CCh and caffeine. Surprisingly, the use of the SERCA inhibitor, CPA (10 μM), in Ca^{2+} -free medium caused a marked Ca^{2+} transient in the BK

channel microdomain (1.88 μM) while only a small Ca^{2+} peak was recorded in the cytosol (0.65 μM). This unexpected result may be explained by a potential coupling between ER Ca^{2+} -release and Ca^{2+} signalling near the BK channel. Furthermore, a mechanism involving IP_3 -induced ER Ca^{2+} -release and mitochondrial buffering has been proposed to account for the local Ca^{2+} -regulation in the vicinity of the BK channel.

CHAPTER 6

GENERAL DISCUSSION

6.1. SUMMARY OF MAIN FINDINGS

The studies outlined in this thesis describe the successful development of a $\beta 2$ -Aeq chimera capable of detecting local Ca^{2+} signals affecting the BK channel. This section presents an overview of the principal findings, the future studies and their significance in the context of the published literature.

The main finding of this thesis was that a highly localised Ca^{2+} signalling controls the BK channel function.

The strategy adopted in this thesis was to measure the intracellular free Ca^{2+} using the Ca^{2+} sensitive photoprotein aequorin targeted to the BK channel complex in living cells, and to investigate the regulation of the Ca^{2+} concentration close to the channel as a signalling mechanism. In the first stage of this work, the $\beta 2$ subunit of the BK channel was cloned using mRNA extracted from osteoblast-like MG63 cells. The aequorin protein was engineered onto the cytosolic C-terminus of the $\beta 2$ subunit and shown to maintain the Ca^{2+} sensitivity in both a cell-free system and living cells. The functional assessment of the protein showed that the new chimera possessed identical reconstitution properties in different conditions but a 10-fold reduction in light emission in comparison to the native aequorin. The recombinant protein targeted effectively the plasma membrane, where it reported changes in free Ca^{2+} .

The $\beta 2$ -Aequorin protein was used in conjunction with a cytosolic Luc-Aeq construct to compare the Ca^{2+} signalling processes in both domains. These two aequorin variants were expressed in two cell lines that contain a high number of BK channels, MG63 and HEK293 stably transfected with the BK channel α subunit. Only HEK293 cells express sufficient aequorin protein to enable Ca^{2+} imaging studies. Evidence of Ca^{2+} release from intracellular stores in response to a mechanical stimuli was found in HEK293 cells in suspension. This Ca^{2+} release indicates the presence of intracellular Ca^{2+} channels that are activated in response to mechanical disturbance.

Store-operated Ca^{2+} entry induced a 3 fold higher Ca^{2+} transient in the vicinity of the channel than that observed in the cytosol in HEK293 cells in monolayers. The individuality of Ca^{2+} signalling in these cells was demonstrated by the wide range of different Ca^{2+} signals detected in the individual cell clusters. Agonist-induced stimuli generated local Ca^{2+} responses near the BK channel. Changes in membrane potential produced no significant Ca^{2+} responses in either the BK channel or cytosol domains. The ER Ca^{2+} release also induced a high Ca^{2+} increase in the BK channel microdomain suggesting a potential coupling between the ER and the BK channel that regulates the Ca^{2+} concentration affecting the channel.

All this evidence proves that this new $\beta 2$ -Aequorin chimera is a powerful tool to clarify the very complex mechanisms involved in cellular Ca^{2+} signalling controlling the BK channel function.

6.2. FUTURE PROSPECTS

The studies reported in this thesis will form the basis of future work on the local regulation and physiological function of free Ca^{2+} near the BK channel.

6.2.1. Further assessment of the functional properties of the $\beta 2$ -Aeq chimera.

The data described in this thesis have provided considerable evidence of the capacity of $\beta 2$ -Aeq for successfully reporting the local Ca^{2+} signals affecting the BK channel. Nonetheless, the correct co-expression of the α subunit with the $\beta 2$ -Aeq has not been studied in detail. An appropriate approach would be immunoassays such as co-immunoprecipitation or immunofluorescence for both α and $\beta 2$ -Aeq proteins. This would also assist in determining whether part of the $\beta 2$ -Aeq is retained in the ER. Previous reports indicate that the α subunit co-assembles effectively with either the $\beta 2$ subunit (Lv *et al.*, 2008) and a $\beta 1$ -GFP chimera (Kim *et al.*, 2007).

A simple estimation of the number of BK channels per cell and the number of $\beta 2$ -Aequorin chimeras present in the cell may suggest that

there was a slightly excess of $\beta 2$ -Aequorin. Assuming that BK channels are uniformly distributed across the cell membrane, an average of three channels per patch (Fig. 3.3) and an average diameter of 30 μm for HEK293 cells, the total number of BK channels per HEK293 cell was estimated to be around 8500 channels. Equally, the amount of total counts can also provide an estimate of the number of $\beta 2$ -Aeq molecules within the cell. Based on the data shown in this thesis (See section 4.3.1) and assuming a transfection efficiency of 20%, a quantum efficiency of 2% for $\beta 2$ -Aeq (10 fold lower than aequorin, Fig. 3.8) and a total quantum collection efficiency of 10% for the luminometer, the number of $\beta 2$ -Aeq molecules was estimated to be of the order of 58000. Each BK channel may potentially bind up to four $\beta 2$ subunits resulting in a maximum of 34000 binding sites available. Consequently, some of the $\beta 2$ -Aeq chimeras may not be co-assembling with the BK channel, although may well be membrane-bound as suggested by the subcellular fraction approach taken in this thesis (Fig. 3.12). The co-immunoprecipitation of both BK α and $\beta 2$ subunits would clarify whether these estimations reflect the precise distribution of these two proteins within the cell.

Patch-clamp studies should also be performed to confirm that the electrophysiological properties of $\beta 2$ subunit remained unchanged following the addition of the aequorin sequence. This would also confirm whether the $\beta 2$ -Aeq chimera co-assemble with the α subunit.

Nevertheless, there is evidence that the addition of GFP to the C-terminus of $\beta 1$ subunit did not modify its expression or electrophysiological properties (Kim *et al.*, 2007). Ideally an equipment that could simultaneously perform bioluminescent Ca^{2+} imaging and patch-clamp would provide the appropriate conditions to correlate the local Ca^{2+} signals detected by $\beta 2\text{-Aeq}$ with the BK channel function.

6.2.2. Investigation of the role of mitochondria on Ca^{2+} signalling near the BK channel.

The work in this thesis has demonstrated that Ca^{2+} signals near the BK channel were locally regulated under certain conditions. As discussed in the previous chapter (See section 5.4.4.) there is a great deal of evidence showing the important role of mitochondria in many cellular processes including the control of Ca^{2+} modulation of the BK channels (Malli *et al.*, 2003). One of the first questions is to determine whether this local Ca^{2+} regulation is affected by mitochondrial buffering. This will be investigated in HEK293 by employing inhibitors of mitochondrial function such as cyanide (CN^-) or *p*-trifluoromethoxyphenyl hydrazone (FCCP). The disruption of the mitochondrial buffering effect will probably result in a rise on Ca^{2+} concentrations in both the BK channel and the cytosol domains. A higher increase of the local Ca^{2+} response near the BK channel in comparison to the cytosol will provide further evidence that there is a subset of mitochondria beneath the plasma membrane acting as a buffering barrier. Conversely if there is no

significant difference between both regions, this would mean that mitochondrial Ca^{2+} uptake operates uniformly across the cell. A better understanding of the role of mitochondria in the modulation of Ca^{2+} signalling is crucial to comprehend BK channel function.

6.2.3. Does the local Ca^{2+} regulation of the BK channel vary with cell function?

The important role of the BK channel in neurotransmitter release, secretion and smooth muscle tone requires a very tight regulation, which has a major impact in cell function. This diverse regulation is achieved by various mechanisms such as expression of different splice variants or co-assembly with different β subunits. Indeed there is evidence of BK channels which exhibited enhanced Ca^{2+} sensitivity (Ransom & Sontheimer, 2002). The majority of the studies reporting these differences were carried out using either excised patches or cytosolic fluorescent dyes. Nonetheless, there is a lack of evidence showing how different cell types handle *in situ* the local Ca^{2+} concentrations affecting the BK channel. There are two potential approaches to examine the specific mechanism of this Ca^{2+} regulation. Firstly the expression of the $\beta 2$ -Aeq construct in other cell lines (i.e. vascular smooth muscle cells, neurons, pancreatic cells...) will provide significant data about how Ca^{2+} regulation of the BK channel is managed by a range of cells with different phenotype. Secondly the co-expression of the $\beta 2$ -Aeq chimera with α subunit variants with different

Ca^{2+} sensitivity (i.e. different splice variants, deletion of the Ca^{2+} bowl...) may reveal that the local Ca^{2+} regulation near the channel is modified as a result. These experiments can bring new insights about how cell function affects the local Ca^{2+} regulation of the BK channel.

6.2.4. Does the BK channel form complexes with Ca^{2+} channels?

Recent studies have reported the co-assembly of BK channels with Ca^{2+} channels resulting in the creation of Ca^{2+} microdomains (Berkefeld *et al.*, 2006; Loane *et al.*, 2007). In these reports the Ca^{2+} chelator BAPTA was capable of diminishing the Ca^{2+} concentrations in these microdomains due to its fast kinetics. In contrast, EGTA was unable to produce the same effect even at high concentrations. The $\beta 2$ -Aeq may prove very useful in determining whether different type of Ca^{2+} channels co-assemble with the BK channel in a range of different cell types. An initial experiment would be to examine whether BAPTA can abolish the local Ca^{2+} increase observed in EGTA medium as a response to CPA (Fig. 5.5). This would demonstrate whether the coupling between the ER Ca^{2+} release and the BK channel is through a microdomain that may be diminished by BAPTA. A series of subsequent experiments using Ca^{2+} channels blockers such as nifedipine and ω -agatoxin in different cell types transfected with $\beta 2$ -Aeq may reveal the existence of these BK- Ca^{2+} channel complexes.

The study of agonist-induced Ca^{2+} transients in the presence of Ca^{2+} channels blockers such as nifedipine and ω -agatoxin in different cell types transfected with $\beta 2$ -Aeq may reveal the existence of these BK- Ca^{2+} channel complexes. If Ca^{2+} channels near the BK channel are blocked a marked decline in the local Ca^{2+} concentration in the proximity of the channel would be observed. Since HEK293 cells possess very low or undetectable endogenous Ca^{2+} channels, these studies should be conducted in other cell lines.

REFERENCES

REFERENCES

- Agbulut O, Coirault C, Niederlander N, Huet A, Vicart P, Hagege A, Puceat M & Menasche P (2006). GFP expression in muscle cells impairs actin-myosin interactions: implications for cell therapy. *Nat Meth* **3**, 331-331.
- Ahluwalia J, Tinker A, Clapp L, Duchen M, Abramov A, Pope S, Nobles M & Segal A. (2004). The large-conductance Ca-activated K channel is essential for innate immunity. *Letters to nature*. **427**, 253-258.
- Ahmed IA, Hopkins PM, Winlow W. (1997) Low concentrations of caffeine raise intracellular calcium concentration only in the presence of extracellular calcium in cultured molluscan neurons. *Gen Pharmacol*. **28**, 245-50.
- Ahring PK, Strøbaek D, Christophersen P, Olesen SP, Johansen TE. (1997) Stable expression of the human large-conductance Ca^{2+} -activated K^{+} channel alpha- and beta-subunits in HEK293 cells. *FEBS Lett*. **415**, 67-70.
- Aidley DJ. (1996). Ion Channels: Molecules in Action.
- Allen DG, Blinks JR, Prendergast FG. (1977) Aequorin luminescence: relation of light emission to calcium concentration--a calcium-independent component. *Science*. **195**, 996-8.
- Allen DG, Eisner DA, Pirolo JS, Smith GL. (1985) The relationship between intracellular calcium and contraction in calcium-overloaded ferret papillary muscles. *J Physiol*. **364**, 169-82.
- Alonso MT, Chamero P, Villalobos C, García-Sancho J. (2003) Fura-2 antagonises calcium-induced calcium release. *Cell Calcium*. Jan;**33**(1):27-35.
- Ataka K & Pieribone V. (2002). A genetically targetable fluorescent probe of channel gating with rapid kinetics. *Biophysical Journal* **82**, 509-516.
- Badminton MN, Kendall JM, Sala-Newby G, Campbell AK. (1995) Nucleoplasmin-targeted aequorin provides evidence for a nuclear calcium barrier. *Exp Cell Res*. **216**, 236-43.

References

- Badminton MN, Sala-Newby GB, Kendall JM, Campbell AK. (1995) Differences in stability of recombinant apoaequorin within subcellular compartments. *Biochem Biophys Res Commun.* **217**, 950-7.
- Badminton MN, Campbell AK, Rembold CM. (1996) Differential regulation of nuclear and cytosolic Ca^{2+} in HeLa cells. *J Biol Chem.* **271**, 31210-4.
- Bailey K. (1942) Myosin and adenosinetriphosphatase. *Biochem J.* **36**, 121-39.
- Bailey M, Cantone A, Yan Q, Macgregor G, Leng Q, Amorim J, Wang T, Hebert S, Giebisch G & Malnic G. (2006). Maxi-K channels contribute to urinary potassium excretion in the ROMK-deficient mouse model of Type II Bartter's syndrome and in adaptation to a high-K diet. *Kidney Int* **70**, 51-9.
- Baker HL, Errington RJ, Davies SC, Campbell AK. (2002) A mathematical model predicts that calreticulin interacts with the endoplasmic reticulum Ca^{2+} -ATPase. *Biophys J.* **82**, 582-90.
- Baker PF. (1972) Transport and metabolism of calcium ions in nerve. *Prog Biophys Mol Biol.* **24**, 177-223.
- Bao L and Cox DH. (2005) Gating and ionic currents reveal how the BKCa channel's Ca^{2+} sensitivity is enhanced by its beta1 subunit. *J Gen Physiol.* **126**, 393-412.
- Barrett JN, Magleby KL, Pallotta BS. (1982) Properties of single calcium-activated potassium channels in cultured rat muscle. *J Physiol.* **331**, 211-30.
- Baubet V, Le Mouellic H, Campbell AK, Lucas-Meunier E, Fossier P, Brúlet P. (2000) Chimeric green fluorescent protein-aequorin as bioluminescent Ca^{2+} reporters at the single-cell level. *Proc Natl Acad Sci U S A.* **97**, 7260-5.
- Bauer T. (2005). Amplification and overexpression of the Ca^{2+} -activated large conductance K^{+} -channel. KCNMA1: a potential therapeutic target in prostate cancer. Patent pending 03/39 KBS University Hospital of Basel.
- Berkefeld H, Sailer CA, Bildl W, Rohde V, Thumfart J-O, Eble S, Klugbauer N, Reisinger E, Bischofberger J, Oliver D, Knaus H-G, Schulte U & Fakler B. (2006). BKCa-Cav Channel Complexes Mediate Rapid and Localized Ca^{2+} -Activated K^{+} Signaling. *Science* **314**, 615-620.
- Bermudez-Fajardo A. (2002) The role of the glucose-regulated protein of 78kDa, Grp78/Bip, in the mammalian ER stress response. *PhD Thesis*
- Berridge MJ. (1984) Inositol trisphosphate and diacylglycerol as second messengers. *Biochem J.* **220**, 345-60.

References

-
- Berridge MJ and Galione A. (1988) Cytosolic calcium oscillators. *FASEB J.* **2**, 3074-82.
- Berrie CP, Cuthbertson KS, Parrington J, Lai FA, Swann K. (1996) A cytosolic sperm factor triggers calcium oscillations in rat hepatocytes. *Biochem J.* **313**, 369-72.
- Bhagavan S, Ibarreta D, Ma D, Kozikowski AP, Etcheberrigaray R. (1998) Restoration of TEA-induced calcium responses in fibroblasts from Alzheimer's disease patients by a PKC activator. *Neurobiol Dis.* **5**, 177-87.
- Bird GS, Putney JW Jr. (2005) Capacitative calcium entry supports calcium oscillations in human embryonic kidney cells. *J Physiol.* **562**, 697-706.
- Birnbaumer L, Zhu X, Jiang M, Boulay G, Peyton M, Vannier B, Brown D, Platano D, Sadeghi H, Stefani E, Birnbaumer M. (1996) On the molecular basis and regulation of cellular capacitative calcium entry: roles for Trp proteins. *Proc Natl Acad Sci U S A.* **93**, 15195-202.
- Blatter LA & Blinks JR. (1991) Simultaneous measurement of Ca^{2+} in muscle with Ca electrodes and aequorin. Diffusible cytoplasmic constituent reduces $\text{Ca}(2+)$ -independent luminescence of aequorin. *J Gen Physiol.* **98**, 1141-60.
- Boehning D, Patterson RL, Sedaghat L, Glebova NO, Kurosaki T, Snyder SH. (2003) Cytochrome c binds to inositol (1,4,5) trisphosphate receptors, amplifying calcium-dependent apoptosis. *Nat Cell Biol.* **5**, 1051-61.
- Boutem N, Pernet K & Issad T. (2001). Monitoring the activation state of the insulin receptor using bioluminescence resonance energy transfer. *Mol Pharmacol* **60**, 640-645.
- Bozler E. (1954) Relaxation in extracted muscle fibers. *J Gen Physiol.* **38**, 149-59.
- Brenner R, Chen QH, Vilaythong A, Toney GM, Noebels JL & Aldrich RW. (2005). BK channel beta4 subunit reduces dentate gyrus excitability and protects against temporal lobe seizures. *Nat Neurosci* **8**, 1752-9
- Brini M, Marsault R, Bastianutto C, Alvarez J, Pozzan T, Rizzuto R. (1995) Transfected aequorin in the measurement of cytosolic Ca^{2+} concentration ($[\text{Ca}^{2+}]_c$). A critical evaluation. *J Biol Chem.* **270**, 9896-903.
- Brini M, De Giorgi F, Murgia M, Marsault R, Massimino ML, Cantini M, Rizzuto R, Pozzan T. (1997) Subcellular analysis of Ca^{2+} homeostasis in primary cultures of skeletal muscle myotubes. *Mol Biol Cell.* **8**, 129-43.
- Brini, M., Pinton, P., Pozzan, T., and Rizzuto, R. (1999) Targeted recombinant aequorins: tools for monitoring $[\text{Ca}^{2+}]$ in the various compartments of a living cell. *Microsc. Res. Technol.* **46**, 380
-

References

- Brini M, Manni S, Pierobon N, Du GG, Sharma P, MacLennan DH, Carafoli E. (2005) Ca^{2+} signalling in HEK-293 and skeletal muscle cells expressing recombinant ryanodine receptors harbouring malignant hyperthermia and central core disease mutations. *J Biol Chem.* **280**, 15380-9.
- Bronstein-Sitton N. (2003). Ion channel in Cancer. Modulator.
- Brown JE and Blinks JR. (1974) Changes in intracellular free calcium concentration during illumination of invertebrate photoreceptors: detection with aequorin. *Journal of General Physiology.* **64**, 643–665.
- Brzyska M., Michalski A., Elbaum D. (2002) Tetraethylammonium-induced changes in intracellular calcium in Alzheimer donor fibroblasts. *Neurosci Res Commun* **30**, 51-61.
- Butcher R and Sutherland E (1962) Adenosine 3,5-phosphate in biological materials. I. Purification and properties of cyclic 3,5-nucleotide phosphodiesterase and use of this enzyme to characterize adenosine 3,5-phosphate in human urine. *J Biol Chem* **237**, 1244-1250.
- Button D and Eidsath A. (1996) Aequorin targeted to the endoplasmic reticulum reveals heterogeneity in luminal Ca^{++} concentration and reports agonist- or IP_3 -induced release of Ca^{++} . *Mol Biol Cell.* **7**, 419-34.
- Cai S-Q, Hernandez, L, Wang, Y, Park, KH, Sesti, F. (2005). MPS-1 is a K^+ channel β -subunit and a serine/threonine kinase. *Nature Neuroscience*, **8**, 1503–1509.
- Campbell, AK. (1983). Intracellular Calcium: Its Universal Role As Regulator. Wiley.
- Campbell, AK. (1988). Chemiluminescence: principles and applications in biology and medicine. Horwood/VCH, Chichester and Weinheim.
- Campbell AK. (1989) Living light: biochemistry, applications. *Essays Biochem.* **24**, 41-81.
- Campbell AK (2003). Rainbow Makers. *Chemistry in Britain* **11**, 30-33.
- Candia S, Garcia ML, Latorre R. (1992) Mode of action of iberiotoxin, a potent blocker of the large conductance $\text{Ca}^{(2+)}$ -activated K^+ channel. *Biophys J.* **63**, 583-90.
- Carafoli E. and Klee CB. (1998) Calcium as a Cellular Regulator. Oxford University Press US.
- Carafoli E. (2002) Calcium signaling: a tale for all seasons. *Proc Natl Acad Sci U S A.* **99**, 1115-22.
- Castro E, Mateo J, Tomé AR, Barbosa RM, Miras-Portugal MT, Rosário LM. (1995) Cell-specific purinergic receptors coupled to Ca^{2+} entry and Ca^{2+} release from

References

- internal stores in adrenal chromaffin cells. Differential sensitivity to UTP and suramin. *J Biol Chem.* **270**, 5098-106.
- Chavis P, Ango F, Michel JM, Bockaert J, Fagni L. (1998) Modulation of big K⁺ channel activity by ryanodine receptors and L-type Ca²⁺ channels in neurons. *Eur J Neurosci.* **10**, 2322-7.
- Chen LY, Chen X, Tian XL, Yu XH. (2000) Effects of tetrandrine on calcium transport, protein fluorescences and membrane fluidity of sarcoplasmic reticulum. *Br J Pharmacol.* **131**, 530-6.
- Cheung C, Webb S, Meng A & Miller A. (2006). Transient expression of apoequorin in zebrafish embryos: extending the ability to image calcium transients during later stages of development *Int J Dev Biol* **50**, 561-569.
- Chi S & Qi Z. (2006). Regulatory effect of sulphatides on BKCa channels. *Br J Pharmacol.* **149**, 1031-8.
- Chittajallu R, Chen Y, Wang H, Yuan X, Ghiani CA, Heckman T, McBain CJ, Gallo V. (2002) Regulation of Kv1 subunit expression in oligodendrocyte progenitor cells and their role in G1/S phase progression of the cell cycle. *Proc Natl Acad Sci U S A.* **99**, 2350-5.
- Ciapa B, Pesando D, Wilding M, Whitaker M. (1994) Cell-cycle calcium transients driven by cyclic changes in inositol trisphosphate levels. *Nature.* **368**, 875-8.
- Clapham DE. (2003) TRP channels as cellular sensors. *Nature.* **426**, 517-24.
- Clapham DE (2007). Calcium signaling. *Cell* **131**, 1047–1058.
- Clapp L & Jabr RI. (2003). Role of BK beta1 and alpha subunit in hypertension. *Circulation research.* **101**, 493-502.
- Claude, A. (1975) The coming of age of the cell. *Science* **189**, 433-435.
- Cobbold PH and Rink TJ. (1987) Fluorescence and bioluminescence measurement of cytoplasmic free calcium. *Biochem J.* **248**, 313-28.
- Cobbold PH and Lee JAC. (1991). Aequorin measurements of cytoplasmic free calcium. In *Cellular calcium: a practical approach*. pp. 55-81. New York: Oxford University Press.
- Coetzee, Amarillo, Chiu, Chow, Lau, McCormack, Moreno, Nadal, Ozaita, Pountney, Saganich, Vega-Saenz de Miera E & Rudy B. (1999). Molecular Diversity of K⁺ Channels *Ann NY Acad Sci* **30**, 233-285.
- Coffey DS. (1998) Self-organization, complexity and chaos: the new biology for medicine. *Nat Med.* **4**, 882-5.

References

- Connecticut College. (2006). <http://www.conncoll.edu/> Data access on Feb 2006.
- Corsi K, Chellat F, Yahia L, Fernandes JC. (2003) Mesenchymal stem cells, MG63 and HEK293 transfection using chitosan-DNA nanoparticles. *Biomaterials*. **24**, 1255-64.
- Cox DH, Aldrich RW. (2000) Role of the beta1 subunit in large-conductance Ca^{2+} -activated K^+ channel gating energetics. Mechanisms of enhanced Ca^{2+} sensitivity. *J Gen Physiol*. **116**, 411-32.
- Cseresnyés Z, Bustamante AI, Klein MG, Schneider MF. (1997) Release-activated Ca^{2+} transport in neurons of frog sympathetic ganglia. *Neuron*. **19**, 403-19.
- Curley M, Morrison J & Smith T. (2004). Analysis of Maxi-K alpha subunit splice variants in human myometrium. *Reproductive Biology and Endocrinology*, **67**.
- Daguzan C, Nicolas MT, Mazars C, Leclerc C, Moreau M. (1995) Expression of membrane targeted aequorin in *Xenopus laevis* oocytes. *Int J Dev Biol*. **39**, 653-7.
- Davies EV, Blanchfield H, Hallett MB. (1997) Use of fluorescent dyes for measurement and localization of organelles associated with Ca^{2+} store release in human neutrophils. *Cell Biol Int*. **21**, 655-63.
- Davies EV, Hallett MB. (1998) High micromolar Ca^{2+} beneath the plasma membrane in stimulated neutrophils. *Biochem Biophys Res Commun*. **248**, 679-83.
- Davies EV and Hallett MB. (1998) Cytosolic Ca^{2+} signalling in inflammatory neutrophils: implications for rheumatoid arthritis. *Int J Mol Med*. **1**, 485-90.
- Day ML, Johnson MH, Cook DI. (1998) Cell cycle regulation of a T-type calcium current in early mouse embryos. *Pflugers Arch*. **436**, 834-42.
- Day ML, Johnson MH, Cook DI. (1998) A cytoplasmic cell cycle controls the activity of a K^+ channel in pre-implantation mouse embryos. *EMBO J*. **17**, 1952-60.
- De Duve, C. (1975) Exploring cells with a centrifuge. *Science* **189**, 186-194.
- Dedkova EN, Sigova AA, Zinchenko VP. (2000) Mechanism of action of calcium ionophores on intact cells: ionophore-resistant cells. *Membr Cell Biol*. **13**, 357-68.
- Del Toro RC, MD. Barneo, JL. . (2005). Down-regulation of Maxi-K channel beta-2 subunit by hypoxia in chromaffin cells. The Physiological Society XXIII Congress.

References

- Deng XL, Lau CP, Lai K, Cheung KF, Lau GK, Li GR. (2007) Cell cycle-dependent expression of potassium channels and cell proliferation in rat mesenchymal stem cells from bone marrow. *Cell Prolif.* **40**, 656-70.
- Diaz L, Meera, P, Amigo, J, Stefani, E, Alvarez, O, Toro, L, Latorre, R. (1998). Role of the S4 Segment in a Voltage-dependent Calcium-sensitive Potassium (hSlo) Channel. *J Biol Chem* **273**, 32430-32436.
- Dray A & Urban L. (1996). New pharmacological strategies for pain relief. *Annu Rev Pharmacol Toxicol*, **36**, 253-280.
- Donoso P, O'Neill SC, Dilly KW, Negretti N, Eisner DA. (1994) Comparison of the effects of caffeine and other methylxanthines on $[Ca^{2+}]_i$ in rat ventricular myocytes. *Br J Pharmacol.* **111**, 455-8.
- Du WB, JF. Yang, H. Diez-Sampedro, A. You, SA. Wang, L. Kotagal, P. Luders, HO. Shi, J. Cui, J. Richerson, GB. Wang, QK. (2005). Calcium-sensitive potassium channelopathy in human epilepsy and paroxysmal movement disorder. *Nature Genetics* **37**, 733-738.
- Dworetzky SI, Trojnecki JT & Gribkoff VK. (1994). Cloning and expression of a human large-conductance calcium-activated potassium channel. *Brain Res Mol Brain Res* **27**, 189-193.
- Eghbali M, Toro L & Stefani E. (2003). Diminished Surface Clustering and Increased Perinuclear Accumulation of Large Conductance Ca^{2+} -activated K^+ Channel in Mouse Myometrium with Pregnancy. *J Biol Chem* **278**, 45311-45317.
- Eichwald C. and Kaiser F. (1993) Model for receptor-controlled cytosolic calcium oscillations and for external influences on the signal pathway. *Biophys J.* **65**, 2047-2058.
- Etter EF, Minta A, Poenie M, Fay FS. (1996) Near-membrane $[Ca^{2+}]$ transients resolved using the Ca^{2+} indicator FFP18. *Proc Natl Acad Sci U S A.* **93**, 5368-73.
- Fanchaouy M, Bychkov R, Meister JJ, Beny JL. (2007). Stretch-elicited calcium responses in the intact mouse thoracic aorta. *Cell Calcium* **41**, 41-50
- Fernandez-Fernandez J, Tomas M, Vazquez E, Orio P, Latorre R, Senti M, Marrugat J & Valverde M. (2004). Gain-of-function mutation in the KCNMB1 potassium channel subunit is associated with low prevalence of diastolic hypertension. *J Clin Invest* **113**, 1032-1039.

References

- Franciolini F, Hogg R, Catacuzzeno L, Petris A, Trequattrini C, Adams DJ. (2001) Large-conductance calcium-activated potassium channels in neonatal rat intracardiac ganglion neurons. *Pflugers Arch.* **441**, 629-38.
- Frieden M, Malli R, Samardzija M, Demareux N, Graier WF. (2002) Subplasmalemmal endoplasmic reticulum controls K(Ca) channel activity upon stimulation with a moderate histamine concentration in a human umbilical vein endothelial cell line. *J Physiol.* **540**, 73-84.
- Gales C, Rebois, RV, Hogue, M, Trieu, P, Breit, A, Hebert, TE, Bouvier, M. (2005). Real-time monitoring of receptor and G-protein interactions in living cells. *Nature Methods* **2**, 177 – 184.
- Garcia-Calvo M, Knaus H, G., McManus OB, Giangiacomo KM, Kaczorowski GJ & Garcia ML. (1994). Purification and reconstitution of the high-conductance, calcium-activated potassium channel from tracheal smooth muscle. *J Biol Chem* **269**, 676-682.
- GeneCards encyclopedia. (2008) <http://www.genecards.org> . Access Data April 2008.
- George, CH. (1998) The molecular assembly of gap junction intercellular communication channels studied using connexin-aequorin probes. *Ph.D. thesis*.
- George CH, Kendall JM, Campbell AK, Evans WH. (1998) Connexin-aequorin chimerae report cytoplasmic calcium environments along trafficking pathways leading to gap junction biogenesis in living COS-7 cells. *J Biol Chem.* **273**, 29822-9.
- Ghatta S, Nimmagadda D, Xu X & O'rourke S. (2005). Large-conductance, calcium-activated potassium channels: Structural and functional implications. *Pharmacol Ther* **110**, 103-16
- Giraldez T, Hughes TE, Sigworth FJ. (2005) Generation of functional fluorescent BK channels by random insertion of GFP variants. *J Gen Physiol.* **126**, 429-38.
- Go LO, Moschella MC, Watras J, Handa KK, Fyfe BS, Marks AR. (1995) Differential regulation of two types of intracellular calcium release channels during end-stage heart failure. *J Clin Invest.* **95**, 888-94.
- Golovina VA, Blaustein MP. (1997) Spatially and functionally distinct Ca²⁺ stores in sarcoplasmic and endoplasmic reticulum. *Science.* **275**, 1643-8.
- Gopalakrishnan M, Monteggia LM, Anderson DJ, Molinari EJ, Piattoni-Kaplan M, Donnelly-Roberts D, Arneric SP, Sullivan JP (1996) Stable expression,

References

- pharmacological properties and regulation of the human neuronal nicotinic acetylcholine $\alpha 4\beta 2$ receptor. *J Pharmacol Exp Ther* **276**, 289-297.
- Graier WF, Paltauf-Doburzynska J, Hill BJ, Fleischhacker E, Hoebel BG, Kostner GM, Sturek M. (1998) Submaximal stimulation of porcine endothelial cells causes focal Ca^{2+} elevation beneath the cell membrane. *J Physiol*. **506**, 109-25.
- Gribkoff VK. (2001). Targeting acute ischemic stroke with a calcium-sensitive opener of maxi-K potassium channels. *Nature Medicine* **7**, 471-477.
- Grynkiewicz G, Poenie M, Tsien RY. (1985) A new generation of Ca^{2+} indicators with greatly improved fluorescence properties. *J Biol Chem*. **260**, 3440-50.
- Hagen B, Bayguinov O & Sanders K. (2003). Beta 1-subunits are required for regulation of coupling between Ca^{2+} transients and Ca^{2+} -activated K^+ (BK) channels by protein kinase C. *Am J Physiol Cell Physiol* **285**, 1270-1280.
- Haghdoust-Yazdi H, Janahmadi M, Behzadi G. (2008) Iberitoxin-sensitive large conductance Ca^{2+} -dependent K^{2+} (BK) channels regulate the spike configuration in the burst firing of cerebellar Purkinje neurons. *Brain Res*. **1212**, 1-8.
- Hamill OP, Marty E, Neher E, Sakmann B & Sigworth FJ. (1981). Improved Patch-Clamp Techniques for High-Resolution Current Recording from Cells and Cell-Free Membrane Patches. . *Pflügers Arch*, **391**, 85-100.
- Harkins AB, Kurebayashi N, Baylor SM. (1993) Resting myoplasmic free calcium in frog skeletal muscle fibers estimated with fluo-3. *Biophys J*. **65**, 865-81.
- Hartness M, Brazier S, Peers C, Bateson A, Ashford M & Kemp P. (2003). Post-transcriptional control of human maxiK potassium channel activity and acute oxygen sensitivity by chronic hypoxia. *J Biol Chem* **278**, 51422-51432.
- Haugland, R. (1993). Intracellular ion indicators. In *Fluorescent and Luminescent Probes for Biological Activity* (Mason, W.T., ed.) Academic Press, London. Pp 34-43.
- Hantusch B, Kalt R, Krieger S, Puri C, Kerjaschki D. (2007) Sp1/Sp3 and DNA-methylation contribute to basal transcriptional activation of human podoplanin in MG63 versus Saos-2 osteoblastic cells. *BMC Mol Biol*. **8**, 20.
- Head JF, Inouye S, Teranishi K & Shimomura O. (2000). The crystal structure of the photoprotein aequorin at 2.3 [angst] resolution. *Nature* **405**, 372-376.
- Heilbrunn, LV. (1940) The action of calcium on muscle protoplasm. *Physiol. Zool*. **13**, 88–94.

References

- Heurteaux C, Lucas G, Guy N, El Yacoubi M, Thummler S, Peng X, Noble F, Blondeau N, Widmann C, Borsotto M, Gobbi G, Vaugeois J, Debonnel G & Lazdunski M. (2006). Deletion of the background potassium channel TREK-1 results in a depression-resistant phenotype. *Nat Neurosci* **9**, 1134-1141.
- Hille B. (2001). Ion channels of excitable membranes, 3th edition, Sinauer.
- Hopf FW, Reddy P, Hong J, Steinhardt RA. (1996) A capacitative calcium current in cultured skeletal muscle cells is mediated by the calcium-specific leak channel and inhibited by dihydropyridine compounds. *J Biol Chem.* **271**, 22358-67.
- Horton RM, Cai ZL, Ho SN, Pease LR. (1990) Gene splicing by overlap extension: tailor-made genes using the polymerase chain reaction. *Biotechniques.* **8**, 528-35.
- Hubner CA & Jentsch TJ. (2002). Ion channel diseases. *Human Molecular Genetics* **11**, 2435-2445.
- Hurwitz, L., Leach, JK. and Partridge, LD. (1991) *Calcium Channels: Their Proper Functions, Regulation and Clinical and Reverance*, Telford Press 1st Ed.
- Inouye S, Noguchi M, Sakaki Y, Takagi Y, Miyata T, Iwanaga S, Miyata T, Tsuji FI. (1985) Cloning and sequence analysis of cDNA for the luminescent protein aequorin. *Proc Natl Acad Sci U S A.* May; **82**, 3154-8.
- Inouye S, Sakaki Y, Goto T, Tsuji F. (1986) Expression of apoaequorin complementary DNA in Escherichia coli. *Biochemistry* **25**, 8425–8429
- Iwata K, Luo J, Penn RB, Benovic JL. (2005) Bimodal regulation of the human H1 histamine receptor by G protein-coupled receptor kinase 2. *J Biol Chem.* **280**, 2197-204.
- James-Kracke MR. (1986) Measurement of cytoplasmic free Ca²⁺ concentration in cultured muscle cells by aequorin and quin 2. *Am J Physiol.* **251**, 512-23.
- Jan L & Jan Y. (1997). Cloned potassium channels from eukaryotes and prokaryotes. *Annu Rev Neurosci* **20**, 91-123.
- Jeffery J, Kendall JM, Campbell AK. (2000) Apoaequorin monitors degradation of endoplasmic reticulum (ER) proteins initiated by loss of ER Ca⁽²⁺⁾. *Biochem Biophys Res Commun.* **268**, 711-5.
- Jiang Y, Pico A, Cadene M, Chait B & MacKinnon R. (2001). Structure of the RCK Domain from the E. coli K⁺ Channel and Demonstration of Its Presence in the Human BK Channel. *Neuron* **29**, 593-601.

References

-
- Karhapää L and Törnquist K. (1997) Effects of caffeine on the influx of extracellular calcium in GH4C1 pituitary cells. *J Cell Physiol.* **171**, 52-60
- Kendall, JM; Dormer, RL; Campbell, AK. (1992) Targeting aequorin to the endoplasmic reticulum of living cells. *Biochem Biophys Res Commun.* **189**, 1008–1016.
- Kerschensteiner D, Soto F & Stocker M. (2005). Fluorescence measurements reveal stoichiometry of K channels formed by modulatory and delayed rectifier α -subunits. *PNAS* **102**, 6150-6165.
- Khan AA, Steiner JP, Klein MG, Schneider MF, Snyder SH. (1992) IP3 receptor: localization to plasma membrane of T cells and cocapping with the T cell receptor. *Science.* **257**, 815-8.
- Kim EY, Ridgway LD, Zou S, Chiu YH, Dryer SE. (2007) Alternatively spliced C-terminal domains regulate the surface expression of large conductance calcium-activated potassium channels. *Neuroscience.* **146**, 1652-61.
- Kim EY, Zou S, Ridgway LD, Dryer SE. (2007) Beta1-subunits increase surface expression of a large-conductance Ca^{2+} -activated K^{2+} channel isoform. *J Neurophysiol.* **97**, 3508-16.
- Komendantov AO, and Kononenko NI. (2000). Caffeine-induced oscillations of membrane potential in Aplysia neurons. *Neurophysiology (Kiev)*, **32**, 77-84.
- Koopman WJ, Scheenen WJ, Roubos EW, Jenks BG. (1997) Kinetics of calcium steps underlying calcium oscillations in melanotrope cells of *Xenopus laevis*. *Cell Calcium.* **22**, 167-78.
- Koval O, Fan Y & Rothberg B. (2007). A Role for the S0 Transmembrane Segment in Voltage-dependent Gating of BK Channels. *J Gen Physiol* **129**, 209-20.
- Krizaj D, Bao JX, Schmitz Y, Witkovsky P, Copenhagen DR. (1999) Caffeine-sensitive calcium stores regulate synaptic transmission from retinal rod photoreceptors. *J Neurosci.* **19**, 7249-61.
- Kummer U, Krajnc B, Pahle J, Green AK, Dixon CJ, Marhl M. (2005) Transition from Stochastic to Deterministic Behavior in Calcium Oscillations. *Biophys J.* September; **89**, 1603–1611.
- Kwan HY, Shen B, Ma X, Kwok YC, Huang Y, Man YB, Yu S, Yao X. (2009) TRPC1 Associates With BKCa Channel to Form a Signal Complex in Vascular Smooth Muscle Cells. *Circ Res.* 2009 **104**, 670-8.
- Latorre R and Brauchi S. (2006) Large conductance Ca^{2+} -activated K^{+} (BK) channel: activation by Ca^{2+} and voltage. *Biol Res.* **39**, 385-401.
-

References

- Laumonnier F, Roger S, Guerin P, Molinari F, M'rad R, Cahard D, Belhadj A, Halayem M, Persico A, Elia M, Romano V, Holbert S, Andres C, Chaabouni H, Colleaux L, Constant J, Le Guennec J & Briault S. (2006). Association of a Functional Deficit of the BKCa Channel, a Synaptic Regulator of Neuronal Excitability, With Autism and Mental Retardation. *Am J Psychiatry* **163**, 1622-1629.
- Leung YM, Kwan CY, Loh TT. (1994) Dual effects of tetrandrine on cytosolic calcium in human leukaemic HL-60 cells: intracellular calcium release and calcium entry blockade. *Br J Pharmacol.* **113**, 767-74.
- Li B, Henney NC, Evans BA, Reviriego P, Campbell AK, Wann KT (2007) BKChannels are Expressed and Functional in Human Osteoblast-like Cells. *Proc Life Sciences*, PC162
- Li D, Wang Z, Sun P, Jin Y, Lin D-H, Hebert SC, Giebisch G & Wang W-H. (2006). Inhibition of MAPK stimulates the Ca^{2+} -dependent big-conductance K channels in cortical collecting duct. *Proc Natl Acad Sci U S A.* **103**, 19569-74.
- Lin M, Hessinger D, Pearce W & Longo L. (2006). Modulation of BK channel calcium affinity by differential phosphorylation in developing ovine basilar artery myocytes. *Am J Physiol Heart Circ Physiol* **291**, 732-740.
- Lin S, Fagan KA, Li KX, Shaul PW, Cooper DM, Rodman DM. (2000) Sustained endothelial nitric-oxide synthase activation requires capacitative Ca^{2+} entry. *J Biol Chem.* **275**, 17979-85.
- Lindaman B, Hinkhouse M, Conklin J, and Cullen J (2002) The effect of phosphodiesterase inhibition on gallbladder motility in vitro. *J Surg Res* **105**: 102-108
- Lippiat JD, Standen NB, Harrow ID, Phillips SC, Davies NW. (2003) Properties of BK(Ca) channels formed by bicistronic expression of hSlo alpha and beta1-4 subunits in HEK293 cells. *J Membr Biol.* **192**, 141-8.
- Liu HS, Jan MS, Chou CK, Chen PH, Ke NJ. (1999) Is green fluorescent protein toxic to the living cells? *Biochem Biophys Res Commun.* **260**, 712-7.
- Loane DJ, Lima PA, Marrion NV. (2007) Co-assembly of N-type Ca^{2+} and BK channels underlies functional coupling in rat brain. *J Cell Sci.* **120**, 985-95.
- Lu R, Alioua A, Kumar Y, Eghbali M, Stefani E & Toro L. (2006). MaxiK channel partners: physiological impact. *J Physiol* **570**, 65-72.
- Luo D, Broad LM, Bird GS, Putney JW Jr. (2001) Signaling pathways underlying muscarinic receptor-induced $[\text{Ca}^{2+}]_i$ oscillations in HEK293 cells. *J Biol Chem.* **276**, 5613-21.

References

- Lv C, Chen M, Gan G, Wang L, Xu T, Ding J. (2008) Four-turn alpha-helical segment prevents surface expression of the auxiliary hbeta2 subunit of BK-type channel. *J Biol Chem.* **283**, 2709-15.
- Malli R, Frieden M, Osibow K, Graier WF. (2003) Mitochondria efficiently buffer subplasmalemmal Ca^{2+} elevation during agonist stimulation. *J Biol Chem.* **278**, 10807-15.
- Manganas L & Trimmer J. (2000). Subunit composition determines Kv1 potassium channel surface expression. *J Biol Chem* **275**, 29685-29693.
- Mansoureh E, Ligia T & Enrico S. (2003). Diminished Surface Clustering and Increased Perinuclear Accumulation of Large Conductance Ca^{2+} -activated K^+ Channel in Mouse Myometrium with Pregnancy. *J Biol Chem* **278**, 45311-45317.
- Marijic J, Li, Q, Song, M, Nishimaru, K, Stefani, E, Toro, L. (2001). Decreased expression of Voltage-and Ca^{2+} -Activated K^+ Channels in coronary smooth muscle during aging. *Circulation research*, **88**, 210-6.
- Markwardt F and Isenberg G. (1992) Gating of maxi K^+ channels studied by Ca^{2+} concentration jumps in excised inside-out multi-channel patches (myocytes from guinea pig urinary bladder). *J Gen Physiol.* **99**, 841-62.
- Marsault R, Murgia M, Pozzan T, Rizzuto R. (1997) Domains of high Ca^{2+} beneath the plasma membrane of living A7r5 cells. *EMBO J.* **16**, 1575-81
- Marshall J, Molloy R, Moss G, Howe J & Hughes T. (1995). The jellyfish green fluorescent protein: a new tool for studying ion channel expression and function. *Neuron*, **14**, 211-5.
- Martin C, Dacquet C, Mironneau C, Mironneau J. (1989) Caffeine-induced inhibition of calcium channel current in cultured smooth cells from pregnant rat myometrium. *Br J Pharmacol.* **98**, 493-8.
- Martin PE, George CH, Castro C, Kendall JM, Capel J, Campbell AK, Revilla A, Barrio LC, Evans WH. (1998) Assembly of chimeric connexin-aequorin proteins into functional gap junction channels. Reporting intracellular and plasma membrane calcium environments. *J Biol Chem.* **273**, 1719-26.
- Marty, A. (1981) Ca^{2+} -dependent K^+ channels with large unitary conductance in chromaffin cell membranes. *Nature.* **291**, 497–500.
- Mattson MP, LaFerla FM, Chan SL, Leissring MA, Shepel PN, Geiger JD. (2000) Calcium signalling in the ER: its role in neuronal plasticity and neurodegenerative disorders. *Trends Neurosci.* **23**, 222-9.

References

- McDonough SI. (2003) *Calcium Channel Pharmacology*. 1st Ed.
- McFadzean, I and Brownlee, C (1995) Ion channels and transduction systems in plant and animal cells. *Ion Channels: A Practical Approach*. Ed R Ashley.
- McGahon MK, Dash DP, Arora A, Wall N, Dawicki J, Simpson DA, Scholfield CN, McGeown JG, Curtis TM. (2007) Diabetes downregulates large-conductance Ca^{2+} -activated potassium beta 1 channel subunit in retinal arteriolar smooth muscle. *Circ Res*. **100**, 703-11.
- McMillian MK, Soltoff SP, Lechleiter JD, Cantley LC, Talamo BR. (1988) Extracellular ATP increases free cytosolic calcium in rat parotid acinar cells. Differences from phospholipase C-linked receptor agonists. *Biochem J*. **255**, 291-300.
- Meera P, Wallner M, Jiang Z, Toro L. (1996) A calcium switch for the functional coupling between alpha (hslo) and beta subunits (K_vCa beta) of maxi K channels. *FEBS Lett*. **382**, 84-8.
- Meera P, Wallner M, Song M & Toro L. (1997). Large conductance voltage- and calcium-dependent K^+ channel, a distinct member of voltage-dependent ion channels with seven N-terminal transmembrane segments (S0-S6), an extracellular N terminus, and an intracellular (S9-S10) C terminus. *Proc Natl Acad Sci USA* **94**, 14066-14071.
- Meera P, Wallner M, Toro L. (2000) A neuronal beta subunit (KCNMB4) makes the large conductance, voltage- and Ca^{2+} -activated K^+ channel resistant to charybdotoxin and iberiotoxin. *Proc Natl Acad Sci U S A*. **97**, 5562-7.
- Meredith AL, Thorneloe KS, Werner ME, Nelson M & Aldrich R. (2004). Overactive bladder and incontinence in the absence of the BK large conductance Ca^{2+} -activated K^+ channel. *The Journal of Biological Chemistry* **279**, 36745-36752.
- Miledi R and Parker I. (1984) Chloride current induced by injection of calcium into *Xenopus* oocytes. *J Physiol*. **357**, 173-83.
- Miller RJ. (1992) Voltage-sensitive Ca^{2+} channels. *J Biol Chem*. **267**, 1403-6.
- Miller A, Karplus E & Jaffe L. (1994). Imaging $[\text{Ca}^{2+}]_i$ with aequorin using a photon imaging detector. *Methods Cell Biol* **40**, 305-338.
- Missiaen L, Parys JB, De Smedt H, Himpens B, Casteels R. (1994) Inhibition of inositol trisphosphate-induced calcium release by caffeine is prevented by ATP. *Biochem J*. **300**, 81-4.
- Miyawaki A, Llopis J, Heim R, McCaffery JM, Adams JA, Ikura M, Tsien RY. (1997) Fluorescent indicators for Ca^{2+} based on green fluorescent proteins and calmodulin. *Nature*. **388**, 882-7.

References

-
- Miyawaki A, Griesbeck O, Heim R, Tsien RY. (1999) Dynamic and quantitative Ca^{2+} measurements using improved cameleons. *Proc Natl Acad Sci U S A.* **96**, 2135-40.
- Miyawaki A & Tsien R. (2000). Monitoring protein conformations and interactions by fluorescence resonance energy transfer between mutants of green fluorescent protein. *Methods in Enzymology* **327**, 472-500.
- Moczydlowski EG. (2004). BK Channel News: Full coverage on the calcium bowl. *Journal of General Physiology* **123**, 471-473.
- Molleman A, Liu LW, Huizinga JD. (2001) Muscarinic activation of transient inward current and contraction in canine colon circular smooth muscle cells. *Can J Physiol Pharmacol.* **79**, 34-42.
- Montero M, Alonso MT, Albillos A, Cuchillo-Ibáñez I, Olivares R, Villalobos C, Alvarez J. (2002) Effect of inositol 1,4,5-trisphosphate receptor stimulation on mitochondrial $[\text{Ca}^{2+}]$ and secretion in chromaffin cells. *Biochem J.* **365**, 451-9.
- Morimoto T, Ohya S, Hayashi H, Onozaki K, Imaizumi Y. (2007) Cell-cycle-dependent regulation of Ca^{2+} -activated K^{+} channel in Jurkat T-lymphocyte. *J Pharmacol Sci.* **104**, 94-8.
- Morita H, Honda A, Inoue R, Ito Y, Abe K, Nelson MT, Brayden JE. (2007) Membrane stretch-induced activation of a TRPM4-like nonselective cation channel in cerebral artery myocytes. *J Pharmacol Sci.* **103**, 417-26.
- Morgan AJ and Jacob R. (1994) Ionomycin enhances Ca^{2+} influx by stimulating store-regulated cation entry and not by a direct action at the plasma membrane. *Biochem J.* **300**, 665-72.
- Morrow JP, Zakharov SI, Liu G, Yang L, Sok AJ, Marx SO. (2006) Defining the BK channel domains required for beta1-subunit modulation. *Proc Natl Acad Sci U S A.* **103**, 5096-101.
- Muñoz A, García L, Guerrero-Hernández A. (1998) In situ characterization of the Ca^{2+} sensitivity of large conductance Ca^{2+} -activated K^{+} channels: implications for their use as near-membrane Ca^{2+} indicators in smooth muscle cells. *Biophys J.* **75**, 1774-82.
- Muschol M, Dasgupta BR, Salzberg BM. (1999) Caffeine interaction with fluorescent calcium indicator dyes. *Biophys J.* **77**, 577-86.
- Myers, MP, Yang, J, Stampe, P. (1999) Visualization and functional analysis of a maxi-K channel (mSlo) fused to green fluorescent protein (GFP). *Electronic Journal of Biotechnology* [online]. **2** [cited 11 November 2008].
-

References

- Nagaya NP, DM. (1997). Potassium channel alpha and beta subunits assemble in the endoplasmic reticulum. *J Biol Chem* **272**, 3022-3027.
- Nakahira K, Shi G, Rhodes K & Trimmer J. (1996). Selective interaction of voltage-gated K⁺ channel beta-subunits with alpha-subunits. *J Biol Chem* **271**, 7084-7089.
- Nakahashi Y, Nelson E, Fagan K, Gonzales E, Guillou JL, Cooper DM. (1997) Construction of a full-length Ca²⁺-sensitive adenylyl cyclase/aequorin chimera. *J Biol Chem.* **272**, 18093-7.
- Nakamura T, Nakamura K, Lasser-Ross N, Barbara JG, Sandler VM, Ross WN. (2000) Inositol 1,4,5-trisphosphate (IP₃)-mediated Ca²⁺ release evoked by metabotropic agonists and backpropagating action potentials in hippocampal CA1 pyramidal neurons. *J Neurosci.* **20**, 8365-76.
- Navarro-Antolin JL, KL. Calderon, E. Ordonez, A. Lopez-Barneo, J. (2005). Decreased expression of maxi-K⁺ channel beta1-subunit and altered vasoregulation in hypoxia. *Circulation* **112**, 1309-1315.
- Neher E (1998). Vesicle pools and Ca²⁺ microdomains: new tools for understanding their roles in neurotransmitter release. *Neuron* **20**, 389–399.
- Neher E and Sakmann B (1976). Single-channel currents recorded from membrane of denervated frog muscle fibres. *Nature.* **260**, 799-802.
- Neher E and Sakmann B. (1992) The patch clamp technique. *Sci Am.***266**, 44-51.
- Nilius B, Schwarz G, Droogmans G. (1993) Control of intracellular calcium by membrane potential in human melanoma cells. *Am J Physiol.***265**, 1501-10.
- Nimigean CM, Magleby KL. (2000) Functional coupling of the beta(1) subunit to the large conductance Ca²⁺-activated K⁺ channel in the absence of Ca²⁺. Increased Ca²⁺ sensitivity from a Ca²⁺-independent mechanism. *J Gen Physiol.* **115**, 719-36.
- Nomura, M., Inouye, S., Ohmiya, Y., and Tsuji, F. I. (1991) A C-terminal proline is required for bioluminescence of the Ca²⁺ binding photoprotein, aequorin. *FEBS Lett.* **295**, 63
- Nowicky AV and Duchen MR. (1998) Changes in [Ca²⁺]_i and membrane currents during impaired mitochondrial metabolism in dissociated rat hippocampal neurons. *J Physiol.* **507**, 131-45.
- Ohi Y, Yamamura H, Nagano N, Ohya S, Muraki K, Watanabe M, Imaizumi Y. (2001) Local Ca²⁺ transients and distribution of BK channels and ryanodine receptors

References

- in smooth muscle cells of guinea-pig vas deferens and urinary bladder. *J Physiol.* **534**, 313-26.
- O'Neil RG and Heller S. (2005) The mechanosensitive nature of TRPV channels. *Pflugers Arch.* **451**, 193-203.
- Orrenius S, Zhivotovsky B, Nicotera P. (2003) Regulation of cell death: the calcium-apoptosis link. *Nat Rev Mol Cell Biol.* **4**, 552-65.
- Ouadid-Ahidouch H, Roudbaraki M, Ahidouch A, Delcourt P, Prevarskaya N. (2004) Cell-cycle-dependent expression of the large Ca^{2+} -activated K^+ channels in breast cancer cells. *Biochem Biophys Res Commun.* **316**, 244-51.
- Orio P, Rojas P, Ferreira G & Latorre R. (2002). New disguises for an old channel: MaxiK channels β -subunits. *News Physiol Sci*, **17**, 156-61
- Orio P, Latorre R. (2005) Differential effects of beta 1 and beta 2 subunits on BK channel activity. *J Gen Physiol.* **125**, 395-411.
- Pallanck L & B. G. (1994). Cloning and characterization of human and mouse homologs of the Drosophila calcium-activated potassium channel gene, slowpoke. *Hum Mol Genet* **3**, 1239-1243.
- Pallotta, BS; Magleby, KL; Barrett, JN. (1981) Single channel recordings of Ca^{2+} -activated K^+ currents in rat muscle cell culture. *Nature.* **293**, 471–474.
- Patel A, Lazdunski M & E. H. (1997). Kv2.1/Kv9.3, a novel ATP-dependent delayed-rectifier K^+ channel in oxygen-sensitive pulmonary artery myocytes. *EMBO J* **16**, 6615–6625. .
- Piston D, Patterson G, Lippincott-Schwartz J, Claxton N & Davidson M. (2006). Fluorescent Microscopy. Nikon's MicroscopyU (www.microscopyu.com), Data access on Aug 2008.
- Parekh AB. (2008) Ca^{2+} microdomains near plasma membrane Ca^{2+} channels: impact on cell function. *J Physiol.* **586**, 3043-54.
- Parker I & Ivorra I. (1991) Caffeine inhibits inositol trisphosphate-mediated liberation of intracellular calcium in *Xenopus* oocytes. *J Physiol.* **433**, 229–240.
- Parker I and Yao Y. (1994) Relation between intracellular Ca^{2+} signals and Ca^{2+} -activated Cl^- current in *Xenopus* oocytes. *Cell Calcium.* **15**, 276-88.
- Pinton P, Pozzan T & Rizzuto R. (1998) The Golgi apparatus is an inositol 1,4,5-trisphosphate-sensitive Ca^{2+} store, with functional properties distinct from those of the endoplasmic reticulum. *EMBO J* **17**, 5298–5308.

References

- Pinton P, Ferrari D, Rapizzi E, Di Virgilio F, Pozzan T, Rizzuto R. (2001) The Ca^{2+} concentration of the endoplasmic reticulum is a key determinant of ceramide-induced apoptosis: significance for the molecular mechanism of Bcl-2 action. *EMBO J.* **20**, 2690-701.
- Pinton P, Bianchi K, Prandini A, Rimessi A, Rizzuto R (2004) Ca^{2+} homeostasis of intracellular compartments: measurements using the jellyfish photo-protein aequorin. *Minerva Biotechnologica*, **16**, 119-26
- Poburko D, Potter K, van Breemen E, Fameli N, Liao CH, Basset O, Ruegg UT, van Breemen C. (2006) *Cell Calcium*. Mitochondria buffer NCX-mediated Ca^{2+} -entry and limit its diffusion into vascular smooth muscle cells. **40**, 359-71.
- Prasher D, McCann RO, Cormier MJ. (1985) Cloning and expression of the cDNA coding for aequorin, a bioluminescent calcium-binding protein. *Biochem Biophys Res Commun.* **126**, 1259-68.
- Putney JW Jr. (1986) A model for receptor-regulated calcium entry. *Cell Calcium.* **7**, 1-12.
- Putney, JW Jr. (2000) Calcium signalling. *Methods in signal transduction*. 2nd Ed.
- Putney JW Jr. (2001) Pharmacology of capacitative calcium entry. *Mol Interv.* **1**, 84-94.
- Putney JW Jr. (2007) Recent breakthroughs in the molecular mechanism of capacitative calcium entry (with thoughts on how we got here). *Cell Calcium.* **42**, 103-10.
- Ransom CB, Liu X, Sontheimer H. (2002) BK channels in human glioma cells have enhanced calcium sensitivity. *Glia.* **38**, 281-91.
- Rao CV, Wolf DM, Arkin AP. (2002) Control, exploitation and tolerance of intracellular noise. *Nature.* **420**, 231-7.
- Reaves BJ and Wolstenholme AJ. (2007) The TRP channel superfamily: insights into how structure, protein-lipid interactions and localization influence function. *Biochem Soc Trans.* **35**, 77-80.
- Rebhan, M., Chalifa-Caspi, V., Prilusky, J., Lancet, D. (1997) GeneCards: integrating information about genes, proteins and diseases. *Trends in Genetics* **13**, 163.
- Rembold CM, Van Riper DA, Chen XL. (1995) Focal $[\text{Ca}^{2+}]_i$ increases detected by aequorin but not by fura-2 in histamine- and caffeine-stimulated swine carotid artery. *J Physiol.* **488**, 549-64.

References

-
- Rhodes KJ, Monaghan MM, Barrezueta N, Nawoschik S, Bekele-Arcuri Z, Matos M, Nakahira K, Schechter L & Trimmer JS. (1996). Voltage-gated K⁺ channel beta subunits: expression and distribution of Kv beta 1 and Kv beta 2 in adult rat brain. *J Neurosci* **16**, 4846-4860.
- Ridgway EB, Ashley CC. (1967) Calcium transients in single muscle fibers. *Biochem Biophys Res Commun.* **29**, 229-34.
- Ringer, S. (1883) A further Contribution regarding the influence of the different Constituents of the Blood on the Contraction of the Heart. *J. Physiol.* **4**, 29–43
- Rizzuto, R; Simpson, AW; Brini, M; Pozzan, T. (1992) Rapid changes of mitochondrial Ca²⁺ revealed by specifically targeted recombinant aequorin. *Nature.* **358**, 325–327.
- Rizzuto R, Pinton P, Ferrari D, Chami M, Szabadkai G, Magalhães PJ, Di Virgilio F, Pozzan T. (2003) Calcium and apoptosis: facts and hypotheses. *Oncogene.* **22**, 8619-27.
- Rizzuto R and Pozzan T (2006). Microdomains of intracellular calcium: molecular determinants and functional consequences. *Physiol Rev* **86**, 369–408.
- Roe MW, Lemasters JJ, Herman B. (1990) Assessment of Fura-2 for measurements of cytosolic free calcium. *Cell Calcium.* **11**, 63-73.
- Rommerts FF, Lyng FM, von Ledeber E, Quinlan L, Jones GR, Warchol JB, Stefanini M, Ravindranath N, Joffre M. (2002) Calcium confusion--is the variability in calcium response by Sertoli cells to specific hormones meaningful or simply redundant? *J Endocrinol.* **167**, 1-5.
- Rossier MF, Python CP, Capponi AM, Schlegel W, Kwan CY, Vallotton MB. (1993) Blocking T-type calcium channels with tetrandrine inhibits steroidogenesis in bovine adrenal glomerulosa cells. *Endocrinology.* **132**, 1035-43.
- Rousseau E, Ladine J, Liu Q, and Meissner G (1988) Activation of the Ca²⁺ release channel of skeletal muscle sarcoplasmic reticulum by caffeine and related compounds. *Arch Biochem Biophys* **267**, 75-86
- Rozen S, Skaletsky H. (2000) Primer3 on the WWW for general users and for biologist programmers. *Methods Mol Biol.* **132**, 365-86.
- Rutter GA, Theler JM, Murgia M, Wollheim CB, Pozzan T, Rizzuto R. (1993) Stimulated Ca²⁺ influx raises mitochondrial free Ca²⁺ to supramicromolar levels in a pancreatic beta-cell line. Possible role in glucose and agonist-induced insulin secretion. *J Biol Chem.* **268**, 22385-90.
-

References

-
- Rüttiger L, Sausbier M, Zimmermann U, Winter H, Braig C, Engel J, Knirsch M, Arntz C, Langer P, Hirt B, Müller M, Kopschall I, Pfister M, Munkner S, Rohbock K, Pfaff I, Rusch A, Ruth P, Knipper M. (2004). Deletion of the Ca^{2+} -activated potassium (BK) α -subunit but not the BK β 1-subunit leads to progressive hearing loss. *PNAS* **101**, 12922-12927.
- Salkoff L, Butler A, Ferreira G, Santi C & Wei A. (2006). High-conductance potassium channels of the SLO family. *Nat Rev Neurosci* **7**, 921-931.
- Santella L. (1998) The role of calcium in the cell cycle: facts and hypotheses. *Biochem Biophys Res Commun.* **244**, 317-24.
- Santarelli L, Chen J, Heinemann S & Hoshi T. (2004). The β 1 subunit enhances oxidative regulation of large-conductance calcium-activated K^+ channels. *J Gen Physiol* **124**, 357-370.
- Scamps F, Valentin S, Dayanithi G, Valmier J. (1998) Calcium channel subtypes responsible for voltage-gated intracellular calcium elevations in embryonic rat motoneurons. *Neuroscience.* **87**, 719-30.
- Schachter JB, Sromek SM, Nicholas RA, Harden TK. (1997) HEK293 human embryonic kidney cells endogenously express the P2Y1 and P2Y2 receptors. *Neuropharmacology.* **36**, 1181-7.
- Scorrano L, Oakes SA, Opferman JT, Cheng EH, Sorcinelli MD, Pozzan T, Korsmeyer SJ. (2003) BAX and BAK regulation of endoplasmic reticulum Ca^{2+} : a control point for apoptosis. *Science.* **300**, 135-9.
- Seidler NW, Jona I, Vegh M, Martonosi A. (1989) Cyclopiazonic acid is a specific inhibitor of the Ca^{2+} -ATPase of sarcoplasmic reticulum. *J Biol Chem.* **264**, 17816–17823
- Seoh SA, Sigg D, Papazian DM, Bezanilla F. (1996) Voltage-sensing residues in the S2 and S4 segments of the Shaker K^+ channel. *Neuron.* **16**, 1159-67.
- Sergeant GP, Hollywood MA, McCloskey KD, McHale NG, Thornbury KD. (2001). Role of IP(3) in modulation of spontaneous activity in pacemaker cells of rabbit urethra. *Am J Physiol Cell Physiol.* **280**, 1349-56.
- Shen NV, Chen X, Boyer MM & Pfaffinger P. (1993). Deletion analysis of K^+ channel assembly. *Neuron* **11**, 67-76.
- Sheridan D, Berlot C, Robert A, Inglis F, Jakobsdottir K, Howe J & Hughes T. (2002). A new way to rapidly create functional, fluorescent fusion proteins: random insertion of GFP with an in vitro transposition reaction. *BMC Neuroscience* **3**.
-

References

- Shiehnm C, Coghlanm M, Sullivanm J & Gopalakrishnanm M. (2000). Potassium channels: molecular defects, diseases, and therapeutic opportunities. *Pharmacology Review* **52**, 557-594.
- Shimomura O, Johnson FH, Saiga Y. (1963) Microdetermination of Calcium by Aequorin Luminescence. *Science*. **140**, 1339-1340.
- Shimomura O, Johnson FH. (1975) Regeneration of the photoprotein aequorin. *Nature*. **256**, 236-8.
- Shimomura O, Kishi Y, Inouye S. (1993) The relative rate of aequorin regeneration from apoaequorin and coelenterazine analogues. *Biochem J*. **296**, 549-51.
- Shimomura, O. (1995) Luminescence of aequorin is triggered by the binding of two calcium ions. *Biochem. Biophys. Res. Commun.* **211**, 359–363.
- Siegel MS & Isacoff EY. (1997). A genetic encoded optical probe of membrane voltage. *Neuron*, **19**, 735-741.
- Sperelakis N. (2001). Cell Physiology Sourcebook: A Molecular Approach. 3rd Edition.
- Smith GL, Valdeolmillos M, Eisner DA, Allen DG. (1988) Effects of rapid application of caffeine on intracellular calcium concentration in ferret papillary muscles. *Journal of General Physiology*. **92**, 351–368.
- Steinhardt RA, Alderton J. (1988) Intracellular free calcium rise triggers nuclear envelope breakdown in the sea urchin embryo. *Nature*. **332**, 364-6.
- Strøbaek D, Christophersen P, Dissing S, Olesen SP. (1996) ATP activates K and Cl channels via purinoceptor-mediated release of Ca^{2+} in human coronary artery smooth muscle. *Am J Physiol*. **271**, 1463-71.
- Streb H, Irvine RF, Berridge MJ, Schulz I. (1983) Release of Ca^{2+} from a nonmitochondrial intracellular store in pancreatic acinar cells by inositol-1,4,5-trisphosphate. *Nature*. **306**, 67-9.
- Stuart GJ, Dodt HU, Sakmann B. (1993) Patch-clamp recordings from the soma and dendrites of neurons in brain slices using infrared video microscopy. *Pflugers Arch*. **423**, 511-8.
- Sutherland ML, Williams SH, Abedi R, Overbeek PA, Pfaffinger PJ, Noebels JL. (1999) Overexpression of a Shaker-type potassium channel in mammalian central nervous system dysregulates native potassium channel gene expression. *Proc Natl Acad Sci U S A*. **96**, 2451-5.
- Syntichaki P, Tavernarakis N. (2003) The biochemistry of neuronal necrosis: rogue biology? *Nat Rev Neurosci*. **4**, 672-84.

References

- Szabo T, Kuo KH, Bernard-Helary K, Poburko D, Lee CH, Seow C, Ruegg UT, van Breemen C. (2003) Agonist-induced mitochondrial Ca^{2+} transients in smooth muscle. *FASEB J.* **17**, 28-37.
- Tani D, Monteilh-Zoller MK, Fleig A, Penner R. (2007) Cell cycle-dependent regulation of store-operated I(CRAC) and Mg^{2+} -nucleotide-regulated MagNuM (TRPM7) currents. *Cell Calcium.* **41**, 249-60.
- Takahashi A, Camacho P, Lechleiter JD, Herman B. (1999) Measurement of intracellular calcium. *Physiol Rev.* **79**, 1089-125.
- Takei D, Ishihara H, Yamaguchi S, Yamada T, Tamura A, Katagiri H, Maruyama Y, Oka Y. (2006) WFS1 protein modulates the free Ca^{2+} concentration in the endoplasmic reticulum. *FEBS Lett.* **580**, 5635-40.
- Tamarina NA, Kuznetsov A, Rhodes CJ, Bindokas VP, Philipson LH. (2005) Inositol (1,4,5)-trisphosphate dynamics and intracellular calcium oscillations in pancreatic beta-cells. *Diabetes.* **54**, 3073-81.
- Thomas P and Smart TG (2005). HEK293 cell line: a vehicle for the expression of recombinant proteins. *J Pharmacol Toxicol Methods.* **51**, 187-200.
- Toma S, Chong KT, Nakagawa A, Teranishi K, Inouye S, Shimomura O. (2005) The crystal structures of semi-synthetic aequorins. *Protein Sci.* **14**, 409-16.
- Tong J, Du GG, Chen SR, MacLennan DH. (1999) HEK-293 cells possess a carbachol- and thapsigargin-sensitive intracellular Ca^{2+} store that is responsive to stop-flow medium changes and insensitive to caffeine and ryanodine. *Biochem J.* **343**, 39-44.
- Toro L. AA, Mahajan A., Garcia j., Nishimaru N., E. Stefani. (2005). Ca^{2+} -activated, voltage dependent K^+ channels. In *Ion Channels in the Pulmonary Vasculature Lung Biology in Health and Disease*. C Lenfant and J X-J Yuan, Ed. Yuan JX-J. Marcel Dekker, Inc.
- Toro B, Cox N, Wilson RJ, Garrido-Sanabria E, Stefani E, Toro L & Zarei MM. (2006). KCNMB1 regulates surface expression of a voltage and Ca^{2+} -activated K^+ channel via endocytic trafficking signals. *Neuroscience* **142**, 661-669.
- Trautmann A and Marty A. (1984) Activation of Ca^{2+} -dependent K^+ channels by carbamoylcholine in rat lacrimal glands. *Proc Natl Acad Sci U S A.* **81**, 611-5.
- Tseng-Crank J, Foster CD, Krause J, Mertz R, Godinot N, DiChiara T & Reinhart P. (1994). Cloning, expression, and distribution of functionally distinct Ca^{2+} -activated K^+ channel isoforms from human brain. *Neuron* **13**, 1315-1330.

References

- Tsien RY. (1980) New calcium indicators and buffers with high selectivity against magnesium and protons: design, synthesis, and properties of prototype structures. *Biochemistry*. **19**, 2396-404.
- Tsien RY. (1998). The Green Fluorescent Protein. *Annu Rev Biochemistry*, 509-544.
- Tsien RW, Lipscombe D, Madison DV, Bley KR, Fox AP. (1988) Multiple types of neuronal calcium channels and their selective modulation. *Trends Neurosci*. **11**, 431-8.
- Tsuji, F. I., Inouye, S., Goto, T., and Sakaki, Y. (1986) Site-specific mutagenesis of the calcium-binding photoprotein aequorin. *Proc. Natl. Acad. Sci U.S.A.* **83**, 8107
- Uebele V, Lagrutta A, Wade T, Figueroa D, Liu Y, McKenna E, Austin C, Bennett P & Swanson R. (2000). Cloning and functional expression of two families of beta-subunits of the large conductance calcium-activated K⁺ channel. *J Biol Chem* **275**, 23211-23218.
- Vandebrouck A, Ducret T, Basset O, Sebillé S, Raymond G, Ruegg U, Gailly P, Cognard C, Constantin B. (2006) Regulation of store-operated calcium entries and mitochondrial uptake by minidystrophin expression in cultured myotubes. *FASEB J*. **20**, 136-8.
- Varadi A, Cirulli V, Rutter GA. (2004) Mitochondrial localization as a determinant of capacitative Ca²⁺ entry in HeLa cells. *Cell Calcium*. **36**, 499-508.
- Voipio J., Pasternack M & Macleod, K. (1994). Ion-sensitive microelectrodes. In *Microelectrode Techniques - The Plymouth Workshop Handbook*, 2nd ed, pp. 275-316. The Company of Biologists Ltd, Cambridge.
- Wang G and Lemos JR. (1992) Tetrandrine blocks a slow, large-conductance, Ca²⁺-activated potassium channel besides inhibiting a non-inactivating Ca²⁺ current in isolated nerve terminals of the rat neurohypophysis. *Pflügers Arch*. **421**, 558-65.
- Wallner M, Meera P, Toro L. (1999) Molecular basis of fast inactivation in voltage and Ca²⁺-activated K⁺ channels: a transmembrane beta-subunit homolog. *Proc Natl Acad Sci U S A*. **96**, 4137-42.
- Wang, G and Lemos, JR (1992) Tetrandrine blocks a slow, large-conductance, Ca²⁺-activated potassium channel besides inhibiting a non-inactivating Ca²⁺ current in isolated nerve terminals of the rat neurohypophysis. *Pflügers Arch* **421**, 558-565.

References

- Wang Y, Ding J, Xia X & Lingle C. (2002). Consequences of the Stoichiometry of Slo1 and Auxiliary Subunits on Functional Properties of Large-Conductance Ca^{2+} -Activated K^{+} Channels The Journal of Neuroscience **22**, 1550-1561.
- Waters M, Minassian N, Stevanin G, Figueroa K, Bannister J, Nolte D, Mock A, Evidente V, Fee D, Muller U, Durr A, Brice A, Papazian D & Pulst S. (2006). Mutations in voltage-gated potassium channel KCNC3 cause degenerative and developmental central nervous system phenotypes. Nat Genet **38**, 447-451.
- Watkins NJ, Campbell AK. (1993) Requirement of the C-terminal proline residue for stability of the Ca^{2+} -activated photoprotein aequorin. *Biochem J.* **293**, 181-5.
- Watkins NJ, Knight MR, Trewavas AJ, Campbell AK. (1995) Free calcium transients in chemotactic and non-chemotactic strains of Escherichia coli determined by using recombinant aequorin. *Biochem J.* **306**, 865-9.
- Watkins, N. (1995) Engineering the calcium activated photoprotein aequorin as an intracellular calcium indicator in bacteria and plants. *Phd. thesis*
- Waud JP, Bermúdez Fajardo A, Sudhaharan T, Trimby AR, Jeffery J, Jones A, Campbell AK. (2001). Measurement of proteases using chemiluminescence-resonance-energy-transfer chimaeras between green fluorescent protein and aequorin. *Biochem J.* **357**, 687-97.
- Wayman CP, McFadzean I, Gibson A, Tucker JF. (1996) Two distinct membrane currents activated by cyclopiazonic acid-induced calcium store depletion in single smooth muscle cells of the mouse anococcygeus. *Br J Pharmacol.* **117**, 566-572.
- Weaver AK, Olsen ML, McFerrin MB, Sontheimer H. (2007) BK channels are linked to inositol 1,4,5-triphosphate receptors via lipid rafts: a novel mechanism for coupling $[\text{Ca}^{2+}]_i$ to ion channel activation. *J Biol Chem.* **282**, 31558-68.
- Wei A, Gutman, G, Aldrich, R, Chandy, K, Grissmer, S, Wulff, H. (2005). International Union of Pharmacology. LII. Nomenclature and Molecular Relationships of Calcium-Activated Potassium Channels. *Pharmacol Rev* **57**, 463-472.
- Wei A, Solaro C, Lingle C & Salkoff L. (1994). Calcium sensitivity of BK-type Kca channels determined by a separable domain. *Neuron* **13**, 671-681.
- Werner M, Zvara P, Meredith A, Aldrich R & Nelson M. (2005). Erectile dysfunction in mice lacking the large conductance calcium-activated potassium (BK) channel. *Journal of Physiology.* **567**, 545-56

References

- Whitaker M. (2006) Calcium microdomains and cell cycle control. *Cell Calcium*. **40**, 585-92.
- White C & McGeown JG. (2002) Carbachol triggers RyR-dependent Ca^{2+} release via activation of IP_3 receptors in isolated rat gastric myocytes. *J Physiol*. **542**, 725-33.
- Woods NM, Cuthbertson KS & Cobbold PH. (1987) Agonist-induced oscillations in cytoplasmic free calcium concentration in single rat hepatocytes. *Cell Calcium*. **8**, 79–100.
- Wu SN, Li HF, Lo YC. (2000) Characterization of tetrandrine-induced inhibition of large-conductance calcium-activated potassium channels in a human endothelial cell line (HUV-EC-C). *J Pharmacol Exp Ther*. **292**, 188-95.
- Xia X, Ding J & Lingle C. (1999). Molecular Basis for the Inactivation of Ca^{2+} - and Voltage-Dependent BK Channels in Adrenal Chromaffin Cells and Rat Insulinoma Tumor Cells. *J Neurosci* **19**, 5255-5264.
- Xie J & McCobb D. (1998). Control of Alternative Splicing of Potassium Channels by *Stress Hormones Science* **280**, 443-446.
- Xiong ZL, Kitamura K, Kuriyama H. (1992) Evidence for contribution of Ca^{2+} storage sites on unitary K^+ channel currents in inside-out membrane of rabbit portal vein. *Pflugers Arch*. **420**, 112-4.
- Xu Y, Piston D & Johnson C. (1999). A bioluminescence resonance energy transfer (BRET) system: application to interacting circadian clock proteins. *Proc Natl Acad Sci U S A* **96**, 151-156.
- Young RC and Zhang P. (2004) Functional separation of deep cytoplasmic calcium from subplasmalemmal space calcium in cultured human uterine smooth muscle cells. *Cell Calcium*. **36**, 11-7.
- Yu J, Upadhyaya A & Atkinson N. (2006). Tissue-specific alternative splicing of BK channel transcripts in Drosophila. *Genes, Brain and Behavior* **5**, 329.
- Zamponi GW. (2005) *Voltage-Gated Calcium Channels*. 1st Ed.
- Zarei MM, Zhu N, Alioua A, Eghbali M, Stefani E, Toro L. (2001) A novel MaxiK splice variant exhibits dominant-negative properties for surface expression. *J Biol Chem*. **276**, 16232-9.
- Zarei M, Song, M, Wilson, RJ, Cox, N, Colom, L, Knaus, HG, Stefani, E, Toro, L. (2005). Endocytic Trafficking Signals in KCNMB2 Regulate Surface Expression of a Voltage and Ca^{2+} -activated K^+ channel. *AHA Research Symposium*

References

- Zeng X, Xia X & Lingle C. (2003). Redox-sensitive extracellular gates formed by auxiliary beta subunits of calcium-activated potassium channels. *Nat Struct Biol* **10**, 448-454.
- Zeng XH, Xia XM, Lingle CJ. (2005) Divalent cation sensitivity of BK channel activation supports the existence of three distinct binding sites. *J Gen Physiol.* **125**, 273-86.
- Zhang L, Li X, Zhou R & Xing G. (2006). Possible role of potassium channel, big K in etiology of Schizophrenia. *Medical Hypotheses* **67**, 41-43.
- Zhuge R, Fogarty KE, Tuft RA, Lifshitz LM, Sayar K, Walsh JV Jr. (2000) Dynamics of signaling between Ca^{2+} sparks and Ca^{2+} -activated K^{+} channels studied with a novel image-based method for direct intracellular measurement of ryanodine receptor Ca^{2+} current. *J Gen Physiol.* **116**, 845-64.
- Zhuge R, Fogarty KE, Tuft RA, Walsh JV Jr. (2002) Spontaneous transient outward currents arise from microdomains where BK channels are exposed to a mean Ca^{2+} concentration on the order of 10 microM during a Ca^{2+} spark. *J Gen Physiol.* **120**, 15-27.
- Ziganshin AU, Hoyle CH, Ziganshina LE, Burnstock G. (1994) Effects of cyclopiazonic acid on contractility and ecto-ATPase activity in guinea-pig urinary bladder and vas deferens. *Br J Pharmacol.* **113**, 669-74.
- Zimmermann B and Walz B (1997) Serotonin-induced intercellular calcium waves in salivary glands of the blowfly *Calliphora erythrocephala*. *J Physiol.* **500**, 17–28.

APPENDIX 1 Oligonucleotide primer sequences.

Primers used to detect the presence of the α and β 1-4 subunits:

Beta Actin sense (20 bp)

CCCAGCCATGTACGTTGCTA

Beta Actin antisense (21 bp)

AGGGCATACCCCTCGTAGATG

α sense (23 bp)

ACGCAATCTGCCTCGCAGAGTTG

α antisense (20 bp)

CATCATGACAGGCCTTGCAG

β 1 sense (21 bp)

CTGTACCACACGGAGGACACT

β 1 antisense (21 bp)

GTAGAGGCGCTGGAATAGGAC

β 2 sense (20 bp)

CATGTCCCTGGTGAATGTTG

β 2 antisense (20 bp)

TTGATCCGTTGGATCCTCTC

β 3 sense (20 bp)

AACCCCCTTTTCATGCTTCT

β3 antisense (20 bp)

TCTTCCTTTGCTCCTCCTCA

β3 sense (20 bp)

GTTTCGAGTGCACCTTCACCT

β4 antisense (20 bp)

TAAATGGCTGGGAACCAATC

Primers used to obtain the full sequence of the β2 subunit:

β2 sense (21 bp)

GAGACCCTGGACCAACATTCT

β2 antisense (25 bp)

AGAACCTTAAGTTTGTAACGTGCAG

Primers used to link the β2 and aequorin sequences:

β2 sense primer (28 bp)

ATGTTTATATGGACCAGTGGCCG

β2 antisense primer (26 bp)

TTATCTATTGATCCGTTGGATCCTCT

β2 antisense primer with aequorin linker (48 bp):

GAAGTCTGATGTAAGCTTGACCATTCTATTGATCCGTTGGATCCTCTC

Aequorin antisense primer (19 bp):

TTAGGGGACAGCTCCACCC

Primer used for plasmid screening in bacteria:

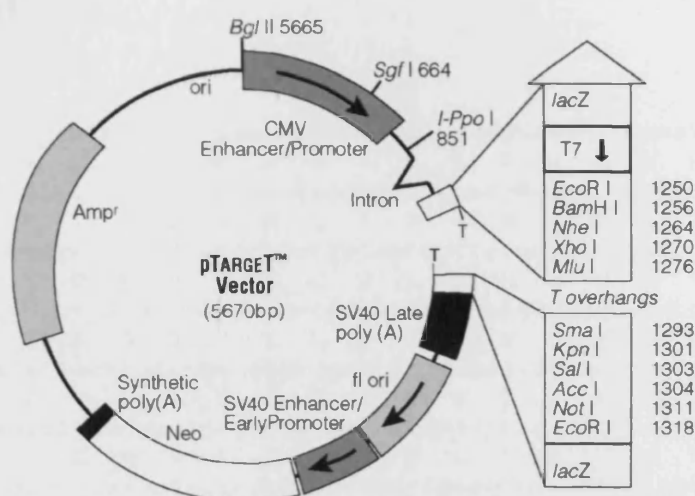
T7 promoter sense primer:

TAATACGACTCACTATAGGG

APPENDIX 2: Vector circle map and sequence reference points.

pTarget: mammalian expression vector

(Promega, Southampton, U.K.)



Sequence reference points

1. Cytomegalovirus immediate-early enhancer
2. Cytomegalovirus immediate-early promoter
3. Chimeric intron
4. *lacZ*α start codon
5. *lacZ*α stop codon
6. *lac* operon sequences
7. *lac* operator
8. T7 promoter
9. Multiple cloning site
10. SV40 late polyadenylation signal
11. Phage f1 region
12. Neomycin selectable marker
13. β-lactamase (Amp^r) coding region

Bases

- 1-659
- 669-750
- 890-1022
- 1377
- 1053
- 1363-1499, 1066-1226
- 1397-1413
- 1227-1251
- 1250-1323
- 1535-1755
- 1798-2252
- 2260-3581
- 3978-4838

APPENDIX 3: cDNA sequences.

A. $\beta 2$ subunit of the BK channel cDNA coding sequence (KCNMB2)

Published sequence of the $\beta 2$ subunit (NM_181361, GenBank). This sequence is listed 5' to 3'. The transcriptional start site is defined as residue +1. Stop codon is indicated by -. The translated amino acid sequence is shown underneath.

```

atgtttatatggaccagtggccggacctcttcatcttatagacatgatgaaaaaagaat 61
  M F I W T S G R T S S S Y R H D E K R N
atttaccagaaaatcagggaccatgacctcctggacaaaaggaaaacagtcacagcactg 121
  I Y Q K I R D H D L L D K R K T V T A L
aaggcaggagaggaccgagctattctcctgggactggctatgatgggtgtgctccatcatg 181
  K A G E D R A I L L G L A M M V C S I M
atgtatcttctgctgggaatcacactcctgcgctcatatgcagagcgtgtggaccgaa 241
  M Y F L L G I T L L R S Y M Q S V W T E
gagtcctcaatgcaccttgctgaatgcgtccatcacggaaacatttaattgctccttcagc 301
  E S Q C T L L N A S I T E T F N C S F S
tgtgggtccagactgctggaaactttctcagtagccctgcctccaggtgtacgttaacctg 361
  C G P D C W K L S Q Y P C L Q V Y V N L
acttcttccggggaaaagctcctcctctaccacacagaagagacaataaaaaatcaatcag 421
  T S S G E K L L L Y H T E E T I K I N Q
aagtgtccttatatacctaaatgtggaaaaaattttgaagaatccatgtccctgggtgaat 481
  K C S Y I P K C G K N F E E S M S L V N
gttgatcatggaaaacttcaggaagtatcaacacttctcctgctattctgaccagaagga 541
  V V M E N F R K Y Q H F S C Y S D P E G
aaccagaagagtgttatcctaacaaaactctacagttccaacgtgctgttccattcactc 601
  N Q K S V I L T K L Y S S N V L F H S L
ttctggccaacctgtatgatggctgggggtgtggcaattgttgccatggtgaaacttaca 661
  F W P T C M M A G G V A I V A M V K L T
cagtacctctccctactatgtgagaggatccaacggatcaatagataa 708
  Q Y L S L L C E R I Q R I N R -

```

B. $\beta 2$ subunit of the BK channel coding sequence.

$\beta 2$ sequence inserted into pTarget. This sequence is listed 5' to 3', left to right. The transcriptional start site is defined as residue +1. Stop codon is indicated by -. The translated amino acid sequence is shown underneath.

```

atgtttatatggaccagtggccggacctcttcattcttatagacatgatgaaaaaagaaat 61
M F I W T S G R T S S S Y R H D E K R N
atttaccagaaaaatcagggaccatgacctcctggacaaaaggaaaacagtcacagcactg 121
I Y Q K I R D H D L L D K R K T V T A L
aaggcaggagaggaccgagctattctcctgggactggctatgatgggtgtgctccatcatg 181
K A G E D R A I L L G L A M M V C S I M
atgtatcttctgctgggaatcacactcctgcgctcatatgcagagcgtgtggaccgaa 241
M Y F L L G I T L L R S Y M Q S V W T E
gagtcctcaatgcaccttgctgaatgcgtccatcacggaaacatttaactgctccttcagc 301
E S Q C T L L N A S I T E T F N C S F S
tgtgggtccagactgctggaaactttctcagtagccctgcctccaggtgtacgttaacctg 361
C G P D C W K L S Q Y P C L Q V Y V N L
acttcttccggggaaaagctcctcctctaccacacagaagagacaataaaaaatcaatcag 421
T S S G E K L L L Y H T E E T I K I N Q
aagtgtcctacatacctaataatgtggaaaaaattttgaagaatccatgtccctgggtgaat 481
K C S Y I P K C G K N F E E S M S L V N
gttgatcatggaaaacttcaggaagtatcaacacttctcctgctattctgacccagaagga 541
V V M E N F R K Y Q H F S C Y S D P E G
aaccagaagagtgttatcctaaccaaactctacagttccaacgtgctgttccattcactc 601
N Q K S V I L T K L Y S S N V L F H S L
ttctggccaacctgtatgatggctgggggtgtggcaattgttgccatggtgaaacttaca 661
F W P T C M M A G G V A I V A M V K L T
cagtacctctccctactatgtgagaggatccaacggatcaatagataa 708
Q Y L S L L C E R I Q R I N R -

```

C. Native aequorin cDNA coding sequence.

Sequence of aequorin cDNA (Badminton, 1996). This sequence is listed 5' to 3', left to right. The transcriptional start site is defined as residue +1. Stop codon is indicated by -. The translated amino acid sequence is shown underneath.

```

atgggtcaagcttacatcagacttcgacaacccaaaatggattggacgacacaagcacatg    61
M V K L T S D F D N P K W I G R H K H M
ttaattttcttgatgtcaaccacaatggaaggatctctcttgacgagatgggtctacaag    121
F N F L D V N H N G R I S L D E M V Y K
Gcgtccgatattgttataaacaatcttgaggagcaacacctgaacaagccaaacgtcacaaa    181
A S D I V I N N L G A T P E Q A K R H K
gatgctgtagaagccttcttcggaggagctggaatgaaatatgggtgtagaaactgaatgg    241
D A V E A F F G G A G M K Y G V E T E W
cctgaatacatcgaaggatggaaaagactggcttccgaggaattgaaaaggtattcaaaa    301
P E Y I E G W K R L A S E E L K R Y S K
aaccaaatcacacttattcgtttatgggggtgatgcattgttcgatatcattgacaaagac    361
N Q I T L I R L W G D A L F D I I D K D
caaaatggagctatttcactggatgaatggaaagcatacacccaaatctgctggcatcatc    421
Q N G A I S L D E W K A Y T K S A G I I
caatcgtcagaagattgcgaggaaacattcagagtgtgcgatattgatgaaagtggacag    481
Q S S E D C E E T F R V C D I D E S G Q
ctcgatgttgatgagatgacaagacaacatttaggattttggtacaccatggaccctgct    541
L D V D E M T R Q H L G F W Y T M D P A
tgcgaaaagctctacgggtggagctgtcccctaa                                573
C E K L Y G G A V P -

```

D. β 2-Aequorin sequence coding sequence.

β 2-Aequorin sequence inserted into pTarget. This sequence is listed 5' to 3', left to right. The transcriptional start site is defined as residue +1. Stop codon is indicated by -. The translated amino acid sequence is shown underneath.

```

atgtttatatggaccagtggccggacctcttcatcttatagacatgatgaaaaaagaaat 61
M F I W T S G R T S S S Y R H D E K R N
atttaccagaaaatcagggaccatgacctcctggacaaaaggaaaacagtcacagcactg 121
I Y Q K I R D H D L L D K R K T V T A L
aaggcaggagaggaccgagctattctcctgggactggctatgatgggtgtgctccatcatg 181
K A G E D R A I L L G L A M M V C S I M
atgtattttctgctgggaatcacactcctgcgctcatagatgcagagcgtgtggaccgaa 241
M Y F L L G I T L L R S Y M Q S V W T E
gagtctcaatgcaccttgctgaatgcgtccatcacggaaacatttaattgctccttcagc 301
E S Q C T L L N A S I T E T F N C S F S
tgtggtccagactgctggaaactttctcagtaccctgcctccaggtgtacgttaacctg 361
C G P D C W K L S Q Y P C L Q V Y V N L
acttcttcggggaaaagctcctcctctaccacacagaagagacaataaaaaatcaatcag 421
T S S G E K L L L Y H T E E T I K I N Q
aagtgtccttatatacctaaatgtggaaaaaattttgaagaatccatgtccctgggtgaat 481
K C S Y I P K C G K N F E E S M S L V N
gttgtcatggaaaacttcaggaagtatcaacacttctcctgctattctgacctcagaagga 541
V V M E N F R K Y Q H F S C Y S D P E G
agccagaagagtgttatcctaacaaaactctacagttccaacgtgctgttccattcactc 601
S Q K S V I L T K L Y S S N V L F H S L
ttctggccaacctgtatgatggctgggggtgtggcaattgttgccatgggtgaaacttaca 661
F W P T C M M A G G V A I V A M V K L T
cagtacctctcctactatgggagaggatccaacggatcaatagaatgggtcaagcttaca 721
Q Y L S L L W E R I Q R I N R M V K L T
tcagacttcgacaacccaaaatggattggacgacacaagcacatgtttaattttcttgat 781
S D F D N P K W I G R H K H M F N F L D
gtcaaccacaatggaaggatctctcttgacgagatgggtctacaaggcgtccgatattgtt 841
V N H N G R I S L D E M V Y K A S D I V
ataaacaatcttggagcaacacactgaacaagccaaacgtcacaaagatgctgtagaagcc 901
I N N L G A T P E Q A K R H K D A V E A
ttcttcggaggagctggaatgaaatatggtgtagaaaactgaatggcctgaatacatcgaa 961
F F G G A G M K Y G V E T E W P E Y I E
ggatggaaaagactggcttcccgaggaattgaaaaggatttcaaaaaaccaaatacacactt 1021
G W K R L A S E E L K R Y S K N Q I T L
attcgtttatggggtgatgcattgttcgatatcattgacaaagaccaaataaggagctatt 1061
I R L W G D A L F D I I D K D Q N G A I
tcactggatgaatggaaagcatacaccaaactctgctggcatcatccaatcgtcagaagat 1121
S L D E W K A Y T K S A G I I Q S S E D
tgcgaggaaacattcagagtgtgcatattgatgaaagtggacagctcgatgttgatgag 1181
C E E T F R V C D I D E S G Q L D V D E
atgacaagacaacatttaggatttttggtacaccatggaccctgcttgcgaaaagctctac 1241
M T R Q H L G F W Y T M D P A C E K L Y
ggtggagctgtcccctaa 1260
G G A V P -

```


APPENDIX 4: Publications, meetings and abstracts.

Publications

Henney N, Li B, Elford C, **Reviriego P**, Campbell A, Wann K, Evans B. (2009) A Large Conductance (BK) Potassium Channel subtype affects both growth and mineralisation of Human Osteoblasts. *Am J Physiol Cell Physiol*.

Peer-reviewed meeting abstracts

B. Li, N.C Henney, B.A.J. Evans, **P. Reviriego**, A.K. Campbell and K.T.Wann (2007) BK channels in human osteoblast-like cells – properties and function. *J. Bone Miner. Res.*, 22, suppl 1, W045.

B. Li, N.C. Henney, B.A.J. Evans, **P. Reviriego**, A.K. Campbell, K.T. Wann (2007) BK Channels are Expressed and Functional in Human Osteoblast-like Cells. *Proc Life Sciences*, PC162

Unrefereed abstracts

P. Reviriego, K.T.Wann and A.K. Campbell. Assessment of the effects of drugs on the Ca^{2+} -activation of the BK channel using a recombinant Aequorin chimera. Ion channels as therapeutic targets meeting, Novartis, Horsham, 2009.

P. Reviriego, K.T.Wann and A.K. Campbell. Bioluminescent indicators for ion channels in living cells. Pharmacy Postgraduate Research Day, Cardiff, 2008.

P. Reviriego, K.T.Wann and A.K. Campbell. Aequorin: the light of knowledge. Speaking of Science meeting, Cardiff, 2007.

P. Reviriego, K.T.Wann and A.K. Campbell. Light at the end of the channel. Biomedical & Life Sciences Annual Lecture, Cardiff, 2006.

